

**Analysis of the expression,
the cellular and the molecular functions
of TBX2 in
murine lung development**

Der Naturwissenschaftlichen Fakultät
der Gottfried Wilhelm Leibniz Universität Hannover

zur Erlangung des Grades
Doktorin der Naturwissenschaften (Dr. rer. nat.)

genehmigte Dissertation

von

Irina Wojahn, M. Sc.

Referent: Prof. Dr. rer. nat. Andreas Kispert

Koreferent: Prof. Dr. rer. nat. Nico Lachmann

Tag der Promotion: 14.04.2021



Angefertigt am
Institut für Molekularbiologie
der Medizinischen Hochschule Hannover
unter der Betreuung von
Prof. Dr. rer. nat. Andreas Kispert

Meiner Familie

"Der Beginn aller Wissenschaften ist das Erstaunen,
dass die Dinge sind, wie sie sind."

Aristoteles

Erklärung zur kumulativen Dissertation von Irina Wojahn (geboren am 20.02.1990 in Cuxhaven)

Diese kumulative Dissertation basiert auf folgendem veröffentlichten Fachartikel und bisher unveröffentlichtem Manuskript:

1. **Irina Wojahn**, Timo H. Lüdtkke, Vincent M. Christoffels, Mark-Oliver Trowe and Andreas Kispert. "TBX2-positive cells represent a multi-potent mesenchymal progenitor pool in the developing lung". *Respiratory Research* (2019) 20:292; DOI:10.1186/s12931-019-1264-y.
2. **Irina Wojahn**, Timo H. Lüdtkke, Marc-Jens Kleppa, Jasper Schierstaedt, Vincent M. Christoffel, Patrick Künzler and Andreas Kispert. "Combined genomic and proteomic approaches reveal DNA binding sites and interaction partners of TBX2 in the developing lung". *Submitted in Respiratory Research*.

In **Artikel 1** habe ich alle Abbildungen (Abb.) experimentell und graphisch erstellt. Die Daten zu den Abb. 1C-E, 2A-B, 5A und 5D, 6A sowie S12A habe ich bereits während meiner Masterarbeit erstellt. Das inhaltliche Konzept des Projekts wurde von Andreas Kispert, Timo Lüdtkke und mir gemeinsam erarbeitet. Das Manuskript wurde von Andreas Kispert und mir gemeinsam geschrieben. Andreas Kispert hat das Projekt finanziert.

In **Artikel 2** habe ich die Abbildungen (Abb.) 2A-C graphisch dargestellt, die Abb. 3 experimentell (mit Ausnahme der massenspektrometrischen Messung und Protein Decodierung) und graphisch erstellt und dazugehörige Tabellen ausgearbeitet, sowie die Abb. 4A experimentell und graphisch erstellt (mit Ausnahme von HMGB2). Ferner habe ich die Abb. S1 und S2 experimentell und graphisch erstellt. Das inhaltliche Konzept des Projekts wurde von Andreas Kispert, Timo Lüdtkke und mir gemeinsam erarbeitet. Initiale und begleitende Experimente (nicht veröffentlicht) wurden von mir durchgeführt. Das Manuskript wurde von Andreas Kispert, Timo Lüdtkke und mir gemeinsam geschrieben. Andreas Kispert hat das Projekt finanziert.

Abstract

The mechanisms underlying organogenesis are based on precisely controlled genetic programs [1-3]. The embryonic development of the respiratory epithelium has been extensively studied [4, 5], while the insights into mesenchymal development are limited. Previous work described the functional requirement of the T-box (*Tbx*) transcription factor genes *Tbx2-Tbx5*, in the development of the pulmonary mesenchyme [6-10], of which the transcriptional repressors TBX2 and TBX3 were shown to control embryonic lung growth and branching morphogenesis by maintaining mesenchymal proliferation [7, 8].

The present study aims to unveil the cellular and molecular mechanisms by which TBX2 exerts its function in the pulmonary mesenchyme. Detailed expression analysis and genetic lineage tracing analyses showed that the majority of mesenchymal cells and approximately half of the mesothelial cells express TBX2 and derive from the TBX2⁺ cell lineage. Analyses in TBX2 loss-and gain-of-function mutant lungs revealed that lineage diversification was independent of TBX2, however, minor defects in the development and physiology of the bronchial smooth muscle layer were observed.

Transcriptomic- and ChIP-seq data identified *Interleukin 33 (Il33)* and *cellular communication network factor 4 (Ccn4)* as additional direct target genes and *de novo* motif analysis of the DNA regions bound by TBX2 revealed an enrichment of homeobox and high-mobility-group (HMG) box consensus sequences. Proteomic analysis revealed that TBX2 interacts with the homeobox transcription factor pre B cell leukemia homeobox 1 (PBX1) and the HMG protein high mobility group box 2 (HMGB2), in consistence with the preceding motif analysis. Further identified interaction partners of TBX2 indicate a function of TBX2 in histone modification and chromatin remodeling. Taking together, TBX2 predominantly controls proliferation of the pulmonary mesenchyme rather than cell fate decisions or differentiation. In order to do so, TBX2 interacts with several proteins to exert DNA binding and histone/chromatin modifications. Thus, this study provides new insight in the cellular and molecular mechanisms by which TBX2 participates in lung development.

Keywords: *Tbx2*, Lung mesenchyme development, Smooth muscle cells, Target genes, Protein interaction

Zusammenfassung

Die Prozesse der Organogenese basieren auf akribisch kontrollierten, genetischen Programmen [1-3]. Im Fall der Lungenentwicklung sind diese Mechanismen für das Epithel bereits eingehend erforscht [4, 5], während das Wissen über die mesenchymale Entwicklung begrenzt ist. Für die T-Box Transkriptionsfaktoren TBX2-TBX5 wurden essenzielle Funktionen für die Entwicklung des Lungenmesenchyms beschrieben [6-10], wobei die transkriptionellen Repressoren TBX2 und TBX3, über die Aufrechterhaltung der mesenchymalen Proliferation, für das Wachstum und die Verzweigungsmorphogenese der embryonalen Lunge notwendig sind [7, 8]. Die vorliegende Arbeit soll die zellulären und molekularen Mechanismen von TBX2 im Lungenmesenchym näher untersuchen. Dafür wurden detaillierte Expressions- und Zellschicksalsanalysen sowie ChIP-Seq-, Transkriptom- und Proteininteraktionsanalysen durchgeführt. Die Expressions- und Zellschicksalsanalyse zeigten, dass ein Großteil der mesenchymalen, sowie in etwa die Hälfte der mesothelialen Zellen TBX2 exprimieren und aus der TBX2⁺ Zelllinie abstammen. Analysen in TBX2 Verlust- und Überexpressionsmutanten verdeutlichten, dass die mesenchymalen Zellschicksale der Lunge unabhängig von TBX2 sind. Allerdings konnten geringe Defekte in der Entwicklung und der Funktion der bronchialen Muskulatur beobachtet werden. Transkriptom- und ChIP-Seq Daten identifizierten *Irf3* und *Ccn4* als weitere Zielgene und eine *de novo* Motivanalyse der von TBX2 gebundenen DNA Regionen zeigte eine Anreicherung von Konsensussequenzen für Homöobox und HMG-Box Proteine. Im Einklang dazu konnten Proteininteraktionsstudien eine Interaktion von TBX2 mit dem Homöobox-Transkriptionsfaktor PBX1 und dem HMG Protein HMGB2 zeigen. Die Betrachtung weiterer Interaktionspartner lieferte Hinweise darauf, dass TBX2 Chromatin und Histon modifizierende Enzyme und Komplexe rekrutiert. Die vorliegende Arbeit verdeutlicht, dass TBX2 vorwiegend die Proliferation des Lungenmesenchyms reguliert, während Zellschicksalsentscheidungen nicht von TBX2 abhängig sind. TBX2 interagiert mit verschiedenen Proteinen, um DNA Regionen spezifisch zu binden und vermutlich um Chromatin und Histone zu modifizierenden. Diese Arbeit liefert neue Erkenntnisse über die zellulären und molekularen Mechanismen mittels derer TBX2 an der Entwicklung der Lunge beteiligt ist.

Schlagnworte: Tbx2, Lungenmesenchym, Glattmuskelzellen, Zielgene, Proteininteraktion

Table of contents

Anfertigungsstätte und Betreuung _____	II
Widmung und Zitat _____	III
Erklärung zur kumulativen Dissertation _____	IV
Abstract _____	V
Zusammenfassung _____	VI
Table of contents _____	VII
Introduction _____	1
Aims of the study _____	16
Part 1 - Lineage tracing of TBX2⁺ cells and the role of TBX2 in cell fate decision _____	18
"TBX2-positive cells represent a multi-potent mesenchymal progenitor pool in the developing lung"	
Part 2 - TBX2 target genes and interaction partners _____	70
"Combined genomic and proteomic approaches reveal DNA binding sites and interaction partners of TBX2 in the developing lung"	
Concluding remarks _____	161
References _____	170
Acknowledgment _____	VIII
Curriculum vitea _____	IX
List of publications _____	XI
Declaration _____	XIII

Introduction

Structure and development of the respiratory system

The physiological function of the mammalian lung is to take up oxygen and discharge carbon dioxide. This gas exchange is based on diffusion and relies on a large air exposed surface closely linked to the vascular network. This is achieved by a complex organ architecture combined with a variety of specialized cell types.

The murine lung consists of one left and four right lobes (superior, middle, inferior and post-caval lobes), one of which (the post-caval lobe) is morphologically shifted to the left side (Fig. 1A). Starting from the trachea, the lung epithelium is organized in a tree like structure of bronchi and bronchioles (Fig. 1B) which conduct the air; the epithelium of the airways is mostly ciliated to remove particles and pathogens from the lung. Distally, the epithelium forms specialized units for the gas exchange, the alveoli (Fig. 1C), which are mostly comprised of alveolar epithelial cells type I and II (AEC I and AEC II). To enable an efficient diffusion of gases, these cells have a flattened morphology and direct contact to the air on one side and to the ramified vascular network on the other.

The epithelium of the trachea, bronchi and bronchioles is surrounded by mesenchymal tissues of differential characters (Fig. 1D, 1D', 1D"). The mesenchymal compartment of the trachea consists of C-shaped cartilaginous rings which enclose the ventral and lateral aspects, while dorsally continuous fibers of SMCs reside (Fig. 1D). The bronchial mesenchyme comprises of irregularly arranged, crescent-shaped cartilaginous plates which surround a periepithelial layer of bSMCs (Fig. 1D'). The bronchioles lack cartilaginous structures, but feature a prominent layer of bSMCs (Fig. 1D"). The bSMCs contract rhythmically to control the diameter of the epithelial tube and thereby support air conduction [17], while the cartilaginous structures stabilize the conducting airways. The mesenchyme of the alveoli is restricted to a sparse population of interstitial fibroblasts and pericytes.

The entire organ is covered by a mono-layer of epithelial-like cells, a mesothelium, also known as the visceral pleura. The mesothelium allows the smooth sliding of the lung along other organs and the body wall and is critically involved in the immune response [18]. [19, 20]

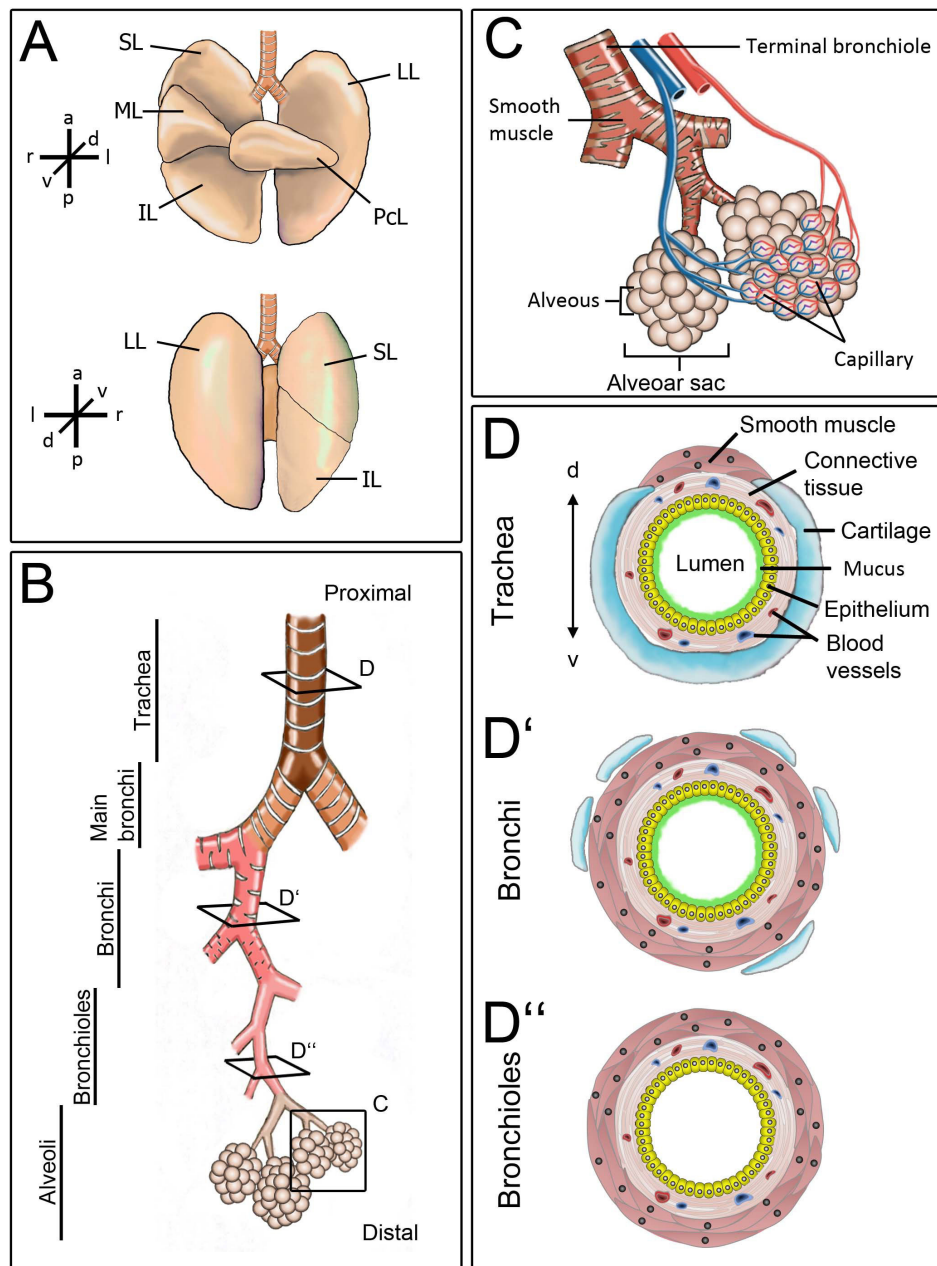


Figure 1: Morphology and histology of the murine lung.

(A) Scheme of the lobes of the adult murine lung. The lung consists of four right lobes (superior, middle, inferior and post-caval) and one left lobe. (B) Scheme of the pulmonary epithelial structure. A magnification of C and cross-sections at the levels D, D' and D'' are depicted in the panels to the right. (C) Illustration of the distal respiratory tree showing alveolar sacs, composed of multiple alveoli and their association with the capillary network. (D, D', D'') Scheme of the circular tissue arrangement of the trachea (D), the bronchi (D') and the bronchioles (D''). Abbreviations: a: anterior; d: dorsal; IL: Inferior lobe; l: left; LL: Left lung; ML: Middle lobe; p: posterior; PCL: Post-caval lobe; r: right; SL: Superior lobe; v: ventral.

The tissue architecture and the cell diversity of the mature lung derives from simple primordia through complex developmental programs, which involve a coordinated interplay of the epithelium, the mesenchyme and the mesothelium [21-23]. At approximately E9.0, a region of the ventral foregut endoderm is specified as lung primordium which will later give rise to entire pulmonary epithelium. This precursor population is marked by the expression of *Nkx2.1* [24], which is induced by two ligands of the canonical WNT-signaling pathway (WNT2 and WNT2B) expressed in the adjacent mesenchyme [25]. In turn, BMP4-signaling from this ventral mesenchyme allows the ventral endoderm to commit to the respiratory lineage by the restriction *Sox2*, and thereby of the esophageal fate, to the dorsal endoderm [26-28] (Fig. 2A).

The initial budding of the lung epithelium critically depends on the expression of the signaling protein FGF10 in the ventral foregut mesoderm. FGF10 acts as a pro-proliferative factor and as chemoattractant, guiding the evagination of the epithelium into the surrounding mesenchyme at approximately E9.75 [29] (Fig. 2B). The initial outpouching immediately forms two separated buds, corresponding to the two primary bronchi. Recent studies in chicken suggest, that these buds originate from a paired primordium, rather than from a subdivision of a single bud [30]. Bud outgrowth is accompanied by the formation of the tracheoesophageal groove (Fig. 2B, arrowhead) which prefigures the separation of the trachea and the esophagus [30-32]. The vascular network develops simultaneously to the respiratory tree and emerges as soon as the initial buds have formed [33-35].

Starting from E9.5, lung development is subdivided into five stages: embryonic, pseudoglandular, canalicular, saccular and alveolar [36-38].

The embryonic and the pseudoglandular stages, which end at E12.5 and at E16.5 respectively, cover most of embryonic development. Both are mainly characterized by branching morphogenesis generating the lower respiratory tract [36-38]. At E12.5 the epithelium is subdivided into a proximal, SOX2⁺ stalk region and a distal, multipotent, highly proliferative region that expresses SOX9 [39-42]. At the distal tips iterative dichotomous branching events take place [43], guided by reciprocal inductive signals of the epithelium and the mesenchyme. Mesenchymal FGF10 expressed around the epithelial tips stimulates and directs the epithelial outgrowth (Fig. 2C(a)). It simultaneously induces *Shh* and *Bmp4* in the most distal epithelium of the tip which repress epithelial proliferation and negatively influence *Fgf10* expression in the mesenchyme (Fig. 2C(b)). This restricts FGF10 expres-

sion and proliferation to the lateral regions of the tip. Subsequently the epithelial growth is directed to the sides (Fig. 2C(c)), forming two new branching endpoints [29, 44-46] (Fig. 2C(d)).

In addition to morphogenesis, the differentiation of the majority of epithelial and mesenchymal cell types takes place in a proximal to distal gradient during the pseudoglandular stage [36-38].

From E16.5 to E17.5, the mouse lung passes through the canalicular stage which is marked by further branching, the refinement of the vascular network and the differentiation of alveolar cell types. The subsequent saccular stage extends until the postnatal day (P)5, followed by the alveolar stage which ends with the full maturation of the lung at P30. Both stages are characterized by maturation of the alveoli, increase of air spaces at the expense of mesenchymal tissue and optimization of the capillary network [36-38].

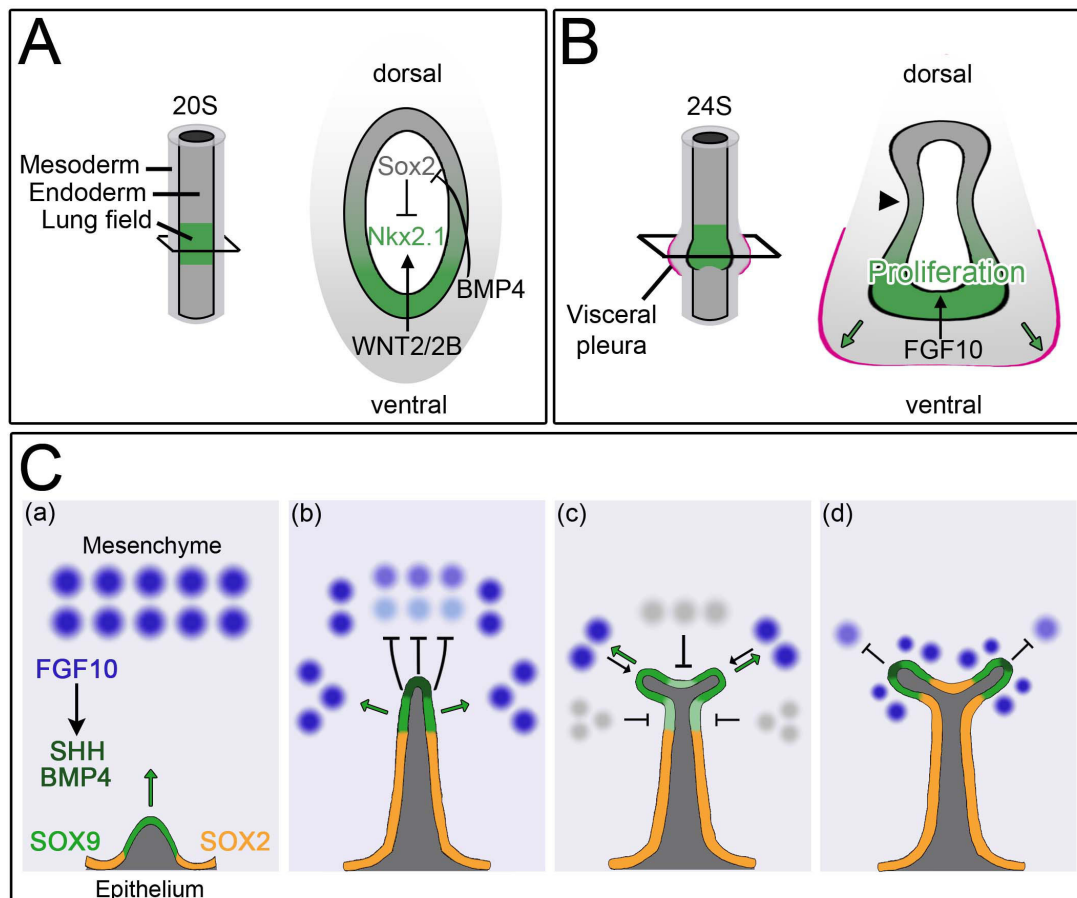


Figure 2: Molecular control of lung specification and branching morphogenesis.

(A) Specification of the lung field within the foregut endoderm. WNT2/2B signals from the mesenchyme induce *Nkx2.1* expression, in the epithelium, which marks the lung primordium. Simultaneously, BMP4 expressed in the ventral mesenchyme represses *Sox2* in the ventral epithelium, thereby restricting the esophageal fate to the dorsal region. (B) Initial budding of the specified endoderm into the surrounding mesenchyme. FGF10 expressed in the mesenchyme promotes the proliferation of the *NKX2.1*⁺ epithelium and additionally directs the ventral outgrowth. (C) Simplified illustration of epithelial bifurcation and its dependence on SHH, BMP4 and FGF10 signals. The epithelium is subdivided into proximal and distal regions marked by the expression of *SOX2* (yellow) and *SOX9* (green), respectively. The multipotent distal epithelium receives FGF10 from the mesenchyme which induces SHH and BMP4 in the epithelium and thereby drives proliferation and directs the pouching of the epithelium towards the FGF10 source. SHH and BMP4 in turn repress FGF10, leading to enhanced FGF10 expression flanking the distal tip, while the central epithelial regions no longer receive FGF10 signals. This results in the outgrowth of the epithelium to the sides and thereby to the bifurcation of the distal tip creating two new branching endpoints. Abbreviations: d: dorsal; S: Somites v: ventral; arrowhead: tracheoesophageal groove; pink arrows: indicates growth direction of the epithelium.

Mesodermal derivatives within the lung: a closer look on origin, precursor populations and differentiation

The complex morphogenesis and the emergence of all specialized cell types are achieved by precisely organized developmental programs depending on tightly regulated gene expression and reciprocal signals from the epithelium, the mesenchyme and the mesothelium. The development and differentiation of the pulmonary epithelium is well studied (for reviews see: [37, 47, 48]), while the knowledge about mesenchymal and mesothelial development lags behind.

In an attempt to systematically characterize mesenchymal cell types and subpopulations of adult lungs broad single-cell RNA-seqs were recently performed. According to their transcriptomic profile endothelial and mesothelial cells as well as different types of fibroblasts (lipofibroblasts, myofibroblasts and two types of matrix fibroblasts) and mesenchymal progenitors were characterized [49]. However, diversification of the pulmonary mesenchyme is still poorly understood. But some studies identified multipotent mesenchymal lineages [50-55]. This was further emphasized by lineage tracings of single mesenchymal cells, which demonstrated that single-potential lineages are rather uncommon in the lung [51], complicating the investigation of genetic control of mesenchymal differentiation. Analyses of different mouse mutants provided some insight into the molecular pathways regulating lineage commitment and differentiation of the major mesodermally derived cell types (mesothelium, bSMCs, vSMCs, cartilage and endothelium), whereas the genetic control of fibroblast differentiation is poorly understood.

The mesodermally derived visceral pleura emerges around E10.5 and grows rapidly to cover the lung [18]. A recent study suggested that the mesothelial lineage is specified and separated from the pulmonary mesenchyme early in development [51]. However, mesothelial cells can contribute, albeit to a limited degree [56], to different mesenchymal cell types, such as endothelial cells, SMCs and fibroblasts [57-59]. More importantly, the visceral pleura serves as an essential signaling center during development [18] which e.g. maintains a multipotent cell population of the mesenchyme or restricts cell differentiation to certain compartments [60-63]. The potential of mesothelial signals to affect the development of the entire mesenchymal compartment was demonstrated by mesothelial-specific loss-and gain-of-function mutant mice. Loss of *Smad4* and gain of SHH-signaling results in a mesenchymal thickening and a reduction of airspaces, while the gain of Notch-signaling

led to an emphysema-like phenotype [56], emphasizing the crosstalk of the mesothelium and the mesenchyme.

The pulmonary mesenchyme is derived from the splanchnic mesoderm and is subdivided into a submesothelial and a subepithelial compartment, which are molecularly distinguishable by the expression of *Wnt2a* and *Noggin*, respectively [63, 64].

FGF10 expressing cells, the descendants of which contribute to both types of SMCs and lipofibroblasts [55, 61, 65] represent the exclusive progenitor population of bSMCs. FGF10 is essential for bSMC lineage commitment [65] and induces *Shh* and *Bmp4* in the epithelium which in turn cause the downregulation of FGF10 in the precursors of the bSMCs. Simultaneously, SHH-signals activate *Foxf1* expression in the mesenchyme, which is suggested to activate WNT2 likewise in the mesenchyme [66]. WNT2 is required and sufficient to initiate the differentiation of bSMCs by inducing the expression of *Myocardin* (*Myocd*) and *Myocardin related transcription factor B* (*Mrtf-B*), two key factors of the myogenic transcriptional program [67, 68]. The specified bSMC progenitors passively relocate to the subepithelial mesenchyme surrounding the stalk epithelium [65] where they mature and express muscle associated genes such as ACTA2 [51, 67]. Mesothelial FGF9, together with mesenchymal β -catenin- and PDGF-signaling maintain the initial precursor population and prevent the differentiation of bSMCs in the submesothelial mesenchyme [61, 63, 69, 70]. Additionally, BMP4 negatively influences *Foxf1* in the distal tip mesenchyme and thereby possibly counteract SMC differentiation in that region [71].

In the upper airways, the reciprocal antagonism of SMCs and juxtaposed cartilaginous structures affect the cell number and the spatial expansion of both cell types [72]. Furthermore, preventing the differentiation of pulmonary SMCs by the inactivation of *Myocd* led to malformations of the cartilaginous structures of the trachea by disturbing the evenly spaced condensation of the future cartilage cells [73].

Cartilage precursors derive from mesenchymal progenitors, commit to the chondrocyte lineage, condense and differentiate to form the tracheal and bronchial cartilage [74, 75]. Cartilage development is mainly driven by WNT-, SHH- and possibly BMP-signals from the epithelium [76-78]. WNT-signaling is required for the condensation of the cartilage precursors and additionally maintains their proliferation [76, 79]. Chondrocyte differentiation is initiated by SHH inducing the expression of SOX9 in certain mesenchymal cells, which in turn activate *Col2a1* a cartilage-specific gene [78]. BMP-signaling acts pro-chondrogenic and is

suggested to stimulate tracheal cartilage formation and chondrocyte maturation [80]. Moreover, the deficiency or reduction of RA-signaling was shown to result in malformed cartilage rings, which was suggested to be the consequence of a reduced blood supply during cartilage formation [81, 82], emphasizing the importance of a functional vascular network not only for later gas exchange, but also for lung development.

The development of the capillary network starts at approximately E10.0 and occurs simultaneously through two mechanisms; angiogenesis, the sprouting of new vessels from pre-existing vessels, and vasculogenesis, the formation of endothelial cells from mesodermal precursors [33, 34, 83, 84]. Endothelial precursor populations are located in proximity to the epithelium and several studies showed a pivotal interaction of these two compartments for proper vasculogenesis [34, 85]. The formation of the first capillary-like structure, the vascular plexus is initiated by FGF-, SHH- and VEGF-signaling from the epithelium to the adjacent mesenchyme. Together these pathways are required and sufficient to induce vascular development [38, 85, 86]. Moreover, VEGFA-signals, conveyed by its receptors VEGFR1 and VEGFR2 expressed in the primitive endothelium, support endothelial proliferation and the formation of angioblasts [25, 84, 87-90]. Endothelial cells are surrounded by a layer of SMCs and connective tissue whose radial patterning is established by a PDGFB-signaling gradient emanating from the endothelium [91]. Vascular SMCs are derived from the mesenchyme around newly generated vessels [91]. It was shown that signals from endothelial cells induce the accumulation of vSMC progenitors [35, 83, 92] which subsequently proliferate and then migrate to enclose the vessel [93, 94]. Analyzing a *Wnt7b*^{LacZ} mutant suggested *Wnt7b* as the major player of canonical WNT-signaling involved in vSMC development, but contradictory results were observed analyzing different *Wnt7b* mutant alleles, questioning its necessity [95]. However, several studies identified β -catenin signaling, together with downstream PDGF-signaling as crucial signals to expand vSMC progenitors and promote their migration [70, 96-98], emphasizing the role of the WNT-signaling pathway.

Thus an orchestrated interplay not only of tissue compartments but also of cell types is essential for proper mesenchymal morphogenesis and differentiation.

From DNA to protein: regulation of gene expression

The generation of complex organs and their multitude of specialized cell types from simple progenitor cell populations is a hallmark of metazoan development [1]. Undifferentiated, homogeneous precursor cells, which contain the same genetic information, have to establish differential gene expression to acquire cell type-specific characteristics. The extensive morphogenesis and cellular diversity occurring during organogenesis are consequences of well-conserved developmental programs driven by precisely controlled patterns of gene expression [2].

Gene expression starts with the transcription of a certain region of genomic DNA (gDNA) by RNA polymerase multiprotein complexes into precursor messenger RNA (pre-mRNA), which is further processed to mature mRNA.

Genomic DNA is present as chromatin, meaning associated with histones and other proteins. Chromatin structure, thus its configuration and the localization of the nucleosomes determines the accessibility of the chromatin for transcription [99].

Chromatin remodeling, meaning ATP dependent nucleosome removal, relocalization by sliding along the DNA and restructuring, is executed by special multiprotein complexes which establish specific nucleosome patterns [100, 101]. These chromatin remodeling complexes are divided - according to their properties and subunits - into four distinct families: the switch/sucrose non-fermenting SWI/SNF (also known as Brg/Brm Associated Factor (BAF)) -family, the chromodomain helicase DNA-binding (CHD) family, the imitation switch (ISWI/SNF2L) family, and INO80 family [100-102].

Chromatin remodeling complexes get recruited to specific target sites in the genome by different modifications of histones, specific DNA features and DNA binding proteins [103, 104], which themselves additionally influence the chromatin structure and chromatin associated proteins [105].

Histone modifications often occur at the N-terminal tails of the histones and include among others methylation of arginine (R) residues as well as methylation and acetylation of lysines (K). These covalent modifications are exerted by specialized enzymes, such as histone acetyltransferases (HATs), histone deacetylases (HDACs), histone demethylases (HDMs) and histone methylases (HMTs).

To allow transcription, the chromatin has to be in an open or "relaxed" state [106]. Hyperacetylation of histones is generally associated with active transcription of a gene, since

acetylation of lysine residues can weaken the binding between the histone and the DNA [107] (Fig. 3A).

In contrast, methylations are associated with gene activation and repression. Here, the exact site and the state of the methylation (mono-, di- and trimethylation) defines the transcriptional outcome [99]. Methylation of histone 3 (H3) at lysine 4 (H3K4), lysine 36 and lysine 79 has been implicated in transcriptional activation, whereas methylations of H3K9, H3K20, and H3K27 serve as repressing marks [108, 109]. Trimethylation of H3K9 (H3K9me3) a repressive histone mark associated with heterochromatin formation is recognized by heterochromatin associated proteins such as HP1 [110-112]. HP1 in turn is able to recruit DNA methyltransferases (DNMTs) [107, 113, 114] which establish DNA modifications associated with transcriptional regulation. Cytosine methylation in the promoter or enhancer region of a gene is the most commonly observed DNA modification which was shown to drive the establishment heterochromatin [115, 116]. Thus, methylated DNA and histones, together with deacetylated histones and binding of heterochromatin proteins result in condensed chromatin, which is transcriptionally inactive [99, 112, 117] (Fig. 3A).

To achieve specificity, chromatin remodeling complexes but also histone modifying enzymes are often recruited to enhancers/silencers and promoters by sequence-specific DNA binding proteins primarily transcription factors (reviewed in: [99, 101, 102]).

Tissue-specific transcription factors (TFs) mediate the spatial and temporal specificity of gene transcription. TFs bind specific DNA sequences within regulatory elements and thereby influence the transcription frequency of the associated transcriptional unit. These regulatory elements can be represented by sites in the promoter region of a gene as well as by enhancers/silencers, located upto thousands of base pairs (bp) away from the transcription start sites [118-120] (Fig. 3B). The DNA sequences which are recognized by TFs are characteristic for all members of a TF family, and are mostly rather short. Therefore, specificity is often achieved by the occurrence of multiple DNA binding sites that are bound by different TFs in concert.

Transcription factors are classified into activators and repressors, which increase or decrease the amount of mRNA transcripts of a gene, respectively. In the case of repressing TFs the transcriptional regulation is achieved by different mechanisms. Transcriptional repressors can bind regulatory elements competitively to an activator, mask the activating site of an enhancing TF or interact with the transcription machinery either directly or via

additional TFs or protein interaction partners [118-120]. As mentioned above, transcription factors can also recruit chromatin remodeling complexes as well as DNA and histone modifying enzymes to modulate DNA accessibility [101, 117, 121-126].

Gene expression is not only controlled on the level of transcription but also at many subsequent steps of mRNA maturation, transport, stability and translation. Eukaryotic pre-mRNA consists of non-coding introns and protein coding exons. During pre-mRNA maturation, the introns are removed by a multiprotein complex, the spliceosome. Thus, alternative splicing of the same pre-mRNA can produce different proteins with different properties and functions. Furthermore, gene expression is influenced by mRNA stability which is determined by different degradation signals [118-120].

After maturation, the mRNA gets translated into a protein by ribosomes. During this step, different modifications such as the attachment of e.g. phosphates or lipids or even the enzymatic cleavage can alter protein appearance and stability and thereby influence gene expression products, levels or duration.

Thus, gene expression is a multi-faceted process which is regulated at various levels. Orchestrating the expression of a multitude of genes allows the establishment of specified tissues and organs during embryonic development whereby transcription factors play a central role in the regulation of gene expression.

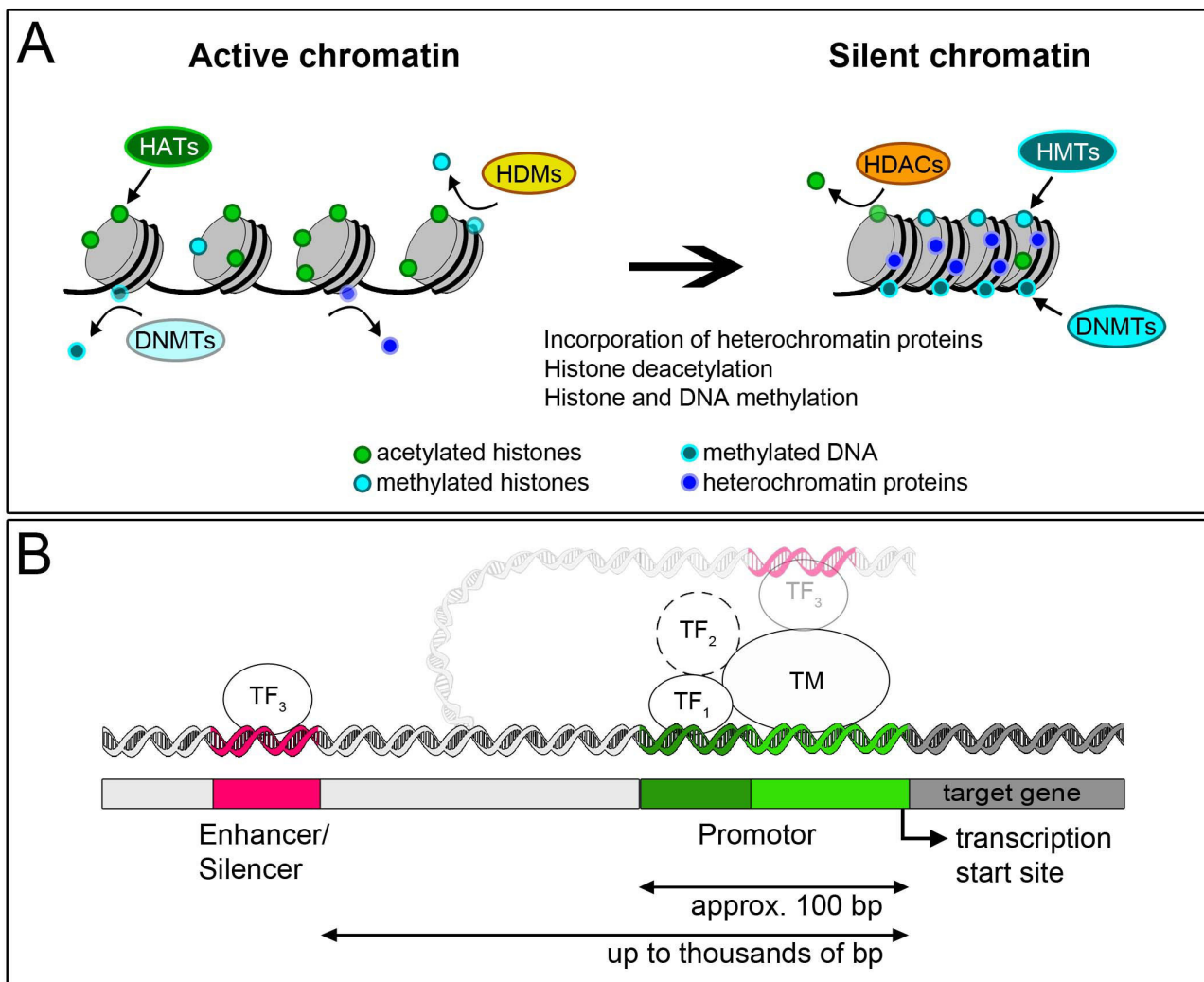


Figure 3: Mechanisms of transcriptional control and chromatin remodeling.

(A) Simplified scheme of epigenetic chromatin silencing. Active chromatin is highly demethylated, contains hyperacetylated histones and is free from heterochromatin proteins. Silencing of the chromatin occurs through deacetylation of histones by HDACs and the methylation of both, histones and DNA by (de-)methylases and methyltransferases. Additionally, heterochromatin proteins get incorporated. (B) Scheme illustrating the general events of transcription. Tissue-specific transcription factors (TF_1 , TF_3) bind to distal regulatory elements (enhancer/silencer)(pink) and (rarely) to proximal regulatory elements in the promoter region (dark green) to recruit the transcription machinery to its specific site at the promoter (light green) in front of the transcription start site of a target gene (dark gray). Moreover, transcription initiation is possibly influenced by the additional interaction with transcriptional co-factors (TF_2). Abbreviations: DNMTs: DNA methyltransferases; HATs: Histone acetyltransferases; HDACs: Histone deacetylases; HDMs: Histone demethylases; HMTs: Histone methylases; TF: Transcription factor; TM: Transcription machinery.

T-box transcription factors: Transcription regulation and their role in development and disease

T-box (*Tbx*) genes encode an evolutionary highly conserved family of transcription factors [127], which is characterized by a conserved DNA binding region of 174-186 amino acids [128], the T-box. In vitro binding site selection experiments identified the sequence 5'-AG-GTGTGA-3' as optimal binding site [129]. This binding site, also referred to as T-box binding element (TBE), is a half site and T-box proteins may bind to one TBE as a monomer or to direct or inverted repeats as dimers [130, 131]. Additionally to interacting with each other, T-box proteins can heterodimerize with transcription factors of other families including homeobox and GATA zinc-finger proteins to regulate target gene transcription [12, 125, 132-136]. Moreover, TBX proteins also interact with proteins that affect the state of the chromatin such as the NuRD or the BAF complex [12, 121, 124, 125, 137].

Specificity of DNA binding is mediated by the T-box, while transcription regulating properties reside outside the T-box [12, 138, 139]. Functionally, T-box transcription factors can be subdivided in activators and repressors [12, 138]; some proteins may act context-dependently either as activator or repressor [12, 132, 138, 140, 141].

In mice, 17 T-box genes have been identified to date, and were grouped into 5 subfamilies (T, *Tbx1*, *Tbx2*, *Tbx6*, *Tbr1*) according to sequence similarity [12, 138]. Divergence of T-box genes is suggested to emerge evolutionarily by (tandem) gene duplication which was best described for the *Tbx2*-subfamily. Its four members, *Tbx2-Tbx5*, emerged from one ancestral locus and duplicated first into *Tbx2/3* and *Tbx4/5* genes which further diversified by an additional duplication event into 4 different genes [127, 142]. As a consequence of the high sequence similarity of e.g. TBX2 and TBX3 these two proteins act redundantly in some contexts, but also have distinct functions [8, 143, 144].

T-box genes are expressed in a multitude of organs and tissues [6, 12] and genetic studies in mice showed that T-box genes are involved in the development of multiple organs and body parts including the heart, the liver, the urogenital system, the limbs and craniofacial structures. Here, they control cell fate decisions, differentiation, patterning and proliferation in both mesenchymal and epithelial tissue primordia and several mutations of T-box genes result in serious defects [12-15, 145, 146].

Mutations of T-box genes also underlie congenital syndromes in humans [147]. For example, mutations of TBX1 results in DiGeorge syndrome, which comprises craniofacial, vas-

cular and heart anomalies [148]. Haploinsufficiency of TBX3 leads to the Ulnar-mammary syndrome. Humans affected by this syndrome suffer among other things, from limb defects, mammary and apocrine gland hypoplasia and dental abnormalities [149]. Heart and skeletal anomalies of the forelimbs are symptoms of Holt-Oram syndrome, which is caused by a mutation of TBX5 [150]. Recent studies showed that the members of the TBX2-subfamily are downregulated in the pulmonary mesenchyme of a nitrofen-induced model of congenital diaphragmatic hernia [151]. Newborns suffering from congenital diaphragmatic hernia display a defective closure of the diaphragm combined with severe hypoplasia of the lung [152]. Moreover, numerous studies demonstrated that the overexpression of TBX2 and TBX3 is associated tumor development in humans [11, 138, 143, 153]. Together this provides strong evidence for the importance of T-box transcription factors for embryonic development and tissue homeostasis in mammals.

T-box transcription factors in murine lung development

Five members of the T-box transcription factor family, namely *Tbx1-5*, are expressed in the embryonic mouse lung [6].

Tbx1 is expressed in the pulmonary epithelium throughout development [6]. The somatic deletion of *Tbx1* leads to a failure of lung inflation at birth [148], but an explicit analysis of *Tbx1* function during lung development has not yet been performed.

In contrast, the members of the TBX2-subfamily (*Tbx2-5*) are expressed in the embryonic lung mesenchyme and the consequences of their loss were analyzed in several studies.

TBX4 and TBX5 act as activators of target gene transcription in the lung mesenchyme [9, 154]. Deletion of *Tbx5* in the entire embryo leads to an unilateral loss of lung bud specification and defective tracheal specification, while mice deficient for *Tbx4* combined with a heterozygote loss of *Tbx5* die shortly after birth due to respiratory distress [9]. Lung-specific deletion of *Tbx4* and/or *Tbx5* results in dose-dependent defects of branching morphogenesis, cartilage formation and expansion of tracheal SMCs [9, 154]. Branching morphogenesis is regulated by the direct activation of *Fgf10*, while the impact of TBX4 and TBX5 on cartilage formation is not yet completely unveiled [9, 154].

TBX2 and TBX3 are transcriptional repressors and were described to act at least partly redundant in the lung mesenchyme [8]. Constitutive expression of TBX2 into adulthood leads to pulmonary hyperplasia including a thickening of the mesenchyme, but mainly unaffected

branching morphogenesis. The loss of *Tbx2* results in hypoplasia and reduced branching of the lung, due to a decrease in proliferation of the mesenchyme [7]. Additionally, a reduced presence of S100A4 expressing interstitial fibroblasts and an increased deposition of extracellular matrix were observed [7]. Indirectly, the loss of *Tbx2* marginally affects also the proliferation of the distal epithelium and the composition of epithelial cell types.

Molecular analyses revealed that TBX2 and TBX3 affect epithelial branching by supporting the proliferation of the mesenchyme by at least two independent mechanisms: the direct repression of the cell cycle inhibitors *Cdkn1a* and *Cdkn1b* [7] and mediation of the pro-proliferative function of the WNT-signaling pathway by direct repression of its antagonists *Frzb* and *Shisa3* [8]. Furthermore, the alterations of mesenchymal composition indicate a role of TBX2 in mesenchymal differentiation.

Thus, several T-box transcription factors are crucial regulators of embryonic lung specification, growth, morphogenesis and mesenchymal cell differentiation. However, the characterization of the cellular and molecular functions of these factors during lung development is not yet complete.

Aims of the study

TBX2, a member of the evolutionary conserved family of T-box DNA-binding proteins, regulates as a transcriptional repressor different cellular programs in the development of numerous organs during mammalian embryogenesis (for review see: [11, 12]).

During murine lung development, TBX2 is expressed in the mesenchyme [6], where it is required for branching morphogenesis and growth of the embryonic lung [7, 8]. Transcriptional analysis and ChIP-seq data identified direct target genes which revealed a crucial function of TBX2 in mesenchymal proliferation. From this, Lütke *et al.* hypothesized that TBX2 maintains the precursor state of lung mesenchymal cells by preserving their ability to proliferate. However, both mesenchymal loss- and gain-of-*Tbx2*, led to mesenchymal and epithelial differentiation defects [7], suggesting that TBX2 also regulates additional cellular programs such as patterning, cell fate decisions and differentiation, as it does in other organ systems [13-16]. Moreover, the molecular mechanisms by which TBX2 achieves target gene specificity and exerts its repressive function in the pulmonary mesenchyme have not yet been examined.

This study aims to provide new insight into the molecular mechanisms of TBX2 function in the pulmonary mesenchyme.

To identify cell types possibly depending on TBX2 function in the developing lung a detailed temporal and spatial expression analyses of TBX2 as well as a lineage tracing analyses of TBX2⁺ cells in the mesenchyme and the mesothelium shall be performed and evaluated in a qualitative and quantitative manner. To address whether TBX2 expression critically affects the differentiation and/or lineage diversification, cell fate analyses will be performed in *Tbx2*-deficient and constitutively overexpressing mutant lungs.

To uncover as yet undescribed cellular and molecular functions of TBX2, existing transcriptional and genomic data sets shall be used to obtain a list of additional direct target genes of TBX2 in the developing pulmonary mesenchyme. The expression and spatial distribution of genes upregulated upon *Tbx2* loss, shall be verified by *in situ* hybridization on E14.5 lung sections. Candidate target genes shall be manually analyzed for the presence of ChIP peaks and TBX2 DNA binding sites located in the peak regions. Subsequently, the binding of TBX2 will be validated by individual ChIP-PCRs of the corresponding DNA fragment.

To characterize the molecular mechanisms by which TBX2 represses its target genes, an unbiased proteomics approach from E14.5 wild-type lung tissue shall be performed to identify TBX2 interaction partners that might serve as cofactors in DNA binding site recognition and transcriptional repression. Subsequently, the interaction of the candidates and TBX2 shall be validated by co-immunoprecipitation assays in HEK293 cells.

Altogether, this study shall further characterize the cellular and molecular mechanisms by which TBX2 regulates murine lung development.

TBX2-positive cells represent a multi-potent mesenchymal progenitor pool in the developing lung

Irina Wojahn¹, Timo H. Lüdtke¹, Vincent M. Christoffels², Mark-Oliver Trowe¹ and Andreas Kispert¹

¹Institut für Molekularbiologie, Medizinische Hochschule Hannover, Hannover, Germany

²Department of Anatomy, Embryology and Physiology, Academic Medical Center, University of Amsterdam, Amsterdam, The Netherlands

Corresponding Author: Andreas Kispert, Medizinische Hochschule Hannover, Institute for Molecular Biology, OE5250, Carl-Neuberg-Str. 1, D-30625 Hannover, Germany. Tel. +49 511 532 4017; Fax: +49 511 5324283; E-mail: kispert.andreas@mh-hannover.de

Type of authorship: First author
Type of article: Research article
Share of the work: 80%
Journal: Respiratory Research
Impact factor: 4.065
Number of citations: 1
Date of publication: 23.12.2019
DOI: 10.1186/s12931-019-1264-y

Rights and permissions

Open Access: This article is distributed under the terms of the Creative Commons Attribution 4.0 International License (<http://creativecommons.org/licenses/by/4.0/>), which permits unrestricted use, distribution, and reproduction in any medium, provided you give appropriate credit to the original author(s) and the source, provide a link to the Creative Commons license, and indicate if changes were made. The Creative Commons Public Domain Dedication waiver (<http://creativecommons.org/publicdomain/zero/1.0/>) applies to the data made available in this article, unless otherwise stated.

RESEARCH

Open Access

TBX2-positive cells represent a multi-potent mesenchymal progenitor pool in the developing lung



Irina Wojahn¹, Timo H. Lüdtke¹, Vincent M. Christoffels², Mark-Oliver Trowe¹ and Andreas Kispert^{1*}

Abstract

Background: In the embryonic mammalian lung, mesenchymal cells act both as a signaling center for epithelial proliferation, differentiation and morphogenesis as well as a source for a multitude of differentiated cell types that support the structure of the developing and mature organ. Whether the embryonic pulmonary mesenchyme is a homogenous precursor pool and how it diversifies into different cell lineages is poorly understood. We have previously shown that the T-box transcription factor gene *Tbx2* is expressed in the pulmonary mesenchyme of the developing murine lung and is required therein to maintain branching morphogenesis.

Methods: We determined *Tbx2*/TBX2 expression in the developing murine lung by in situ hybridization and immunofluorescence analyses. We used a genetic lineage tracing approach with a *Cre* line under the control of endogenous *Tbx2* control elements (*Tbx2*^{Cre}), and the *R26*^{mTmG} reporter line to trace TBX2-positive cells in the murine lung. We determined the fate of the TBX2 lineage by co-immunofluorescence analysis of the GFP reporter and differentiation markers in normal murine lungs and in lungs lacking or overexpressing TBX2 in the pulmonary mesenchyme.

Results: We show that TBX2 is strongly expressed in mesenchymal progenitors in the developing murine lung. In differentiated smooth muscle cells and in fibroblasts, expression of TBX2 is still widespread but strongly reduced. In mesothelial and endothelial cells expression is more variable and scattered. All fetal smooth muscle cells, endothelial cells and fibroblasts derive from TBX2⁺ progenitors, whereas half of the mesothelial cells have a different descent. The fate of TBX2-expressing cells is not changed in *Tbx2*-deficient and in TBX2-constitutively overexpressing mice but the distribution and abundance of endothelial and smooth muscle cells is changed in the overexpression condition.

Conclusion: The fate of pulmonary mesenchymal progenitors is largely independent of TBX2. Nevertheless, a successive and precisely timed downregulation of TBX2 is necessary to allow proper differentiation and functionality of bronchial smooth muscle cells and to limit endothelial differentiation. Our work suggests expression of TBX2 in an early pulmonary mesenchymal progenitor and supports a role of TBX2 in maintaining the precursor state of these cells.

Keywords: *Tbx2*, Lineage tracing, Pulmonary mesenchyme, Smooth muscle cells, Lung development

Background

The primary function of the lung, the exchange of oxygen in the air with carbon dioxide in the vascular system, is supported by a multitude of differentiated cell types in a highly organized tissue architecture. Predominant are epithelial cells that line both the conducting airways of the trachea and the bronchial tree as well as the distal gas-exchange

units, the alveoli. According to their position, epithelial cells are diversified to support the exclusion of solid particles and fight microorganisms on the one hand, and to allow intimate association and gas exchange with the highly elaborated vascular system on the other hand [1, 2]. Mesenchymal cells line the respiratory epithelium and are similarly specialized along the proximal to distal axis of the lung. From the trachea down to the bronchi they form cartilaginous rings and smooth muscle cells (SMCs) in an alternating fashion to stabilize the airways. In the bronchial tree SMCs are highly abundant, while only a sparse population of

* Correspondence: kispert.andreas@mh-hannover.de

¹Institut für Molekularbiologie, Medizinische Hochschule Hannover, Hannover, Germany

Full list of author information is available at the end of the article



© The Author(s). 2019 **Open Access** This article is distributed under the terms of the Creative Commons Attribution 4.0 International License (<http://creativecommons.org/licenses/by/4.0/>), which permits unrestricted use, distribution, and reproduction in any medium, provided you give appropriate credit to the original author(s) and the source, provide a link to the Creative Commons license, and indicate if changes were made. The Creative Commons Public Domain Dedication waiver (<http://creativecommons.org/publicdomain/zero/1.0/>) applies to the data made available in this article, unless otherwise stated.

fibroblasts resides in the alveolar interstitium. In the entire organ, mesenchymal cells associate as pericytes and SMCs with the endothelial network [3]. Finally, a layer of mesothelium, the visceral pleura, covers the outside of the organ possibly to synthesize lubricating factors and help in defense of pathogens [4].

Mesenchymal cells provide structural support to the respiratory epithelium and the vessels under homeostatic conditions but also play an indispensable instructive role at all steps of pulmonary epithelial development in embryogenesis (for reviews see [5, 6]). At the onset of lung development, in the mouse around embryonic day (E)9.0, mesenchyme surrounding the ventral anterior foregut endoderm acts as a critical source of signals that specifies the pulmonary epithelium [7] and induces its evagination and division into the first two lung buds. Throughout the extended pseudoglandular stage, which in the mouse ends around E16.5, mesenchymal signals direct the elongation and branching of the lung buds into the bronchial tree [8, 9], and account for their correct proximal-distal patterning and differentiation [10]. Finally, the mesenchyme is important for septation of the distal air-sacs, the alveoli, in the canalicular and sacular phases from E16.5 onwards [11, 12].

During this developmental time-line mesenchymal progenitors residing at the distal lung buds differentiate in a temporally and spatially specific manner into a multitude of cell types starting proximally with airway and vascular SMCs, pericytes, and airway cartilage cells, and ending with distal alveolar lipo- and myofibroblasts [3]. Mesenchymal and epithelial development is also supported by the embryonic mesothelium which forms shortly after specification of the lung bud. The mesothelium provides crucial signals to maintain mesenchymal proliferation and may act as a minor cell source for the pulmonary mesenchyme [13–15] (for recent reviews on lung development and structure see [16, 17]).

Despite its important developmental function, our knowledge of mesenchymal (and mesothelial) differentiation clearly lags behind that of the epithelium. We have recently characterized TBX2, a member of the T-box family of transcription factors, as a crucial mesenchymal factor for embryonic lung development. Expression of *Tbx2* occurs in the pulmonary mesenchyme from E9.5 to at least E18.5. Loss of *Tbx2* function leads to reduced mesenchymal proliferation, but also affects in a non cell-autonomous fashion proliferation of the distal epithelium and branching morphogenesis resulting in lung hypoplasia from E14.5 onwards. Epithelial patterning is not affected upon loss of *Tbx2* in the mesenchyme, but the number of alveolar epithelial cells type I is mildly reduced at E18.5. Constitutive TBX2 expression in mature lungs results in mesenchymal hyperproliferation, but does not affect branching morphogenesis or epithelial

differentiation [18]. Molecular analysis showed that TBX2 maintains mesenchymal proliferation by repressing *Cdkn1a* (p21) and *Cdkn1b* (p27), two members of the Cip/Kip family of cell cycle inhibitor genes [18], and independently, by maintaining pro-proliferative WNT signaling through repression of WNT antagonist genes *Frzb* and *Shisa3* [19].

Here, we further characterize the pool of TBX2 positive cells in the developing lung, and determine its contribution to differentiated mesenchymal cell types in normal development but also under conditions of mesenchymal loss and gain of *Tbx2*. We provide evidence that TBX2 not only marks a multipotent precursor population in the pulmonary mesenchyme and maintains its undifferentiated state, but is also essential for proper SMC functionality.

Materials and methods

Mouse strains and genotyping

Tbx2^{tm1.1(cre)Vmc} (synonym: *Tbx2*^{cre}) [20], *Tbx2*^{tm2.2Vmc} (synonym: *Tbx2*^{fl}) [21], *Gt* (ROSA)26^{Sortm4(ACTB-tdTomato-EGFP)Luo/J} (synonym: *R26*^{mTmG}) [22] and *Hprt*^{tm2(CAG-TBX2-EGFP)Akis} (synonym: *Hprt*^{TBX2}) [23] mice were maintained on an NMRI outbred background. Embryos for phenotype analysis were derived from matings of *Tbx2*^{cre/+} males with *Tbx2*^{fl/fl}; *R26*^{mTmG/mTmG}, *Hprt*^{TBX2/TBX2} or *R26*^{mTmG/mTmG} females. For timed pregnancies, vaginal plugs were checked on the morning after mating and noon was taken as embryonic day (E) 0.5. Pregnant females were sacrificed by cervical dislocation. Embryos were isolated in PBS, decapitated, rinsed and fixed in 4% paraformaldehyde (PFA)/PBS overnight and stored in 100% methanol at –20 °C until use. Genotypes of embryos were assigned by epifluorescence analysis of GFP expression from the reporter allele or from the *Hprt* allele.

All animal work conducted for this study was performed according to European and German legislation. The breeding, handling and sacrifice of mice for embryo isolation was approved by the Niedersächsisches Landesamt für Verbraucherschutz und Lebensmittelsicherheit (Permit Number: AZ33.12–42,502–04-13/1356).

Organ culture

Lung rudiments of E12.5 embryos were explanted on 0.4 µm polyester membrane Transwell supports (#3450, Corning Inc., Lowell, MA, USA) and cultivated at the air-liquid interface for 36 h, 6 days or 8 days at 37 °C and 5% CO₂ in RPMI medium (#61870044, ThermoFisher Scientific, Waltham, MA, USA) supplemented with 10% FCS (#S0115, Biochrom, Berlin, Germany), 100 units/ml Penicillin/100 µg/ml Streptomycin (#15140 122, ThermoFisher Scientific).

To record contractility in cultures, videos of 2 min length were taken 12 h, 18 h, 24 h and 36 h after explantation. Only lungs of comparable developmental stage as

judged by the number of branching endpoints were included in this assay. Contraction intensity was measured by computational Fiji Multi-Kymograph analysis (www.imagej.net) [24]. To compare these intensities over a full contraction wave, we determined the area below the intensity curves. Results of both were statistically evaluated by two-tailed Student's t-test and considered significant ($P < 0.05$), highly significant ($P < 0.01$), or extremely significant ($P < 0.001$).

Immunofluorescence

Detection of antigens was performed on 5 μ m paraffin sections. Endogenous peroxidases were blocked by incubation in 6% H₂O₂ for 20 min. For antigen retrieval either 0.05% Triton X-100 (PDGFRA/B) or citrate-based heat unmasking (all others) was employed. The following primary antibodies were used: anti-ALDH1A2 (1:200; #ab96060, Abcam plc, Cambridge, UK), anti-CDH1 (1:500; a kind gift of Rolf Kemler, MPI Freiburg), anti-EMCN (1:2; a kind gift of Prof. Dietmar Vestweber, MPI M \ddot{u} nster), mouse-anti-GFP (1:50, 1:200; #11814460001, Roche, Basel, Switzerland), rabbit-anti-GFP (1:100; #ab290, Abcam), anti-KDR (1:50, 1:200; #BAF644, R&D Systems, Minneapolis, MN, USA), anti-PDGFRA (1:200; #AF1062-SP, R&D Systems), anti-PDGFRB (1:200; #AF1042-SP, R&D Systems), anti-POSTN (1:200; #ab14041, Abcam), anti-S100A4 (1:200; #ab27957-250, Abcam), anti-ACTA2 (1:200; #A5228, Sigma-Aldrich, St. Louis, MO, USA), anti-TAGLN (1:400; #ab14106-100, Abcam), anti-TBX2 (1:200, 1:2000; #07-318, Merck Millipore, Darmstadt, Germany), anti-TBX2 (1:200; #sc-514,291 X, Santa Cruz Biotechnology, Inc., Dallas, TX, USA), anti-TBX3 (1:50; #sc-31,656, Santa Cruz), anti-WT1 (1:500; #CA1026, Calbiochem, San Diego, CA, USA). Primary antibodies were detected by directly labeled fluorescence- or biotin-conjugated secondary antibodies (1:200; Invitrogen, Carlsbad, CA, USA; Dianova, Hamburg, Germany; Jackson ImmunoResearch, Cambridgeshire, UK). Signal amplification was performed with the Tyramide Signal Amplification (TSA) system (NEL702001KT, PerkinElmer, Waltham, MA, USA) according to the manufacturer's instruction. Nuclei were stained with 4',6-diamidino-2-phenylindole (DAPI, # 6335.1, Carl Roth, Karlsruhe, Germany). To exclude unspecific binding of secondary or tertiary antibodies, we performed as a control immunofluorescence stainings without primary antibody and if required without primary and secondary antibodies (Additional file 1: Figure S1).

Quantification of immunofluorescence staining

We used Fiji freeware (www.imagej.net) to quantify the relative expression of TBX2 and of the lineage reporter GFP at different developmental time-points in the entire lung mesenchyme (10.5, E12.5), in the mesenchyme of the right lung lobe (E14.5, E16.5) and in regions of specific cell types (E14.5) in a semi-quantitative manner.

The mesenchymal compartment was defined by DAPI-signal based histology, whereas cell-type specific areas were defined by marker gene expression. The specific immunofluorescence signals of each single color-channel picture were converted into black pixels, while signal negative areas of the picture were displayed in white. The area of black pixels was measured. The relative area of DAPI or of a specific marker was set to 100%. Within this area, the proportion representing TBX2 or GFP expression was calculated as the ratio of TBX2 (or GFP) area to DAPI (or marker) area and expressed in %. Measurements were performed for at least three individuals (exception: $n = 2$ for TBX2 expression in PDGFRA⁺ and PDGFRB⁺ cells) and data were expressed as means \pm SD. Differences in GFP expression of control and *Tbx2*-deficient mice were compared and considered significant with * $p \leq 0.05$, ** $p \leq 0.01$, *** $p \leq 0.005$, using two-tailed Student's t-test. The complete data set is provided in Additional file 2: Table S1.

RNA in situ hybridization analysis

In situ hybridization were performed on 5- μ m or 10- μ m paraffin sections as described [25]. For each marker, at least three independent specimens were analyzed.

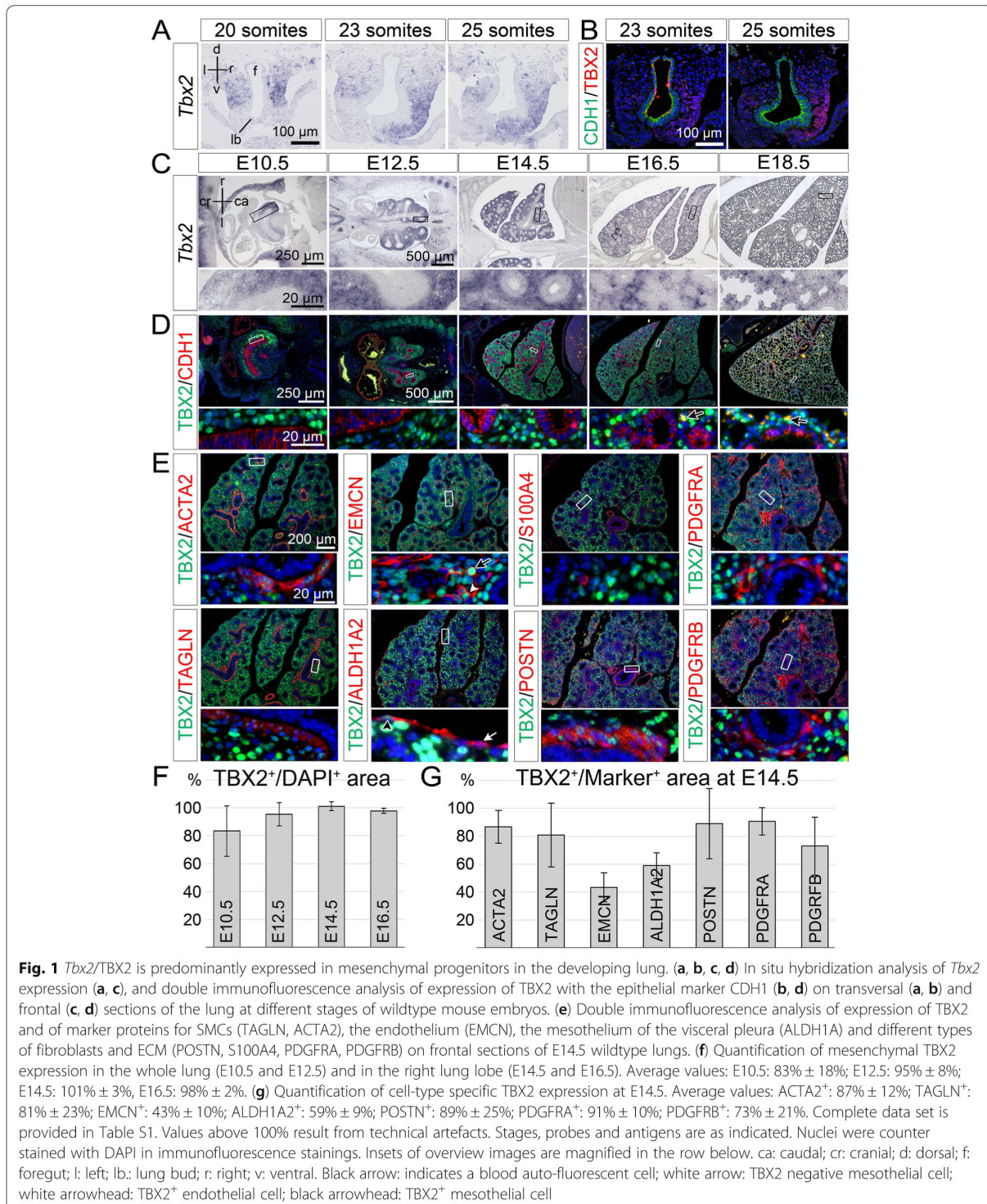
Documentation

Overviews of sectioned lungs were documented either with a DM5000 or DM6000 microscope (Leica Camera, Wetzlar, Germany) equipped with a Leica DFC300FX or Leica DFC350FX digital camera, respectively. For higher magnifications confocal microscopy was performed using a Leica DM IRB with a TCS SP2 AOBs scan head. Organ cultures were photographed with the DM6000 microscope, a Leica M420 microscope with a Fujix digital camera HC-300Z (Fujifilm Holdings, Minato/Tokyo, Japan) or a Leica MZFLIII with a Leica DFC420C digital camera. Images were processed and analyzed in Adobe Photoshop CS5 (Adobe, San Jose, CA, USA).

Results

TBX2 is expressed in a variety of cells excluding the airway epithelium during lung development

To define the spatial and temporal expression of *Tbx2* mRNA and TBX2 protein during murine lung development in greater detail as previously reported [18], we performed in situ hybridization and (co-)immunofluorescence analysis on lung sections of different developmental stages (Fig. 1). At E9.0 to E9.5, we visualized the lung bud as a *Nkx2.1*⁺ epithelium ventral to the foregut (Additional file 1: Figure S2). In embryos with 20 somites, *Tbx2* mRNA was restricted to the lateral foregut mesenchyme. At the 23-somite stage, both *Tbx2* mRNA and TBX2 protein expression expanded into the mesenchyme on the right side of the lung bud (Fig. 1A and B). At the 25-somite stage, *Tbx2*/TBX2 expression was increased in this



region (Fig. 1a and b, Additional file 1: Figure S2A). From E10.5 to E16.5, *Tbx2* mRNA was robustly detected in the entire pulmonary mesenchyme, i.e. both in the undifferentiated mesenchyme surrounding the distal tip regions and

more weakly in proximal regions where differentiated cell types reside. At E18.5, *Tbx2* expression was strongly decreased. The epithelium lacked *Tbx2* expression at all stages (Fig. 1a and c).

Double immunofluorescence analysis with the epithelial marker cadherin 1 (CDH1) confirmed complete absence of TBX2 protein from the airway epithelium. In the pulmonary mesenchyme, TBX2 expression was strongest in cells surrounding the distal epithelial lung buds. There as well as in more proximal regions some cells lacked TBX2 or expressed low levels only (Fig. 1d). To investigate whether this variable expression reflects a cell-type specific restriction, we performed double immunofluorescence stainings of TBX2 and markers of various differentiated cell-types that reside outside the airway epithelium (Fig. 1e). We performed this analysis at E14.5 when these cell-types are established and easy to visualize. TBX2 expression was found at low levels in actin, alpha 2, smooth muscle, aorta positive (ACTA2⁺) and transgelin positive (TAGLN⁺) bronchial SMCs and in some scattered endomucin positive (EMCN⁺) endothelial cells. Similarly, the mesothelial lining of the visceral pleura, which is marked by aldehyde dehydrogenase family 1, subfamily A2 (ALDH1A2) expression [26], contained TBX2⁺ cells. Fibroblasts constitute a heterogeneous, poorly characterized mesenchymal cell type in the lung. Some interstitial fibroblasts are marked by the expression of the S100 calcium binding protein A4 (S100A4) [27–29]. We did not find expression of this marker in TBX2⁺ cells. However, weak TBX2 expression was found in association with cells expressing periostin (POSTN), an extracellular matrix protein produced by fibroblasts surrounding the main bronchi at this stage [30], in cells expressing platelet derived growth factor receptor, alpha polypeptide (PDGFRA), a marker for (myo-)fibroblasts and SMC precursors [11, 12] and in cells positive for platelet derived growth factor receptor, beta polypeptide (PDGFRB), a marker for vascular SMC precursors and pericytes [31].

Quantification of TBX2 expression by Fiji-based measurement of the immunofluorescent signals confirmed TBX2 expression in most (E10.5) and almost all mesenchymal cells of the developing lung (E12.5, E14.5, E16.5) (Fig. 1f, Additional file 2: Table S1), and revealed that low level expression of TBX2 at E14.5 was detected in 40% of EMCN⁺ endothelial cells, 60% of ALDH1A2⁺ mesothelial cells and over 80% of ACTA2⁺, TAGLN⁺ SMCs and POSTN⁺, PDGFRA⁺ or PDGFRB⁺ (myo-)fibroblasts (Fig. 1g, Additional file 2: Table S1). Thus, TBX2 is strongly expressed in mesenchymal precursors, and persists at lower levels and to various degrees in differentiated cell-types including SMCs, pericytes and (myo-)fibroblasts, endothelial and mesothelial cells at this stage.

Fibroblasts, endothelial, mesothelial and SM cells derive from a TBX2⁺ precursor population

Since some mesenchymal (progenitor) cells surrounding the distal lung buds and most differentiated pulmonary cells lacked TBX2 or expressed only low levels, we questioned whether these cells are descendants of cells

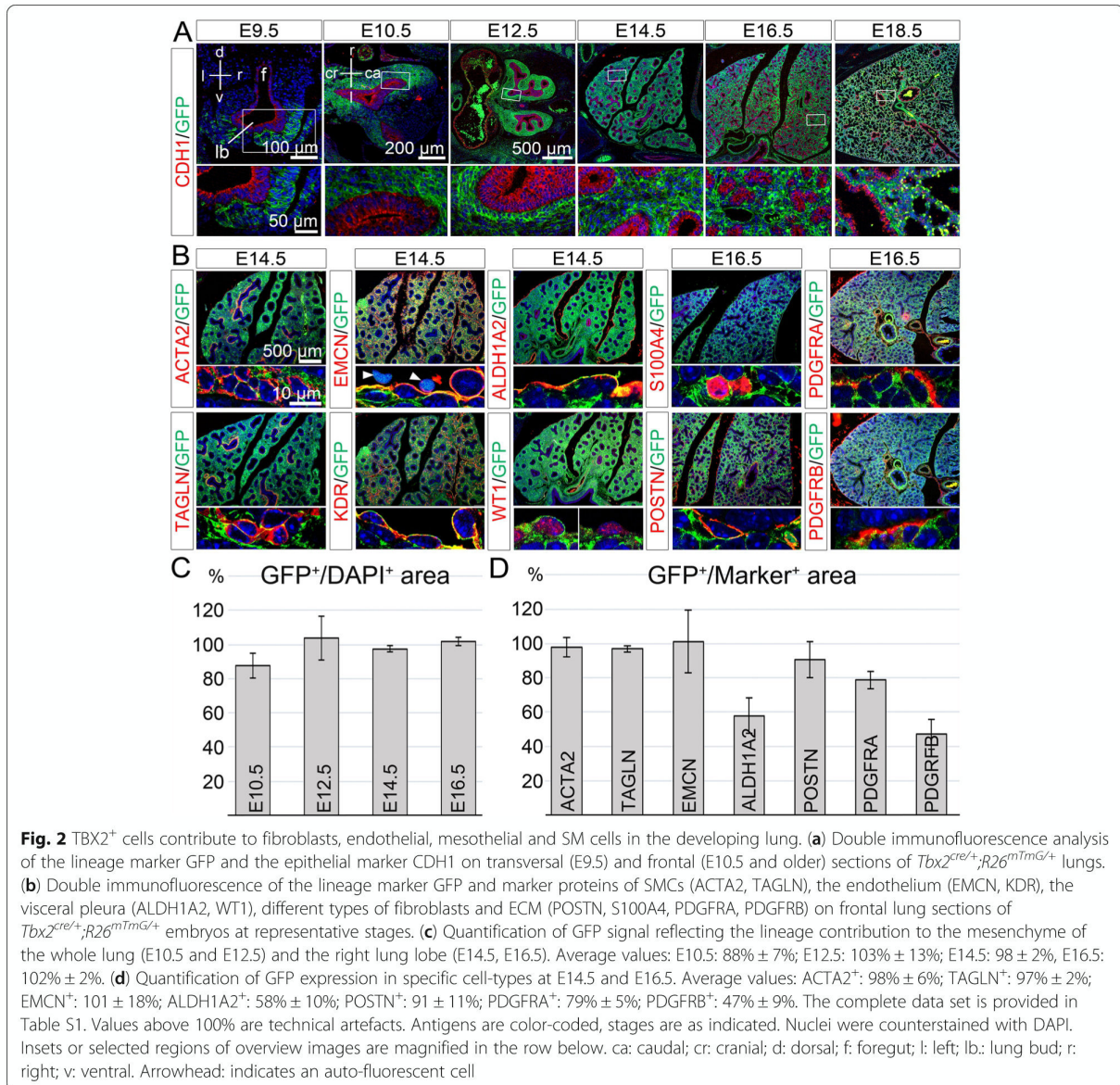
initially positive for the protein. To test this hypothesis, we used a genetic lineage tracing approach with a *Cre* line under the control of endogenous *Tbx2* control elements (*Tbx2^{cre}*) [20], and the *R26^{mTmG}* reporter line which switches from membrane-bound RFP to membrane bound GFP expression upon *Cre*-mediated recombination [22]. We performed co-stainings of the lineage marker GFP with CDH1 during development (Fig. 2a), and of GFP with differentiation markers at E14.5 and E16.5 (Fig. 2b) on lung sections of *Tbx2^{cre/+};R26^{mTmG/+}* embryos, and quantified the signals to judge the overall contribution of TBX2⁺ cells to the epithelial and mesenchymal compartment (Fig. 2c, Additional file 2: Table S1) and to differentiated cell-types in the pulmonary mesenchyme (Fig. 2d, Additional file 2: Table S1).

GFP⁺ cells were found in a scattered fashion in the pulmonary mesenchyme at E9.5 (Fig. 2a). At E10.5, the contribution of TBX2⁺ cells to cell types outside the airway epithelium was 88% and increased to almost 100% at E12.5, E14.5 and E16.5 (Fig. 2a and c, Additional file 2: Table S1). All ACTA2⁺ and TAGLN⁺ SMCs were positive for the lineage marker GFP at E14.5, as were EMCN- and kinase insert domain protein receptor (KDR) [32, 33] positive endothelial cells (Fig. 2b and d, Additional file 2: Table S1). We also observed co-expression of ALDH1A2 (58%) and wilms tumor 1 homolog (WT1) [34], two mesothelial markers, with GFP. Moreover, most if not all S100A4⁺ cells (not quantifiable by Fiji-based tools), 91% of POSTN-, 79% of PDGFRA- and 47% of PDGFRB-expressing cells were positive for GFP expression at E16.5 (Fig. 2b and d, Additional file 2: Table S1). Together this analysis shows that SMCs, endothelial cells and fibroblasts of the fetal lung derive almost completely, mesothelial cells to about 50% from cells positive for TBX2 expression.

Lineage contribution of TBX2⁺ cells is not changed upon loss or gain of TBX2

Loss of *Tbx2* in the pulmonary mesenchyme leads to hypoplasia whereas overexpression results in tissue thickening and organ overgrowth possibly by altering the balance between progenitor proliferation and differentiation [18, 19]. To determine whether these manipulations of TBX2 expression affect the lineage diversification of TBX2⁺ cells, we performed cell fate analysis in lungs of mice with conditional loss or gain of *Tbx2* expression in the pulmonary mesenchyme.

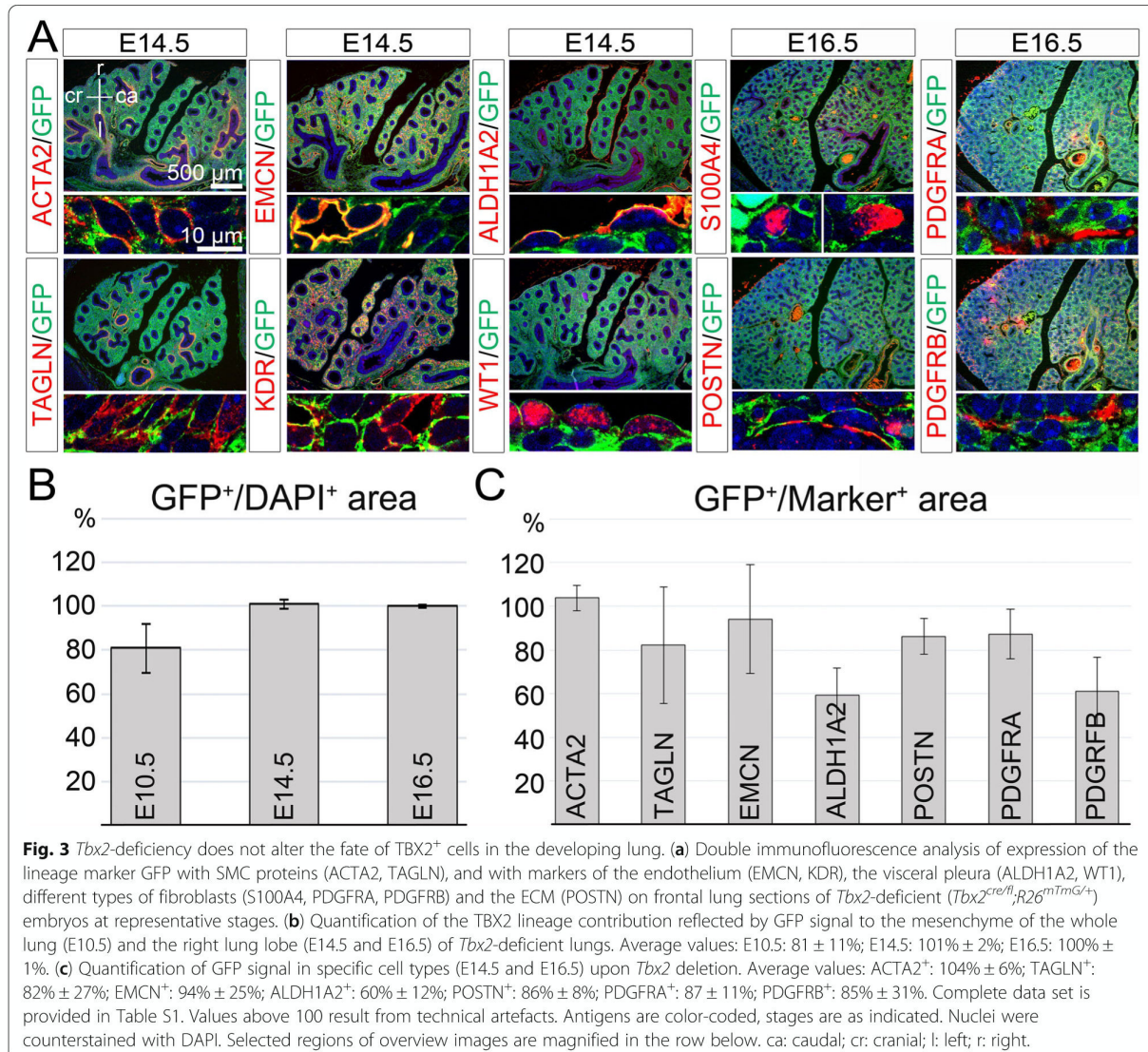
For this purpose, we combined the *Tbx2^{cre}* allele with a *Tbx2^{loxed}* allele [21] and the *R26^{mTmG}* reporter line [22]. Immunofluorescence analysis on lung sections of these *Tbx2^{cre/fl};R26^{mTmG/+}* embryos at E9.5, E10.5 and E11.5 confirmed the absence of TBX2 protein in the entire pulmonary mesenchyme from the onset of lung development (Additional file 1: Figures S3 and S4). Double



immunofluorescence analysis showed that GFP⁺, i.e. lineage positive cells did not contribute to the respiratory epithelium at all analyzed stages (Additional file 1: Figure S5). Quantification of GFP expression within the pulmonary mesenchyme at different developmental stages showed that *Tbx2* deletion did not alter the overall contribution of lineage positive cells in this tissue (Fig. 3a and b, Additional file 2: Table S1). Furthermore, GFP expression was detected in all ACTA2- and most TAGLN- positive SMCs, in a large fraction of EMCN- and KDR- positive endothelial cells and to a lower extent in the ALDH1A2- and WT1- positive mesothelium at E14.5. We found GFP expression in all S100A4- positive interstitial fibroblasts, as well as in over 85% of

the POSTN-, in 87% of the PDGFRA- and in 61% of the PDGFRB- positive area at E16.5 (Fig. 3a, and c, Additional file 2: Table S1). Hence, loss of TBX2 does not affect the differentiation and lineage distribution of mesenchymal precursors initially positive for TBX2 in the developing lung.

To analyze the gain-of-function situation, we used an *Hprt* knock-in allele of human *TBX2* (*Hprt^{TBX2}*) [23] which upon combination with the *Tbx2^{cre}* allele leads to ectopic expression in all cells of the TBX2 lineage. Due to the X-chromosomal localization of the *Hprt* locus, females exhibit mosaic overexpression, while in males all recombined cells express TBX2 ectopically. Cre-mediated recombination was visualized by co-expression of a YFP from the *Hprt^{TBX2}*



allele. Since overexpression of TBX2 is lethal to male embryos at approximately E13.0, lung rudiments of E12.5 embryos were explanted and analyzed after culturing for 6 or 8 days (Fig. 4).

On the morphological level, explants of male (*Tbx2*^{cre/+};*Hprt*^{TBX2/y}) and female (*Tbx2*^{cre/+};*Hprt*^{TBX2/+}) mutant embryos did not show any obvious defects. Male explants exhibited homogenous YFP epifluorescence during the whole culture period, while explants of female mutants showed a mosaic pattern as expected (Fig. 4a). Starting from day 2 of culture, YFP⁺ cells in females formed clusters at the rim of the explants which increased with time. Similar clusters were observed in control cultures, however, they emerged approximately three days later and were unevenly distributed over the entire organ (Fig. 4a, Additional file 1: Figure S6).

We also determined TBX2 expression and lineage contribution in these cultures. In *Tbx2*^{cre/+};*R26*^{mTmG/+} control cultures both TBX2 expression as well as the TBX2⁺ cell lineage was restricted to the CDH1 negative population. The same was true for male and female overexpression mutants (Additional file 1: Figure S7). To decipher the cell-types to which the TBX2 overexpressing cells contribute in these cultures, we first validated the differentiation markers on control cultures. KDR, ALDH1A2 and WT1 were not faithfully expressed, whereas ACTA2, TAGLN, EMCN, POSTN and S100A4 were expressed in a similar fashion as in vivo (Additional file 1: Figure S8B).

In cultures of *Tbx2*^{cre/+};*Hprt*^{TBX2} embryos, TBX2⁺ cells contributed to ACTA2⁺ and TAGLN⁺ SMCs but with reduced frequency in comparison to *Tbx2*^{cre/+};*R26*^{mTmG/+} control cultures. In *Tbx2*^{cre/+};*Hprt*^{TBX2/y} cultures we

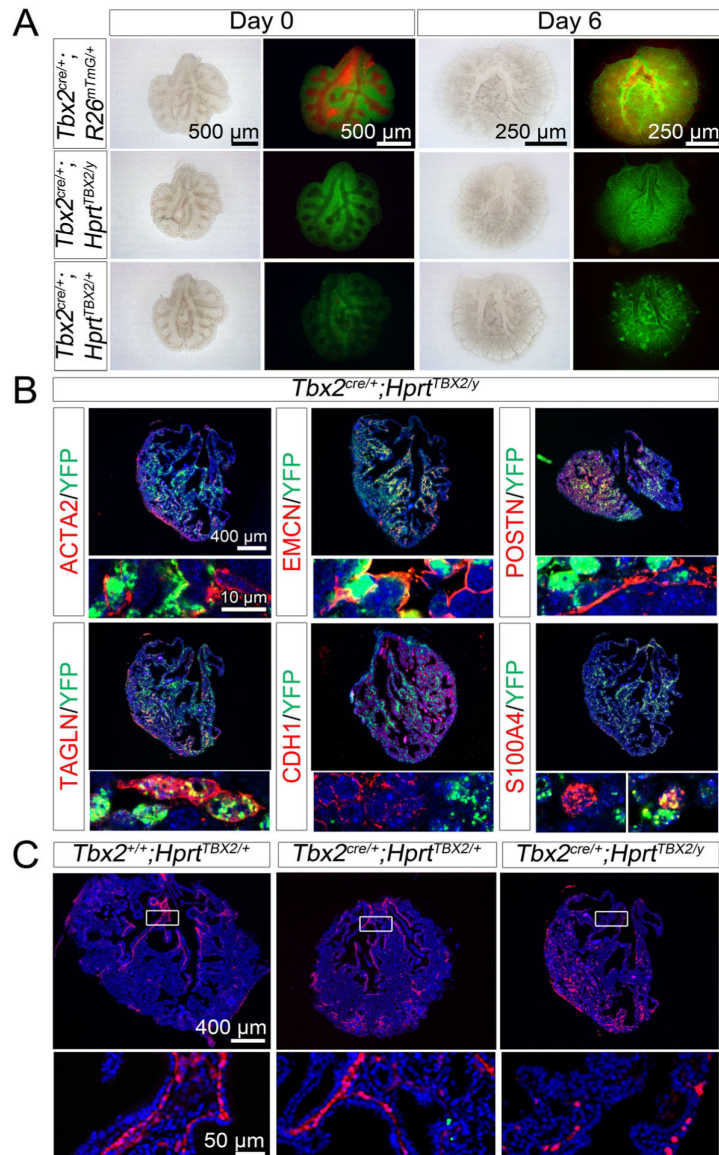


Fig. 4 *Tbx2*-overexpression does not alter the fate of TBX2⁺ cells in the developing lung. **(a)** Morphology and GFP/RFP epifluorescence of lung explants of E12.5 *Tbx2*^{cre/+};*R26*^{mTmG/+} (control), *Tbx2*^{cre/+};*Hprt*^{TBX2/+} (female) and *Tbx2*^{cre/+};*Hprt*^{TBX2/y} (male) embryos at day 0 and day 6 of culture. **(b)** Double immunofluorescence analysis of YFP (indicating TBX2 expression from the *Hprt* allele) and cell-type specific marker proteins (TAGLN, ACTA2 for SMCs; EMCN for the endothelium; CDH1 for the epithelium; S100A4 for different types of fibroblasts and POSTN for the ECM) on sections of *Tbx2*^{cre/+};*Hprt*^{TBX2/y} lung rudiments after 8 days of culture. Antigens are color-coded. Selected regions of overview images are magnified in the row below. **(c)** Immunofluorescent analysis of TAGLN expression on frontal sections of *Tbx2*^{cre/+};*R26*^{mTmG/+} (control), *Tbx2*^{cre/+};*Hprt*^{TBX2/+} and *Tbx2*^{cre/+};*Hprt*^{TBX2/y} lung cultures. Genotypes are as indicated. Insets or selected regions in overview images are magnified in the row below. Nuclei were counterstained with DAPI

observed an increase of interstitial ACTA2- and TAGLN-positive cells at the expense of SMCs lining the trachea and bronchi (Fig. 4b and c). The EMCN⁺ vasculature was composed of YFP-positive and negative cells as in the control. However, the *Tbx2*^{cre/+};*Hprt*^{TBX2/y} culture harbored clearly more EMCN⁺ cells than the female mutant or the

control (Fig. 4b, Additional file 1: Figures S8, S9). Double immunofluorescence analysis for S100A4 and YFP revealed that S100A4⁺ cells partially derived from the TBX2 lineage. Similarly, YFP⁺ cells expressed POSTN both in male (Fig. 4b) and female overexpression mutants (Additional file 1: Figure S9).

To exclude that changes of TBX2 expression are compensated by opposing expression changes of the closely related TBX3 protein, we analyzed TBX3 expression in the context of the TBX2⁺ lineage both in control and in loss- and gain-of-function conditions. In the control condition, TBX3 expression was confined to the TBX2 cell lineage in the pulmonary mesenchyme at all analyzed stages of lung development (Additional file 1: Figure S10A) as well as in lung explant cultures (Additional file 1: Figure S10B). Neither loss nor gain of TBX2 in the pulmonary mesenchyme affected TBX3 expression in this tissue (Additional file 1: Figures S10C and S10D). Together, this analysis shows that prolonged expression of TBX2 in the pulmonary mesenchyme affects the contribution of TBX2-positive cells to SMCs as well as the differentiation of SMCs and endothelial cells.

SMC differentiation and functionality depends on TBX2

In our *Tbx2* overexpression mutants, we found a strongly reduced number of bronchial SMCs in cultured explants of embryonic lungs (Fig. 4b and c). To more carefully explore the relation of TBX2 expression and SMC differentiation, we analyzed the expression of TBX2 in bronchial SMCs in more detail. Immunofluorescence stainings and quantifications indicated that in control lungs expression of TBX2 was inversely correlated with that of SMC markers (Fig. 5a and b, Additional file 2: Table S1). In *Tbx2^{cre/+};Hprt^{TBX2/y}* lungs, bronchial SMCs were established normally at E12.5 (Fig. 5c, Additional file 1: Figure S11). After 8 days of culture, only few bronchial SMCs remained in *Tbx2^{cre/+};Hprt^{TBX2/y}* lung explants as mentioned before (Fig. 4b) but interestingly, some of them were still TBX2⁺, whereas TBX2 expression was excluded from SMCs in the controls (Fig. 5c, Additional file 1: Figure S11).

Although *Tbx2* was not required for SMC differentiation at E14.5 (Fig. 3), its loss may affect the initiation of this program. We therefore examined expression of TAGLN (Fig. 5d) and ACTA2 (Additional file 1: Figure S12) in control and *Tbx2*-deficient lungs at E10.5, E11.5 and E12.5. However, no changes in SMC differentiation were observed at these stages. Further, the SMC related genes *myosin heavy chain 11* (*Myh11*), *calponin1* (*Cnn1*) and *desmin* (*Des*) showed no differential expression in *Tbx2^{cre/fl}* mice at E12.5 and E14.5 compared to controls (Additional file 1: Figure S12). We also analyzed expression of S100A4, which was previously described as SMC-associated Calcium-binding protein, involved in SMC function in other contexts [35]. In the control, S100A4 was first detected in bronchial SMCs at E14.5, whereas *Tbx2^{cre/fl}* mice showed premature expression of this protein at E12.5 (Fig. 6a).

To find out whether changes of TBX2 expression affect the functionality of pulmonary SMCs, we analyzed muscular contractions in lung explant cultures. *Tbx2^{cre/fl}* lungs cultured for 36 h showed an increase in contraction

intensity to 45.3% compared to 39.3% of control cultures, associated with a significantly slower relaxation of the contracted muscles. *Tbx2^{cre/+};Hprt^{TBX2/y}* explants displayed a significant reduction to 21.3% contraction intensity compared to the control (32.4%) and a faster relaxation of the musculature after 36 h of culture (Fig. 6b). Calculating the areas below the curves clearly demonstrated the significant differences in both mutants compared to the control cultures in overall contraction intensities. In *Tbx2^{cre/fl};R26^{mTmG/+}* lungs, the average integral significantly increased from 4.7 to 6.7. In *Tbx2^{cre/+};Hprt^{TBX2/y}* lungs a significant decrease from 5.4 to 3.3 was observed (Fig. 6c, Additional file 3: Table S2). Together this suggests that TBX2 influences the differentiation and functionality of bronchial SMCs.

Discussion

TBX2 expression marks a multipotent mesenchymal progenitor population in the developing lung

To explore the lineage relation between TBX2 expressing cells and differentiated cell types in the fetal lung we performed genetic lineage tracing with a cre knock-in line into the *Tbx2* locus. Notably, previous work established that the *Tbx2^{cre}* allele is suited for this purpose, since *cre* expression faithfully reflects endogenous expression of *Tbx2* [20]. We found that most cells outside the respiratory epithelium, including SMCs of the airways and the vasculature, fibroblasts, a large part of endothelial cells as well as mesothelial cells of the visceral pleura were positive for the reporter. Together with the fact that TBX2 expression does not occur in the respiratory epithelium, it confirms other studies that the lineages of the respiratory epithelium and of all surrounding cell-types are completely segregated from onset of lung development ([32–34]). It also implies that TBX2 expression occurs in a common or in distinct progenitor pools of endothelial, mesothelial and mesenchymal cells of the embryonic lung. In fact, our expression analysis revealed that TBX2 is activated shortly after emergence of the lung buds, is predominantly and strongly expressed in undifferentiated cells that surround the distal lung buds and declines in differentiated SMCs and fibroblasts. It is noteworthy that TBX2 expression in the mesenchyme surrounding the distal lung buds was very heterogenous. Most cells expressed high levels, other expressed low levels or were negative for TBX2. It is conceivable that TBX2-negative cells get actually lost during lung development since they do not proliferate. Alternatively, expression levels of TBX2 in this population may fluctuate with all cells activating expression of TBX2 at some point. Notably, TBX2 expression in the endothelium and mesothelium was more variable and appeared scattered.

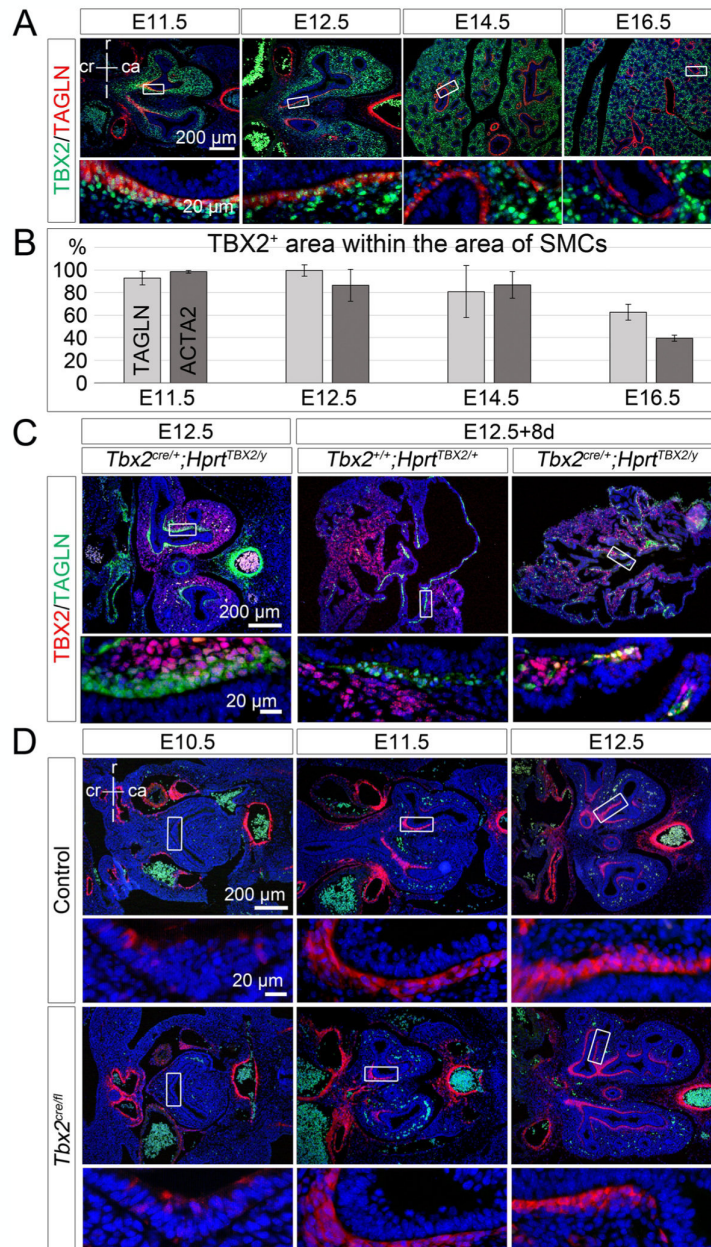


Fig. 5 SMC development and its correlation with TBX2 expression. **(a, c)** Double immunofluorescence analysis of expression of TBX2 with the SMC protein TAGLN on frontal lung sections of control mice **(a)**, of *Tbx2^{cre/+};Hprt^{TBX2/y}* lungs at E12.5, and of 8-day cultures of E12.5 *Tbx2^{+/+};Hprt^{TBX2/+}* and *Tbx2^{cre/+};Hprt^{TBX2/y}* lung explants **(c)**. **(b)** Quantification of TBX2 expression in pulmonary SMCs marked by TAGLN or ACTA2 of control embryos at different embryonic stages. Average values: TAGLN⁺: 93% ± 6% (E11.5); 99% ± 5% (E12.5); 81% ± 23% (E14.5); 63% ± 3% (E16.5); ACTA2⁺: 98 ± 1% (E11.5); 87% ± 14% (E12.5); 87 ± 12% (E14.5); 39% ± 3% (E16.5). Complete data set is provided in Table S1. Technical artefacts produce values above 100%. **(d)** Immunofluorescence of TAGLN (red) on control and *Tbx2^{cre/fl};R26^{mTmG/+}* frontal lung sections at different developmental stages. Antigens are color-coded. Stages are as indicated. Nuclei were counter stained with DAPI. Insets of overview images are magnified in the row below. ca: caudal; cr: cranial; d: dorsal; f: foregut; l: left; lb: lung bud; r: right; v: ventral

Besides *Tbx2*, the early pulmonary mesenchyme expresses the WNT ligand genes *Wnt2/2b*, the T-box transcription factor gene *Tbx4* and the fibroblast growth

factor gene *Fgf10*. Lineage tracing of *Fgf10*-expressing cells, revealed that these cells in an early embryonic wave give rise to bronchial and vascular SMCs as well as

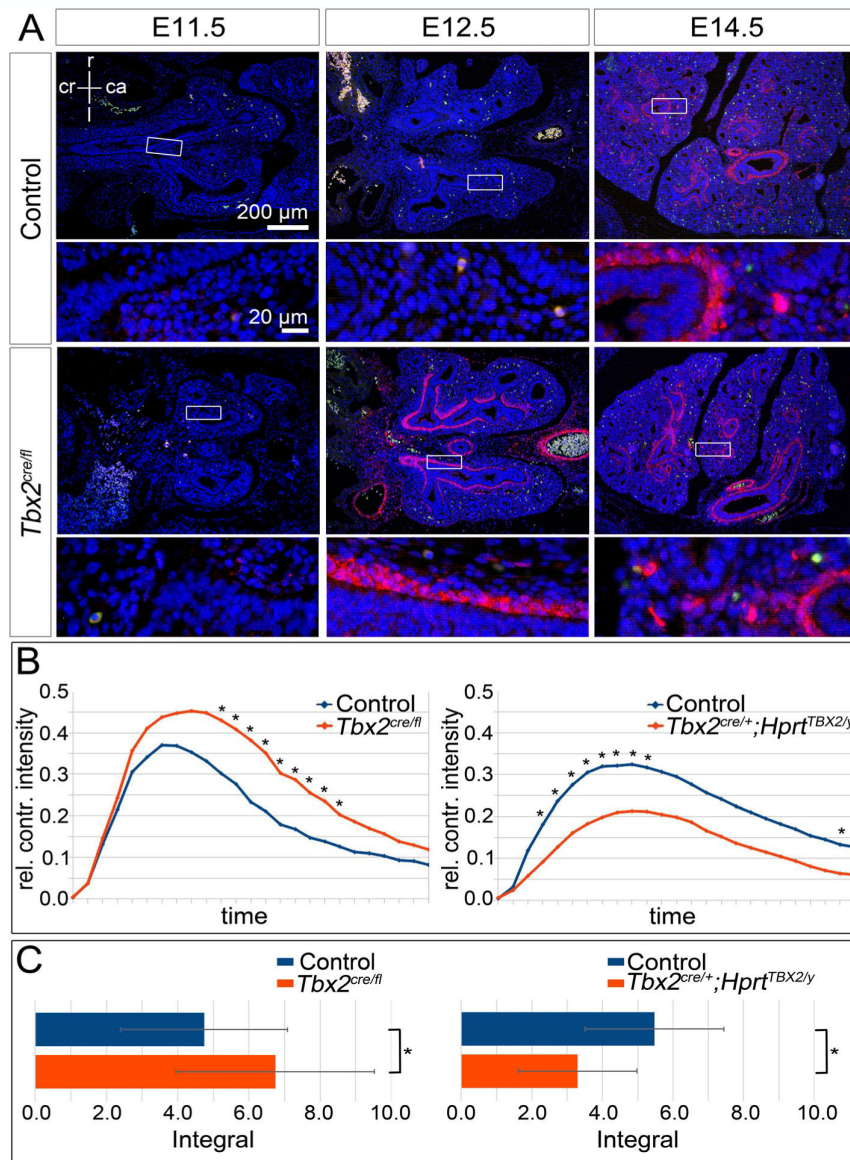


Fig. 6 Premature S100A4 expression in TBX2-deficient bSMCs correlates with altered contraction in *Tbx2*^{cre/fl} and *Tbx2*^{cre/+}; *Hprt*^{TBX2/y} lungs. **(a)** Immunofluorescence staining of S100A4 (red) on frontal lung section of different stages of control and *Tbx2*^{cre/fl}; *R26*^{mTmG/+} embryos. Stages are as indicated. Nuclei were counterstained with DAPI. Insets of overview images are magnified in the row below. **(b, c)** Diagrams of relative contraction intensity **(b)** and bar graphs of corresponding integral calculation **(c)**, Average values: Control (left): 4.7 ± 2.3, *Tbx2*^{cre/fl}; *R26*^{mTmG/+}: 6.7 ± 2.8; Control (right): 5.4 ± 2, *Tbx2*^{cre/+}; *Hprt*^{TBX2/y}: 3.3 ± 1.7) of the right main bronchi of lungs explanted at E12.5 and cultured for 36 h. Differences were considered significant with **p* ≤ 0.05, ***p* ≤ 0.01, ****p* ≤ 0.005, using two-tailed Student's t-test. Statistical values are provided in Table S2

lipofibroblasts, whereas during alveologenesis they contribute to lipofibroblasts and myofibroblasts only [35]. Even though *Fgf10* is already expressed very early and *Fgf10* is a critical factor for lung development [8, 36], the TBX2 lineage contributes to more cells within the pulmonary mesenchyme.

Fgf10 is induced by TBX4, a T-box transcription factor that belongs with *Tbx2* to the same T-box subfamily [37,

38]. *Tbx4* is expressed in the embryonic lung mesenchyme from E9.25 onwards and lineage tracing using a *Tbx4* lung enhancer *Cre* line showed that TBX4-expressing cells give rise to a subset of fibroblasts (lipofibroblasts and myofibroblasts), SMCs, endothelial and mesothelial cells in the fetal and adult lung [38, 39]. Given the similarities of the TBX4 and the TBX2 lineages and expression patterns in the developing pulmonary mesenchyme, one might conclude that

TBX2 similar to TBX4 is one of the factors, which defines the early lung mesenchyme. However, *Tbx2* deletion only affects branching morphogenesis around E14.5, i.e. much later than TBX4 [38, 40].

Previous work revealed that *Wnt2* is expressed in the ventral region of the mesenchyme surrounding the lung buds, and that these cells are able to generate most of the mesoderm/mesenchymal lineages within the lung, including bronchial and vascular SMCs, fibroblasts and proximal endothelium [7]. *Wnt2*⁺ cells also generate cardiomyocytes and endocardial cells within the inflow tract of the heart, demonstrating the existence of a common cardiopulmonary progenitor (CPP) that orchestrates pulmonary and cardiac development [33, 34]. Given the well-known fact that *Tbx2* is expressed early in the heart anlage and that TBX2⁺ cells also generate cardiomyocytes [20], it seems possible that TBX2 expression similar to *Wnt2* marks the CPP.

Our study observed that approximately half of pleural cells expressed TBX2 and descended from that lineage, respectively. Whether this mesothelial TBX2 progenitor is identical with the CPP or whether it represents an uncharacterized expression of TBX2 in the coelomic epithelium from which the mesothelium derives, remains unclear at this point. However, our analysis points to a molecular heterogeneity within the pleura previously not appreciated. We conclude that TBX2 expression marks an early progenitor for mesenchymal, endothelial and mesothelial cells in the lung.

TBX2 plays a minor role in differentiation of the pulmonary mesenchyme

We have previously shown that TBX2 is required to maintain the proliferation in the lung mesenchyme by two independent molecular mechanisms: maintenance of WNT signaling and repression of cell-cycle inhibitor genes [18, 19]. In this study we found that TBX2 expression is strongly reduced upon differentiation of bronchial SMCs. Since proliferation and differentiation are often inversely correlated, we expected to see premature expression of TBX2-derived cell types, particularly SMCs and fibroblasts. However, we did not detect changes of bronchial SMCs or fibroblasts nor did we see altered lineage segregation in our loss-of-function mutants. A possible explanation is redundancy with TBX3 as in many other organ contexts [23, 41]. TBX3 is expressed in an overlapping pattern with TBX2 from E9.5 to E14.5 and then diminishes in the pulmonary mesenchyme. Combined systemic deletion of *Tbx2* and *Tbx3* leads to early embryonic death due to cardiovascular defects. In explant cultures of rare surviving double mutants the lung was severely hypoplastic and branching morphogenesis stopped very early [18, 19].

Prolonged expression of TBX2 maintained mesenchymal proliferation [18] but did not affect lineage segregation and differentiation potential of TBX2⁺ cells since SMCs, the endothelium, the mesothelium as well as fibroblasts were all found as descendants in *Tbx2*^{cre/+}; *Hprt*^{TBX2/y} lungs. However, *Tbx2*^{cre/+}; *Hprt*^{TBX2/y} mutants harbored strikingly more EMCN-positive cells than the female overexpression mutant or the control. Conceivably, TBX2 is sufficient to maintain the proliferative precursor population of the endothelium or ectopically induces endothelial proliferation. This is in line with our observation that TBX2 is expressed in endothelial progenitors but is less strongly expressed in endothelial cells.

We also observed in our *Tbx2* gain-of-function cultures that bronchial SMCs were established in a very small number but that interstitial or peripheral SMCs were greatly increased. Together with the observation that onset of SMC differentiation is not altered in these mutants this argues that down-regulation of TBX2 is not required for the commitment into the SMC fate but for the correct spatial allocation of these cells at the proximal airways.

Our data also suggest that TBX2 expression levels are critical for the correct physiology of SMCs in the lung. In *Tbx2* loss-of-function mutants the contraction intensity was increased whereas it was decreased in gain-of-function lung cultures. We did not find changes of major SMC structural proteins but a premature activation of S100A4 in (prospective) bronchial SMCs. Further, S100A4 is transiently expressed in bronchial SMC of controls from E14.5 to E16.5, matching the time-point when TBX2 gets reduced in this cell layer. Unfortunately, we were not able to analyze whether S100A4 expression is delayed or even completely abolished in *Tbx2*^{cre/+}; *Hprt*^{TBX2/y} mice, since they do not survive until E14.5 or later, and the in vivo expression pattern is not completely reflected in culture conditions. Studies in the coronary system showed, that S100A4 promotes proliferation and migration of SMCs and that it is associated with SMC contractility [42]. Hence, repression of S100A4 by TBX2 may be one means in which this transcription factor modulates SMC physiology.

Conclusions

Our work shows that TBX2 is expressed in an early pulmonary progenitor pool and supports a role of TBX2 in maintaining the precursor state in the pulmonary mesenchyme. The fate of pulmonary mesenchymal progenitors is largely independent of TBX2. Nevertheless, a successive and precisely timed downregulation of TBX2 is necessary to allow proper differentiation and functionality of bronchial smooth muscle cells and to limit endothelial differentiation.

Supplementary information

Supplementary information accompanies this paper at <https://doi.org/10.1186/s12931-019-1264-y>.

Additional file 1: Figure S1. Secondary and tertiary antibodies do not exhibit unspecific binding. **Figure S2.** *Tbx2*/TBX2 expression and lineage contribution to the lung mesenchyme at E9.5. **Figure S3.** *Tbx2*/TBX2 expression and lineage contribution in the lung bud mesenchyme of *Tbx2*-deficient embryos. **Figure S4.** TBX2 expression is lost in the pulmonary mesenchyme of *Tbx2*^{cre/f1}; *R26*^{mTmG/+} embryos in early lung development. **Figure S5.** The TBX2⁺ lineage does not contribute to the pulmonary epithelium in *Tbx2*-deficient embryos. **Figure S6.** Overexpression of TBX2 leads to enhanced and premature formation of lineage positive cell clusters. **Figure S7.** TBX2 expression and TBX2 lineage contribution in control and constitutively TBX2 overexpressing lung explant cultures. **Figure S8.** Validation of cell-type specific markers and of TBX2⁺ cell lineage contribution in lung explant cultures. **Figure S9.** Mesenchymal mosaic overexpression of TBX2 does not affect the lineage diversification of TBX2-expressing cells. **Figure S10.** Expression analysis of TBX3 and TBX2⁺ cell lineage contribution to TBX3 expressing cells. **Figure S11.** Analysis of ACTA2 expression in *Tbx2*^{cre/f1}; *Hprt*^{TBX2/y} lungs. **Figure S12.** Analysis of SMC differentiation in *Tbx2*^{cre/f1}; *R26*^{mTmG/+} lungs.

Additional file 2: Table S1. Quantification of immunofluorescence staining. Raw measuring data and calculations of immunofluorescence signals. Quantification of TBX2 and GFP expression in the whole lung and in areas of cell type specific marker expression at different embryonic stages analyzed in this study for control and *Tbx2*^{cre/f1}; *R26*^{mTmG/+} mice.

Additional file 3: Table S2. Statistical evaluation of contraction behavior of lung explant cultures. Raw measuring data, integral calculations and counted branching endpoints are depicted in "LOF data" and "GOF data" for controls and corresponding mutants. Statistical calculations are summarized in "LOF statistics" and "GOF statistics".

Abbreviations

Acta2: Actin, alpha 2, smooth muscle, aorta, (synonym: SmaA); Aldh1a2: Aldehyde dehydrogenase family 1, subfamily A2; bSMCs: Bronchial smooth muscle cells; ca: Caudal; Cdh1: Cadherin 1; Cdkn: Cyclin-dependent kinase inhibitor; Cnn1: Calponin 1; CPP: Cardio-pulmonary precursor; cr: Cranial; d: Dorsal; DAPI: 4',6-diamidino-2-phenylindole; Des: Desmin; E: Embryonic day; Emcn: Endomucin; f: Foregut; FCS: Fetal calf serum; Fgf10: Fibroblast growth factor 10; Frzb: Frizzled-related protein; GFP: Green fluorescent protein; GOF: Gain-of-function; Hprt: Hypoxanthine guanine phosphoribosyl transferase; hrs: Hours; Kdr: Kinase insert domain protein receptor; l: Left; lb: Lung bud; LOF: Loss-of-function; Myh11: Myosin, heavy polypeptide 11, smooth muscle; PBS: Phosphate-buffered saline; Pdgfr: Platelet derived growth factor receptor; PFA: Paraformaldehyde; Postn: Periostin; r: Right; R26: Rosa26; S100A4: S100 calcium binding protein A4; Shisa3: Shisa family member 3; SMC: Smooth muscle cell; SMCs: Smooth muscle cells; TAGLN: Transgelin (synonym: SM22); Tbx: T-box; v: Ventral; Wnt: Wingless-type MMTV integration site family; Wt1: Wilms tumor 1 homolog; YFP: Yellow fluorescent protein

Acknowledgements

We thank Rolf Kemler for the anti-CDH1 antiserum and Dietmar Vestweber for the anti-EMCN antiserum.

Authors' contributions

Concept and design: IW, THL, AK; mouse and laboratory work and data analysis: IW, THL, MOT, AK; Animals: VMC; preparation of manuscript & figures: IW, THL, AK. All authors have read and approved the manuscript.

Funding

This work was funded by a grant from the Deutsche Forschungsgemeinschaft (DFG KI728/11 to AK).

Availability of data and materials

All datasets and reagents are available from the corresponding author on reasonable request.

Ethics approval and consent to participate

All animal work conducted for this study was performed according to European and German legislation. The breeding, handling and sacrifice of mice for embryo isolation was approved by the Niedersächsisches Landesamt für Verbraucherschutz und Lebensmittelsicherheit (Permit Number: AZ33.12–42502–04-13/1356).

Consent for publication

Not applicable.

Competing interests

The authors declare that they have no competing interest.

Author details

¹Institut für Molekularbiologie, Medizinische Hochschule Hannover, Hannover, Germany. ²Department of Anatomy, Embryology and Physiology, Academic Medical Center, University of Amsterdam, Amsterdam, Netherlands.

Received: 14 September 2019 Accepted: 18 December 2019

Published online: 23 December 2019

References

- Plasschaert LW, Zilionis R, Choo-Wing R, Savova V, Knehr J, Roma G, et al. A single-cell atlas of the airway epithelium reveals the CFTR-rich pulmonary ionocyte. *Nature*. 2018;560:377–81.
- Montoro DT, Haber AL, Biton M, Vinarsky V, Lin B, Birket SE, et al. A revised airway epithelial hierarchy includes CFTR-expressing ionocytes. *Nature*. 2018;560:319–24.
- Zepp JA, Zacharias WJ, Frank DB, Cavanaugh CA, Zhou S, Morley MP, et al. Distinct Mesenchymal lineages and niches promote epithelial self-renewal and Myofibrogenesis in the lung. *Cell*. 2017;170:1134–48 e10.
- Charalampidis C, Youroukou A, Lazaridis G, Baka S, Mpoukovinas I, Karavasilis V, et al. Physiology of the pleural space. *J Thorac Dis*. 2015;7:S33–7.
- Shannon JM, Hyatt BA. Epithelial-mesenchymal interactions in the developing lung. *Annu Rev Physiol*. 2004;66:625–45.
- McCulley D, Wienhold M, Sun X. The pulmonary mesenchyme directs lung development. *Curr Opin Genet Dev*. 2015;32:98–105.
- Goss AM, Tian Y, Tsukiyama T, Cohen ED, Zhou D, Lu MM, et al. Wnt2/2b and beta-catenin signaling are necessary and sufficient to specify lung progenitors in the foregut. *Dev Cell*. 2009;17:290–8.
- Belluscio S, Grindley J, Emoto H, Itoh N, Hogan BL. Fibroblast growth factor 10 (FGF10) and branching morphogenesis in the embryonic mouse lung. *Development*. 1997;124:4867–78.
- Miller RK, McCrea PD. Wnt to build a tube: contributions of Wnt signaling to epithelial tubulogenesis. *Dev Dyn*. 2009;239:77–93.
- Shannon JM, Nielsen LD, Gebb SA, Randell SH. Mesenchyme specifies epithelial differentiation in reciprocal recombinants of embryonic lung and trachea. *Dev Dyn*. 1998;212:482–94.
- Bostrom H, Willetts K, Pekny M, Leveen P, Lindahl P, Hedstrand H, et al. PDGF-A signaling is a critical event in lung alveolar myofibroblast development and alveogenesis. *Cell*. 1996;85:863–73.
- Lindahl P, Karlsson L, Hellstrom M, Gebre-Medhin S, Willetts K, Heath JK, et al. Alveogenesis failure in PDGF-A-deficient mice is coupled to lack of distal spreading of alveolar smooth muscle cell progenitors during lung development. *Development*. 1997;124:3943–53.
- Que J, Wilm B, Hasegawa H, Wang F, Bader D, Hogan BL. Mesothelium contributes to vascular smooth muscle and mesenchyme during lung development. *Proc Natl Acad Sci U S A*. 2008;105:16626–30.
- Yin Y, Wang F, Ornitz DM. Mesothelial- and epithelial-derived FGF9 have distinct functions in the regulation of lung development. *Development*. 2011;138:3169–77.
- Ludtke TH, Rudat C, Kurz J, Hafner R, Greulich F, Wojahn I, et al. Mesothelial mobilization in the developing lung and heart differs in timing, quantity, and pathway dependency. *Am J Physiol Lung Cell Mol Physiol*. 2019;316:L767–L83.
- Morrissey EE, Hogan BL. Preparing for the first breath: genetic and cellular mechanisms in lung development. *Dev Cell*. 2010;18:8–23.
- Zepp JA, Morrissey EE. Cellular crosstalk in the development and regeneration of the respiratory system. *Nat Rev Mol Cell Biol*. 2019;20(9):551–66.

18. Ludtke TH, Farin HF, Rudat C, Schuster-Gossler K, Petry M, Barnett P, et al. Tbx2 controls lung growth by direct repression of the cell cycle inhibitor genes Cdkn1a and Cdkn1b. *PLoS Genet.* 2013;9:e1003189.
19. Ludtke TH, Rudat C, Wojahn I, Weiss AC, Kleppa MJ, Kurz J, et al. Tbx2 and Tbx3 act downstream of Shh to maintain canonical Wnt signaling during branching morphogenesis of the murine lung. *Dev Cell.* 2016;39:239–53.
20. Aanhaanen WT, Brons JF, Dominguez JN, Rana MS, Norden J, Airik R, et al. The Tbx2⁺ primary myocardium of the atrioventricular canal forms the atrioventricular node and the base of the left ventricle. *Circ Res.* 2009;104:1267–74.
21. Wakker V, Brons JF, Aanhaanen WT, van Roon MA, Moorman AF, Christoffels VM. Generation of mice with a conditional null allele for Tbx2. *Genesis.* 2010;48:195–9.
22. Muzumdar MD, Tasic B, Miyamichi K, Li L, Luo L. A global double-fluorescent Cre reporter mouse. *Genesis.* 2007;45:593–605.
23. Singh R, Hoogaars WM, Barnett P, Grieskamp T, Rana MS, Buermans H, et al. Tbx2 and Tbx3 induce atrioventricular myocardial development and endocardial cushion formation. *Cell Mol Life Sci.* 2012;69:1377–89.
24. Schindelin J, Arganda-Carreras I, Frise E, Kaynig V, Longair M, Pietzsch T, et al. Fiji: an open-source platform for biological-image analysis. *Nat Methods.* 2012;9:676–82.
25. Moorman AF, Houweling AC, de Boer PA, Christoffels VM. Sensitive nonradioactive detection of mRNA in tissue sections: novel application of the whole-mount in situ hybridization protocol. *J Histochem Cytochem.* 2001;49:1–8.
26. Niederreither K, McCaffery P, Drager UC, Chambon P, Dolle P. Restricted expression and retinoic acid-induced downregulation of the retinaldehyde dehydrogenase type 2 (RALDH-2) gene during mouse development. *Mech Dev.* 1997;62:67–78.
27. Strutz F, Okada H, Lo CW, Danoff T, Carone RL, Tomaszewski JE, et al. Identification and characterization of a fibroblast marker: FSP1. *J Cell Biol.* 1995;130:393–405.
28. Kaarteenaho-Wiik R, Paakko P, Sormunen R. Ultrastructural features of lung fibroblast differentiation into myofibroblasts. *Ultrastruct Pathol.* 2009;33:6–15.
29. Lawson WE, Polosukhin W, Zoia O, Stathopoulos GT, Han W, Plieth D, et al. Characterization of fibroblast-specific protein 1 in pulmonary fibrosis. *Am J Respir Crit Care Med.* 2005;171:899–907.
30. Horiuchi K, Amizuka N, Takeshita S, Takamatsu H, Katsuura M, Ozawa H, et al. Identification and characterization of a novel protein, periostin, with restricted expression to periosteum and periodontal ligament and increased expression by transforming growth factor beta. *J Bone Miner Res.* 1999;14:1239–49.
31. Hellstrom M, Kalen M, Lindahl P, Abramsson A, Betsholtz C. Role of PDGF-B and PDGFR-beta in recruitment of vascular smooth muscle cells and pericytes during embryonic blood vessel formation in the mouse. *Dev.* 1999;126:3047–55.
32. Rawlins EL, Clark CP, Xue Y, Hogan BL. The Id2⁺ distal tip lung epithelium contains individual multipotent embryonic progenitor cells. *Dev.* 2009;136:3741–5.
33. Peng T, Tian Y, Boogerd CJ, Lu MM, Kadzik RS, Stewart KM, et al. Coordination of heart and lung co-development by a multipotent cardiopulmonary progenitor. *Nature.* 2013;500:589–92.
34. Herriges M, Morrisey EE. Lung development: orchestrating the generation and regeneration of a complex organ. *Development.* 2014;141:502–13.
35. El Agha E, Herold S, Al Alam D, Quantius J, MacKenzie B, Carraro G, et al. Fgf10-positive cells represent a progenitor cell population during lung development and postnatally. *Development.* 2014;141:296–306.
36. Sekine K, Ohuchi H, Fujiwara M, Yamasaki M, Yoshizawa T, Sato T, et al. Fgf10 is essential for limb and lung formation. *Nat Genet.* 1999;21:138–41.
37. Cebra-Thomas JA, Bromer J, Gardner R, Lam GK, Sheipe H, Gilbert SF. T-box gene products are required for mesenchymal induction of epithelial branching in the embryonic mouse lung. *Dev Dyn.* 2003;226:82–90.
38. Arora R, Metzger RJ, Papaioannou VE. Multiple roles and interactions of Tbx4 and Tbx5 in development of the respiratory system. *PLoS Genet.* 2012;8:e1002866.
39. Zhang W, Menke DB, Jiang M, Chen H, Warburton D, Turcatel G, et al. Spatial-temporal targeting of lung-specific mesenchyme by a Tbx4 enhancer. *BMC Biol.* 2013;11:111.
40. Sakiyama J, Yamagishi A, Kuroiwa A. Tbx4-Fgf10 system controls lung bud formation during chicken embryonic development. *Development.* 2003;130:1225–34.
41. Zirzow S, Ludtke TH, Brons JF, Petry M, Christoffels VM, Kispert A. Expression and requirement of T-box transcription factors Tbx2 and Tbx3 during secondary palate development in the mouse. *Dev Biol.* 2009;336:145–55.
42. Brisset AC, Hao H, Camenzind E, Bacchetta M, Geinoz A, Sanchez JC, Chaponnier C, Gabbiani G, Bochaton-Piallat ML. Intimal smooth muscle cells of porcine and human coronary artery express S100A4, a marker of the rhomboid phenotype in vitro. *Circ Res.* 2007;100:1055–62.

Publisher's Note

Springer Nature remains neutral with regard to jurisdictional claims in published maps and institutional affiliations.

Ready to submit your research? Choose BMC and benefit from:

- fast, convenient online submission
- thorough peer review by experienced researchers in your field
- rapid publication on acceptance
- support for research data, including large and complex data types
- gold Open Access which fosters wider collaboration and increased citations
- maximum visibility for your research: over 100M website views per year

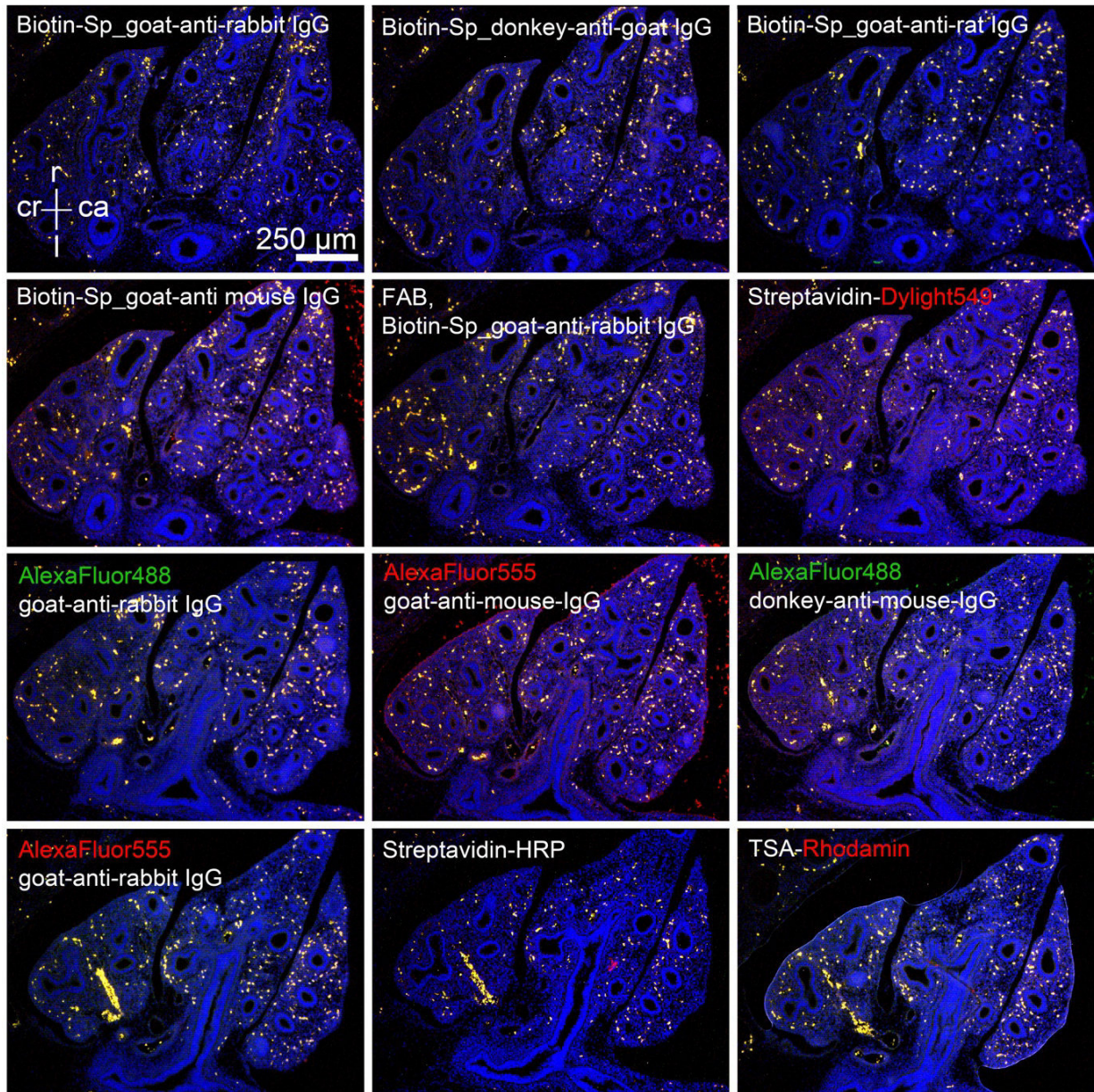
At BMC, research is always in progress.

Learn more biomedcentral.com/submissions



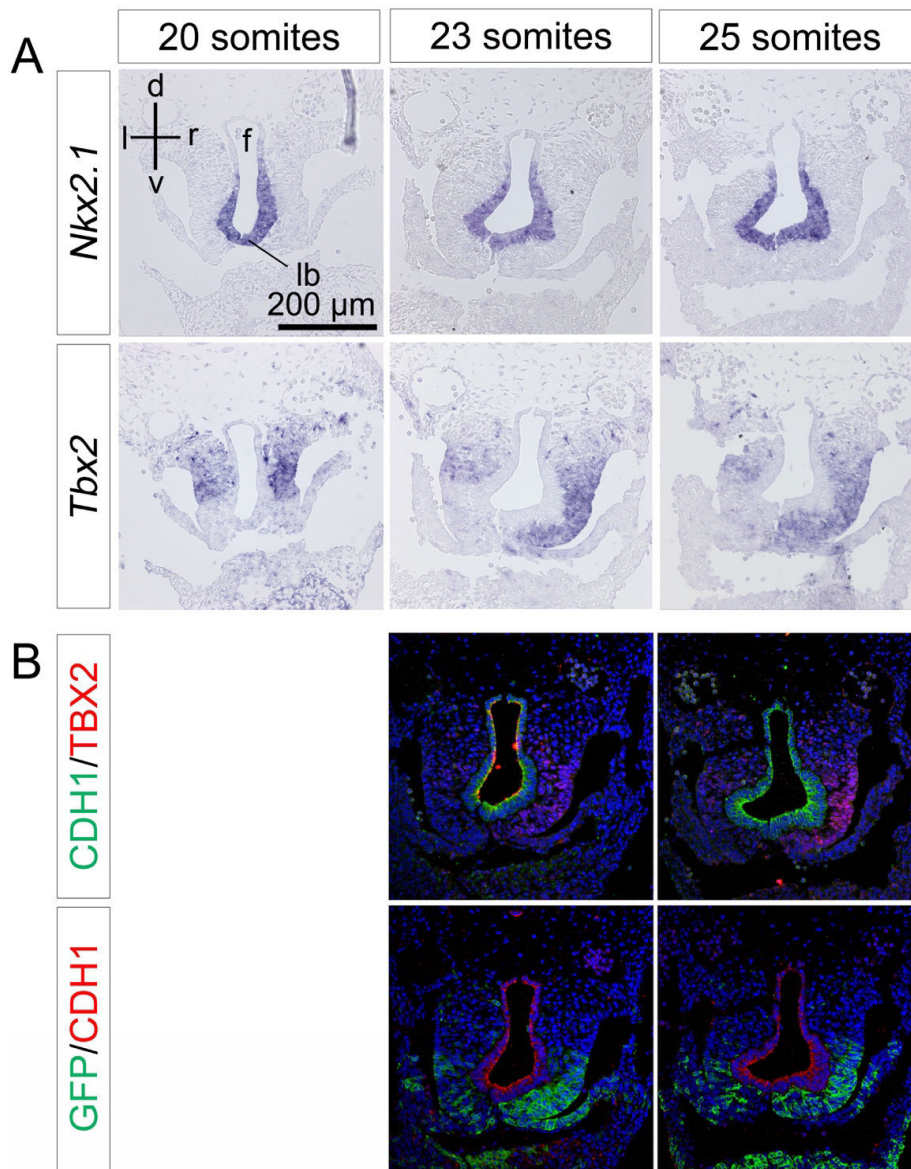
Supplemental Data

Additional file 1



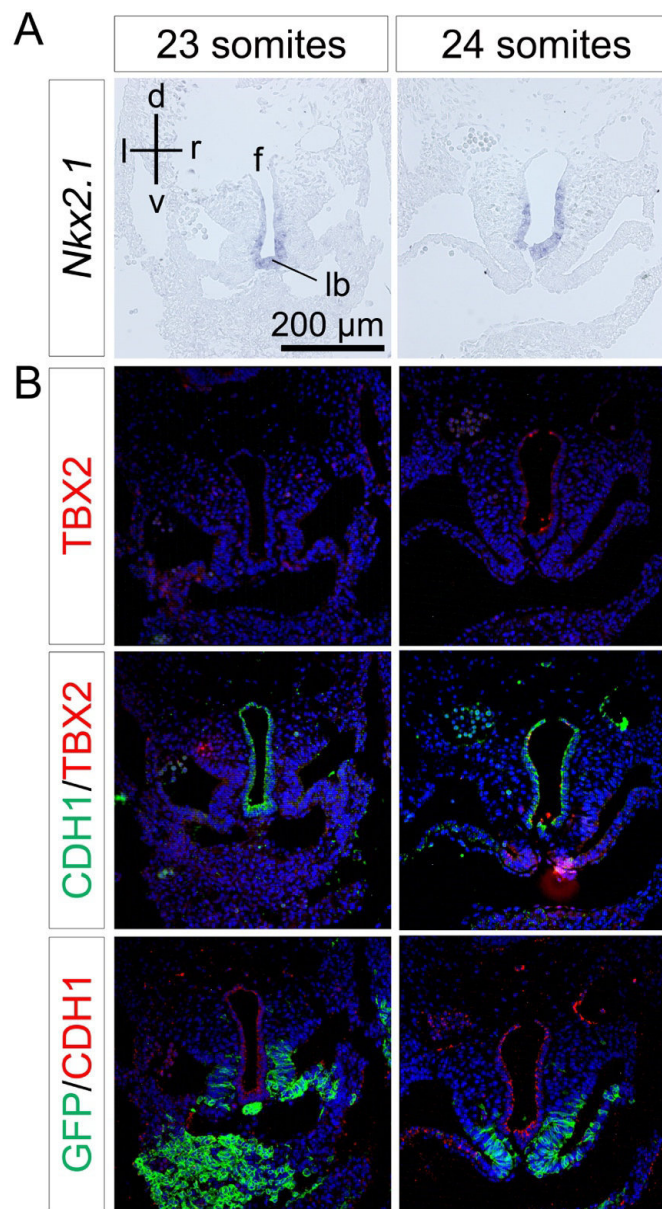
SFigure 1. Secondary and tertiary antibodies do not exhibit unspecific binding.

Control immunofluorescence stainings of secondary and tertiary antibodies without primary antibody on frontal lung sections of E14.5 control embryos. Antibodies and fluorophores are indicated. Incubation with a biotinylated antibody was followed by a streptavidin-HRP conjugated antibody and TSA-Rhodamine. ca: caudal; cr: cranial; l: left; r: right.



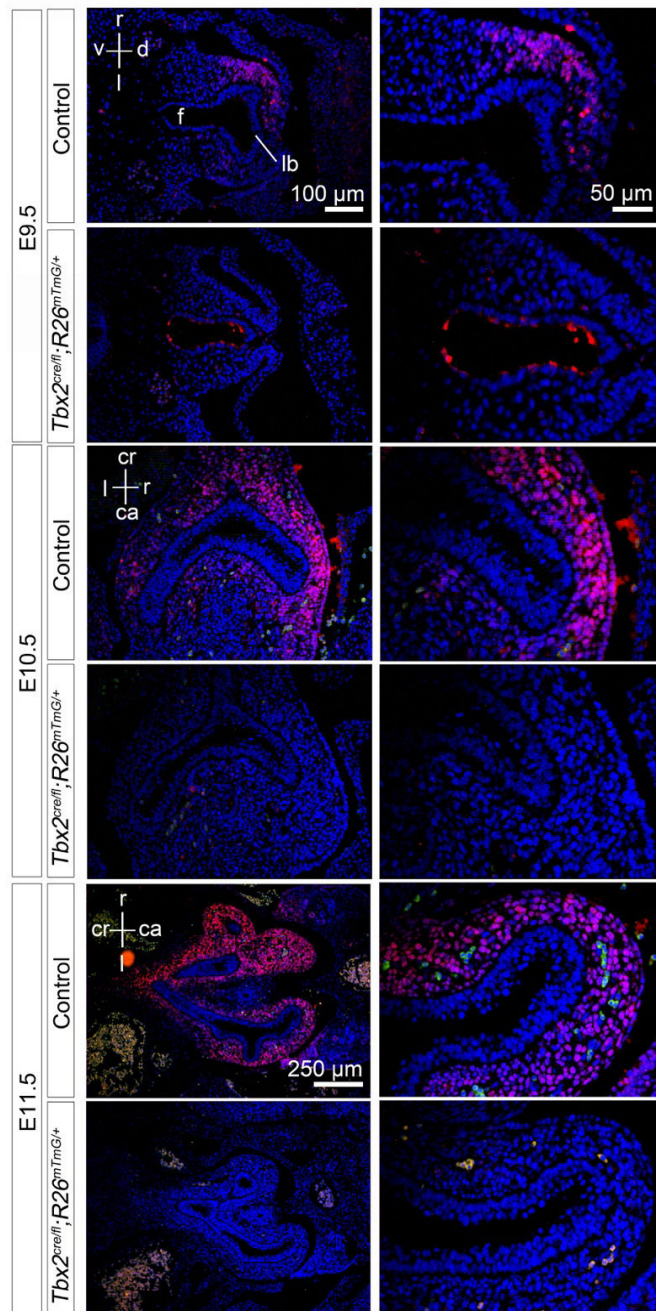
SFigure 2. *Tbx2*/TBX2 expression and lineage contribution to the lung mesenchyme at E9.5.

(A) *In situ* hybridization analysis of expression of the lung bud marker *Nkx2.1* and of *Tbx2* on adjacent transverse sections of wildtype embryos at the indicated somite numbers. (B) Double immunofluorescence analysis of expression of TBX2 with the epithelial marker CDH1 on sections of wildtype embryos, and of the lineage marker GFP with the epithelial marker CDH1 on sections of *Tbx2^{cre/+};R26^{mTmG/+}* embryos. Antigens are color-coded, stages are as indicated. Nuclei were counterstained with DAPI. d: dorsal; f: foregut; l: left; lb: lung bud; r: right; v: ventral.



SFigure 3. *Tbx2*/TBX2 expression and lineage contribution in the lung bud mesenchyme of *Tbx2*-deficient embryos.

(A) *In situ* hybridization analysis of expression of the lung bud marker *Nkx2.1* and (B) immunofluorescence analysis of expression of TBX2 and the epithelial marker CDH1 and of the lineage marker GFP together with the epithelial marker CDH1 on transverse sections of *Tbx2*^{cre/fl};*R26*^{mTmG/+} embryos at a developmental stage of 23 and 24 somites. Antigens are color-coded, stages are as indicated. Nuclei were counterstained with DAPI. d: dorsal; f: foregut; l: left; lb: lung bud; r: right; v: ventral.



SFigure 4. TBX2 expression is lost in the pulmonary mesenchyme of *Tbx2*^{cre/fl};*R26*^{mTmG/+} embryos in early lung development.

Immunofluorescence staining of TBX2 expression (red) on transverse (E9.5) and frontal (E10.5, E11.5) sections of control and *Tbx2*-deficient embryos. Higher magnifications are shown on the right panel. Stages and genotypes are as indicated. Nuclei were counterstained with DAPI. ca: caudal; cr: cranial; d: dorsal; f: foregut; l: left; lb: lung bud; r: right; v: ventral.

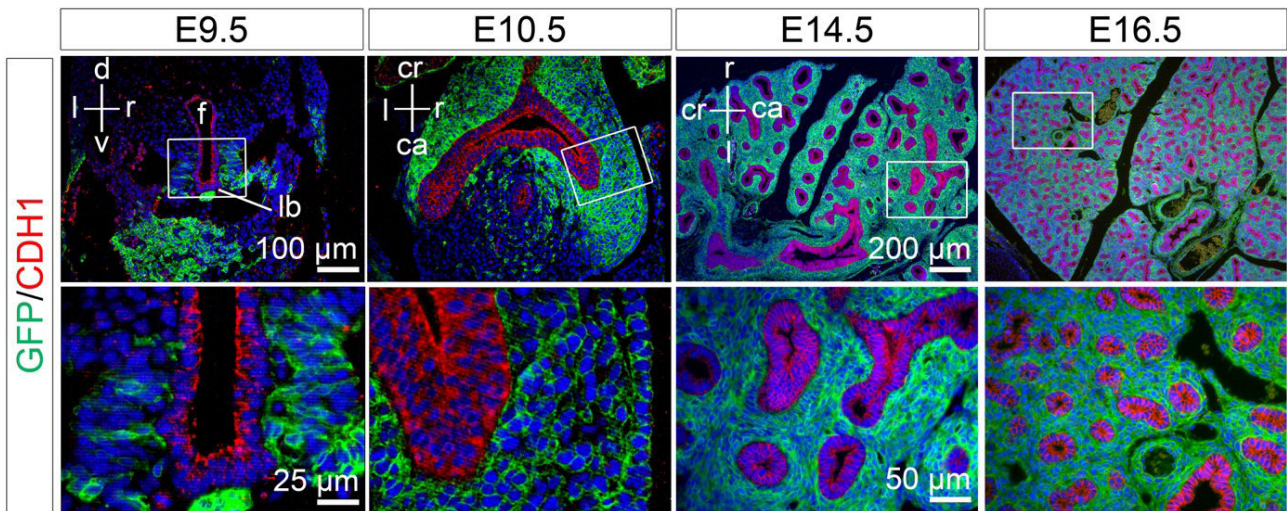


Figure 5. The TBX2⁺ lineage does not contribute to the pulmonary epithelium in *Tbx2*-deficient embryos.

Double immunofluorescence analysis of the lineage marker GFP and the epithelial marker CDH1 on transverse (E9.5) and frontal (E10.5, E14.5, E16.5) sections of *Tbx2^{cre/fl};R26^{mTmG}*⁺ lungs at different developmental stages. Antigens are color-coded, stages and genotypes are as indicated. Nuclei were counterstained with DAPI. Insets in overview images are magnified in the row below. ca: caudal; cr: cranial; d: dorsal; f: foregut; l: left; lb: lung bud; r: right; v: ventral.

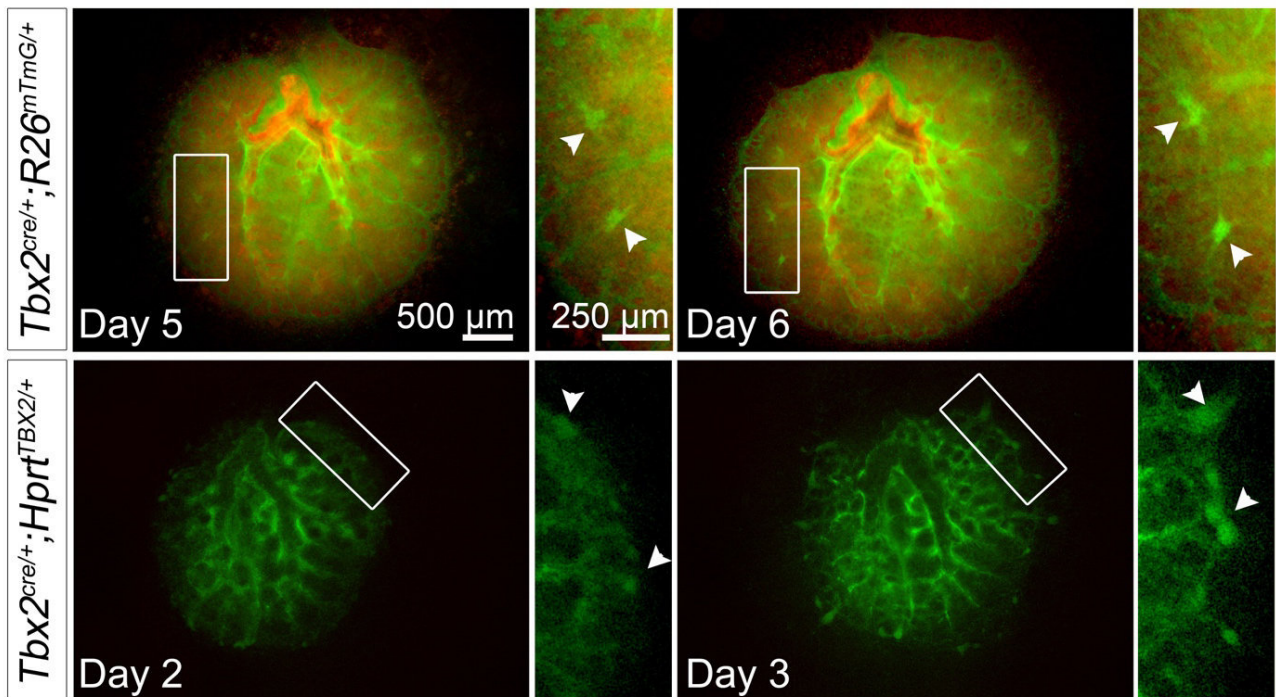
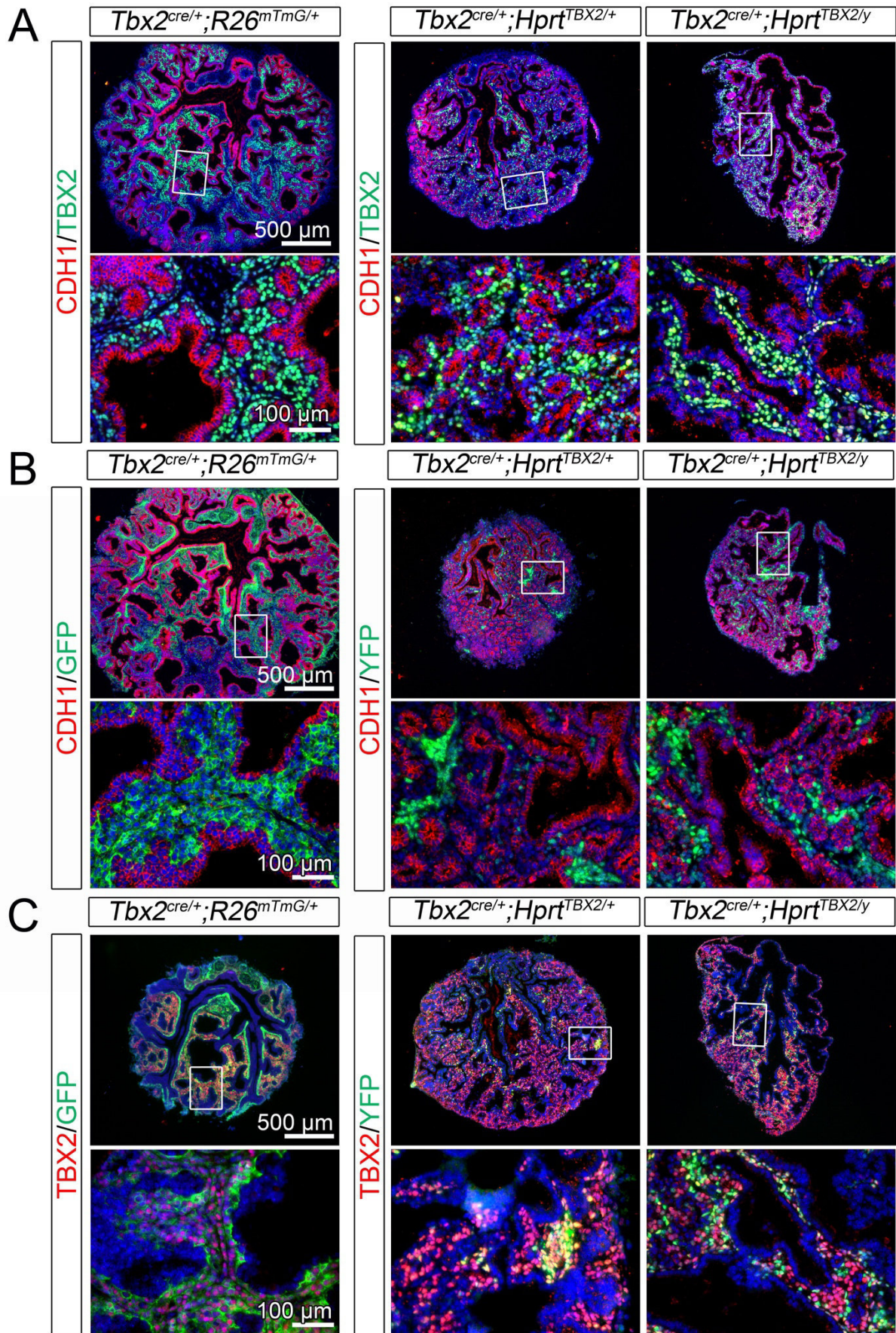


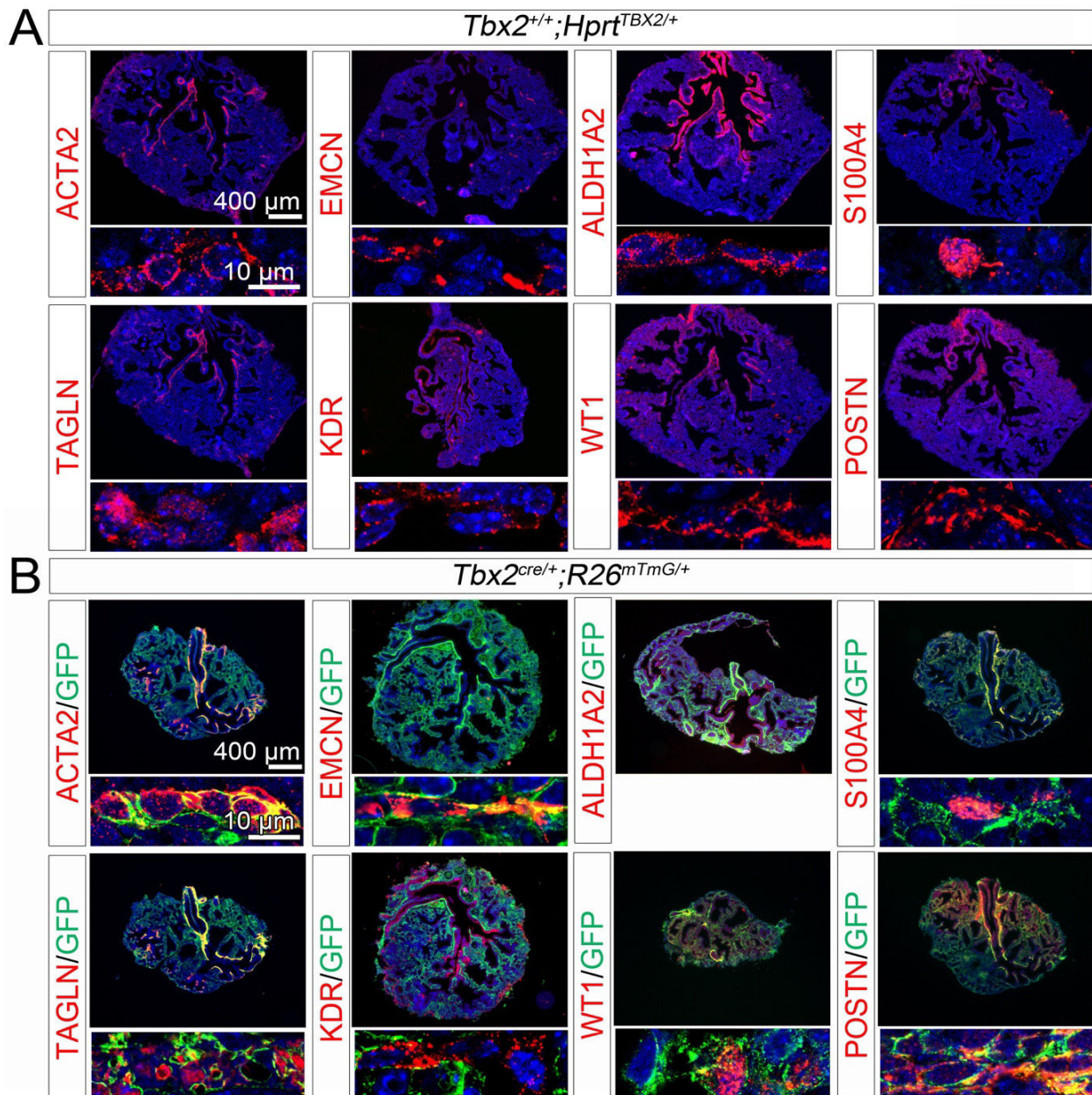
Figure 6. Overexpression of TBX2 leads to enhanced and premature formation of lineage positive cell clusters.

Analysis of GFP/RFP epifluorescence of *Tbx2*^{cre/+};*R26*^{mTmG/+} (control) and *Tbx2*^{cre/+};*Hprt*^{TBX2/+} lung explants at different time-points of the culture. Clusters of irregularly distributed GFP⁺ cells (arrowheads) were observed in *Tbx2*^{cre/+};*R26*^{mTmG/+} controls at day 5 of the culture. In *Tbx2*^{cre/+};*Hprt*^{TBX2/+} mutant lungs GFP⁺ clusters appeared at day 2 of the culture and were evenly arranged at the rim. Stages and genotypes are as indicated. Insets in overview images are magnified on the panels on the right.



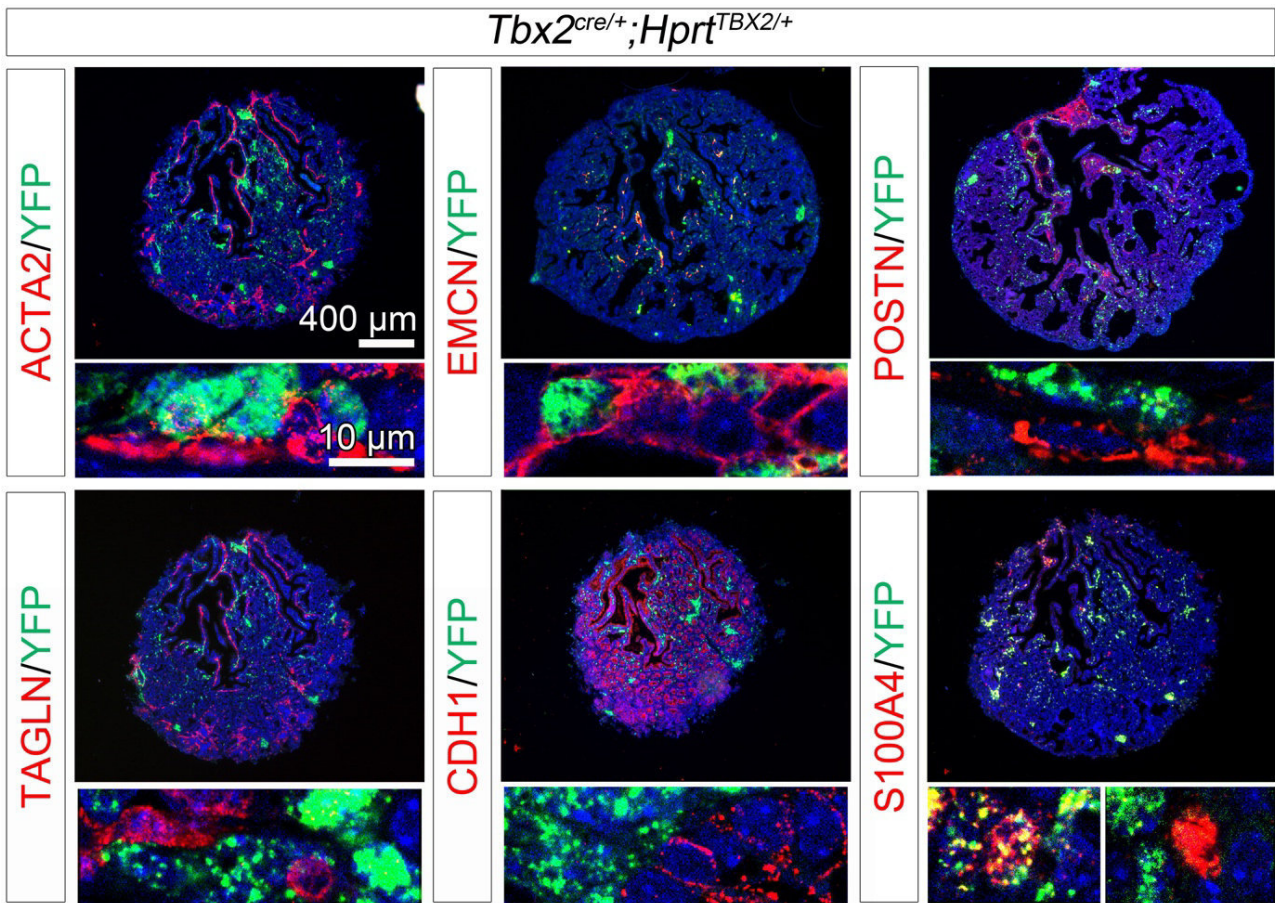
SFigure 7. TBX2 expression and TBX2 lineage contribution in control and constitutively TBX2 overexpressing lung explant cultures.

(A) Double immunofluorescence analysis of expression of TBX2 and the epithelial marker CDH1 in lung explants of *Tbx2^{cre/+};R26^{mTmG/+}* (control), *Tbx2^{cre/+};Hprt^{TBX2/+}* and *Tbx2^{cre/+};Hprt^{TBX2/y}* embryos cultured for 6 or 8 days. (B) The distribution of lineage positive cells was analyzed by double immunofluorescence stainings of the epithelial marker CDH1 and the lineage marker GFP and YFP, respectively. (C) The correlation of TBX2 expression with TBX2 lineage was investigated using TBX2/GFP and TBX2/YFP co-stainings. Antigens are color-coded, genotypes are as indicated. Nuclei were counterstained with DAPI. Insets of overview images are magnified in the row below.



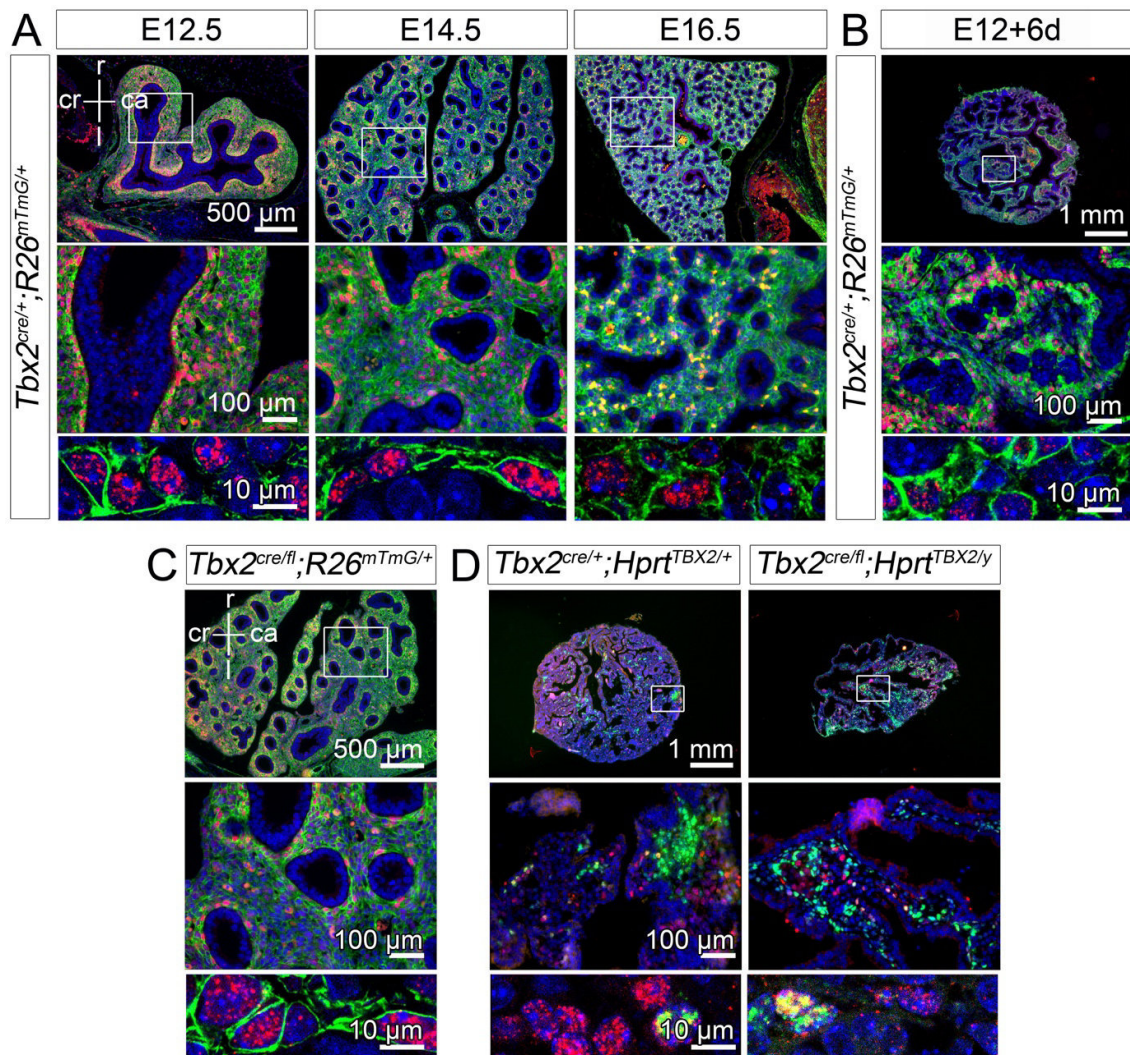
SFigure 8. Validation of cell-type specific markers and of TBX2⁺ cell lineage contribution in lung explant cultures.

(A) *Ex vivo* validation of the expression pattern of different cell-type specific markers on sections of *Cre*-negative control cultures explanted at E12.5 and cultured for 8 days. (B) Lineage tracing of TBX2-positive cells in E12.5 *Tbx2^{cre/+};R26^{mTmG/+}* lung explants cultured for 6 days. Antigens are color-coded, stages and genotypes are as indicated. Nuclei were counterstained with DAPI. Selected regions of overview images are magnified in the row below.



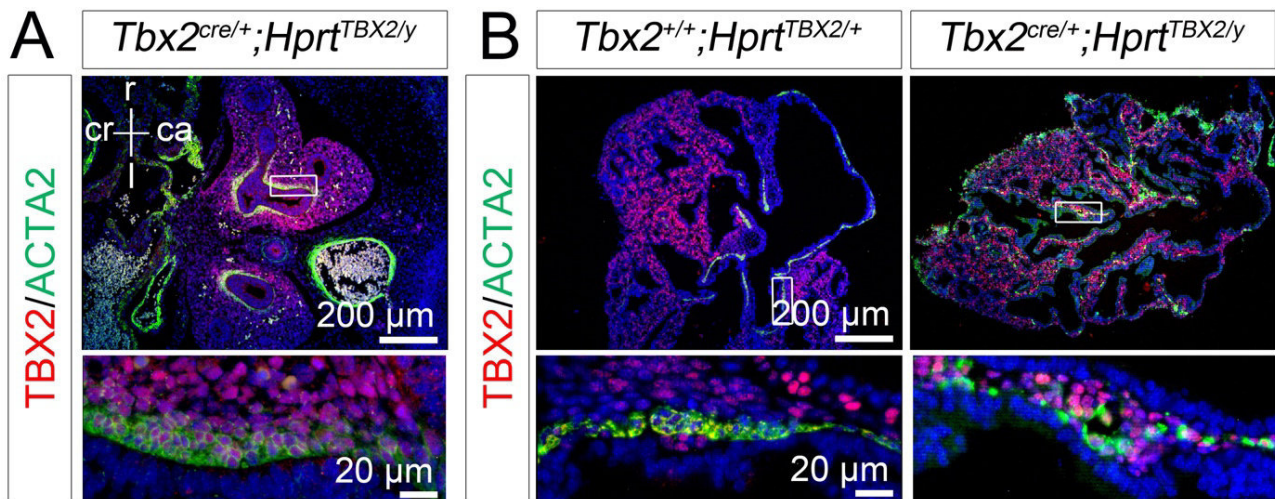
SFigure 9. Mesenchymal mosaic overexpression of TBX2 does not affect the lineage diversification of TBX2-expressing cells.

Double immunofluorescence analysis of expression of cell-type specific marker proteins (TAGLN, ACTA2 for SMCs; EMCN for the endothelium; CDH1 for the epithelium; S100A4 for different types of fibroblasts, and POSTN for the ECM) and of the TBX2 lineage marker YFP on frontal sections of explants of E12.5 *Tbx2^{cre/+};Hprt^{TBX2/+}* lungs cultured for 8 days. Antigens are color-coded. Nuclei were counterstained with DAPI. Selected regions of overview images are magnified in the row below.



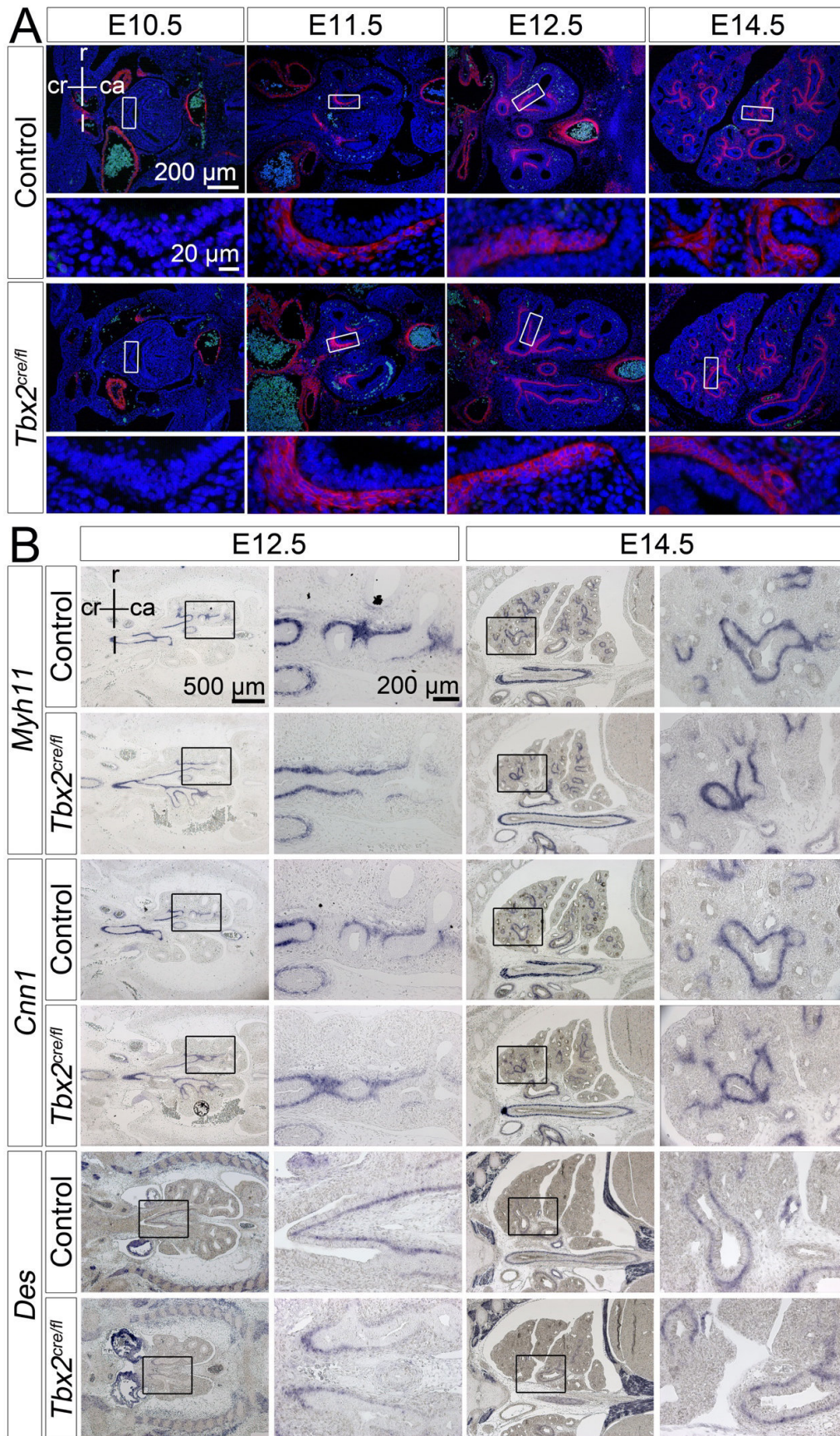
SFigure 10. Expression analysis of TBX3 and TBX2⁺ cell lineage contribution to TBX3 expressing cells.

(A, B, C) Co-immunofluorescence analysis of expression of TBX3 (in red) and the lineage marker GFP (in green) on frontal sections of lungs from *Tbx2^{cre/+};R26^{mTmG/+}* control embryos at E12.5, E14.5, E16.5 (A), in 6-day cultures of E12.5 lung explants (B), and on lungs with conditional loss of *Tbx2* (*Tbx2^{cre/fl};R26^{mTmG/+}*) at E14.5 (C). (D) Co-immunofluorescence analysis of expression of TBX3 (in red) and the lineage marker YFP (in green) on sections of E12.5 lung explants from *Tbx2^{cre/+};Hprt^{TBX2/+}* and *Tbx2^{cre/+};Hprt^{TBX2/y}* mutant embryos cultured for 8 days. Stages and genotypes are as indicated. Nuclei were counterstained with DAPI. Insets or selected regions of overview images are magnified in the rows below. ca: caudal; cr: cranial; l: left; r: right.



SFigure 11. Analysis of ACTA2 expression in *Tbx2*^{cre/+};*Hprt*^{TBX2/y} lungs.

Double immunofluorescence analysis of expression of TBX2 and the SMC marker ACTA2 on frontal sections of E12.5 embryos (A) and on 8-day cultures of E12.5 lung explants (B). Antigens are color-coded, stages and genotypes are as indicated. Nuclei were counterstained with DAPI. Insets of overview images are magnified in the rows below. ca: caudal; cr: cranial; l: left; r: right.



SFigure 12. Analysis of SMC differentiation in *Tbx2*^{cre/fl};*R26*^{mTmG/+} lungs.

(A) Immunofluorescence analysis of ACTA2 expression on frontal sections of the lung of control and *Tbx2*^{cre/fl};*R26*^{mTmG/+} mice at E10.5, E11.5, E12.5 and E14.5. Nuclei were counterstained with DAPI. (B) *In situ* hybridization analysis of expression of the SMC marker genes *Myh11*, *Cnn1* and *Des* on frontal lung sections of *Tbx2*-deficient and control embryos at E12.5 and E14.5. Probes, stages and genotypes are as indicated. Insets of overview images are magnified in the row below (A) or in the column to the right (B). ca: caudal; cr: cranial; l: left; r: right.

Additional file 2

Table S1: refers to Fig. 1F, 1G, 2C, 2D, 3B, 3C and 5B

<i>Tbx2^{fl/yf};R26^{mTmG*}</i> (Control)		Stage	staining	positive area (%)	TBX2+ cells (%)	positive area (%)	TBX2+ cells (%)	positive area (%)	TBX2+ cells (%)	positive area (%)	TBX2+ cells (%)	average positive area (%)	TBX2+ cells (%)		
refers to Fig. 1F		E10.5	TBX2	4,866	100,89	4,281	84,29	3,641	64,83			83,34	18,05		
			DAPI	4,823		5,079		5,616							
		E12.5	TBX2	22,416	80,71	25,115	99,17	12,471	99,55	14,745	96,37	30,485	100,54	95,27	8,29
			DAPI	27,774		25,324		12,527		15,3		30,321		101,12	3,09
refers to Fig. 1G		E14.5	TBX2	30,836	103,66	30,179	97,68	30,922	102,03				97,87	1,96	
			DAPI	29,748		30,896		30,306							
		E16.5	TBX2	30,094	99,71	30,214	98,10	13,447	95,80	14,036					
			DAPI	30,181		30,799									
refers to Fig. 2C		E14.5	TBX2	5,05	100,20	3,67	78,00	2,66	82,17			86,79	11,80		
			ACTA2	5,04		4,705		3,237					80,88	22,94	
		E14.5	TBX2	5,14	101,60	6,465	84,82	4,153	56,23						
			TAGLN	5,059		7,622		7,386							
		E14.5	TBX2	6,831	40,92	2,57	52,95	4,656	29,68	7,2	49,49		43,26	10,37	
			EMCN	16,695		4,854		15,687		14,549					
		E14.5	TBX2	0,873	57,93	0,965	68,54	1,015	49,68				58,72	9,45	
			ALDH1A2	1,507		1,408		2,043							
		E14.5	TBX2	6,203	113,38	2,558	63,13	2,689	90,63				89,05	25,16	
			POSTN	5,471		4,052		2,967							
		E14.5	TBX2	3,003	83,63	3,276	97,70						90,66	9,95	
			PDGFRA	3,591		3,353									
		E14.5	TBX2	2,483	58,11	9,166	87,51						72,81	20,79	
			PDGFRB	4,273		10,474									
refers to Fig. 2C		E10.5	GFP	20,823	94,49	17,476	79,94	19,515	89,11			87,84	7,36		
			DAPI	22,037		21,862		21,901							
		E12.5	GFP	7,068	102,24	7,233	117,15	4,167	91,95				103,78	12,67	
			DAPI	6,913		6,174		4,532							
		E14.5	GFP	44,283	95,72	46,742	99,44	52,192	97,58				97,58	1,86	
			DAPI	46,264		47,007		53,484							
refers to Fig. 2C		E16.5	GFP	50,83	99,59	52,521	102,29	44,374	104,32			102,07	2,37		
			DAPI	51,039		51,346		42,536							

Stage	staining	positive area (%)	TBX2+ cells (%)	positive area (%)	TBX2+ cells (%)	positive area (%)	TBX2+ cells (%)	positive area (%)	TBX2+ cells (%)	positive area (%)	TBX2+ cells (%)	average positive TBX2+ cells (%)
refers to Fig. 2D	E14.5	GFP	4,684	100,43	2,746	102,16	4,883	91,24	4,883	91,24	97,94	5,87
		ACTA2	4,664		2,688		5,352		5,352		97,04	1,83
	E14.5	GFP	8,037	96,51	4,84	99,08	6,488	95,54	6,488	95,54		
		TAGLN	8,328		4,885		6,791		6,791			
	E14.5	GFP	17,146	122,25	18,946	91,08	14,815	89,89	14,815	89,89	101,07	18,35
		EMCN	14,025		20,802		16,481		16,481			
	E14.5	GFP	0,877	46,35	1,17	66,36	0,914	60,81	0,914	60,81	57,84	10,33
		ALDH1A2	1,892		1,763		1,503		1,503			
	E16.5	GFP	3,174	100,06	5,514	93,00	8,212	79,25	8,212	79,25	90,77	10,58
		POSTN	3,172		5,929		10,362		10,362			
	E16.5	GFP	0,636	77,94	4,781	74,04	3,13	83,87	3,13	83,87	78,62	4,95
		PDGFRA	0,816		6,457		3,732		3,732			
	E16.5	GFP	1,039	37,00	1,503	49,93	1,096	53,94	1,096	53,94	46,96	8,85
		PDGFRB	2,808		3,01		2,032		2,032			
	refers to Fig. 5B	E11.5	TBX2	2,449	97,07	1,698	88,58					92,82
		TAGLN	2,523		1,917							
E12.5		TBX2	1,472	103,59	4,643	104,03	4,479	95,06	4,479	95,06	99,43	5,06
		TAGLN	1,421		4,463		4,712		4,712			
E14.5		TBX2	5,14	101,60	6,465	84,82	4,153	56,23	4,153	56,23	80,88	22,94
		TAGLN	5,059		7,622		7,386		7,386			
E16.5		TBX2	4,047	70,25	2,388	56,18	2,848	61,34	2,848	61,34	62,59	7,12
		TAGLN	5,761		4,251		4,643		4,643			
E11.5		TBX2	2,801	97,19	3,061	99,42	3,071	98,87	3,071	98,87	98,49	1,16
		ACTA2	2,882		3,079		3,106		3,106			
E12.5		TBX2	1,996	102,10	0,705	62,17	0,933	84,28	0,933	84,28	86,52	14,18
		ACTA2	1,955		1,134		1,107		1,107			
E14.5		TBX2	5,05	100,20	3,67	78,00	2,66	82,17	2,66	82,17	86,79	11,80
		ACTA2	5,04		4,705		3,237		3,237			
E16.5		TBX2	4,062	42,15	5,818	39,26	1,787	36,77	1,787	36,77	39,39	2,70
	ACTA2	9,636		14,821		4,86		4,86				

Tbx2^{creffl};R26^{mTmG+} (Mutant)

refers to Fig. 3B

Stage	staining	positive area (%)	TBX2+ cells (%)	positive area (%)	TBX2+ cells (%)	positive area (%)	TBX2+ cells (%)	positive area (%)	TBX2+ cells (%)	positive area (%)	TBX2+ cells (%)	average positive area (%)	average TBX2+ cells (%)
E10.5	GFP	21,983	95.52	11.62	69.44	13,723	76.02	20,283	82.79	20,283	82.79	80.95	11.14
	DAPI	23,013		16,734		18,051		24,498		24,498			
	GFP	50,098	102.19	46,135	98.43	49,391	102.37					101.00	2.23
E16.5	DAPI	49,023		46,873		48,249						99.96	0.87
	GFP	49,838	100.96	41,624	99.35	41,136	99.57						
	DAPI	49,364		41,896		41,313							
E14.5	GFP	4,229	110.33	2.55	99.18	6,243	101.84					103.79	5.82
	ACTA2	3,833		2,571		6.13							
E14.5	GFP	6,991	97.10	4,409	51.45	12,789	98.23					82.26	26.68
	TAGLN	7.2		8.569		13.02							
E14.5	GFP	15,238	110.36	11,684	106.55	15,534	65.43					94.11	24.91
	EMCN	13,807		10,966		23,741							
E14.5	GFP	1,635	68.76	1,871	64.10	0,998	45.47					59.44	12.32
	ALDH1A2	2,378		2,919		2,195							
E16.5	GFP	13,522	93.99	2,118	77.87	9,719	87.06					86.31	8.09
	POSTN	14,387		2.72		11,163							
E16.5	GFP	6,106	98.63	7,363	87.70	5,821	75.97					87.43	11.33
	PDGFRA	6,191		8,396		7,662							
E16.5	GFP	1,633	43.11	5,153	71.61	2.61	68.76					61.16	15.70
	PDGFRB	3,788		7,196		3,796							

refers to Fig. 3C

Part 1 - Lineage tracing of TBX2⁺ cells and the role of TBX2 in cell fate decision

Table S1: refers to Fig. 1F, 1G, 2C, 2D, 3B, 3C and 5B

Tbx2^{+/fl};R26^{mTmG/+} (Control)

Tbx2^{cre/fl};R26^{mTmG/+} (Mutant)

	Stage	staining		average % of TBX2+ cells	sd		Stage	staining		average % of TBX2+ cells	sd
refers to Fig. 1F	E10.5	TBX2	DAPI	83,34	18,05	refers to Fig. 3B	E10.5	GFP	DAPI	80,95	11,14
	E12.5	TBX2	DAPI	95,27	8,29		E14.5	GFP	DAPI	101,00	2,23
	E14.5	TBX2	DAPI	101,12	3,09		E16.5	GFP	DAPI	99,96	0,87
	E16.5	TBX2	DAPI	97,87	1,96	refers to Fig. 3C	E14.5	GFP	ACTA2	103,79	5,82
refers to Fig. 1G	E14.5	TBX2	ACTA2	86,79	11,80		E14.5	GFP	TAGLN	82,26	26,68
	E14.5	TBX2	TAGLN	80,88	22,94		E14.5	GFP	EMCN	94,11	24,91
	E14.5	TBX2	EMCN	43,26	10,37		E14.5	GFP	ALDH1A2	59,44	12,32
	E14.5	TBX2	ALDH1A2	58,72	9,45		E16.5	GFP	POSTN	86,31	8,09
	E14.5	TBX2	POSTN	89,05	25,16		E16.5	GFP	PDGFRA	87,43	11,33
	E14.5	TBX2	PDGFRA	90,66	9,95		E16.5	GFP	PDGRFB	61,16	15,70
	E14.5	TBX2	PDGRFB	72,81	20,79						
	refers to Fig. 2C	E10.5	GFP	DAPI	87,84	7,36					
E12.5		GFP	DAPI	103,78	12,67						
E14.5		GFP	DAPI	97,58	1,86						
E16.5		GFP	DAPI	102,07	2,37						
refers to Fig. 2D	E14.5	GFP	ACTA2	97,94	5,87						
	E14.5	GFP	TAGLN	97,04	1,83						
	E14.5	GFP	EMCN	101,07	18,35						
	E14.5	GFP	ALDH1A2	57,84	10,33						
	E16.5	GFP	POSTN	90,77	10,58						
	E16.5	GFP	PDGFRA	78,62	4,95						
	E16.5	GFP	PDGRFB	46,96	8,85						
refers to Fig. 5B	E11.5	TBX2	TAGLN	92,82	6,00						
	E12.5	TBX2	TAGLN	99,43	5,06						
	E14.5	TBX2	TAGLN	80,88	22,94						
	E16.5	TBX2	TAGLN	62,59	7,12						
refers to Fig. 5B	E11.5	TBX2	ACTA2	98,49	1,16						
	E12.5	TBX2	ACTA2	86,52	14,18						
	E14.5	TBX2	ACTA2	86,79	11,80						
	E16.5	TBX2	ACTA2	39,39	2,70						

Tbx2^{+/fl};26R^{mTmG/+} (Control)				Tbx2^{cre/fl};R26^{mTmG/+} (Mutant)											
	N1	N2	N3	average	sd		N1	N2	N3	N4	average	sd	t-test		
E10.5	GFP	94.5	79.94	89.11	87.84	7.36	E10.5	GFP	95.52	69.44	76.02	82.79	80.95	11.14	0.446
	DAPI							DAPI							
E14.5	GFP	95.72	99.44	97.58	97.58	1.86	E14.5	GFP	102.19	98.43	102.37		100.995	2.23	0.111
	DAPI							DAPI							
E16.5	GFP	99.59	102.29	104.32	102.07	2.37	E16.5	GFP	100.96	99.35	99.57		99.9609	0.87	0.223
	DAPI							DAPI							
E14.5	GFP	100.43	102.16	91.24	97.94	5.87	E14.5	GFP	110.33	99.18	101.84		103.786	5.82	0.288
	ACTA2							ACTA2							
E14.5	GFP	96.51	99.08	95.54	97.04	1.83	E14.5	GFP	97.10	51.45	98.23		82.2586	26.68	0.393
	TAGLN							TAGLN							
E14.5	GFP	122.25	91.08	89.89	101.07	18.35	E14.5	GFP	110.36	106.55	65.43		94.1143	24.91	0.717
	EMCN							EMCN							
E14.5	GFP	46.35	66.36	60.81	57.84	10.33	E14.5	GFP	68.76	64.10	45.47		59.4398	12.32	0.872
	ALDH1A2							ALDH1A2							
E16.5	GFP	100.06	93.00	79.25	90.77	10.58	E16.5	GFP	93.99	77.87	87.06		86.3066	8.09	0.593
	POSTN							POSTN							
E16.5	GFP	77.94	74.04	83.87	78.62	4.95	E16.5	GFP	98.63	87.70	75.97		87.432	11.33	0.284
	PDGFRA							PDGFRA							
E16.5	GFP	37.00	49.93	53.94	46.96	8.85	E16.5	GFP	43.11	71.61	68.76		61.1585	31.14	0.244
	PDGFRB							PDGFRB							

Additional file 3

Table S2: refers to Fig. 6B and 6C
Tbx2^{fl/y};R26^{mTmG/+} and Tbx2^{cre/fl/y};R26^{mTmG/+}

24hr	Kymograph measurement														
	Culture 1					Culture 2					Culture 3				
Control 1	Control 2	Control 3	Control 4	Control 5	Control 6	Control 7	Control 8	Control 9	Control 10	Control 11	Control 12	Control 13	Control 14	Control 15	
0.004	0.006	0.000	0.009	0.001	0.005	0.043	0.000	0.010	0.005	0.002	0.003	0.002	0.009	0.000	
0.042	0.076	0.028	0.122	0.031	0.104	0.050	0.087	0.010	0.014	0.042	0.020	0.050	0.033	0.011	
0.181	0.188	0.093	0.193	0.119	0.341	0.235	0.168	0.034	0.041	0.166	0.110	0.166	0.072	0.038	
0.199	0.309	0.198	0.258	0.174	0.399	0.267	0.222	0.110	0.064	0.243	0.130	0.150	0.132	0.072	
0.299	0.293	0.317	0.420	0.251	0.429	0.357	0.314	0.132	0.064	0.246	0.208	0.244	0.170	0.105	
0.361	0.318	0.329	0.456	0.279	0.407	0.391	0.408	0.149	0.088	0.269	0.233	0.273	0.203	0.152	
0.406	0.320	0.341	0.450	0.310	0.374	0.386	0.428	0.141	0.105	0.302	0.229	0.337	0.207	0.170	
0.426	0.347	0.352	0.454	0.339	0.324	0.372	0.428	0.145	0.124	0.309	0.239	0.360	0.216	0.181	
0.422	0.335	0.358	0.449	0.341	0.285	0.360	0.422	0.149	0.145	0.297	0.274	0.398	0.212	0.167	
0.395	0.333	0.353	0.451	0.325	0.276	0.311	0.417	0.140	0.138	0.286	0.289	0.407	0.219	0.159	
0.371	0.342	0.350	0.444	0.314	0.242	0.284	0.402	0.139	0.140	0.278	0.277	0.385	0.204	0.169	
0.302	0.316	0.347	0.439	0.298	0.228	0.261	0.392	0.155	0.124	0.265	0.284	0.382	0.203	0.159	
0.276	0.257	0.326	0.427	0.254	0.187	0.280	0.366	0.135	0.129	0.228	0.291	0.356	0.194	0.158	
0.200	0.240	0.323	0.427	0.235	0.172	0.258	0.304	0.130	0.116	0.204	0.297	0.348	0.185	0.137	
0.125	0.246	0.317	0.421	0.226	0.140	0.243	0.267	0.115	0.123	0.204	0.300	0.339	0.162	0.116	
0.101	0.232	0.312	0.382	0.206	0.120	0.227	0.238	0.092	0.119	0.212	0.282	0.288	0.155	0.100	
0.070	0.210	0.312	0.320	0.165	0.102	0.195	0.205	0.100	0.116	0.217	0.261	0.265	0.123	0.077	
0.058	0.184	0.310	0.267	0.146	0.086	0.167	0.205	0.091	0.096	0.195	0.259	0.242	0.090	0.048	
0.056	0.171	0.284	0.261	0.130	0.059	0.138	0.196	0.081	0.076	0.164	0.255	0.251	0.073	0.040	
0.087	0.161	0.232	0.243	0.115	0.049	0.122	0.197	0.081	0.078	0.172	0.249	0.200	0.047	0.030	
0.071	0.170	0.200	0.225	0.120	0.033	0.109	0.186	0.080	0.087	0.152	0.223	0.200	0.032	0.052	
0.077	0.137	0.186	0.202	0.122	0.032	0.109	0.181	0.064	0.088	0.131	0.190	0.192	0.029	0.052	
0.079	0.096	0.146	0.155	0.113	0.023	0.092	0.176	0.086	0.097	0.094	0.166	0.198	0.026	0.051	
0.078	0.087	0.133	0.162	0.110	0.027	0.068	0.173	0.082	0.094	0.067	0.137	0.188	0.024	0.046	
0.089	0.055	0.124	0.151	0.110	0.032	0.065	0.150	0.081	0.091	0.076	0.100	0.162	0.020	0.043	
0.078	0.065	0.118	0.160	0.107	0.029	0.055	0.146	0.062	0.085	0.066	0.102	0.146	0.033	0.034	

Table S2: refers to Fig. 6B and 6C
Tbx2^{+/fl};R26^{mTmG/+} and Tbx2^{cre/fl};R26^{mTmG/+}

Kymograph measurement

36hr	Control 1	Control 2	Control 3	Control 4	Control 5	Control 6	Control 7	Control 8	Control 9	Control 10	Control 11	Control 12	Control 13	Control 14	Control 15
0.001	0.003	0.009	0.009	0.000	0.000	0.000	0.001	0.014	0.013	0.011	0.001	0.000	0.000	0.000	0.006
0.033	0.128	0.004	0.004	0.114	0.010	0.003	0.010	0.027	0.044	0.050	0.016	0.025	0.032	0.025	0.031
0.245	0.275	0.038	0.038	0.208	0.070	0.164	0.196	0.132	0.126	0.116	0.043	0.101	0.082	0.047	0.051
0.369	0.461	0.084	0.084	0.276	0.187	0.242	0.292	0.353	0.138	0.150	0.061	0.178	0.168	0.054	0.098
0.481	0.590	0.206	0.206	0.412	0.386	0.347	0.383	0.493	0.180	0.206	0.100	0.226	0.195	0.073	0.136
0.586	0.595	0.245	0.245	0.465	0.397	0.368	0.422	0.528	0.174	0.210	0.197	0.276	0.224	0.087	0.171
0.665	0.633	0.319	0.319	0.449	0.492	0.356	0.438	0.512	0.180	0.242	0.254	0.292	0.266	0.083	0.193
0.671	0.621	0.333	0.333	0.448	0.504	0.309	0.396	0.512	0.199	0.236	0.273	0.285	0.291	0.082	0.240
0.669	0.601	0.340	0.340	0.444	0.503	0.202	0.348	0.497	0.193	0.220	0.265	0.264	0.304	0.089	0.276
0.636	0.557	0.325	0.325	0.443	0.494	0.177	0.281	0.478	0.162	0.204	0.270	0.233	0.305	0.080	0.288
0.599	0.507	0.296	0.296	0.449	0.477	0.154	0.237	0.388	0.127	0.160	0.247	0.210	0.299	0.074	0.286
0.519	0.465	0.259	0.259	0.448	0.451	0.144	0.211	0.333	0.102	0.156	0.219	0.183	0.300	0.077	0.286
0.382	0.438	0.212	0.212	0.415	0.345	0.115	0.147	0.253	0.101	0.128	0.195	0.162	0.289	0.076	0.267
0.355	0.404	0.188	0.188	0.377	0.297	0.122	0.144	0.195	0.086	0.104	0.176	0.146	0.296	0.068	0.248
0.314	0.302	0.149	0.149	0.301	0.288	0.111	0.099	0.174	0.086	0.080	0.129	0.132	0.279	0.068	0.216
0.299	0.298	0.125	0.125	0.261	0.269	0.104	0.102	0.185	0.080	0.073	0.099	0.108	0.282	0.068	0.164
0.287	0.265	0.078	0.078	0.227	0.209	0.102	0.088	0.191	0.062	0.058	0.094	0.098	0.256	0.051	0.124
0.291	0.261	0.072	0.072	0.218	0.186	0.099	0.079	0.178	0.065	0.058	0.070	0.090	0.228	0.044	0.106
0.302	0.222	0.053	0.053	0.184	0.153	0.085	0.062	0.171	0.063	0.065	0.059	0.082	0.225	0.041	0.089
0.284	0.204	0.048	0.048	0.183	0.141	0.074	0.037	0.159	0.044	0.050	0.054	0.088	0.192	0.027	0.056
0.284	0.204	0.055	0.055	0.180	0.125	0.068	0.029	0.149	0.050	0.056	0.038	0.085	0.181	0.035	0.058
0.277	0.197	0.058	0.058	0.165	0.116	0.053	0.036	0.133	0.044	0.061	0.026	0.083	0.170	0.031	0.032
0.254	0.183	0.055	0.055	0.131	0.104	0.055	0.033	0.109	0.041	0.059	0.004	0.078	0.163	0.039	0.022
0.239	0.197	0.058	0.058	0.126	0.103	0.059	0.036	0.096	0.021	0.060	0.009	0.098	0.144	0.032	0.011
0.222	0.189	0.053	0.053	0.091	0.081	0.041	0.030	0.086	0.017	0.068	0.012	0.094	0.127	0.038	0.014

Table S2: refers to Fig. 6B and 6C

Tbx2^{+/fl};R26^{tmTmG/+} and Tbx2^{cre/fl};R26^{tmTmG/+}

		Kymograph measurement														
		Culture 1							Culture 2							Culture 3
24hr	Mutant 1	Mutant 2	Mutant 3	Mutant 4	Mutant 5	Mutant 6	Mutant 7	Mutant 8	Mutant 9	Mutant 10	Mutant 11	Mutant 12	Mutant 13	Mutant 14		
0.000	0.004	0.000	0.030	0.005	0.007	0.009	0.009	0.009	0.000	0.006	0.027	0.008	0.009	0.003		
0.224	0.085	0.052	0.052	0.043	0.080	0.059	0.011	0.011	0.000	0.014	0.018	0.014	0.014	0.047		
0.360	0.183	0.059	0.063	0.072	0.081	0.128	0.119	0.119	0.000	0.041	0.097	0.072	0.040	0.222		
0.439	0.288	0.102	0.098	0.086	0.148	0.142	0.159	0.159	0.000	0.064	0.165	0.146	0.044	0.220		
0.417	0.309	0.165	0.119	0.090	0.250	0.165	0.136	0.136	0.000	0.061	0.214	0.203	0.079	0.270		
0.445	0.300	0.163	0.107	0.105	0.276	0.160	0.145	0.145	0.000	0.063	0.244	0.236	0.097	0.357		
0.470	0.293	0.186	0.125	0.109	0.274	0.161	0.199	0.199	0.000	0.057	0.292	0.268	0.116	0.418		
0.480	0.287	0.197	0.137	0.084	0.266	0.169	0.207	0.207	0.000	0.057	0.305	0.310	0.135	0.465		
0.465	0.291	0.186	0.101	0.079	0.258	0.171	0.207	0.207	0.000	0.049	0.307	0.313	0.135	0.475		
0.446	0.288	0.187	0.100	0.069	0.236	0.170	0.213	0.213	0.000	0.077	0.306	0.308	0.135	0.481		
0.418	0.297	0.187	0.118	0.058	0.216	0.171	0.219	0.219	0.000	0.079	0.296	0.304	0.133	0.487		
0.403	0.315	0.195	0.125	0.052	0.189	0.156	0.215	0.215	0.000	0.092	0.277	0.300	0.135	0.505		
0.396	0.288	0.161	0.105	0.018	0.153	0.121	0.206	0.206	0.000	0.091	0.261	0.305	0.138	0.499		
0.404	0.260	0.151	0.102	0.015	0.112	0.094	0.206	0.206	0.000	0.096	0.240	0.285	0.130	0.489		
0.413	0.246	0.136	0.092	0.022	0.072	0.068	0.190	0.190	0.000	0.093	0.230	0.270	0.132	0.467		
0.412	0.229	0.116	0.097	0.036	0.064	0.064	0.179	0.179	0.000	0.078	0.194	0.258	0.131	0.448		
0.405	0.172	0.111	0.093	0.035	0.068	0.050	0.165	0.165	0.000	0.085	0.180	0.241	0.124	0.436		
0.387	0.142	0.098	0.089	0.043	0.063	0.028	0.135	0.135	0.000	0.078	0.173	0.213	0.112	0.428		
0.363	0.117	0.088	0.089	0.055	0.052	0.029	0.122	0.122	0.000	0.071	0.160	0.180	0.100	0.388		
0.333	0.076	0.057	0.078	0.047	0.057	0.013	0.116	0.116	0.000	0.068	0.157	0.167	0.101	0.360		
0.321	0.071	0.064	0.088	0.049	0.051	0.000	0.100	0.100	0.000	0.067	0.153	0.142	0.096	0.330		
0.307	0.068	0.067	0.101	0.047	0.044	0.005	0.091	0.091	0.000	0.073	0.130	0.125	0.086	0.316		
0.299	0.047	0.048	0.104	0.057	0.031	0.016	0.089	0.089	0.000	0.065	0.105	0.089	0.079	0.281		
0.281	0.037	0.019	0.108	0.060	0.028	0.029	0.102	0.102	0.000	0.059	0.076	0.082	0.071	0.261		
0.235	0.026	0.023	0.133	0.024	0.013	0.052	0.104	0.104	0.000	0.038	0.063	0.067	0.068	0.265		
0.216	0.021	0.016	0.117	0.026	0.014	0.047	0.096	0.096	0.000	0.043	0.051	0.051	0.068	0.261		

Table S2: refers to Fig. 6B and 6C

Tbx2^{fl/fl};R26^{mTmG/+}* and *Tbx2^{cre/fl};R26^{mTmG/+}

Kymograph measurement

36hr		Mutant 1	Mutant 2	Mutant 3	Mutant 4	Mutant 5	Mutant 6	Mutant 7	Mutant 8	Mutant 9	Mutant 10	Mutant 11	Mutant 12	Mutant 13	Mutant 14
0.000	0.000	0.000	0.004	0.002	0.007	0.002	0.007	0.002	0.008	0.005	0.001	0.018	0.020	0.000	0.001
0.003	0.021	0.099	0.018	0.016	0.116	0.021	0.116	0.021	0.023	0.029	0.015	0.040	0.014	0.089	0.022
0.266	0.119	0.285	0.097	0.060	0.264	0.081	0.264	0.081	0.138	0.154	0.172	0.129	0.035	0.152	0.092
0.440	0.293	0.444	0.196	0.172	0.311	0.192	0.311	0.192	0.215	0.197	0.308	0.106	0.128	0.256	0.143
0.676	0.496	0.553	0.340	0.301	0.351	0.302	0.351	0.302	0.318	0.416	0.388	0.139	0.185	0.273	0.260
0.707	0.557	0.610	0.371	0.384	0.361	0.375	0.361	0.375	0.448	0.484	0.397	0.183	0.209	0.276	0.390
0.715	0.619	0.654	0.395	0.499	0.330	0.379	0.330	0.379	0.510	0.478	0.389	0.181	0.238	0.332	0.412
0.688	0.605	0.672	0.433	0.518	0.308	0.377	0.308	0.377	0.514	0.480	0.394	0.198	0.300	0.376	0.403
0.680	0.592	0.681	0.457	0.541	0.289	0.373	0.289	0.373	0.503	0.480	0.382	0.189	0.346	0.418	0.407
0.686	0.588	0.683	0.464	0.546	0.284	0.313	0.284	0.313	0.477	0.475	0.362	0.179	0.362	0.443	0.413
0.692	0.590	0.683	0.455	0.525	0.247	0.224	0.247	0.224	0.405	0.454	0.357	0.191	0.348	0.444	0.409
0.703	0.588	0.675	0.437	0.504	0.192	0.173	0.192	0.173	0.338	0.445	0.311	0.174	0.336	0.433	0.407
0.712	0.556	0.658	0.382	0.421	0.174	0.131	0.174	0.131	0.290	0.419	0.265	0.173	0.327	0.428	0.406
0.711	0.532	0.647	0.342	0.331	0.154	0.073	0.154	0.073	0.226	0.355	0.263	0.173	0.308	0.414	0.385
0.623	0.472	0.596	0.273	0.179	0.122	0.052	0.122	0.052	0.179	0.284	0.256	0.144	0.301	0.386	0.365
0.627	0.431	0.570	0.249	0.137	0.118	0.101	0.118	0.101	0.181	0.270	0.213	0.136	0.284	0.363	0.334
0.588	0.310	0.520	0.276	0.063	0.107	0.119	0.107	0.119	0.162	0.252	0.143	0.121	0.258	0.326	0.329
0.544	0.264	0.497	0.262	0.046	0.093	0.127	0.093	0.127	0.141	0.226	0.100	0.127	0.229	0.304	0.325
0.431	0.197	0.449	0.223	0.025	0.070	0.128	0.070	0.128	0.110	0.201	0.081	0.099	0.202	0.287	0.341
0.401	0.171	0.426	0.207	0.017	0.067	0.111	0.067	0.111	0.078	0.176	0.077	0.097	0.175	0.263	0.344
0.356	0.145	0.406	0.200	0.020	0.037	0.087	0.037	0.087	0.083	0.162	0.078	0.092	0.153	0.236	0.326
0.336	0.117	0.383	0.194	0.018	0.027	0.085	0.027	0.085	0.072	0.130	0.093	0.104	0.133	0.210	0.294
0.295	0.081	0.362	0.181	0.011	0.027	0.070	0.027	0.070	0.063	0.116	0.098	0.087	0.098	0.199	0.250
0.280	0.064	0.358	0.162	0.012	0.015	0.068	0.015	0.068	0.080	0.120	0.097	0.090	0.078	0.180	0.211
0.263	0.039	0.361	0.139	0.025	0.014	0.055	0.014	0.055	0.057	0.111	0.089	0.089	0.078	0.171	0.178

Table S2: refers to Fig. 6B and 6C
Tbx2^{+/fl};R26^{mTmG/+} and *Tbx2^{cre/fl};R26^{mTmG/+}*

Integral calculation	Culture 1			Culture 2			Culture 3									
	24hr	Control 1	Control 2	Control 3	Control 4	Control 5	Control 6	Control 7	Control 8	Control 9	Control 10	Control 11	Control 12	Control 13	Control 14	Control 15
	0.023	0.041	0.132	0.061	0.158	0.075	0.223	0.047	0.043	0.010	0.009	0.022	0.012	0.026	0.021	0.005
	0.190	0.249	0.301	0.146	0.226	0.370	0.251	0.127	0.127	0.022	0.027	0.104	0.065	0.080	0.053	0.024
	0.249	0.301	0.306	0.257	0.339	0.414	0.312	0.268	0.195	0.072	0.053	0.205	0.120	0.130	0.102	0.055
	0.384	0.319	0.335	0.323	0.438	0.418	0.374	0.361	0.288	0.121	0.064	0.244	0.169	0.197	0.151	0.088
	0.416	0.334	0.346	0.346	0.453	0.390	0.388	0.418	0.361	0.140	0.076	0.258	0.220	0.258	0.186	0.129
	0.424	0.341	0.355	0.355	0.452	0.340	0.366	0.425	0.425	0.145	0.096	0.286	0.231	0.305	0.205	0.161
	0.409	0.334	0.335	0.335	0.450	0.333	0.336	0.419	0.419	0.143	0.115	0.305	0.234	0.348	0.212	0.176
	0.383	0.338	0.351	0.351	0.447	0.320	0.298	0.409	0.409	0.147	0.134	0.303	0.257	0.379	0.214	0.174
	0.336	0.329	0.348	0.348	0.441	0.306	0.273	0.397	0.397	0.139	0.139	0.282	0.283	0.396	0.211	0.163
	0.289	0.286	0.336	0.336	0.433	0.276	0.208	0.379	0.379	0.147	0.132	0.271	0.281	0.384	0.203	0.164
	0.238	0.248	0.324	0.324	0.427	0.245	0.180	0.270	0.335	0.145	0.127	0.247	0.288	0.369	0.198	0.158
	0.162	0.243	0.320	0.320	0.424	0.231	0.156	0.251	0.286	0.133	0.120	0.216	0.294	0.352	0.190	0.148
	0.113	0.239	0.314	0.314	0.402	0.216	0.130	0.235	0.253	0.123	0.120	0.204	0.299	0.344	0.174	0.127
	0.086	0.221	0.312	0.312	0.351	0.185	0.111	0.211	0.221	0.096	0.117	0.215	0.272	0.277	0.159	0.108
	0.064	0.197	0.311	0.311	0.294	0.155	0.094	0.181	0.205	0.096	0.106	0.206	0.260	0.253	0.139	0.089
	0.057	0.177	0.297	0.297	0.264	0.138	0.073	0.152	0.200	0.086	0.106	0.206	0.257	0.246	0.107	0.063
	0.071	0.166	0.258	0.258	0.252	0.122	0.054	0.130	0.196	0.081	0.077	0.168	0.252	0.235	0.060	0.035
	0.079	0.165	0.216	0.216	0.234	0.117	0.041	0.116	0.191	0.081	0.083	0.162	0.236	0.209	0.039	0.041
	0.074	0.154	0.193	0.193	0.213	0.121	0.033	0.109	0.184	0.072	0.087	0.141	0.206	0.196	0.031	0.052
	0.078	0.117	0.166	0.166	0.178	0.117	0.027	0.101	0.178	0.075	0.092	0.112	0.178	0.195	0.028	0.052
	0.079	0.091	0.139	0.139	0.158	0.111	0.025	0.080	0.174	0.084	0.095	0.080	0.152	0.193	0.025	0.048
	0.084	0.071	0.129	0.129	0.157	0.110	0.029	0.067	0.162	0.081	0.092	0.071	0.118	0.175	0.022	0.044
	0.083	0.060	0.121	0.121	0.156	0.109	0.030	0.060	0.148	0.071	0.088	0.071	0.101	0.154	0.026	0.038
	0.039	0.033	0.059	0.059	0.080	0.054	0.015	0.027	0.073	0.031	0.042	0.033	0.051	0.073	0.017	0.017
Integral sum	4.852	5.494	6.388	6.388	7.944	4.940	4.505	5.425	6.677	2.587	2.443	4.887	5.407	6.489	3.069	2.366

Table S2: refers to Fig. 6B and 6C
Tbx2^{fl/y};R26^{mTmG*}* and *Tbx2^{crefl/y};R26^{mTmG*}

Integral calculation														
36hr														
Control 1	Control 2	Control 3	Control 4	Control 5	Control 6	Control 7	Control 8	Control 9	Control 10	Control 11	Control 12	Control 13	Control 14	Control 15
0.017	0.066	0.007	0.057	0.005	0.002	0.006	0.020	0.029	0.031	0.008	0.013	0.016	0.012	0.019
0.139	0.201	0.021	0.161	0.040	0.084	0.103	0.079	0.085	0.083	0.029	0.063	0.057	0.036	0.041
0.307	0.368	0.061	0.242	0.128	0.203	0.244	0.242	0.132	0.133	0.052	0.139	0.125	0.051	0.075
0.425	0.525	0.145	0.344	0.287	0.295	0.337	0.423	0.159	0.178	0.080	0.202	0.182	0.064	0.117
0.534	0.592	0.225	0.439	0.392	0.358	0.403	0.511	0.177	0.208	0.148	0.251	0.210	0.080	0.153
0.626	0.614	0.282	0.457	0.445	0.362	0.430	0.520	0.177	0.226	0.226	0.284	0.245	0.085	0.182
0.668	0.627	0.326	0.448	0.498	0.332	0.417	0.512	0.189	0.239	0.264	0.288	0.278	0.082	0.216
0.670	0.611	0.336	0.446	0.503	0.255	0.372	0.505	0.196	0.228	0.269	0.274	0.297	0.086	0.258
0.652	0.579	0.332	0.444	0.499	0.189	0.314	0.487	0.177	0.212	0.268	0.248	0.304	0.085	0.282
0.618	0.532	0.310	0.446	0.486	0.165	0.259	0.433	0.144	0.182	0.259	0.221	0.302	0.077	0.287
0.559	0.486	0.278	0.449	0.464	0.149	0.224	0.361	0.114	0.158	0.233	0.197	0.299	0.076	0.286
0.451	0.451	0.236	0.431	0.398	0.130	0.179	0.293	0.101	0.142	0.207	0.172	0.294	0.077	0.276
0.369	0.421	0.200	0.396	0.321	0.119	0.145	0.224	0.093	0.116	0.166	0.154	0.292	0.072	0.257
0.335	0.353	0.168	0.339	0.293	0.117	0.121	0.184	0.086	0.092	0.152	0.139	0.288	0.068	0.232
0.307	0.300	0.137	0.281	0.279	0.108	0.100	0.179	0.083	0.077	0.114	0.120	0.281	0.068	0.190
0.293	0.281	0.102	0.244	0.239	0.103	0.095	0.188	0.071	0.065	0.097	0.103	0.269	0.060	0.144
0.289	0.263	0.075	0.223	0.197	0.100	0.083	0.184	0.064	0.058	0.082	0.094	0.242	0.048	0.115
0.297	0.242	0.063	0.201	0.169	0.092	0.071	0.174	0.064	0.062	0.065	0.086	0.226	0.042	0.097
0.293	0.213	0.051	0.184	0.147	0.079	0.049	0.165	0.054	0.058	0.056	0.085	0.209	0.034	0.072
0.284	0.204	0.052	0.182	0.133	0.071	0.033	0.154	0.047	0.053	0.046	0.086	0.187	0.031	0.057
0.281	0.201	0.056	0.173	0.121	0.061	0.033	0.141	0.047	0.059	0.032	0.084	0.176	0.033	0.045
0.265	0.190	0.056	0.148	0.110	0.054	0.035	0.121	0.043	0.060	0.015	0.080	0.166	0.035	0.027
0.246	0.190	0.057	0.129	0.104	0.057	0.035	0.102	0.031	0.060	0.006	0.088	0.154	0.035	0.017
0.230	0.193	0.056	0.109	0.092	0.050	0.033	0.091	0.019	0.064	0.011	0.096	0.136	0.035	0.013
0.111	0.095	0.026	0.046	0.041	0.020	0.015	0.043	0.009	0.034	0.006	0.047	0.063	0.019	0.007
Integral sum	9.264	8.799	7.018	6.388	3.554	4.137	6.338	2.392	2.877	2.912	3.615	5.297	1.388	3.466

Table S2: refers to Fig. 6B and 6C
Tbx2^{+/fl};R26^{tmTmG/+} and *Tbx2^{cre/fl};R26^{tmTmG/+}*

Integral calculation	Culture 1				Culture 2				Culture 3					
	24hr Mutant 1	Mutant 2	Mutant 3	Mutant 4	Mutant 5	Mutant 6	Mutant 7	Mutant 8	Mutant 9	Mutant 10	Mutant 11	Mutant 12	Mutant 13	Mutant 14
	0.112	0.045	0.026	0.041	0.024	0.044	0.034	0.010	0.000	0.010	0.022	0.011	0.012	0.025
	0.292	0.134	0.055	0.057	0.057	0.081	0.093	0.065	0.000	0.028	0.058	0.043	0.027	0.135
	0.399	0.235	0.080	0.081	0.079	0.115	0.135	0.139	0.000	0.053	0.131	0.109	0.042	0.221
	0.428	0.298	0.133	0.109	0.088	0.199	0.153	0.148	0.000	0.062	0.190	0.174	0.061	0.245
	0.431	0.304	0.164	0.113	0.098	0.263	0.162	0.140	0.000	0.062	0.229	0.219	0.088	0.313
	0.457	0.296	0.175	0.116	0.107	0.275	0.160	0.172	0.000	0.060	0.268	0.252	0.107	0.387
	0.475	0.290	0.192	0.131	0.096	0.270	0.165	0.203	0.000	0.057	0.298	0.289	0.126	0.441
	0.473	0.289	0.191	0.119	0.081	0.262	0.170	0.207	0.000	0.053	0.306	0.312	0.135	0.470
	0.456	0.290	0.186	0.101	0.074	0.247	0.170	0.210	0.000	0.063	0.307	0.310	0.135	0.478
	0.432	0.293	0.187	0.109	0.063	0.226	0.171	0.216	0.000	0.078	0.301	0.306	0.134	0.484
	0.410	0.306	0.191	0.121	0.055	0.202	0.164	0.217	0.000	0.086	0.287	0.302	0.134	0.496
	0.399	0.302	0.178	0.115	0.035	0.171	0.138	0.211	0.000	0.092	0.269	0.302	0.137	0.502
	0.400	0.274	0.156	0.103	0.017	0.132	0.107	0.206	0.000	0.093	0.250	0.295	0.134	0.494
	0.408	0.253	0.143	0.097	0.018	0.092	0.081	0.198	0.000	0.094	0.235	0.278	0.131	0.478
	0.412	0.237	0.126	0.094	0.029	0.068	0.066	0.184	0.000	0.085	0.212	0.264	0.131	0.458
	0.408	0.200	0.114	0.095	0.036	0.066	0.057	0.172	0.000	0.081	0.187	0.250	0.128	0.442
	0.396	0.157	0.105	0.091	0.039	0.066	0.039	0.150	0.000	0.081	0.177	0.227	0.118	0.432
	0.375	0.129	0.093	0.089	0.049	0.058	0.028	0.129	0.000	0.074	0.166	0.196	0.106	0.408
	0.348	0.096	0.072	0.083	0.051	0.054	0.021	0.119	0.000	0.069	0.158	0.173	0.101	0.374
	0.327	0.073	0.061	0.083	0.048	0.054	0.006	0.108	0.000	0.067	0.155	0.155	0.099	0.345
	0.314	0.070	0.065	0.094	0.048	0.048	0.003	0.096	0.000	0.070	0.141	0.134	0.091	0.323
	0.303	0.057	0.058	0.102	0.052	0.037	0.011	0.090	0.000	0.069	0.117	0.107	0.082	0.299
	0.290	0.042	0.034	0.106	0.058	0.030	0.023	0.095	0.000	0.062	0.090	0.085	0.075	0.271
	0.258	0.031	0.021	0.121	0.042	0.021	0.040	0.103	0.000	0.049	0.070	0.074	0.069	0.263
	0.226	0.024	0.019	0.125	0.025	0.013	0.049	0.100	0.000	0.041	0.057	0.059	0.068	0.263
	0.108	0.011	0.008	0.059	0.013	0.007	0.023	0.048	0.000	0.022	0.025	0.026	0.034	0.131
Integral sum	9.340	4.737	2.834	2.555	1.383	3.099	2.271	3.737	0.000	1.662	4.707	4.952	2.504	9.178

Table S2: refers to Fig. 6B and 6C
Tbx2^{+/fl};R26^{mTmG/+} and Tbx2^{cre/fl};R26^{mTmG/+}

36hr	Integral calculation												
	Culture 1				Culture 2				Culture 3				
Mutant 1	Mutant 2	Mutant 3	Mutant 4	Mutant 5	Mutant 6	Mutant 7	Mutant 8	Mutant 9	Mutant 10	Mutant 11	Mutant 12	Mutant 13	Mutant 14
0,001	0,010	0,049	0,011	0,009	0,061	0,012	0,016	0,017	0,008	0,029	0,017	0,045	0,011
0,134	0,070	0,192	0,057	0,038	0,190	0,051	0,081	0,091	0,093	0,085	0,024	0,120	0,057
0,353	0,206	0,365	0,146	0,116	0,288	0,136	0,177	0,175	0,240	0,117	0,081	0,204	0,118
0,558	0,394	0,498	0,268	0,236	0,331	0,247	0,267	0,307	0,348	0,122	0,157	0,265	0,201
0,691	0,526	0,581	0,356	0,342	0,356	0,339	0,383	0,450	0,393	0,161	0,197	0,275	0,325
0,711	0,588	0,632	0,383	0,442	0,346	0,377	0,479	0,481	0,393	0,182	0,223	0,304	0,401
0,702	0,612	0,663	0,414	0,509	0,319	0,378	0,512	0,479	0,391	0,189	0,269	0,354	0,408
0,684	0,598	0,676	0,445	0,529	0,298	0,375	0,509	0,480	0,388	0,193	0,323	0,397	0,405
0,683	0,590	0,682	0,461	0,543	0,286	0,343	0,490	0,477	0,372	0,184	0,354	0,397	0,410
0,689	0,589	0,683	0,460	0,535	0,265	0,269	0,441	0,464	0,359	0,185	0,355	0,444	0,411
0,697	0,589	0,679	0,446	0,514	0,220	0,198	0,371	0,449	0,334	0,183	0,342	0,439	0,408
0,707	0,572	0,666	0,410	0,463	0,183	0,152	0,314	0,432	0,288	0,173	0,331	0,431	0,407
0,712	0,544	0,652	0,362	0,376	0,164	0,102	0,258	0,387	0,264	0,173	0,318	0,421	0,395
0,667	0,502	0,621	0,307	0,255	0,138	0,063	0,202	0,319	0,260	0,158	0,304	0,400	0,375
0,625	0,451	0,583	0,261	0,158	0,120	0,076	0,180	0,277	0,235	0,140	0,292	0,375	0,350
0,607	0,370	0,545	0,262	0,100	0,113	0,110	0,171	0,261	0,178	0,128	0,271	0,344	0,332
0,566	0,287	0,508	0,269	0,055	0,100	0,123	0,152	0,239	0,121	0,124	0,243	0,315	0,327
0,488	0,230	0,473	0,242	0,035	0,082	0,127	0,126	0,213	0,091	0,113	0,215	0,295	0,333
0,416	0,184	0,437	0,215	0,021	0,069	0,119	0,094	0,188	0,079	0,098	0,189	0,275	0,342
0,378	0,158	0,416	0,204	0,019	0,052	0,099	0,081	0,169	0,077	0,095	0,164	0,249	0,335
0,346	0,131	0,395	0,197	0,019	0,032	0,086	0,078	0,146	0,085	0,098	0,143	0,223	0,310
0,316	0,099	0,373	0,187	0,014	0,027	0,078	0,068	0,123	0,095	0,095	0,115	0,205	0,272
0,287	0,073	0,360	0,172	0,012	0,021	0,069	0,071	0,118	0,098	0,089	0,088	0,189	0,231
0,272	0,052	0,359	0,151	0,019	0,015	0,061	0,068	0,115	0,093	0,090	0,078	0,175	0,195
0,132	0,020	0,180	0,069	0,012	0,007	0,027	0,028	0,055	0,044	0,044	0,039	0,085	0,089
Integral sum	12,422	8,446	12,270	6,755	4,083	4,016	5,617	6,914	5,329	3,249	5,133	7,259	7,446

Table S2: refers to Fig. 6B and 6C
Tbx2^{+/fl};R26^{mTmG/+} and *Tbx2^{cre/fl};R26^{mTmG/+}*

Branching endpoints								
	12 hr		18 hr		24 hr		36 hr	
	Control	Mutant	Control	Mutant	Control	Mutant	Control	Mutant
1	8	9	8	9	9	9	10	10
2	8	8	8	8	8	8	9	9
3	9	7	9	7	9	10	10	12
4	8	7	8	8	8	8	9	10
5	9	9	9	9	9	9	10	11
6	9	9	10	10	10	9	10	10
7	9	9	9	9	9	10	11	11
8	9	8	10	8	10	8	12	10
9	9	9	9	9	10	9	11	11
10	9	9	10	9	10	9	11	11
11	9	9	10	10	11	10	12	12
12	9	9	9	9	10	10	12	11
13	9	9	9	9	9	9	10	10
14	8		8		9		10	
15	8		9		9		9	

Table S2: refers to Fig. 6B and 6C

Tbx2^{+fl};*R26*^{mTmG/+} and *Tbx2*^{cre/fl};*R26*^{mTmG/+}

Kymograph measurement

24hr	Control		Mutant		t-test	
	average	sd	average	sd		
	0.007	0.011	0.008	0.009	0.636	n.s
	0.048	0.035	0.051	0.056	0.863	n.s
	0.139	0.084	0.110	0.092	0.374	n.s
	0.195	0.091	0.150	0.110	0.240	n.s
	0.257	0.108	0.177	0.110	0.060	n.s
	0.288	0.108	0.193	0.123	0.035	*
	0.300	0.107	0.212	0.133	0.058	n.s
	0.308	0.104	0.221	0.142	0.070	n.s
	0.308	0.101	0.217	0.144	0.059	n.s
	0.300	0.100	0.215	0.140	0.072	n.s
	0.289	0.096	0.213	0.137	0.092	n.s
	0.277	0.092	0.211	0.138	0.141	n.s
	0.257	0.088	0.196	0.141	0.166	n.s
	0.239	0.089	0.185	0.140	0.222	n.s
	0.223	0.094	0.174	0.139	0.269	n.s
	0.204	0.089	0.165	0.134	0.353	n.s
	0.183	0.083	0.155	0.130	0.491	n.s
	0.163	0.083	0.142	0.126	0.602	n.s
	0.149	0.085	0.129	0.115	0.603	n.s
	0.139	0.076	0.116	0.108	0.528	n.s
	0.129	0.069	0.109	0.101	0.537	n.s
	0.119	0.061	0.104	0.096	0.614	n.s
	0.107	0.053	0.094	0.089	0.632	n.s
	0.098	0.051	0.087	0.084	0.652	n.s
	0.090	0.044	0.079	0.081	0.663	n.s

36hr	Control		Mutant		t-test	
	average	sd	average	sd		
1	0.004	0.005	0.005	0.007	0.702	n.s
2	0.053	0.049	0.038	0.036	0.958	n.s
3	0.149	0.086	0.146	0.078	0.493	n.s
4	0.240	0.123	0.243	0.106	0.410	n.s
5	0.331	0.151	0.357	0.143	0.274	n.s
6	0.371	0.153	0.411	0.145	0.170	n.s
7	0.394	0.156	0.438	0.153	0.195	n.s
8	0.394	0.151	0.448	0.142	0.136	n.s
9	0.386	0.154	0.453	0.140	0.075	n.s
10	0.369	0.157	0.448	0.146	0.045	*
11	0.344	0.159	0.430	0.156	0.033	*
12	0.317	0.159	0.408	0.171	0.031	*
13	0.284	0.156	0.382	0.175	0.013	*
14	0.256	0.152	0.351	0.182	0.020	*
15	0.221	0.137	0.302	0.172	0.025	*
16	0.205	0.132	0.287	0.164	0.021	*
17	0.182	0.123	0.255	0.155	0.024	*
18	0.168	0.117	0.235	0.148	0.034	*
19	0.147	0.105	0.203	0.132	0.059	n.s
20	0.134	0.103	0.186	0.129	0.060	n.s
21	0.126	0.096	0.170	0.121	0.101	n.s
22	0.115	0.090	0.157	0.112	0.112	n.s
23	0.103	0.083	0.139	0.104	0.138	n.s
24	0.098	0.079	0.130	0.099	0.174	n.s
25	0.078	0.074	0.119	0.097	0.182	n.s

Integral calculation

24hr	Integral		Integral		t-test	
Control 1	4.852	Mutant 1	9.340	0.189	n.s	
Control 2	5.494	Mutant 2	4.737			
Control 3	6.388	Mutant 3	2.834			
Control 4	7.944	Mutant 4	2.555			
Control 5	4.940	Mutant 5	1.383			
Control 6	4.505	Mutant 6	3.099			
Control 7	5.425	Mutant 7	2.271			
Control 8	6.677	Mutant 8	3.737			
Control 9	2.587	Mutant 9	0.000			
Control 10	2.443	Mutant 10	1.662			
Control 11	4.887	Mutant 11	4.707			
Control 12	5.407	Mutant 12	4.952			
Control 13	6.489	Mutant 13	2.504			
Control 14	3.069	Mutant 14	9.178			
Control 15	2.366					
average	4.898		3.783			
sd	1.67681517		2.69592228			

36hr	Integral		Integral		t-test	
Control 1	9.264	Mutant 1	12.422	0.046	*	
Control 2	8.799	Mutant 2	8.446			
Control 3	3.658	Mutant 3	12.270			
Control 4	7.018	Mutant 4	6.755			
Control 5	6.388	Mutant 5	5.372			
Control 6	3.554	Mutant 6	4.083			
Control 7	4.137	Mutant 7	4.016			
Control 8	6.338	Mutant 8	5.617			
Control 9	2.392	Mutant 9	6.914			
Control 10	2.877	Mutant 10	5.329			
Control 11	2.912	Mutant 11	3.249			
Control 12	3.615	Mutant 12	5.133			
Control 13	5.297	Mutant 13	7.259			
Control 14	1.388	Mutant 14	7.446			
Control 15	3.466					
average	4.740		6.736			
sd	2.34682313		2.7866796			

Branching endpoints

	Control		Mutant		ttest	
	average	sd	average	sd		
12hr	9	0.488	9	0.776	0.600	n.s
18hr	9	0.756	9	0.832	0.449	n.s
24hr	9	0.816	9	0.760	0.400	n.s
36hr	10	1.056	11	0.870	0.565	n.s

Table S2: refers to Fig. 6B and 6C
Tbx2^{+/+};Hprt^{TBX2/+}* and *Tbx2^{cre/+};Hprt^{TBX2/y}

Kymograph measurement		Culture 3														
		Control 1	Control 2	Control 3	Control 4	Control 5	Control 6	Control 7	Control 8	Control 9	Control 10	Control 11	Control 12	Control 13	Control 14	Control 15
24hr	0.018	0.335	0.015	0.029	0.017	0.012	0.019	0.004	0.010	0.011	0.000	0.000	0.000	0.005	0.000	0.008
	0.018	0.339	0.040	0.023	0.029	0.024	0.039	0.011	0.112	0.029	0.000	0.000	0.000	0.007	0.021	0.010
	0.065	0.394	0.204	0.188	0.061	0.080	0.080	0.022	0.310	0.105	0.000	0.000	0.000	0.036	0.094	0.066
	0.089	0.470	0.265	0.438	0.118	0.185	0.112	0.090	0.379	0.124	0.000	0.000	0.000	0.070	0.141	0.123
	0.121	0.495	0.302	0.493	0.160	0.262	0.192	0.149	0.421	0.144	0.000	0.000	0.000	0.138	0.187	0.165
	0.128	0.512	0.308	0.502	0.155	0.319	0.284	0.174	0.435	0.163	0.000	0.000	0.000	0.180	0.226	0.193
	0.133	0.517	0.318	0.512	0.163	0.352	0.294	0.192	0.438	0.147	0.000	0.000	0.000	0.235	0.242	0.197
	0.142	0.516	0.302	0.502	0.154	0.368	0.296	0.177	0.423	0.133	0.000	0.000	0.000	0.282	0.283	0.208
	0.147	0.510	0.298	0.513	0.150	0.387	0.306	0.156	0.402	0.120	0.000	0.000	0.000	0.312	0.297	0.202
	0.137	0.509	0.285	0.501	0.143	0.380	0.287	0.139	0.387	0.132	0.000	0.000	0.000	0.327	0.300	0.195
	0.110	0.485	0.254	0.494	0.124	0.378	0.278	0.101	0.373	0.133	0.000	0.000	0.000	0.337	0.299	0.188
	0.102	0.473	0.206	0.481	0.111	0.369	0.245	0.104	0.353	0.126	0.000	0.000	0.000	0.356	0.296	0.171
	0.095	0.456	0.179	0.482	0.096	0.335	0.195	0.080	0.325	0.103	0.000	0.000	0.000	0.368	0.284	0.173
	0.102	0.464	0.182	0.447	0.089	0.304	0.173	0.083	0.286	0.087	0.000	0.000	0.000	0.369	0.265	0.161
	0.084	0.455	0.175	0.411	0.088	0.287	0.158	0.074	0.253	0.061	0.000	0.000	0.000	0.366	0.258	0.138
	0.092	0.425	0.150	0.341	0.093	0.234	0.145	0.075	0.218	0.071	0.000	0.000	0.000	0.366	0.257	0.132
	0.086	0.410	0.133	0.322	0.085	0.223	0.162	0.055	0.168	0.074	0.000	0.000	0.000	0.343	0.220	0.114
	0.087	0.399	0.113	0.302	0.093	0.217	0.141	0.048	0.148	0.077	0.000	0.000	0.000	0.325	0.202	0.092
	0.084	0.390	0.101	0.249	0.084	0.189	0.113	0.044	0.127	0.066	0.000	0.000	0.000	0.327	0.166	0.087
	0.090	0.379	0.089	0.223	0.087	0.190	0.089	0.036	0.125	0.062	0.000	0.000	0.000	0.309	0.148	0.087
	0.087	0.378	0.068	0.209	0.075	0.177	0.053	0.022	0.111	0.052	0.000	0.000	0.000	0.302	0.128	0.092
	0.082	0.369	0.060	0.176	0.066	0.182	0.052	0.045	0.101	0.043	0.000	0.000	0.000	0.285	0.129	0.084
	0.095	0.356	0.061	0.166	0.077	0.162	0.058	0.046	0.102	0.022	0.000	0.000	0.000	0.266	0.123	0.084
	0.092	0.345	0.059	0.133	0.072	0.160	0.046	0.051	0.088	0.010	0.000	0.000	0.000	0.256	0.123	0.088
	0.088	0.352	0.049	0.106	0.070	0.162	0.054	0.058	0.093	0.010	0.000	0.000	0.000	0.253	0.123	0.075

Table S2: refers to Fig. 6B and 6C

Tbx2^{Cre/+};*Hprt*^{TBX2/+} and *Tbx2*^{Cre/+};*Hprt*^{TBX2/y}

Kymograph measurement		Culture 3														
		Culture 1					Culture 2					Culture 3				
36hr		Control 1	Control 2	Control 3	Control 4	Control 5	Control 6	Control 7	Control 8	Control 9	Control 10	Control 11	Control 12	Control 13	Control 14	Control 15
0.015	0.003	0.000	0.000	0.000	0.000	0.000	0.000	0.000	0.000	0.007	0.027	0.004	0.000	0.000	0.002	0.009
0.015	0.007	0.037	0.039	0.045	0.011	0.015	0.027	0.027	0.146	0.146	0.028	0.026	0.011	0.010	0.038	0.023
0.111	0.039	0.095	0.142	0.078	0.106	0.106	0.104	0.106	0.301	0.301	0.212	0.085	0.075	0.039	0.162	0.147
0.151	0.079	0.236	0.191	0.152	0.139	0.121	0.150	0.150	0.362	0.362	0.281	0.139	0.101	0.105	0.192	0.317
0.257	0.112	0.231	0.239	0.196	0.182	0.192	0.219	0.219	0.431	0.431	0.353	0.210	0.122	0.156	0.243	0.409
0.339	0.127	0.213	0.276	0.227	0.238	0.261	0.251	0.251	0.433	0.433	0.411	0.251	0.175	0.212	0.266	0.455
0.373	0.132	0.219	0.294	0.260	0.326	0.260	0.255	0.255	0.419	0.419	0.482	0.259	0.242	0.248	0.315	0.490
0.412	0.139	0.217	0.281	0.287	0.390	0.278	0.275	0.275	0.345	0.345	0.478	0.253	0.259	0.282	0.384	0.512
0.417	0.134	0.205	0.275	0.327	0.418	0.278	0.282	0.282	0.282	0.282	0.453	0.248	0.268	0.305	0.406	0.519
0.412	0.122	0.193	0.279	0.344	0.452	0.307	0.299	0.256	0.256	0.256	0.406	0.257	0.286	0.313	0.418	0.522
0.411	0.107	0.192	0.254	0.340	0.446	0.314	0.303	0.244	0.244	0.244	0.345	0.260	0.271	0.319	0.427	0.520
0.389	0.093	0.166	0.237	0.342	0.462	0.305	0.306	0.229	0.229	0.229	0.299	0.249	0.272	0.309	0.429	0.510
0.364	0.070	0.131	0.218	0.329	0.473	0.280	0.313	0.214	0.214	0.214	0.305	0.234	0.250	0.311	0.426	0.506
0.322	0.053	0.087	0.212	0.312	0.464	0.272	0.304	0.204	0.204	0.204	0.285	0.198	0.245	0.296	0.411	0.487
0.301	0.041	0.044	0.211	0.315	0.455	0.240	0.311	0.197	0.197	0.197	0.228	0.145	0.231	0.271	0.390	0.470
0.287	0.042	0.043	0.189	0.288	0.449	0.218	0.287	0.179	0.179	0.179	0.242	0.103	0.224	0.265	0.342	0.448
0.252	0.053	0.031	0.183	0.251	0.438	0.205	0.267	0.179	0.179	0.179	0.227	0.067	0.219	0.249	0.323	0.417
0.237	0.054	0.026	0.178	0.203	0.412	0.166	0.244	0.185	0.185	0.185	0.243	0.058	0.191	0.238	0.274	0.384
0.205	0.058	0.040	0.161	0.185	0.397	0.145	0.216	0.168	0.168	0.168	0.234	0.056	0.164	0.225	0.256	0.344
0.190	0.061	0.053	0.155	0.155	0.395	0.142	0.211	0.163	0.163	0.163	0.226	0.055	0.148	0.207	0.216	0.312
0.161	0.067	0.049	0.136	0.154	0.381	0.123	0.204	0.155	0.155	0.155	0.211	0.056	0.131	0.166	0.195	0.274
0.130	0.070	0.070	0.136	0.145	0.351	0.118	0.205	0.157	0.157	0.157	0.175	0.031	0.118	0.134	0.173	0.253
0.115	0.089	0.057	0.121	0.134	0.332	0.110	0.197	0.144	0.144	0.144	0.168	0.027	0.099	0.121	0.154	0.226
0.105	0.087	0.070	0.125	0.135	0.300	0.096	0.190	0.148	0.148	0.148	0.134	0.025	0.088	0.106	0.145	0.198
0.094	0.095	0.058	0.116	0.136	0.288	0.074	0.197	0.144	0.144	0.144	0.140	0.039	0.075	0.099	0.117	0.190
												0.028	0.081	0.099	0.106	0.176

Table S2: refers to Fig. 6B and 6C

Tbx2^{+/+};*Hprt*^{TBX2/+} and *Tbx2*^{cre/+};*Hprt*^{TBX2/y}

Kymograph measurement					
Culture 1		Culture 2		Culture 3	
24hr					
Mutant 1	Mutant 2	Mutant 3	Mutant 4	Mutant 5	Mutant 6
0.000	0.011	0.003	0.000	0.000	0.002
0.008	0.055	0.013	0.000	0.000	0.006
0.052	0.115	0.025	0.000	0.000	0.031
0.086	0.119	0.062	0.000	0.000	0.051
0.137	0.160	0.131	0.000	0.000	0.065
0.146	0.148	0.162	0.000	0.000	0.072
0.179	0.159	0.199	0.000	0.000	0.066
0.177	0.140	0.201	0.000	0.000	0.097
0.183	0.130	0.199	0.000	0.000	0.096
0.186	0.120	0.164	0.000	0.000	0.094
0.170	0.116	0.159	0.000	0.000	0.084
0.152	0.082	0.139	0.000	0.000	0.080
0.129	0.074	0.126	0.000	0.000	0.071
0.090	0.051	0.116	0.000	0.000	0.073
0.084	0.051	0.093	0.000	0.000	0.059
0.068	0.027	0.089	0.000	0.000	0.053
0.048	0.023	0.078	0.000	0.000	0.042
0.041	0.007	0.080	0.000	0.000	0.054
0.035	0.007	0.076	0.000	0.000	0.046
0.037	0.006	0.061	0.000	0.000	0.042
0.019	0.001	0.066	0.000	0.000	0.036
0.025	0.018	0.058	0.000	0.000	0.043
0.024	0.006	0.055	0.000	0.000	0.054
0.016	0.021	0.063	0.000	0.000	0.038
0.016	0.001	0.047	0.000	0.000	0.027
0.013	0.017	0.055	0.000	0.000	0.027
36hr					
Mutant 1	Mutant 2	Mutant 3	Mutant 4	Mutant 5	Mutant 6
0.007	0.000	0.000	0.004	0.000	0.024
0.025	0.019	0.009	0.026	0.010	0.055
0.039	0.068	0.032	0.085	0.039	0.087
0.064	0.084	0.067	0.139	0.105	0.091
0.088	0.093	0.103	0.210	0.156	0.114
0.118	0.106	0.153	0.252	0.212	0.124
0.146	0.091	0.214	0.259	0.248	0.137
0.167	0.085	0.260	0.253	0.282	0.141
0.179	0.088	0.290	0.248	0.305	0.148
0.201	0.057	0.306	0.257	0.313	0.145
0.191	0.048	0.318	0.260	0.319	0.136
0.187	0.026	0.330	0.249	0.309	0.127
0.190	0.018	0.315	0.234	0.311	0.121
0.179	0.025	0.311	0.198	0.296	0.112
0.168	0.021	0.300	0.145	0.271	0.092
0.160	0.018	0.286	0.103	0.265	0.082
0.147	0.020	0.268	0.067	0.249	0.067
0.129	0.020	0.255	0.058	0.238	0.053
0.099	0.017	0.247	0.056	0.225	0.047
0.081	0.018	0.220	0.055	0.207	0.046
0.076	0.021	0.207	0.056	0.166	0.037
0.068	0.020	0.199	0.031	0.134	0.035
0.051	0.017	0.183	0.027	0.121	0.028
0.056	0.018	0.164	0.025	0.106	0.015
0.041	0.021	0.155	0.039	0.099	0.010
0.026	0.022	0.139	0.028	0.099	0.013

Table S2: refers to Fig. 6B and 6C
Tbx2^{Cre/+};Hprt^{TBX2/+} and Tbx2^{Cre/+};Hprt^{TBX2/y}

Integral calculation	Culture 3															
	Culture 1					Culture 2					Culture 3					
	24hr	Control 1	Control 2	Control 3	Control 4	Control 5	Control 6	Control 7	Control 8	Control 9	Control 10	Control 11	Control 12	Control 13	Control 14	Control 15
	0.018	0.337	0.027	0.026	0.023	0.018	0.029	0.007	0.007	0.051	0.020	0.000	0.000	0.006	0.010	0.009
	0.042	0.366	0.122	0.106	0.045	0.071	0.059	0.016	0.016	0.211	0.067	0.000	0.000	0.022	0.057	0.038
	0.077	0.432	0.235	0.313	0.089	0.152	0.096	0.056	0.056	0.345	0.115	0.000	0.000	0.063	0.117	0.095
	0.105	0.483	0.283	0.465	0.139	0.224	0.152	0.120	0.120	0.400	0.134	0.000	0.000	0.104	0.164	0.144
	0.125	0.503	0.305	0.497	0.158	0.291	0.238	0.161	0.161	0.428	0.153	0.000	0.000	0.159	0.206	0.179
	0.131	0.514	0.313	0.507	0.159	0.336	0.289	0.183	0.183	0.436	0.155	0.000	0.000	0.207	0.234	0.195
	0.137	0.517	0.310	0.507	0.158	0.360	0.295	0.185	0.185	0.430	0.140	0.000	0.000	0.258	0.262	0.203
	0.144	0.513	0.300	0.507	0.152	0.377	0.301	0.167	0.167	0.413	0.127	0.000	0.000	0.297	0.290	0.205
	0.142	0.510	0.292	0.507	0.146	0.384	0.296	0.148	0.148	0.395	0.126	0.000	0.000	0.319	0.298	0.198
	0.123	0.497	0.269	0.498	0.134	0.379	0.283	0.120	0.120	0.380	0.133	0.000	0.000	0.332	0.299	0.191
	0.106	0.479	0.230	0.488	0.118	0.374	0.261	0.103	0.103	0.363	0.130	0.000	0.000	0.346	0.297	0.179
	0.099	0.464	0.192	0.481	0.104	0.352	0.220	0.092	0.092	0.339	0.115	0.000	0.000	0.362	0.290	0.172
	0.099	0.460	0.180	0.464	0.092	0.319	0.184	0.082	0.082	0.306	0.095	0.000	0.000	0.368	0.275	0.167
	0.093	0.460	0.179	0.429	0.088	0.295	0.165	0.079	0.079	0.270	0.074	0.000	0.000	0.367	0.261	0.149
	0.089	0.448	0.171	0.391	0.092	0.271	0.151	0.074	0.074	0.235	0.066	0.000	0.000	0.366	0.257	0.135
	0.093	0.433	0.159	0.356	0.094	0.245	0.151	0.070	0.070	0.203	0.072	0.000	0.000	0.357	0.248	0.126
	0.089	0.417	0.142	0.332	0.089	0.229	0.160	0.060	0.060	0.178	0.073	0.000	0.000	0.346	0.230	0.117
	0.086	0.404	0.123	0.312	0.089	0.220	0.151	0.052	0.052	0.158	0.075	0.000	0.000	0.334	0.211	0.103
	0.085	0.395	0.107	0.276	0.088	0.203	0.127	0.046	0.046	0.138	0.072	0.000	0.000	0.326	0.184	0.090
	0.087	0.384	0.095	0.236	0.085	0.189	0.101	0.040	0.040	0.126	0.064	0.000	0.000	0.318	0.157	0.087
	0.089	0.378	0.079	0.216	0.081	0.183	0.071	0.029	0.029	0.118	0.057	0.000	0.000	0.305	0.138	0.090
	0.084	0.373	0.064	0.192	0.070	0.180	0.052	0.033	0.033	0.106	0.048	0.000	0.000	0.293	0.128	0.088
	0.088	0.363	0.061	0.171	0.072	0.172	0.055	0.046	0.046	0.101	0.032	0.000	0.000	0.276	0.126	0.084
	0.093	0.351	0.060	0.149	0.075	0.161	0.052	0.048	0.048	0.095	0.016	0.000	0.000	0.261	0.123	0.086
	0.090	0.349	0.054	0.119	0.071	0.161	0.050	0.054	0.054	0.091	0.010	0.000	0.000	0.254	0.123	0.082
	0.044	0.176	0.024	0.053	0.035	0.081	0.027	0.029	0.029	0.047	0.005	0.000	0.000	0.126	0.062	0.037
Integral sum	2.459	11.007	4.377	8.599	2.546	6.226	4.019	2.100	2.100	6.373	2.173	0.000	0.000	6.765	5.049	3.249

Table S2: refers to Fig. 6B and 6C
Tbx2^{cre/+};Hprt^{TBX2/+} and Tbx2^{cre/+};Hprt^{TBX2/y}

Integral calculation	Culture 3														
	Culture 1					Culture 2					Culture 3				
	36hr	Control 1	Control 2	Control 3	Control 4	Control 5	Control 6	Control 7	Control 8	Control 9	Control 10	Control 11	Control 12	Control 13	Control 14
	0.015	0.005	0.018	0.019	0.022	0.005	0.007	0.013	0.077	0.027	0.015	0.005	0.005	0.020	0.016
	0.063	0.023	0.066	0.090	0.069	0.045	0.060	0.065	0.224	0.120	0.056	0.043	0.025	0.100	0.085
	0.131	0.059	0.165	0.167	0.122	0.109	0.113	0.127	0.331	0.246	0.112	0.088	0.072	0.177	0.232
	0.204	0.095	0.233	0.215	0.174	0.160	0.156	0.184	0.396	0.317	0.175	0.112	0.131	0.218	0.363
	0.298	0.119	0.222	0.258	0.212	0.210	0.226	0.235	0.432	0.382	0.231	0.149	0.184	0.255	0.432
	0.356	0.129	0.216	0.285	0.243	0.282	0.261	0.253	0.426	0.446	0.255	0.209	0.230	0.291	0.472
	0.392	0.135	0.218	0.287	0.274	0.358	0.269	0.265	0.382	0.480	0.256	0.251	0.265	0.350	0.501
	0.415	0.128	0.199	0.277	0.335	0.435	0.292	0.291	0.269	0.430	0.252	0.277	0.309	0.412	0.520
	0.412	0.114	0.193	0.267	0.342	0.449	0.310	0.301	0.250	0.376	0.258	0.272	0.316	0.422	0.521
	0.400	0.100	0.179	0.246	0.341	0.454	0.310	0.305	0.237	0.322	0.254	0.272	0.314	0.428	0.515
	0.376	0.082	0.149	0.227	0.336	0.467	0.293	0.309	0.222	0.302	0.242	0.261	0.310	0.428	0.508
	0.343	0.062	0.109	0.215	0.321	0.468	0.276	0.308	0.209	0.295	0.216	0.248	0.304	0.419	0.496
	0.311	0.047	0.066	0.211	0.314	0.460	0.256	0.307	0.201	0.256	0.172	0.238	0.284	0.400	0.479
	0.294	0.041	0.043	0.200	0.302	0.452	0.229	0.299	0.197	0.235	0.124	0.228	0.268	0.366	0.459
	0.280	0.042	0.030	0.189	0.270	0.444	0.211	0.277	0.188	0.234	0.085	0.222	0.257	0.332	0.433
	0.262	0.047	0.024	0.186	0.245	0.425	0.185	0.255	0.182	0.235	0.063	0.205	0.243	0.298	0.400
	0.244	0.053	0.028	0.181	0.221	0.409	0.165	0.230	0.176	0.238	0.057	0.177	0.232	0.265	0.364
	0.221	0.056	0.033	0.170	0.194	0.401	0.155	0.213	0.166	0.230	0.056	0.156	0.216	0.236	0.328
	0.198	0.060	0.047	0.158	0.170	0.396	0.144	0.209	0.159	0.218	0.055	0.140	0.187	0.206	0.293
	0.175	0.064	0.051	0.146	0.155	0.388	0.133	0.206	0.155	0.193	0.043	0.124	0.150	0.184	0.264
	0.145	0.068	0.060	0.136	0.150	0.366	0.121	0.205	0.156	0.172	0.029	0.108	0.128	0.164	0.240
	0.122	0.079	0.064	0.129	0.140	0.342	0.114	0.201	0.151	0.151	0.026	0.093	0.114	0.149	0.212
	0.110	0.088	0.063	0.123	0.135	0.316	0.103	0.194	0.146	0.134	0.032	0.082	0.103	0.131	0.194
	0.099	0.091	0.064	0.120	0.136	0.294	0.085	0.193	0.146	0.137	0.034	0.078	0.099	0.111	0.183
	0.047	0.047	0.029	0.058	0.068	0.144	0.037	0.098	0.072	0.070	0.014	0.040	0.049	0.053	0.088
Integral sum	6.330	1.974	2.782	4.839	5.595	8.683	4.790	5.824	5.863	6.711	3.362	4.347	5.088	6.809	9.115

Table S2: refers to Fig. 6B and 6C

Tbx2^{+/+};*Hprt*^{TBX2/+} and *Tbx2*^{cre/+};*Hprt*^{TBX2/y}

Integral calculation						
	Culture 1		Culture2		Culture 3	
	24hr					
	Mutant 1	Mutant 2	Mutant 3	Mutant 4	Mutant 5	Mutant 6
	0.004	0.033	0.008	0.000	0.000	0.004
	0.030	0.085	0.019	0.000	0.000	0.019
	0.069	0.117	0.043	0.000	0.000	0.041
	0.112	0.139	0.096	0.000	0.000	0.058
	0.141	0.154	0.146	0.000	0.000	0.068
	0.162	0.154	0.180	0.000	0.000	0.069
	0.178	0.150	0.200	0.000	0.000	0.081
	0.180	0.135	0.200	0.000	0.000	0.096
	0.184	0.125	0.182	0.000	0.000	0.095
	0.178	0.118	0.162	0.000	0.000	0.089
	0.161	0.099	0.149	0.000	0.000	0.082
	0.140	0.078	0.133	0.000	0.000	0.076
	0.110	0.063	0.121	0.000	0.000	0.072
	0.087	0.051	0.104	0.000	0.000	0.066
	0.076	0.039	0.091	0.000	0.000	0.056
	0.058	0.025	0.084	0.000	0.000	0.048
	0.044	0.015	0.079	0.000	0.000	0.048
	0.038	0.007	0.078	0.000	0.000	0.050
	0.036	0.006	0.068	0.000	0.000	0.044
	0.028	0.004	0.064	0.000	0.000	0.039
	0.022	0.009	0.062	0.000	0.000	0.039
	0.025	0.012	0.056	0.000	0.000	0.048
	0.020	0.013	0.059	0.000	0.000	0.046
	0.016	0.011	0.055	0.000	0.000	0.033
	0.015	0.009	0.051	0.000	0.000	0.027
	0.007	0.008	0.028	0.000	0.000	0.014
Integral sum	2.120	1.658	2.519	0.000	0.000	1.408
	36hr					
	Mutant 1	Mutant 2	Mutant 3	Mutant 4	Mutant 5	Mutant 6
	0.016	0.010	0.004	0.015	0.005	0.039
	0.032	0.044	0.020	0.056	0.025	0.071
	0.052	0.076	0.049	0.112	0.072	0.089
	0.076	0.089	0.085	0.175	0.131	0.102
	0.103	0.100	0.128	0.231	0.184	0.119
	0.132	0.099	0.184	0.255	0.230	0.131
	0.157	0.088	0.237	0.256	0.265	0.139
	0.173	0.086	0.275	0.251	0.294	0.145
	0.190	0.073	0.298	0.252	0.309	0.147
	0.196	0.053	0.312	0.258	0.316	0.140
	0.189	0.037	0.324	0.254	0.314	0.131
	0.189	0.022	0.323	0.242	0.310	0.124
	0.184	0.021	0.313	0.216	0.304	0.116
	0.173	0.023	0.306	0.172	0.284	0.102
	0.164	0.019	0.293	0.124	0.268	0.087
	0.153	0.019	0.277	0.085	0.257	0.075
	0.138	0.020	0.261	0.063	0.243	0.060
	0.114	0.018	0.251	0.057	0.232	0.050
	0.090	0.018	0.233	0.056	0.216	0.047
	0.079	0.020	0.214	0.055	0.187	0.041
	0.072	0.021	0.203	0.043	0.150	0.036
	0.060	0.018	0.191	0.029	0.128	0.031
	0.054	0.018	0.173	0.026	0.114	0.022
	0.048	0.020	0.159	0.032	0.103	0.013
	0.034	0.022	0.147	0.034	0.099	0.012
	0.013	0.011	0.069	0.014	0.049	0.006

Table S2: refers to Fig. 6B and 6C

Tbx2^{+/+};*Hprt*^{TBX2/+} and *Tbx2*^{cre/+};*Hprt*^{TBX2/y}

Branching endpoints								
	12 hr		18 hr		24 hr		36 hr	
	Control	Mutant	Control	Mutant	Control	Mutant	Control	Mutant
1	7	8	8	8	9	8	10	9
2	9	9	9	10	10	11	10	13
3	7	9	9	9	8	9	10	10
4	9	8	9	8	10	8	11	13
5	7	8	8	7	9	8	10	10
6	7	7	8	8	8	9	8	11
7	8	8	8	8	9	9	9	10
8	9		9		9		11	
9	9		10		11		15	
10	9		10		10		11	
11	8		9		9		9	
12	7		9		9		10	
13	8		9		9		10	
14	9		9		9		12	
15	9		10		11		13	

Table S2: refers to Fig. 6B and 6C

Tbx2^{+/+};*Hprt*^{TBX2/+} and *Tbx2*^{cre/+};*Hprt*^{TBX2/y}

Kymograph measurement

24hr	Control		Mutant		ttest
	average	sd	average	sd	
	0,032	0,084	0,003	0,004	0,407 n.s
	0,047	0,085	0,014	0,021	0,364 n.s
	0,116	0,113	0,037	0,043	0,118 n.s
	0,174	0,148	0,053	0,047	0,068 n.s
	0,215	0,154	0,082	0,071	0,058 n.s
	0,239	0,157	0,088	0,075	0,038 *
	0,249	0,159	0,100	0,090	0,046 *
	0,252	0,158	0,102	0,087	0,043 *
	0,253	0,161	0,102	0,087	0,044 *
	0,248	0,159	0,094	0,080	0,037 *
	0,237	0,159	0,088	0,075	0,043 *
	0,226	0,157	0,076	0,065	0,036 *
	0,211	0,156	0,067	0,057	0,041 *
	0,201	0,149	0,055	0,048	0,032 *
	0,187	0,145	0,048	0,040	0,034 *
	0,179	0,136	0,039	0,037	0,024 *
	0,169	0,128	0,032	0,030	0,020 *
	0,160	0,123	0,030	0,033	0,022 *
	0,150	0,118	0,027	0,031	0,023 *
	0,135	0,113	0,024	0,026	0,030 *
	0,128	0,108	0,020	0,027	0,028 *
	0,117	0,108	0,024	0,023	0,054 n.s
	0,112	0,103	0,023	0,026	0,055 n.s
	0,108	0,098	0,023	0,024	0,053 n.s
	0,102	0,095	0,015	0,019	0,042 *
	0,100	0,095	0,019	0,021	0,057 n.s

36hr	Control		Mutant		ttest
	average	sd	average	sd	
0	0,004	0,008	0,006	0,009	0,748 n.s
1	0,032	0,034	0,024	0,017	0,600 n.s
2	0,119	0,068	0,058	0,025	0,048 *
3	0,181	0,083	0,092	0,028	0,020 *
4	0,237	0,094	0,127	0,047	0,015 *
5	0,276	0,094	0,161	0,059	0,013 *
6	0,305	0,099	0,183	0,067	0,012 *
7	0,320	0,100	0,198	0,079	0,016 *
8	0,321	0,102	0,210	0,086	0,030 *
9	0,324	0,104	0,213	0,100	0,037 *
10	0,317	0,105	0,212	0,108	0,054 n.s
11	0,306	0,110	0,205	0,116	0,074 n.s
12	0,295	0,118	0,198	0,115	0,105 n.s
13	0,277	0,121	0,187	0,109	0,130 n.s
14	0,257	0,126	0,166	0,106	0,139 n.s
15	0,242	0,122	0,152	0,106	0,133 n.s
16	0,224	0,120	0,136	0,103	0,133 n.s
17	0,210	0,108	0,125	0,100	0,116 n.s
18	0,195	0,102	0,115	0,097	0,116 n.s
19	0,182	0,094	0,105	0,087	0,097 n.s
20	0,170	0,087	0,094	0,075	0,078 n.s
21	0,154	0,085	0,081	0,071	0,079 n.s
22	0,145	0,077	0,071	0,067	0,053 n.s
23	0,133	0,072	0,064	0,060	0,051 n.s
24	0,127	0,063	0,061	0,055	0,037 *
25	0,122	0,063	0,055	0,052	0,032 *

Integral calculation

24hr	Integral		ttest
	Control	Mutant	
Control 1	2,459	2,120	0,030 *
Control 2	11,007	1,658	
Control 3	4,377	2,519	
Control 4	8,599	0,000	
Control 5	2,546	0,000	
Control 6	6,226	1,408	
Control 7	4,019		
Control 8	2,100		
Control 9	6,373		
Control 10	2,173		
Control 11	0,000		
Control 12	0,000		
Control 13	6,765		
Control 14	5,049		
Control 15	3,249		
average	4,329	1,284	
sd	3,0716355	1,0654622	

36hr	Integral		ttest
	Control	Mutant	
Control 1	6,330	2,880	0,028 *
Control 2	1,974	1,043	
Control 3	2,782	5,331	
Control 4	4,839	3,362	
Control 5	5,595	5,088	
Control 6	8,683	2,075	
Control 7	4,790		
Control 8	5,824		
Control 9	5,863		
Control 10	6,711		
Control 11	3,362		
Control 12	4,347		
Control 13	5,088		
Control 14	6,809		
Control 15	9,115		
average	5,474	3,296	
sd	1,9665178	1,6789714	

Branching endpoints

	Control		Mutant		ttest
	average	sd	average	sd	
12hr	8	0,913	8	0,548	0,377 n.s
18hr	9	0,689	8	1,140	0,319 n.s
24hr	9	0,832	9	1,304	0,412 n.s
36hr	10	1,653	11	1,871	0,453 n.s

Combined genomic and proteomic approaches reveal DNA binding sites and interaction partners of TBX2 in the developing lung

Timo H. Lüdtkke^{1,§}, Irina Wojahn^{1,§}, Marc-Jens Kleppa¹, Jasper Schierstaedt^{1,&}, Vincent M. Christoffels², Patrick Künzler³ and Andreas Kispert¹

¹Institut für Molekularbiologie, Medizinische Hochschule Hannover, Hannover, Germany

²Department of Anatomy, Embryology and Physiology, Academic Medical Center, University of Amsterdam, Amsterdam, The Netherlands

³Institut für Pflanzengenetik, Leibniz Universität Hannover, Hannover, Germany

§ Equal contribution

& Current address: Plant-Microbe Systems, Leibniz Institute of Vegetable and Ornamental Crops, Großbeeren, Germany.

Corresponding Author: Andreas Kispert, Medizinische Hochschule Hannover, Institute for Molecular Biology, OE5250, Carl-Neuberg-Str. 1, D-30625 Hannover, Germany. Tel. +49 511 532 4017; Fax: +49 511 5324283; E-mail: kispert.andreas@mh-hannover.de

Type of authorship:	Co-First author
Type of article:	Research article
Share of the work:	35%
Journal:	Respiratory Research
Impact factor:	4.065
Number of citations:	0
Date of publication:	submitted
DOI:	-

Abstract

Background

Tbx2 encodes a transcriptional repressor implicated in the development of numerous organs in mouse. During lung development TBX2 maintains the proliferation of mesenchymal progenitors, and hence, epithelial proliferation and branching morphogenesis. The pro-proliferative function was traced to direct repression of the cell-cycle inhibitor genes *Cdkn1a* and *Cdkn1b*, as well as of genes encoding WNT antagonists, *Frzb* and *Shisa3*, to increase pro-proliferative WNT signaling. Despite these important molecular insights, we still lack knowledge of the DNA occupancy of TBX2 in the genome, and of the protein interaction partners involved in transcriptional repression of target genes.

Methods

We used chromatin immunoprecipitation (ChIP)-sequencing and expression analyses to identify genomic DNA-binding sites and transcription units directly regulated by TBX2 in the developing lung. Moreover, we purified TBX2 containing protein complexes from embryonic lung tissue and identified potential interaction partners by subsequent liquid chromatography/mass spectrometry. The interaction with candidate proteins was validated by immunofluorescence and individual co-immunoprecipitation analyses.

Results

We identified *Irf3* and *Ccn4* as additional direct target genes of TBX2 in the pulmonary mesenchyme. Analyzing TBX2 occupancy data unveiled the enrichment of five consensus sequences, three of which match T-box binding elements. The remaining two correspond to a high mobility group (HMG)-box and a homeobox consensus sequence motif. We found and validated binding of TBX2 to the HMG-box transcription factor HMG2 and the homeobox transcription factor PBX1, to the heterochromatin protein CBX3, and to various members of the nucleosome remodeling and deacetylase (NuRD) chromatin remodeling complex including HDAC1, HDAC2 and CHD4.

Conclusion

Our data suggest that TBX2 interacts with homeobox and HMG-box transcription factors as well as with the NuRD chromatin remodeling complex to repress transcription of anti-proliferative genes in the pulmonary mesenchyme.

Keywords:

Tbx2, pulmonary mesenchyme, lung development, NuRD, HDAC, CBX3, HMGB2, PBX1

Background

In the mammalian lung, trachea, bronchi and bronchioles form a tree-like system of tubes that conduct the air to thin-walled terminal sacs, the alveoli, where the exchange of carbon dioxide and oxygen occurs. This elaborate epithelial system arises from a simple out-growth of the foregut endoderm by a complex program of specification, proliferative expansion, branching morphogenesis, proximal-distal patterning and differentiation during embryonic development [1]. All of these epithelial processes depend on cues from surrounding mesenchymal cells and the visceral pleura, the mesothelial lining of the lung. Branching morphogenesis occurs mostly during the pseudoglandular stage of lung development which extends in mice from embryonic day (E)12.5 to E16.5. Here, the pulmonary mesenchyme acts as a source for signals that direct the proliferative expansion and branching of the distal epithelial tips of the developing airways. In turn, endodermal and mesothelial signals maintain a proliferative undifferentiated state of the pulmonary mesenchyme, thus, preventing its differentiation into chondrocytes, smooth muscle cells (SMCs) and various types of fibroblasts that will later ensheath the epithelial components of the mature lung [2, 3]. The cross-talk between all three pulmonary tissue compartments is executed by a number of different signaling molecules including SHH, BMPs, FGFs and WNTs [4-9].

Orchestration and interpretation of these reciprocal signaling cascades require the activity of transcription factors that regulate the signals and their activities in time and space but also impinge onto the cell-cycle machinery to assure the pro-proliferative undifferentiated state in either tissue compartment. T-box proteins are members of a large, evolutionary conserved family of transcriptional regulators that share a highly conserved DNA-binding region, namely the T-box [10]. Transcriptional regulation by T-box proteins underlies a multitude of cellular processes including proliferation and differentiation in diverse contexts of germ layer, tissue and organ development as evidenced by severe embryonic defects in men and animals with loss- and gain-of-function of these genes [11, 12].

Our previous work characterized the T-box transcription factor TBX2 as a mesenchymal regulatory hub during lung development. *Tbx2* and the closely related *Tbx3* gene are predominantly expressed in mesenchymal precursors that surround the distal endodermal tips. The expression largely depends on epithelial SHH signals with modulatory input from epithelial BMP4, mesenchymal TGFs, and WNTs possibly emerging from both compartments [13, 14]. Loss of *Tbx2* and even more, the combined loss of *Tbx2* and *Tbx3* in mice,

results in arrest of mesenchymal proliferation, premature mesenchymal differentiation and an arrest of epithelial branching morphogenesis leading to lung hypoplasia at birth. Prolongation of TBX2 expression into adulthood leads to hyperproliferation and maintenance of mesenchymal progenitor cells. These cellular changes were traced to a molecular function of TBX2 to directly repress expression of the cell-cycle inhibitor genes *Cdkn1a* and *Cdkn1b*, as well as of genes encoding WNT antagonists, *Frzb* and *Shisa3*, which in turn increases pro-proliferative WNT signaling [13, 15].

Despite these important molecular insights, we still lack a survey of all direct target genes of TBX2 in the mesenchyme of the developing lung and of the nature and configuration of DNA-binding sites present in these genes. Moreover, we do not know with which other transcription factors, corepressors and chromatin remodeling complexes TBX2 interacts to achieve target gene specificity and repression in this developmental context.

Here, we set out to experimentally address these questions. Using a combination of transcriptional profiling by microarrays and ChIP-Seq technology, we identified additional targets of TBX2 activity including *Ccn4* and *I133*, and describe the consensus binding site of TBX2 in the developing lung. Additionally, we identified and characterized protein binding partners of TBX2 that may aid in specific repression of these target genes.

Methods

Mouse strains and genotyping

All mouse strains used in this study: *Tbx2*^{tm1.1(cre)Vmc} (synonym: *Tbx2*^{cre}) [16], *Tbx2*^{tm2.2Vmc} (synonym: *Tbx2*^{fl}) [17], *Gt(ROSA)26*^{Sortm4(ACTB-tdTomato,-EGFP)Luo/J} (synonym: *R26*^{mTmG}) [18] were maintained on an NMRI outbred background. Embryos for analysis were obtained from matings of NMRI wildtype mice, and from matings of *Tbx2*^{cre/+} males with *R26*^{mTmG/mTmG}; *Tbx2*^{fl/fl} or *Tbx2*^{cre/+} females. To time the pregnancy, vaginal plugs were checked on the morning after mating and noon was taken as embryonic day (E) 0.5. On the day of harvest, pregnant females were sacrificed by cervical dislocation. Embryos and lungs were dissected in PBS. For both *in situ* hybridization and immunofluorescence analyses, embryos were fixed in 4% PFA/PBS, transferred to methanol and stored at -20°C. PCR genotyping was performed on genomic DNA prepared from ear clips of adult mice or from embryonic tissues.

All animal work conducted for this study was approved by the local authorities (Niedersächsisches Landesamt für Verbraucherschutz und Lebensmittelsicherheit; permit number AZ33.12-42502-04-13/1356) and was performed at the central animal laboratory of the Medizinische Hochschule Hannover in accordance with the National Institute of Health guidelines for the care and use of laboratory animals.

Chromatin immunoprecipitation DNA-sequencing (ChIP-seq) assays

For ChIP-Seq analysis, a total of 100 E14.5 wildtype lungs were minced in PBS into pieces of 100-500 µm. The tissue was incubated in 1.6% formaldehyde/PBS for 20 min before glycine was added to a final concentration of 1% and incubation continued for 10 min at room temperature. After a washing step with PBS, the tissue was stored at -80°C until further use. ChIP reactions were performed with the SimpleChIP® Plus Enzymatic Chromatin IP Kit (Magnetic Beads) (#9005, Cell Signaling Technology, Danvers, MA, USA) following manufacturer's instructions. Nuclease treatment for fragmentation of chromatin was prolonged to 30 min and nuclease concentration was doubled to obtain fragments of 300 bp in average. The DNA-containing supernatants were incubated with a ChIP grade anti-TBX2 antibody (1:50; sc-514291 X, Santa Cruz Biotechnology Inc., Santa Cruz, CA, USA), anti-Histone H3 (1:50; #9005, Cell Signaling Technology) or an IgG control (1:50; #9005, Cell Signaling Technology) for 1 h at room temperature, and together with ChIP-

Grade ProteinG Magnetic Beads (#9006S, Cell Signaling Technology) overnight at 4°C. The DNA precipitates were passed to the Research Core Unit Genomics of Hannover Medical School. Library preparation was performed with NEBNext® Ultra™ II DNA Library Prep Kit for Illumina® (E7645S, New England Biolabs, Ipswich, MA, USA) and next generation sequencing was performed on Illumina NextSeq High Output 500/550 flow cells with a reading depth of 15 million 75 bp paired-end reads (FC-404-2005, Illumina, San Diego, CA, USA) using NEBNext® Multiplex Oligos for Illumina® (96 Unique Dual Index Primer Pairs) (E6440S, New England Biolabs,) following manufacturer's instructions. ChIP peaks were mapped against the GRC38/mm10 genome (NCBI BioProject Accession: PRJNA20689) using MACS2 callpeak integrated in Galaxy version 2.1.1.20160309.1 [19]. ChIP peaks were visualized and manually analyzed using IGV software v.2.5.3 [20, 21]. Associated gene names were determined in Galaxy with "Fetch closest non-overlapping feature", version 4.0.1. (<https://usegalaxy.org>). Gene ontology (GO) term analysis was performed with Genomic Regions Enrichment of Annotations Tool (GREAT, version 4.0.4, <http://great.stanford.edu/public/html>). *De novo* motif analysis on the data was performed with the FIMO tool in Galaxy (Version 4.11.1.0, <https://usegalaxy.org>) [22] for palindromic and non-palindromic sequences. For that purpose, sequence information from Macs2 callpeak data was gathered in Galaxy with the "Extract Genomic DNA" plugin (Version 2.2.3). Enriched motifs were compared to known transcription factor binding profiles with the TomTom Motif Comparison Tool version 5.1.1 (<http://meme-suite.org/tools/tomtom>) [23], using annotated sequences stored in Jaspas (<http://jaspar.genereg.net>) and footprintDB (<http://floresta.eead.csic.es/footprintdb>) databases.

GO-term analysis of gene lists

Lists of gene symbols were imported into DAVID Bioinformatics Resources version 6.8 (<https://david.ncifcrf.gov>) [24] with annotations restricted to mouse. Gene lists imported into MouseMine websoftware (MGI 6.14) [25] were analyzed for ontology terms of biological processes determined with Holm-Bonferroni test correction and p-values smaller than 0.05.

ChIP-PCR assays

Chromatin of ~20 wildtype and *Tbx2*-mutant lungs was isolated as described for ChIP-seq

experiments and subjected to PCR amplification of gene-specific peak regions. Primers for a peak in *Ccn4*, chr15:66,883,385-66,883,657 were: 5'- CCAGAGAATGTCACACTCCAC-3' and 5'- GCAGCTACTGGGTCTCTCA-3'. For peak #1 in *Il33* (chr19:29,925,062-29,925,237): 5'-TGGTTCTCTGCCAAGTTCTG-3' and 5'- TGCTCCACAGGTCCTAAGAT-3'; for peak #2 in *Il33* (chr19:29,924,808-29,924,983): 5'-GGCTAAGGCAAGAAGATCATG-3' and 5'-CCTGCCAATGTTACTGTTATC-3'.

Proteomic analysis

Three independent proteomic analyses were performed using material of 100 E14.5 lungs each. The lung tissue was fixed and stored until further use as described for ChIP-seq assays. Tissue dissociation was achieved following the RIME protocol [26] utilizing a Minilys homogenizer (#P000673-MLYS0-A, Bertin Technologies, Montigny-le-Bretonneux, France) with mixed 1.4/2.8 mm ceramic beads (#91-PCS-CKM, VWR International, Radnor, PA, USA) and a sonification step of 3 x 20 pulses of an amplitude of 60% with a duty cycle of 75% (UP200H, Sonotrode S1, Ø1mm, Hielscher Ultrasonic GmbH, Teltow, Germany). Cell lysates were incubated overnight at 4°C under constant rotation with ChIP-Grade ProteinG Magnetic Beads (#9006S, Cell Signaling Technology) conjugated either with normal rabbit IgG (#9005, Cell Signaling Technology) or ChIP grade mouse-anti-TBX2 antibody (1:50; sc-514291X, Santa Cruz). Enzymatic digestion and raw data processing steps were performed by the Research Core Unit Proteomics of the MHH. Liquid chromatography with subsequent tandem mass spectrometry (LC-MS/MS) was performed by the Department of Plant Proteomics of the Institute of Plant Genetics of the Leibniz-University Hannover. Extracted proteins were alkylated with iodacetamide and digested with trypsin overnight at 37°C in 40 mM ammonium hydrocarbonate buffer containing 10% acetonitrile. The reaction was stopped by increasing the concentration of trifluoroacetic acid (TFA) to 5%. Samples were centrifuged at high speed and supernatants containing peptides were dried and stored at -20°C.

Apart from minor modifications, LC-MS/MS was performed as previously described [27]. Peptides were resuspended in 20 µl of 5% [v/v] acetonitrile and 0.1% [v/v] TFA, of which 1 µl were loaded onto a 2 cm C18 reversed phase trap column (Acclaim PepMap100, diameter: 100 µm, granulometry: 5 µm, pore size: 100 Å; Thermo Fisher Scientific, Waltham, MA, USA). Separation took place on a 50 cm C18 reversed phase analytical

column (Acclaim PepMap100, diameter: 75 μm , granulometry: 3 μm , pore size: 100 \AA ; Thermo Fisher Scientific, Dreieich, Germany) using a 60 min non-linear 5-36% [v/v] acetonitrile gradient in 0.1% [v/v] formic acid for elution (250 nl/min; 33°C). Eluting peptides were transferred into a Q-Exactive mass spectrometer (Thermo Fisher Scientific) by electrospray ionization (ESI) using a NSI source (Thermo Fisher Scientific) equipped with a stainless steel nano-bore emitter (Thermo Fisher Scientific). A spray voltage of 2.2 kV, capillary temperature of 275°C, and S-lens RF level of 50% were selected. The data-dependent MS/MS run was conducted in positive ion mode using a top-10 method. MS1 spectra (resolution 70,000) and MS2 spectra (resolution 17,500) were recorded in profile mode from 20 to 100 min. Automatic gain control (AGC) targets for MS and MS/MS were set to 1E6 and 1E5, respectively. Only peptides with 2, 3, or 4 positive charges were considered. Raw data were processed using Max Quant (version 1.5, [28]), and Perseus software (version 1.6.2.3, [29]) and human and virus entries of Uniprot databases containing common contaminants. Proteins were stated identified by a false discovery rate of 0.01 on protein and peptide level and quantified by extracted ion chromatograms of all peptides.

Protein network analysis was performed using the STRING protein-protein interaction networks functional enrichment analysis tool v11 (<https://string-db.org>) [30] with MCL clustering with an inflation parameter of 2 as suggested by STRING, an interaction score of high confidence (0.700) and deactivating text mining as least meaningful interaction source.

RNA *in situ* hybridization analysis

Non-radioactive *in situ* hybridization analysis of gene expression was performed on 10- μm paraffin sections of embryos using digoxigenin-labeled antisense riboprobes as described previously [31]. For each marker, sections from at least three mutant and control lungs were analyzed.

Immunofluorescence

Detection of antigens was performed on 5- μm or 10- μm frontal sections through the lung region of paraffin-embedded embryos. Endogenous peroxidases were blocked by incubation in 6% H_2O_2 for 20 min. Antigen retrieval was achieved by citrate-based heat

unmasking (H-3300, Vector Laboratories Inc., Burlingame, CA, USA). The following primary antibodies were used: anti-CBX3 (1:200; #PA5-30954, ThermoFisher Scientific, Waltham, MA, USA), anti-CHD4 (1:200; ab70469, Abcam plc, Cambridge, UK), anti-HDAC1 (1:200; #PA1-860, ThermoFisher Scientific), anti-HDAC2 (1:200; #51-5100, ThermoFisher Scientific), anti-HMGB2 (1:200; #ab124670, Abcam plc), anti-PBX1 (1:100; #PA5-82100, ThermoFisher Scientific), anti-TBX2 (1:200 or 1:2000; #07-318, Merck Millipore, Darmstadt, Germany), anti-TBX2 (1:200; #sc-514291X, Santa Cruz Biotechnology Inc.). Primary antibodies were detected by directly labeled fluorescence- or biotin-conjugated secondary antibodies (1:200; Invitrogen, Carlsbad, CA, USA; Dianova, Hamburg, Germany). The signal was amplified using a tyramide signal amplification (TSA) system (NEL702001KT, PerkinElmer, Waltham, MA, USA) according to the manufacturer's instruction. Nuclei were stained with 4',6-diamidino-2-phenylindole (DAPI, #6335.1, Carl Roth, Karlsruhe, Germany).

Cell culture, co-transfections and co-immunoprecipitations

HEK293 cells (ACC 305, DSMZ, Braunschweig, Germany) were cultured in DMEM medium with GlutaMax™ (#61965-059, ThermoFisher Scientific) containing 10% FCS (#F2442, Merck), 100 units/ml penicillin, 100 µg/ml streptomycin (#15140122, ThermoFisher Scientific), 5% sodium pyruvate (#11360070; ThermoFisher Scientific) and 5% non-essential amino acids (#11140035; ThermoFisher Scientific) and kept in an incubator at 37°C with 5% CO₂. The transient transfections were performed with the calcium phosphate method as previously described [32]. For this, cells were plated on 6 well plates (#657160, Cellstar, Greiner, Germany) and grown for approximately 6 hours to reach 80-90% confluence. 5 µg of expression plasmid each for TBX2 and its interaction candidate were co-transfected. Transfection efficiency was verified by epifluorescence of EGFP co-transfected with an empty *pcDNA3* vector.

We used the following expression vectors for transfections in HEK293 cells: *pcDNA3.huTBX2.HA* encoding N-terminally HA-tagged full-length human TBX2; *pCS2.Pbx1b* encoding full-length mouse PBX1B, (gift from Heike Pöpperl, Institute for Biophysical Chemistry, Hannover Medical School, Germany); *pd2EGFP-N1* (EGFP-expression vector) [33]; *pCMV6-Entry.Cbx3-Myc-DDK* encoding full-length mouse CBX3 (#MR224357, OriGene, Rockville, Maryland, USA); *pCMV-SPORT6.Hdac1* encoding full-

length mouse HDAC1 (#4217199, Sourcebioscience, Nottingham, UK); *pCMV6-Entry.Hdac2-Myc-DDK* encoding full-length mouse HDAC2 (#MR226709, OriGene); *pCMV-SPORT6.Chd4* encoding full-length mouse CHD4 (#6489649, Sourcebioscience); *pCMV-Entry.Hmgb2-GFP* encoding full-length mouse HMGB2 (#MR202276, OriGene).

Cell lysates were obtained following the RIME protocol [26] as described for MS analysis. Immunoprecipitations were performed using primary antibodies against potential interaction partners of TBX2 either exploiting MYC protein tags (mouse anti-MYC monoclonal antibody (9E10), MA1-980, Thermo Fisher Scientific) or with antibodies directed against the respective protein (rabbit anti-HP1 gamma (CBX3) polyclonal antibody, #PA5-30954, ThermoFisher Scientific; mouse anti-CHD4 antibody [3F2/4], ab70469, Abcam; rabbit anti-HDAC1 polyclonal antibody, #PA1-860, ThermoFisher Scientific; rabbit anti-HDAC2 polyclonal antibody, #51-5100, ThermoFisher Scientific; rabbit anti-PBX1 polyclonal antibody, #PA5-82100, ThermoFisher Scientific). Antibodies for IP reactions were diluted according to manufacturers' instructions. Cell lysates were incubated with respective antibodies for 1 hr at room temperature, followed by incubation with ProteinG Magnetic Beads (#9006S, Cell Signaling Technology) overnight at 4°C. After washing, beads were boiled in 1x Laemmli buffer with 2.5% β -mercaptoethanol (CAS 60-24-2, Sigma Aldrich). Proteins were separated by SDS-PAGE and blotted onto PVDF membranes (T830.1, Carl Roth, Karlsruhe, Germany). Western blots were stained using HRP coupled mouse anti HA (#ab1265, Abcam) antibodies for detection of HA tagged TBX2. Bands were visualized using CheLuminate-HRP FemtoDetect chemiluminescent substrate (#A7807, AppliChem, Darmstadt, Germany).

Documentation

Lung sections were documented with a DM5000 microscope (Leica Camera, Wetzlar, Germany) equipped with a Leica DFC300FX digital camera. Images were processed and analyzed with Adobe Photoshop CS5 (Adobe, San Jose, CA, USA) and ImageJ software (<https://imagej.nih.gov>). Western blots Blots were documented on a LAS-4000 luminescent Image Analyzer (Fuji, Tokyo, Japan).

Results

ChIP-Seq analysis identifies genome-wide TBX2 binding sites in the developing lung

To obtain an unbiased view of TBX2-bound genomic regions in the pseudoglandular stage of lung development, we performed *in vivo* ChIP-Seq analysis on E14.5 wildtype lungs using an anti-TBX2 antibody. Mapping of sequenced tags using MACS2 callpeak [19] identified 3062 peaks that were at least 3.5 fold enriched with $-\log_{10}$ p-values between 4 and 256. Peak scores ranged from 7 to 2470 (Table S1). We mapped TBX2 ChIP-sequencing peaks to genes with the Genomic Regions Enrichment of Annotations Tool (GREAT, version 4.0.4, <http://great.stanford.edu/public/html>) [34]. With respect to the transcription start site (TSS), 177 TBX2-binding sites mapped 5 kbp upstream, 174 mapped 5 kbp downstream; an additional 1150 TBX2-binding sites were located within 50 kbp up- or downstream; 3648 TBX2-binding sites were located at a greater distance (Figure 1A). Since TBX2-binding sites can be associated with more than one gene, the number of total localizations does not sum up to the number of peaks found.

Gene ontology (GO) annotation of biological function and processes by GREAT revealed enrichment of peak-associated genes with various mouse phenotypes. "Abnormal pulmonary trunk morphology" and "dilated respiratory conducting tubes" were the top enriched clusters in mouse phenotypes indicating significant affiliation of TBX2-bound regions to pulmonary development. Additional peak clusters were affiliated with the terms "abnormal digit development", "failure of palatal shelf elevation", "development of the urogenital system" and "limbs" reflecting known functions of TBX2 in mouse development [35-38]. "Abnormal otic vesicle development", "decreased cochlear coiling" and "abnormal tympanic membrane morphology" within the top 15 clusters may indicate an as yet unexplored function associated with TBX2 expression in the otic vesicle [39] (Figure 1B, Table S2-S4). We next performed *de novo* sequence motif analysis on the sequenced tags with the FIMO tool in Galaxy [22] (Figure 1C). Using the TomTom Motif Comparison Tool version 5.1.1 [23], we compared enriched motifs with experimentally determined transcription factor binding profiles deposited in Jaspar (<http://jaspar.genereg.net>) and footprintDB (<http://floresta.eead.csic.es/footprintdb>) databases. We found five enriched binding motifs in our ChIP-Seq data set with three strongly resembling previously described binding sites for T-box proteins. Two of them, one palindromic, the other non-palindromic, demonstrated

high similarity to a known binding motif for TBX2 (entry MA0688.1 in Jaspar) (Fig. 1C, highlighted in grey); a third (palindromic) motif was highly similar to a TBX21 binding site (entry TBX21_full_1 in footprintDB HumanTF 1.0) (Figure 1C, highlighted in green). The fourth motif matched a high mobility group (HMG)-box binding site (Fig. 1C, highlighted in blue), the fifth one resembled a composite of an erythroblast transformation specific (ETS) transcription factor binding site and a homeobox consensus sequence (Fig. 1C, highlighted in red). Strikingly, the TBX21-like binding motif occurred in different spatial combinations with the ETS-/homeobox- and HMG-motifs (Figure 1D), raising the possibility of cooperative binding of TBX2 with transcription factors harboring the respective DNA binding domains.

Microarray analysis identifies functional targets of TBX2 activity in the pulmonary mesenchyme

ChIP provides genomic DNA fragments bound by TBX2 but does not necessarily reflect a biological functionality of near-by genes. To identify genes whose expression depends on TBX2 in lung development, we interrogated a microarray-based gene expression profiling data set previously generated from E14.5 lungs of *Tbx2*-deficient and control mice [13]. Filtering each of the four individual microarray data sets by thresholds for intensity (>100) and fold change (>1.4) delivered a set of 36 genes with reduced and a set of 70 genes with increased expression (Figure 2A, Table S5-6).

Since TBX2 is a potent transcriptional repressor [40-43], we intersected the list of upregulated genes with the list of genes with an associated TBX2 ChIP-peak, and obtained 39 genes that are potentially directly repressed by TBX2 in the developing lung (Figure 2B,C). Functional annotation using MouseMine websoftware MGI 6.14 [25]) revealed an enrichment of clusters of GO terms related to “response to stress” (GO:0006950); “regulation of cell population proliferation” (GO:0042127) and “positive regulation of cell growth in cardiac muscle development” (GO:0061051) implicating TBX2 transcriptional activity in proliferative growth control (Figure 2D, Table S7-8). RNA *in situ* hybridization analysis on sections revealed a clear mesenchymal upregulation in *Tbx2*-deficient lungs for five genes: *Cdkn1a*, *Frzb1* and *Shisa3* as previously reported [13, 15], and additionally *Ccn4* (also known as *Wisp1*) and *Ii33* (Figure 2E, Figure S1). Analysis at earlier stages showed that derepression starts around E12.5 in *Tbx2*-deficient lungs

(Figure S2). Ectopic expression of *I33* occurred in the mesothelium and the sub-mesothelial mesenchyme (Figure 2E, Figure S2).

To gain further evidence for a direct regulation of *Ccn4* and *I33* by TBX2, we manually analyzed the ChIP-peak landscape for both genes (Figure 2F). We detected peaks upstream of or within the promoter region that we evaluated by ChIP-PCR on wildtype and *Tbx2*-mutant lungs (Figure 2G). Input control was comparable in wildtype and mutant chromatin for all tested peak regions. PCR signals in mutant chromatin were strongly reduced for all tested ChIP regions further implicating *I33* and *Ccn4* as direct targets of TBX2 repressive activity in the pulmonary mesenchyme.

Proteomic analysis identifies binding partners of TBX2 in the developing lung

To identify protein interaction partners that may explain target specificity and transcriptional repressive activity of TBX2 in the pulmonary mesenchyme, we used an *in vivo* co-immunoprecipitation (Co-IP) approach from E14.5 lungs with subsequent liquid chromatography - tandem mass spectrometry analysis (LC-MS/MS) (Figure 3A). For this, TBX2 containing complexes were purified from formaldehyde fixed lungs of E14.5 wildtype mice by affinity purification using an anti-TBX2 antibody coupled to Protein-G magnetic beads. The purified protein complexes of three independent experiments were sent to the proteomics facility of Hannover Medical School for protein extraction, and subsequently handed over to the Institute of Plant Genetics of Leibniz-University Hannover for LC-MS/MS analysis. In the three experiments, fragments of 919 mouse proteins were identified. An enrichment of 2 or larger (Student's t-test) against the control (immunoprecipitates in absence of the anti-TBX2 primary antibody) was found for 219 proteins (Figure 3A, Table S9). We rejected hemoglobins, immunoglobins and proteins associated with the terms "ribosomal", "mitochondrial" and "proteasomal" in the DAVID functional annotation tool (v6.8, david.ncifcrf.gov) reducing the list of candidates to 183 proteins. GO enrichment analysis using DAVID revealed that 119 of these proteins were associated with the term "nucleus", i.e. were likely to colocalize with TBX2 in the nucleus (Figure 3A, Table S10). Out of this list, 29 proteins were annotated by DAVID with the GO term "regulation of transcription", 14 proteins were associated with "histones or histone modification", implicating a role in transcriptional regulation. Seven proteins were in common between the two lists: CBX3, HDAC1/2, HNRNPD, RBBP4/7 and RBM14 (Figure

3A-C, Table S10). Analysis of the protein association network of these 36 proteins using the STRING Protein-Protein Interaction Networks Functional Enrichment analysis tool (v11, <https://string-db.org>) [30] uncovered three distinct protein interaction clusters (Figure 3D). Within the largest cluster (in red in Figure 3D) five proteins are known to be part of the transcriptional corepressor nucleosome remodeling and deacetylase (NuRD) core complex: the histone deacetylases HDAC1 and HDAC2, the histone-binding proteins RBBP4 and RBBP7, and the ATP-dependent chromatin-remodeling enzyme chromodomain-helicase-DNA-binding protein CHD4 [44, 45]. Proteins associated with this core complex included CBX3 (aka HP1 γ), a chromatin organization modifier (Chromo) domain protein associated with heterochromatin [46], the homeobox transcription factor PBX1 that interacts with HOX proteins and is able to repress transcription [47], the HMG box containing protein HMGB2, which binds to DNA in a DNA structure-dependent but nucleotide sequence-independent manner to function in chromatin remodeling [48], the DNA (cytosine-5) methyltransferase DNMT1 that acts in gene silencing [49], and the transcriptional corepressor MYBBP1A [50].

The second cluster (green in Figure 3D) contained several proteins implicated in RNA metabolism and splicing (HNRNs, DDX5, RBM39, CDC5L, ILF2). Further, members of the SWI/SNF chromatin remodeling complex were present (SMARCC1/2, DPF2). However, important core proteins of this complex including the ATPase (SMARCA2/4) were not enriched in our anti-TBX2 immunoprecipitation experiments. The third cluster (blue in Figure 3D) represents a very small group of WNT-signaling associated proteins correlated with cell adhesion. For the two latter clusters interactions have been found only between individual components indicating lack of functional complex formation.

TBX2 colocalizes and interacts with members of the NuRD complex (CHD4, HDAC1, HDAC2) as well as with PBX1, HMGB2 and CBX3

For further validation, we decided to employ candidate proteins found in the repressive NuRD complex (CHD4, HDAC1, HDAC2) as well as the proteins possibly associated with this complex (PBX1, HMGB2, CBX3) since they are likely to explain the target specificity and repressive activity of TBX2 in the pulmonary mesenchyme.

Co-immunofluorescence analysis of the candidate proteins and TBX2 on transverse sections of E14.5 lungs revealed that all six candidates were widely coexpressed with

TBX2 in the nuclei of pulmonary mesenchymal cells (Figure 4A).

In co-transfection/co-immunoprecipitation experiments in HEK293 cells, TBX2 interacted with all six candidates (Figure 4B). Hence, TBX2 interacts in the mesenchymal compartment of the developing lung with proteins implicated in transcriptional repression.

Discussion

***I/33* and *Ccn4* are novel direct targets of TBX2 in the lung mesenchyme**

We previously performed a ChIP-Seq experiment to validate *Cdkn1a*, *Cdkn1b*, *Frzb* and *Shisa3* as direct targets of TBX2 repressive activity in the pulmonary mesenchyme [13]. Here, we performed a new ChIP-Seq experiment to survey in an unbiased fashion the genomic binding sites of TBX2 in this organ. Importantly, we increased the chromatin input to obtain higher signals and performed bioinformatical analysis on the obtained called peak data set. We identified 3062 significantly enriched binding sites in the mouse genome that were variably spaced from TSSs indicating distant enhancer-promoter interactions. By a number of criteria, we deem that these binding peaks represent or at least contain *bona fide* TBX2 genomic binding sites. First, our motif analysis found a highly significant enrichment of DNA sequences similar to a T-box binding element initially identified in an *in vitro* binding site selection approach for the prototypical T-box protein Brachyury and to a consensus sequence previously identified by ChIP-Seq for TBX2 in neuroblastoma cell lines [51, 52]. Second, we recovered binding peaks in those genes previously characterized as direct targets of TBX2 repressive activity in the lung, including *Cdkn1a*, *Shisa3* and *Frzb* [13, 15]. Third, GO annotation of biological function and processes revealed enrichment of peak-associated genes with mouse phenotypes previously associated with TBX2 function in various embryological contexts [35-38].

The intersection of transcriptional profiling and ChIP-seq data sets provided a list of 39 genes that might be directly regulated by TBX2. In line with our previous phenotypic characterization, we found enrichment of genes annotated with proliferation and stress control, indicating that TBX2 predominantly represses anti-proliferative genes. To our surprise, we failed to detect increased expression of most candidate genes in the pulmonary mesenchyme of *Tbx2*-deficient embryos by *in situ* hybridization analysis. We assume that the overall expression of these genes is too low in the pulmonary mesenchyme of *Tbx2*-deficient embryos to reliably detect it by this method. Since many of

these candidate genes are strongly expressed in the epithelium, changes in the mesenchyme are unlikely to be detected either by alternative approaches including RT-PCRs of whole lung tissue. However, we confirmed increased expression of *Ccn4* and *Il33* in the lung mesenchyme of mutant embryos, and validated them as additional direct targets of TBX2 by ChIP-PCR. CCN4, also known as WISP-1, is a member of the WNT1 inducible signaling pathway protein (WISP) subfamily of the connective tissue growth factor/CCN family of matricellular proteins. CCN proteins, which are secreted, interact with cell surface receptors (e.g., integrins) and extracellular matrix components to modulate cellular functions. CCN4 can stimulate proliferation, adhesion, invasion, metastasis and epithelial-to-mesenchymal transition of cells [53]. The significance of repression of *Ccn4*, and thus, of these cell programs in the lung mesenchyme cannot be answered at this point. *Il33* codes for a cytokine which mediates inflammatory responses [54]. Its repression by TBX2 in the mesothelium and the submesothelial mesenchyme might prevent a premature activation of these responses in lung development, and thus avoid excessive immune cell infiltration at this stage.

TBX2 interacts with homeobox and HMG-box transcription factors in the lung mesenchyme

Our *de novo* motif analysis of the TBX2-ChIP-seq data set did not only reveal binding sites highly similar to the consensus binding site(s) of the T-box DNA-binding domain [11, 51] but also in variable spatial association for homeobox-, ETS-domain and HMG-box proteins, indicating concerted or even cooperative DNA-binding of TBX2 with members of other transcription factor families. Since DNA-binding sites are normally rather short, concerted binding of several transcription factors to adjacent binding sites dramatically increases target specificity [55]. It may further enhance the transcriptional outcome and may serve architectural purposes. In fact, high-mobility group (HMG) proteins are architectural DNA bending proteins that promote DNA loop structures and tether distant regulatory elements to gene promoters [56].

Most satisfyingly, we identified the homeobox transcription factor PBX1 and the HMG-box protein HMGB2 that have both been implicated in transcriptional repression [57, 58], amongst TBX2 interaction partners in our unbiased proteomic screen in the E14.5 lung. We validated binding of these candidates to TBX2 in co-immunoprecipitations in HEK

cells, and showed that they are largely coexpressed with TBX2 in the lung mesenchyme at E14.5. Mice with loss of *Hmgb2* do not exhibit lung defects, while *Pbx1*-deficiency results in lung hypoplasia and alveolar defects [59, 60]. In either case it is conceivable that the interaction with TBX2 is irrelevant for mesenchymal proliferation and branching morphogenesis in the pseudoglandular stage. Alternatively, redundancy with closely related family members (*Hmgb1* and *Pbx2-4*) may conceal the requirement of these genes in these cellular programs.

Although our *de novo* motif analysis found an enrichment of an ETS-domain binding motif in the TBX2-ChIP peaks, we did not identify a member of this protein family in our proteomic screen. This seems plausible since members of the ETS transcription factor family (e.g. ETV4, ERG, ELF1, ELK1) act as transcriptional activators [61-63] and would interfere with the repressive activity of TBX2, PBX and HMGB2 complexes. However, localization of these motifs might not occur coincidentally. It is conceivable that TBX2 inhibits ETS-mediated transcriptional activation competitively or by displacement of ETS transcription factor complexes from the promoter without necessarily interacting directly.

It is important to note that interaction of TBX2 and the closely related TBX3 with HMG-box and homeobox proteins has been documented before for other developmental contexts in which these closely related T-box proteins act [64-66] while interaction with ETS domain proteins is unreported. This further substantiates the possibility that TBX2 preferentially interacts with HMG and homeobox proteins in target gene repression in the lung.

TBX2 interacts with the components and interaction partners of the repressive NuRD complex

It is long known that TBX2 acts as repressor of target gene transcription both *in vitro* and *in vivo* [40-43] but evidence has accumulated that the molecular mechanisms of repression may differ in different developmental contexts. In the developing heart, TBX2 achieves repression of chamber specific genes in the atrioventricular canal by competing with the transcriptional activator TBX5 for binding to both conserved T-box binding elements as well as cooperating transcription factors including NKX2-5 and GATA4 [64]. In breast cancer cell lines, TBX2 interacts with EGR1 to co-repress EGR1-target genes including the breast tumor suppressor gene *NDRG1*. To do so, TBX2 recruits the DNA methyltransferase DNMT3B and histone methyltransferase complex components to set a

repressive chromatin mark (H3K9me3) within the proximal promoter of *NDRG1* [67]. In contrast, the repression of *Cdkn1a*, *Cdkn2a*, *Adam10*, *Pten* and muscle-specific genes in different cancer cell lines or myoblasts cells depends on recruitment of HDAC1, hence, deacetylation of lysine residues in N-terminal tails of histones [68-71]. The closely related T-box factor TBX3 also binds to HDACs (1,2,3 and 5) to repress target genes including *Cdkn1a* and *Cdkn2a* [72, 73].

Our proteomic analysis argues that HDACs namely, HDAC1 and HDAC2, are also involved in repression of TBX2 target genes including *Cdkn1a* and *Cdkn1b* in the lung mesenchyme. Both proteins were enriched in our proteomic screen, both bound to TBX2 in HEK cells and both genes were largely coexpressed with TBX2 in the lung mesenchyme. Our proteomic analysis further identified RBBP4, RBBP7 and CHD4 which are known to interact with HDAC1 and HDAC2 in the CHD/NuRD complex [44, 45] implicating for the first time this chromatin remodeling/histone deacetylase complex in the repression of TBX2 target genes in the lung mesenchyme.

CHD proteins like CHD4 are known to bind to methylated histone tails (H3K9me3) most likely via their PHD2 finger [74]. Similarly, CBX3 (aka HP1 γ), another protein for which we confirmed TBX2 binding, recognizes H3K9me3 marks and is involved in heterochromatin formation and transcriptional silencing including that of *Cdkn1a* by TBX2 [46, 67, 75, 76]. Together, this would argue for TBX2 interaction with histone-methyltransferases such as was shown for repression of *NDRG1* in tumor cells [67]. The identity of such histone methyltransferases in the lung mesenchyme remains open since we did not detect such enzymes in our proteomic screen. However, similar to the control of *NDRG1* by TBX2, we found that a DNA methyltransferase, namely (maintenance) DNMT1 coprecipitated with TBX2 from lung tissue implicating DNA methylation in transcriptional repression by TBX2 [49]. Intriguingly, cooperation of DNMTs with HDACs and the NuRD complex, and of DNMTs with CBX3/HP1 γ and the NuRD complex in gene silencing including that of sFRPs (such as *Frzb*) and of *Cdkn1a* has been reported, substantiating the relevance of TBX2 interaction with these components [77-80].

We also found MYBBP1A as an interaction partner in the proteomic analysis. MYBBP1A acts as a corepressor for different transcription factors and is possibly involved in chromatin compaction by recruiting negative epigenetic modifiers, such as HDAC1/2 and histone methyltransferase [50, 81]. Finally, in the group of 119 enriched nuclear proteins

LMNB1 was present, localizing TBX2 targets to the heterochromatic region associated with the nuclear lamina.

Conclusion

Our work identified *I/33* and *Ccn4* as additional direct target genes of TBX2 in the lung mesenchyme. It revealed combinations of T-box binding elements with binding sites for HMG-box and homeobox proteins in the TBX2 genomic binding peaks, and characterized the transcription factors PBX1 and HMGB2, and components and interaction partners of the NuRD complex as TBX2 protein binding partners. We suggest TBX2 cooperates with homeobox and HMG-box transcription factors in transcriptional repression of anti-proliferative genes in the lung mesenchyme, and that this repressive activity relies on histone deacetylation and chromatin remodeling mediated by the NuRD complex but also on DNA methylation, histone H3K9 trimethylation and subsequent heterochromatin formation by CBX3 at the nuclear lamina.

Availability of data and materials

All datasets and reagents are available from the corresponding author on reasonable request.

Abbreviations

Å:	Ångström
α-:	Anti-
ADAM10:	A disintegrin and metallopeptidase domain 10
ATP:	Adenosintriphosphat
avgFC:	Average fold change
BMP4 :	Bone morphogenetic protein 4
°C:	Degree Celsius
CBX3:	Chromobox 3
CCN4:	Cellular communication network factor 4
CDC5L:	Cell division cycle 5-like
CDKN1A:	Cyclin-dependent kinase inhibitor 1A (P21)
CDKN1B:	Cyclin-dependent kinase inhibitor 1B (P27)
CHD:	Chromodomain helicase DNA binding protein
CHD4:	Chromodomain helicase DNA binding protein 4
ChIP:	Chromatin immunoprecipitation
ChIP-Seq:	Chromatin immunoprecipitation sequencing
Chromo:	Chromatin organization modifier
cm:	Centimeter
CO₂:	Carbon dioxide
Co-IP:	Co-Immunoprecipitation
DAPI:	4',6-diamidino-2-phenylindole
DDX5:	DEAD box helicase 5
DNA:	Deoxyribonucleic acid
DNMTs:	DNA methyltransferases
DNMT1:	DNA (cytosine-5) methyltransferase 1
DNMT3B:	DNA methyltransferase 3B
DMEM:	Dulbecco's Modified Eagle's Medium

DPF2:	D4, zinc and double PHD fingers family 2
E:	Embryonic day
EGFP:	Enhanced green fluorescent protein
EGR1:	Early growth response 1
ELF1:	E74-like factor 1
ELK1:	ELK1, member of ETS oncogene family
ERG:	ETS transcription factor
ETS:	Erythroblast transformation specific
ETV4:	Ets variant 4
FC:	Fold change
FCS:	Fetal calf serum
Frzb:	Fizzled-related protein
GATA4:	GATA binding protein 4
GO:	Gene ontology
GREAT:	Genomic Regions Enrichment of Annotations Tool
H₂O₂:	Hydrogen peroxide
HDACs:	Histone deacetylases
HDAC1:	Histone deacetylase 1
HDAC2:	Histone deacetylase 12
HEK293 cells:	Human embryonic kidney 293 cells
HMG:	High mobility group
HMGB2:	High mobility group box 2
HNRNs:	Heterogeneous nuclear ribonucleoproteins
HNRNPD:	Heterogeneous nuclear ribonucleoprotein D
HOX:	Homeobox
HP1γ	Heterochromatin Protein 1, gamma
hr:	Hour
IgG:	Immunoglobulin G
IL33:	Interleukin 33
ILF2:	Interleukin enhancer binding factor 2
IP:	Immunoprecipitation
kbp:	Kilo base pairs

kDa:	Kilodalton
kV:	Kilovolt
LC-MS/MS:	Liquid chromatography tandem mass spectrometry
LMNB1:	Lamin B1
min:	Minute
µg:	Microgram
µl:	Microliter
µm:	Micrometer
mM:	Millimolar
MS:	Mass spectrometry
MYBBP1A:	MYB binding protein (P160) 1a
NDRG1:	N-myc downstream regulated gene 1
NKX2-5:	NK2 homeobox 5
nl:	Nanoliter
NuRD:	Nucleosome remodeling and deacetylase
PBS:	Phosphate-buffered saline
PBX1:	Pre B cell leukemia homeobox 1
PCR:	Polymerase chain reaction
PFA:	Paraformaldehyde
PHD2:	Plant homeodomain
PTEN:	Phosphatase and tensin homolog
RBBP4:	Retinoblastoma binding protein 4, chromatin remodeling factor
RBBP7:	Retinoblastoma binding protein 7, chromatin remodeling factor
RBM14:	RNA binding motif protein 14
RBM39:	RNA binding motif protein 39
RNA:	Ribonucleic acid
RT-PCR:	Reverse transcription polymerase chain reaction
SDS:	Sodium dodecyl sulfate
sFRPs:	Secreted frizzled-related protein
SHISA3:	Shisa family member 3

SMARCC1:	SWI/SNF related, matrix associated, actin dependent regulator of chromatin, subfamily c, member 1
SMARCC2:	SWI/SNF related, matrix associated, actin dependent regulator of chromatin, subfamily c, member 12
SMARCA2:	SWI/SNF related, matrix associated, actin dependent regulator of chromatin, subfamily a, member 4
SMARCA4:	SWI/SNF related, matrix associated, actin dependent regulator of chromatin, subfamily a, member 2
SMC:	Smooth muscle cell
SWI/SNF:	SWItch/Sucrose Non-Fermentable
TBX2:	T-box 2
TBX21:	T-box 21
TBX3:	T-box 3
TBX5:	T-box 5
TFA:	Trifluoroacetic acid
TGFs:	Transforming Growth Factors
TSA:	Tyramide signal amplification
TSS:	Transcription start site
v/v:	Volume percent
WISP:	WNT1 inducible signaling pathway protein
WISP-1:	WNT1 inducible signaling pathway protein 1
WNT:	Wingless-type MMTV integration site family
WNT1:	Wingless-type MMTV integration site family, member 1

Acknowledgements

We thank Dr. Imke Peters for excellent technical support, Dr. Heike Pöpperl for antibodies, Dr. Carsten Rudat and Dr. Mark-Oliver Trowe for critical reading of the manuscript.

Funding

This work was funded by a grant from the Deutsche Forschungsgemeinschaft (DFG KI728/11 to AK).

Declarations

Ethics approval and consent to participate

All animal work conducted for this study was performed according to European and German legislation. The breeding, handling and sacrifice of mice for embryo isolation was approved by the Niedersächsisches Landesamt für Verbraucherschutz und Lebensmittelsicherheit (Permit Number: AZ33.12-42502-04-13/1356).

Consent for publication

Not applicable.

Competing interests

The authors declare that they have no competing interest.

Author information

Timo H. Lüdtkke and Irina Wojahn contributed equally to the work.

Affiliations

Institut für Molekularbiologie, Medizinische Hochschule Hannover, Hannover, Germany

Timo H. Lüdtkke, Irina Wojahn, Marc-Jens Kleppa, Jasper Schierstaedt, Andreas Kispert
Department of Anatomy, Embryology and Physiology, Academic Medical Center, University of Amsterdam, Amsterdam, The Netherlands

Vincent M. Christoffels

Institut für Pflanzengenetik, Leibniz Universität Hannover, Hannover, Germany

Patrick Künzler

Plant-Microbe Systems, Leibniz Institute of Vegetable and Ornamental Crops, Großbeeren, Germany (current address)

Jasper Schierstaedt

Authors' contributions

Concept and design: THL, IW, AK; mouse and laboratory work and data analysis: THL, IW, JS, MJK, PK, AK; Animals: VMC; preparation of manuscript & figures: THL, IW, AK. All authors have read and approved the manuscript.

Corresponding author

Andreas Kispert, Medizinische Hochschule Hannover, Institut für Molekularbiologie,
OE5250, Carl-Neuberg-Str. 1, 30625 Hannover, Germany

E-mail: kispert.andreas@mh-hannover.de (AK)

References

1. Morrisey EE, Hogan BL: **Preparing for the first breath: genetic and cellular mechanisms in lung development.** *Dev Cell* 2010, **18**:8-23.
2. Shannon JM, Hyatt BA: **Epithelial-mesenchymal interactions in the developing lung.** *Annu Rev Physiol* 2004, **66**:625-645.
3. McCulley D, Wienhold M, Sun X: **The pulmonary mesenchyme directs lung development.** *Curr Opin Genet Dev* 2015, **32**:98-105.
4. Bellusci S, Furuta Y, Rush MG, Henderson R, Winnier G, Hogan BL: **Involvement of Sonic hedgehog (Shh) in mouse embryonic lung growth and morphogenesis.** *Development* 1997, **124**:53-63.
5. Bellusci S, Grindley J, Emoto H, Itoh N, Hogan BL: **Fibroblast growth factor 10 (FGF10) and branching morphogenesis in the embryonic mouse lung.** *Development* 1997, **124**:4867-4878.
6. Weaver M, Dunn NR, Hogan BL: **Bmp4 and Fgf10 play opposing roles during lung bud morphogenesis.** *Development* 2000, **127**:2695-2704.
7. Li C, Xiao J, Hormi K, Borok Z, Minoo P: **Wnt5a participates in distal lung morphogenesis.** *Dev Biol* 2002, **248**:68-81.
8. Shu W, Jiang YQ, Lu MM, Morrisey EE: **Wnt7b regulates mesenchymal proliferation and vascular development in the lung.** *Development* 2002, **129**:4831-4842.
9. Rajagopal J, Carroll TJ, Guseh JS, Bores SA, Blank LJ, Anderson WJ, Yu J, Zhou Q, McMahon AP, Melton DA: **Wnt7b stimulates embryonic lung growth by coordinately increasing the replication of epithelium and mesenchyme.** *Development* 2008, **135**:1625-1634.
10. Sebe-Pedros A, Ruiz-Trillo I: **Evolution and Classification of the T-Box Transcription Factor Family.** *Curr Top Dev Biol* 2017, **122**:1-26.
11. Naiche LA, Harrelson Z, Kelly RG, Papaioannou VE: **T-box genes in vertebrate development.** *Annu Rev Genet* 2005, **39**:219-239.
12. Ghosh TK, Brook JD, Wilsdon A: **T-Box Genes in Human Development and Disease.** *Curr Top Dev Biol* 2017, **122**:383-415.
13. Ludtke TH, Rudat C, Wojahn I, Weiss AC, Kleppa MJ, Kurz J, Farin HF, Moon A, Christoffels VM, Kispert A: **Tbx2 and Tbx3 Act Downstream of Shh to Maintain**

- Canonical Wnt Signaling during Branching Morphogenesis of the Murine Lung.** *Dev Cell* 2016, **39**:239-253.
14. Wojahn I, Ludtke TH, Christoffels VM, Trowe MO, Kispert A: **TBX2-positive cells represent a multi-potent mesenchymal progenitor pool in the developing lung.** *Respir Res* 2019, **20**:292.
 15. Ludtke TH, Farin HF, Rudat C, Schuster-Gossler K, Petry M, Barnett P, Christoffels VM, Kispert A: **Tbx2 controls lung growth by direct repression of the cell cycle inhibitor genes Cdkn1a and Cdkn1b.** *PLoS Genet* 2013, **9**:e1003189.
 16. Aanhaanen WT, Brons JF, Dominguez JN, Rana MS, Norden J, Airik R, Wakker V, de Gier-de Vries C, Brown NA, Kispert A, et al: **The Tbx2+ primary myocardium of the atrioventricular canal forms the atrioventricular node and the base of the left ventricle.** *Circ Res* 2009, **104**:1267-1274.
 17. Wakker V, Brons JF, Aanhaanen WT, van Roon MA, Moorman AF, Christoffels VM: **Generation of mice with a conditional null allele for Tbx2.** *Genesis* 2010, **48**:195-199.
 18. Muzumdar MD, Tasic B, Miyamichi K, Li L, Luo L: **A global double-fluorescent Cre reporter mouse.** *Genesis* 2007, **45**:593-605.
 19. Zhang Y, Liu T, Meyer CA, Eeckhoutte J, Johnson DS, Bernstein BE, Nusbaum C, Myers RM, Brown M, Li W, Liu XS: **Model-based analysis of ChIP-Seq (MACS).** *Genome Biol* 2008, **9**:R137.
 20. Robinson JT, Thorvaldsdottir H, Winckler W, Guttman M, Lander ES, Getz G, Mesirov JP: **Integrative genomics viewer.** *Nat Biotechnol* 2011, **29**:24-26.
 21. Thorvaldsdottir H, Robinson JT, Mesirov JP: **Integrative Genomics Viewer (IGV): high-performance genomics data visualization and exploration.** *Brief Bioinform* 2013, **14**:178-192.
 22. Grant CE, Bailey TL, Noble WS: **FIMO: scanning for occurrences of a given motif.** *Bioinformatics* 2011, **27**:1017-1018.
 23. Gupta S, Stamatoyannopoulos JA, Bailey TL, Noble WS: **Quantifying similarity between motifs.** *Genome Biol* 2007, **8**:R24.
 24. Huang da W, Sherman BT, Lempicki RA: **Systematic and integrative analysis of large gene lists using DAVID bioinformatics resources.** *Nat Protoc* 2009, **4**:44-57.

25. Motenko H, Neuhauser SB, O'Keefe M, Richardson JE: **MouseMine: a new data warehouse for MGI.** *Mamm Genome* 2015, **26**:325-330.
26. Mohammed H, Taylor C, Brown GD, Papachristou EK, Carroll JS, D'Santos CS: **Rapid immunoprecipitation mass spectrometry of endogenous proteins (RIME) for analysis of chromatin complexes.** *Nat Protoc* 2016, **11**:316-326.
27. Thal B, Braun HP, Eubel H: **Proteomic analysis dissects the impact of nodulation and biological nitrogen fixation on *Vicia faba* root nodule physiology.** *Plant Molecular Biology* 2018, **97**:233-251.
28. Cox J, Mann M: **MaxQuant enables high peptide identification rates, individualized p.p.b.-range mass accuracies and proteome-wide protein quantification.** *Nat Biotechnol* 2008, **26**:1367-1372.
29. Cox J, Mann M: **1D and 2D annotation enrichment: a statistical method integrating quantitative proteomics with complementary high-throughput data.** *BMC Bioinformatics* 2012:S12.
30. Szklarczyk D, Gable AL, Lyon D, Junge A, Wyder S, Huerta-Cepas J, Simonovic M, Doncheva NT, Morris JH, Bork P, et al: **STRING v11: protein-protein association networks with increased coverage, supporting functional discovery in genome-wide experimental datasets.** *Nucleic Acids Res* 2019, **47**:D607-D613.
31. Moorman AF, Houweling AC, de Boer PA, Christoffels VM: **Sensitive nonradioactive detection of mRNA in tissue sections: novel application of the whole-mount in situ hybridization protocol.** *J Histochem Cytochem* 2001, **49**:1-8.
32. Pear WS, Nolan GP, Scott ML, Baltimore D: **Production of high-titer helper-free retroviruses by transient transfection.** *Proc Natl Acad Sci U S A* 1993, **90**:8392-8396.
33. Rivera-Reyes R, Kleppa MJ, Kispert A: **Proteomic analysis identifies transcriptional cofactors and homeobox transcription factors as TBX18 binding proteins.** *PLoS One* 2018, **13**:e0200964.
34. McLean CY, Bristor D, Hiller M, Clarke SL, Schaar BT, Lowe CB, Wenger AM, Bejerano G: **GREAT improves functional interpretation of cis-regulatory regions.** *Nat Biotechnol* 2010, **28**:495-501.
35. Zirzow S, Ludtke TH, Brons JF, Petry M, Christoffels VM, Kispert A: **Expression**

- and requirement of T-box transcription factors Tbx2 and Tbx3 during secondary palate development in the mouse.** *Dev Biol* 2009, **336**:145-155.
36. Suzuki T, Takeuchi J, Koshiba-Takeuchi K, Ogura T: **Tbx Genes Specify Posterior Digit Identity through Shh and BMP Signaling.** *Dev Cell* 2004, **6**:43-53.
37. Aydogdu N, Rudat C, Trowe MO, Kaiser M, Ludtke TH, Taketo MM, Christoffels VM, Moon A, Kispert A: **TBX2 and TBX3 act downstream of canonical WNT signaling in patterning and differentiation of the mouse ureteric mesenchyme.** *Development* 2018, **145**.
38. Farin HF, Ludtke TH, Schmidt MK, Placzko S, Schuster-Gossler K, Petry M, Christoffels VM, Kispert A: **Tbx2 terminates shh/fgf signaling in the developing mouse limb bud by direct repression of gremlin1.** *PLoS Genet* 2013, **9**:e1003467.
39. Chapman DL, Garvey N, Hancock S, Alexiou M, Agulnik SI, Gibson-Brown JJ, Cebra-Thomas J, Bollag RJ, Silver LM, Papaioannou VE: **Expression of the T-box family genes, Tbx1-Tbx5, during early mouse development.** *Dev Dyn* 1996, **206**:379-390.
40. Brummelkamp TR, Kortlever RM, Lingbeek M, Trettel F, MacDonald ME, van Lohuizen M, Bernards R: **TBX-3, the gene mutated in Ulnar-Mammary Syndrome, is a negative regulator of p19ARF and inhibits senescence.** *J Biol Chem* 2002, **277**:6567-6572.
41. Carreira S, Dexter TJ, Yavuzer U, Easty DJ, Goding CR: **Brachyury-related transcription factor Tbx2 and repression of the melanocyte-specific TRP-1 promoter.** *Mol Cell Biol* 1998, **18**:5099-5108.
42. Jacobs JJ, Keblusek P, Robanus-Maandag E, Kristel P, Lingbeek M, Nederlof PM, van Welsem T, van de Vijver MJ, Koh EY, Daley GQ, van Lohuizen M: **Senescence bypass screen identifies TBX2, which represses Cdkn2a (p19(ARF)) and is amplified in a subset of human breast cancers.** *Nat Genet* 2000, **26**:291-299.
43. Lingbeek ME, Jacobs JJ, van Lohuizen M: **The T-box repressors TBX2 and TBX3 specifically regulate the tumor suppressor gene p14ARF via a variant T-site in the initiator.** *J Biol Chem* 2002, **277**:26120-26127.
44. Xue Y, Wong J, Moreno GT, Young MK, Cote J, Wang W: **NURD, a novel complex with both ATP-dependent chromatin-remodeling and histone deacetylase**
-

- activities.** *Mol Cell* 1998, **2**:851-861.
45. Torchy MP, Hamiche A, Klaholz BP: **Structure and function insights into the NuRD chromatin remodeling complex.** *Cell Mol Life Sci* 2015, **72**:2491-2507.
 46. Minc E, Allory Y, Worman HJ, Courvalin JC, Buendia B: **Localization and phosphorylation of HP1 proteins during the cell cycle in mammalian cells.** *Chromosoma* 1999, **108**:220-234.
 47. Saleh M, Rambaldi I, Yang XJ, Featherstone MS: **Cell signaling switches HOX-PBX complexes from repressors to activators of transcription mediated by histone deacetylases and histone acetyltransferases.** *Mol Cell Biol* 2000, **20**:8623-8633.
 48. Paull TT, Haykinson MJ, Johnson RC: **The nonspecific DNA-binding and -bending proteins HMG1 and HMG2 promote the assembly of complex nucleoprotein structures.** *Genes Dev* 1993, **7**:1521-1534.
 49. Siegfried Z, Eden S, Mendelsohn M, Feng X, Tsuberi BZ, Cedar H: **DNA methylation represses transcription in vivo.** *Nat Genet* 1999, **22**:203-206.
 50. Yang CC, Liu H, Chen SL, Wang TH, Hsieh CL, Huang Y, Chen SJ, Chen HC, Yung BY, Chin-Ming TB: **Epigenetic silencing of myogenic gene program by Myb-binding protein 1a suppresses myogenesis.** *EMBO J* 2012, **31**:1739-1751.
 51. Kispert A, Herrmann BG: **The Brachyury gene encodes a novel DNA binding protein.** *EMBO J* 1993, **12**:3211-3220.
 52. Decaestecker B, Denecker G, Van Neste C, Dolman EM, Van Loocke W, Gartlgruber M, Nunes C, De Vloed F, Depuydt P, Verboom K, et al: **TBX2 is a neuroblastoma core regulatory circuitry component enhancing MYCN/FOXM1 reactivation of DREAM targets.** *Nat Commun* 2020, **9**:4866.
 53. Gurbuz I, Chiquet-Ehrismann R: **CCN4/WISP1 (WNT1 inducible signaling pathway protein 1): A focus on its role in cancer.** *Int J Biochem Cell Biol* 2015, **62**:142-146.
 54. Cayrol C, Girard JP: **Interleukin-33 (IL-33): A nuclear cytokine from the IL-1 family.** *Immunol Rev* 2018:154-168.
 55. Hill CS: **Transcriptional control by the SMADs.** *Cold Spring Harb Perspect Biol* 2016, **8**:a022079.
 56. Bustin M: **Regulation of DNA-dependent activities by the functional motifs of**
-

- the high-mobility group chromosomal proteins. *Mol Cell Biol* 1999, **19**:5237–5246. .
57. Stelzer G, Goppelt A, Lottspeich F, Meisterernst M: **Repression of basal transcription by HMG2 is counteracted by TFIIH-associated factors in an ATP-dependent process.** *Mol Cell Biol* 1994, **14**:4712-4721.
58. Lu Q, Kamps MP: **Selective repression of transcriptional activators by Pbx1 does not require the homeodomain.** *Proc Natl Acad Sci U S A* 1996, **93**:470-474.
59. Sato M, Miyata K, Tian Z, Kadomatsu T, Ujihara Y, Morinaga J, Horiguchi H, Endo M, Zhao J, Zhu S, et al: **Loss of Endogenous HMGB2 Promotes Cardiac Dysfunction and Pressure Overload-Induced Heart Failure in Mice.** *Circ J* 2019, **83**:368-378.
60. Li W, Lin CY, Shang C, Han P, Xiong Y, Lin CJ, Jang J, Selleri L, Chang CP: **Pbx1 activates Fgf10 in the mesenchyme of developing lungs.** *Genesis* 2014, **52**:399-407.
61. Tsokos GC, Nambiar MP, Y.T. J: **Activation of the Ets transcription factor Elf-1 requires phosphorylation and glycosylation: defective expression of activated Elf-1 is involved in the decreased TCR zeta chain gene expression in patients with systemic lupus erythematosus.** *Ann N Y Acad Sci* 2003, **987**:240-245.
62. Kasza A, Wyrzykowska P, Horwacik I, Tymoszek P, Mizgalska D, Palmer K, Rokita H, Sharrocks AD, Jura J: **Transcription factors Elk-1 and SRF are engaged in IL1-dependent regulation of ZC3H12A expression.** *BMC Mol Biol* 2010, **11**:14.
63. Wollenick K, Hu J, Kristiansen G, Schraml P, Rehrauer H, Berchner-Pfannschmidt U, Fandrey J, Wenger RH, Stiehl DP: **Synthetic transactivation screening reveals ETV4 as broad coactivator of hypoxia-inducible factor signaling.** *Nucleic Acids Res* 2012, **40**:1928-1943
64. Habets PE, Moorman AF, Clout DE, van Roon MA, Lingbeek M, van Lohuizen M, Campione M, Christoffels VM: **Cooperative action of Tbx2 and Nkx2.5 inhibits ANF expression in the atrioventricular canal: implications for cardiac chamber formation.** *Genes Dev* 2002, **16**:1234-1246.
65. Boogerd KJ, Wong LY, Christoffels VM, Klarenbeek M, Ruijter JM, Moorman AF, Barnett P: **Msx1 and Msx2 are functional interacting partners of T-box factors in the regulation of Connexin43.** *Cardiovasc Res* 2008, **78**:485-493.
-

66. Saadi I, Das P, Zhao M, Raj L, Ruspita I, Xia Y, Papaioannou VE, Bei M: **Msx1 and Tbx2 antagonistically regulate Bmp4 expression during the bud-to-cap stage transition in tooth development.** *Development* 2013, **140**:2697-2702.
67. Crawford NT, McIntyre AJ, McCormick A, D'Costa ZC, Buckley, N.E., Mullan PB: **TBX2 interacts with heterochromatin protein 1 to recruit a novel repression complex to EGR1-targeted promoters to drive the proliferation of breast cancer cells.** *Oncogene* 2019, **38** 5971-5986.
68. Vance KW, Carreira S, Brosch G, Goding CR: **Tbx2 is overexpressed and plays an important role in maintaining proliferation and suppression of senescence in melanomas.** *Cancer Res* 2005, **65** 2260-2268.
69. Zhu B, Zhang M, Byrum SD, Tackett AJ, Davie JK: **TBX2 blocks myogenesis and promotes proliferation in rhabdomyosarcoma cells.** *Int J Cancer* 2014, **135**:785-797.
70. Zhu B, Zhang M, Williams EM, Keller C, Mansoor A, Davie JK: **TBX2 represses PTEN in rhabdomyosarcoma and skeletal muscle.** 2016, **35**: 4212-4224
71. Reinhardt S, Schuck F, Stoye N, Hartmann T, Grimm MOW, Pflugfelder G, Endres K: **Transcriptional repression of the ectodomain sheddase ADAM10 by TBX2 and potential implication for Alzheimer's disease.** *Cell Mol Life Sci* 2019, **76** 1005-1025
72. Yarosh W, Barrientos T, Esmailpour T, Lin L, Carpenter PM, Osann K, Anton-Culver H, Huang T: **TBX3 is overexpressed in breast cancer and represses p14 ARF by interacting with histone deacetylases.** *Cancer Res* 2008, **68**: 693-699.
73. Dong L, Dong Q, Chen Y, Li Y, Zhang B, Zhou F, Lyu X, Chen GG, Lai P, Kung HF, He ML: **Novel HDAC5-interacting motifs of Tbx3 are essential for the suppression of E-cadherin expression and for the promotion of metastasis in hepatocellular carcinoma.** *Signal Transduct Target Ther* 2018, **3**: 22
74. Musselman CA, Mansfield RE, Garske AL, Davrazou F, Kwan AH, Oliver SS, O'Leary H, Denu JM, Mackay JP, Kutateladze TG: **Binding of the CHD4 PHD2 finger to histone H3 is modulated by covalent modifications.** *Biochem J* 2009, **423**:179-187.
75. Fan Y, Li H, Liang X, Xiang Z: **CBX3 promotes colon cancer cell proliferation by CDK6 kinase-independent function during cell cycle.** *Oncotarget* 2017, **8**:CBX3

promotes colon cancer cell proliferation by CDK6 kinase-independent function during 19934-19946.

76. van Wijnen AJ, Bagheri L, Badreldin AA, Larson AN, Dudakovic A, Thaler R, Paradise CR, Wu Z: **Biological functions of chromobox (CBX) proteins in stem cell self-renewal, lineage-commitment, cancer and development.** *Bone*. 2020 Sep 24:115659. doi: 10.1016/j.bone.2020.115659. Online ahead of print.
77. Nan X, Ng HH, Johnson CA, Laherty CD, Turner BM, Eisenman RN, Bird A: **Transcriptional repression by the methyl-CpG-binding protein MeCP2 involves a histone deacetylase complex.** *Nature* 1998, **393**:386-389.
78. Fuks F, W.A. B, Brehm A, L. H-D, T. K: **DNA methyltransferase Dnmt1 associates with histone deacetylase activity.** *Nat Genet* 2000, **24**:88-91.
79. Choi WI, Jeon BN, Yoon JH, Koh DI, Kim MH, Yu MY, Lee KM, Kim Y, Kim K, Hur SS, et al: **The proto-oncoprotein FBI-1 interacts with MBD3 to recruit the Mi-2/NuRD-HDAC complex and BCoR and to silence p21WAF/CDKN1A by DNA methylation.** *Nucleic Acids Res* 2013, **41**: 6403-6420
80. Cai Y, Geutjes EJ, de Lint K, Roepman P, Bruurs L, Yu LR, Wang W, van Blijswijk J, Mohammad H, de Rink I, et al: **The NuRD complex cooperates with DNMTs to maintain silencing of key colorectal tumor suppressor genes.** *Oncogene* 2014, **33**:2157-2168.
81. Felipe-Abrio B, Carnero A: **The Tumor Suppressor Roles of MYBBP1A, a Major Contributor to Metabolism Plasticity and Stemness.** *Cancers* 2020, **2**:254.

Figures

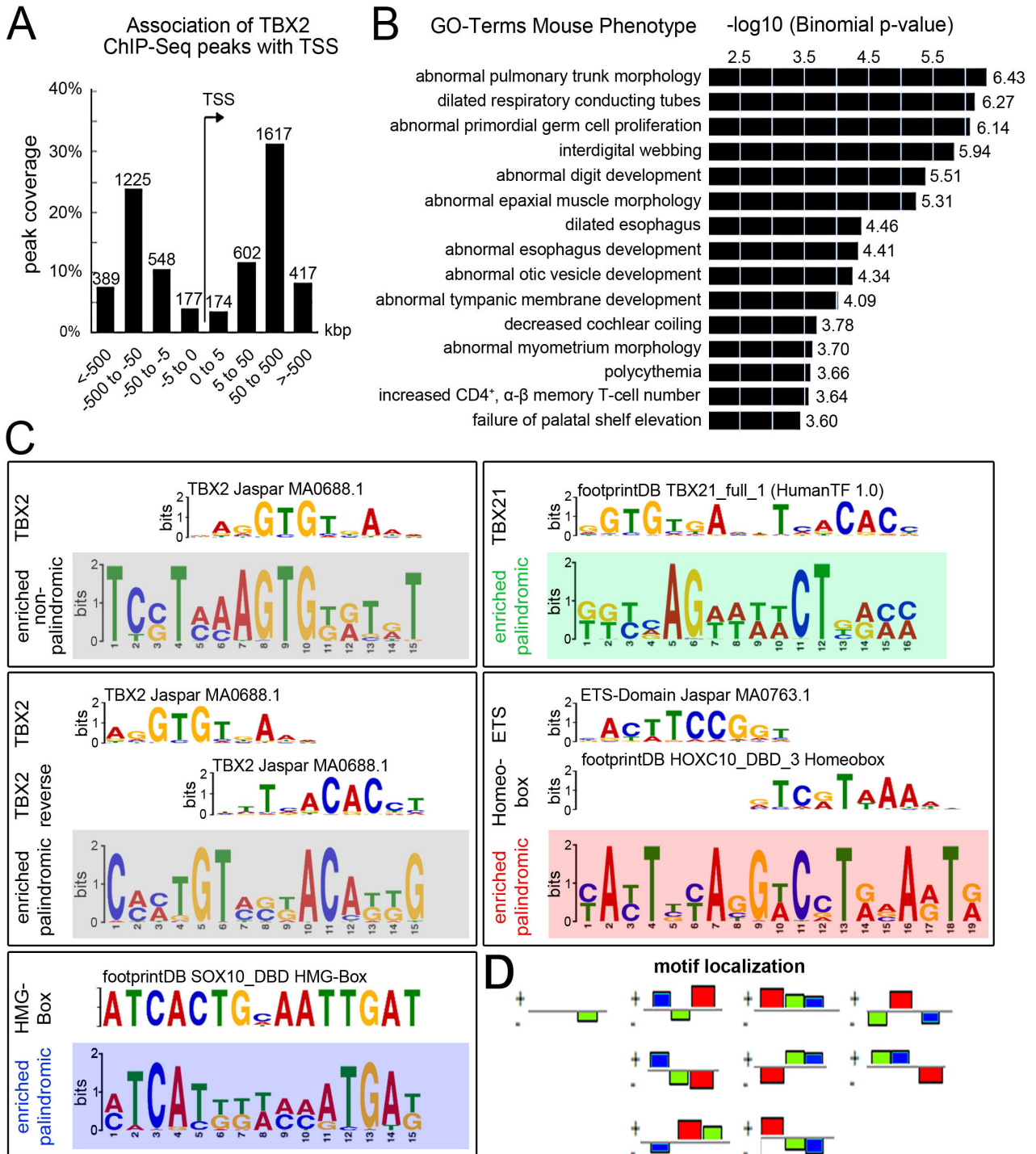


Figure 1. ChIP-Seq analysis identifies genomic binding sites of TBX2 in E14.5 lungs.

(A,B) Analysis of TBX2 ChIP-sequencing peaks with Genomic Regions Enrichment of Annotations Tool (GREAT, version 4.0.4). (A) Bar diagram showing the orientation and distance of TBX2 ChIP peaks to a transcription start site (TSS). (B) Functional annotation shows enrichment of genes associated with TBX2 ChIP peaks in clusters with annotated mouse phenotypes and biological processes sorted by $-\log_{10}$ binomial p-value. (C) *De novo* motif analysis was performed in Galaxy using FIMO - Scan a set of sequences for motifs (Galaxy v4.11.1.0) Novel consensus sequences are highlighted in colored boxes and compared to known motifs with TomTom Motif Comparison Tool v5.1.1. One palindromic and one non-palindromic motif with similarities to a known TBX2 binding element in the Jaspas database were discovered with E-values of $5.9e-198$ and $4.6e-152$ (grey boxes). Additional novel palindromic sequences show similarities to a TBX21 binding site in the footprint database, $E=1.7e-252$ (green box), an ETS (Jaspas database) and homeobox (footprint database) binding motif, $E=6.8e-497$ (red box), and an HMG-Box binding site (footprintDB), $E=4.4e-300$ (blue box). (E) Analysis of motif localization by GREAT discovered conjunct motifs for TBX2 (green), ETS/homeobox (red) and HMG-box proteins (blue) in TBX2 ChIP-Seq peaks. Motifs are colored as in C and colored boxes in D reflect spatial arrangement and interconnection of motifs on both DNA strands (+ and -).

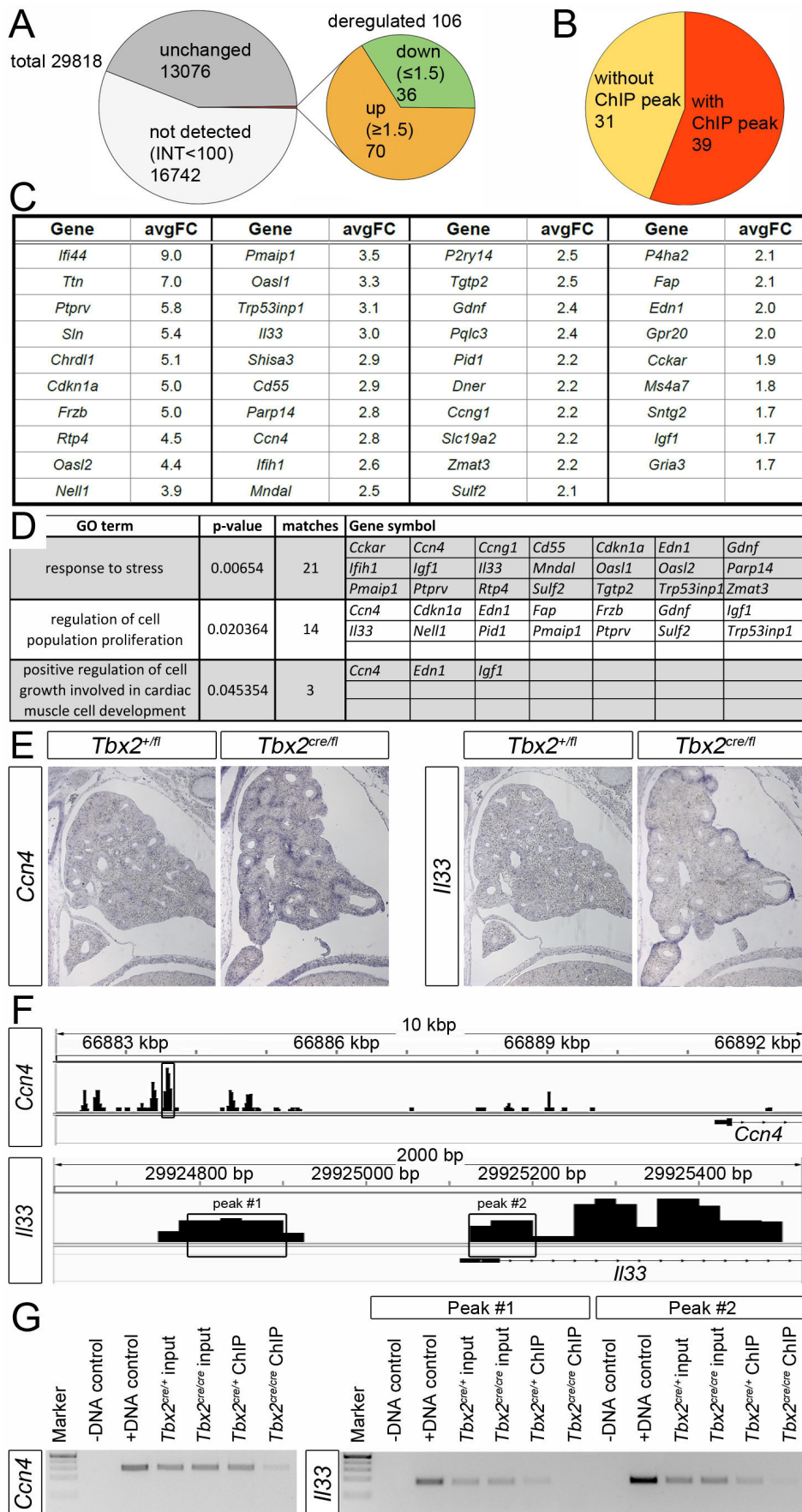
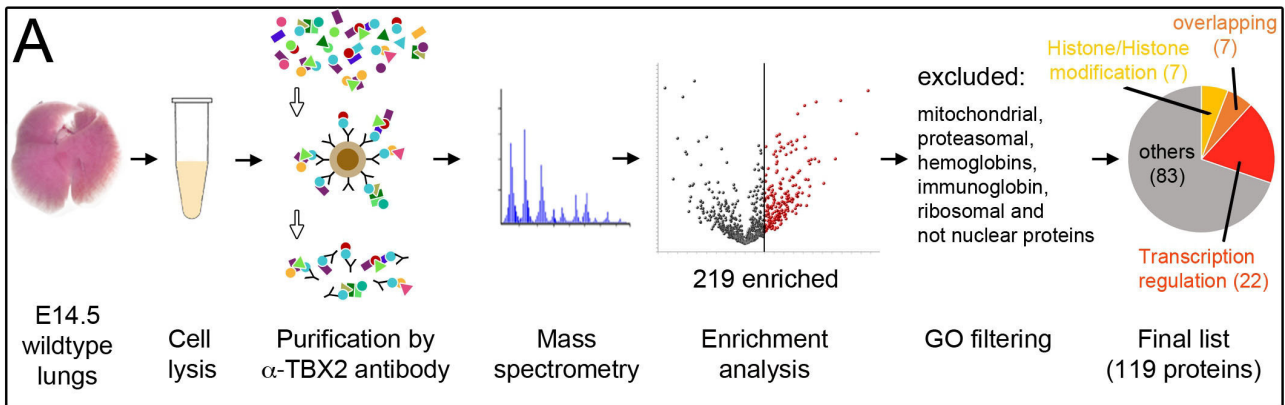


Figure 2. Microarray analysis identifies functional targets of TBX2 activity in E14.5 lungs.

(A) Pie-chart summarizing the results of 4 individual transcriptional profiling experiments by microarrays of E14.5 control and *Tbx2*-deficient lungs. (B) Intersection of the list of genes upregulated in the microarrays of E14.5 *Tbx2*-deficient lungs and the list of genes associated with TBX2 ChIP peaks in the E14.5 lung. (C) List of genes upregulated in the microarrays of E14.5 *Tbx2*-deficient lungs and having a TBX2 ChIP-peak. Shown are the average fold changes (avgFC) of the 4 individual microarray data sets. (D) Functional annotation analysis by MouseMine websoftware identifies functional enrichment of terms related to stress response and growth control in the set of 39 genes upregulated in the microarrays of E14.5 *Tbx2*-deficient lungs and having a TBX2 ChIP-peak. (E) RNA *in situ* hybridization analysis of *Ccn4* and *I133* expression on sections of E14.5 control and *Tbx2*-deficient lungs. (F) Scheme depicting the genomic loci of *Ccn4* and *I133*. Binding peaks identified by ChIP-Seq analysis are indicated above. Black boxes indicate peaks further validated by ChIP-PCR. (G) ChIP-PCR-validation of peaks in *I133* and *Ccn4* as indicated in (F). Lanes were loaded as indicated.



B

Transcription regulation	
ID	Gene Name
Adnp	activity-dependent neuroprotective protein
Cbx3	chromobox 3
Cdc5l	cell division cycle 5-like
Chd4	chromodomain helicase DNA binding protein 4
Ctnnb1	catenin (cadherin associated protein), beta 1
Ctnd1	catenin (cadherin associated protein), delta 1
Ddx5	DEAD (Asp-Glu-Ala-Asp) box polypeptide 5
Dnmt1	DNA methyltransferase (cytosine-5) 1
Dpf2	D4, zinc and double PHD fingers family 2
Fubp1	far upstream element (FUSE) binding protein 1
Hdac1	histone deacetylase 1
Hdac2	histone deacetylase 2
Hmgb2	high mobility group box 2
Hnrnpab	heterogeneous nuclear ribonucleoprotein A/B
Hnrnpd	heterogeneous nuclear ribonucleoprotein D
Hspa4	heat shock protein 4
Ilf2	interleukin enhancer binding factor 2

Transcription regulation	
ID	Gene Name
Mybbp1a	MYB binding protein (P160) 1a
Parp1	poly (ADP-ribose) polymerase family, member 1
Pbx1	pre B cell leukemia homeobox 1
Rbbp4	retinoblastoma binding protein 4
Rbbp7	retinoblastoma binding protein 7
Rbm14	RNA binding motif protein 14
Rbm39	RNA binding motif protein 39
Smarcc1	SWI/SNF related, matrix associated, actin dependent regulator of chromatin, subfamily c, member 1
Smarcc2	SWI/SNF related, matrix associated, actin dependent regulator of chromatin, subfamily c, member 2
Snd1	staphylococcal nuclease and tudor domain containing 1
Sub1	SUB1 homolog
Tbx2	T-box 2

C

Histone/Histone modification	
ID	Gene Name
Anp32e	Acidic leucine-rich nuclear phosphoprotein 32 family member E
Cbx3	Chromobox protein homolog 3
Cdk1	Cyclin-dependent kinase 1
H1fx	H1.10 Linker Histone
H2afv	H2A histone family, member V
H2afy2	H2A histone family, member Y2
H2afz	H2A histone family, member Z
Hdac1	histone deacetylase 1
Hdac2	histone deacetylase 2
Hnrnpd	Heterogeneous nuclear ribonucleoprotein D0
Rac1	Ras-related C3 botulinum toxin substrate 1
Rbbp4	Histone-binding protein RBBP4
Rbbp7	Histone-binding protein RBBP7
Rbm14	RNA binding motif protein 14

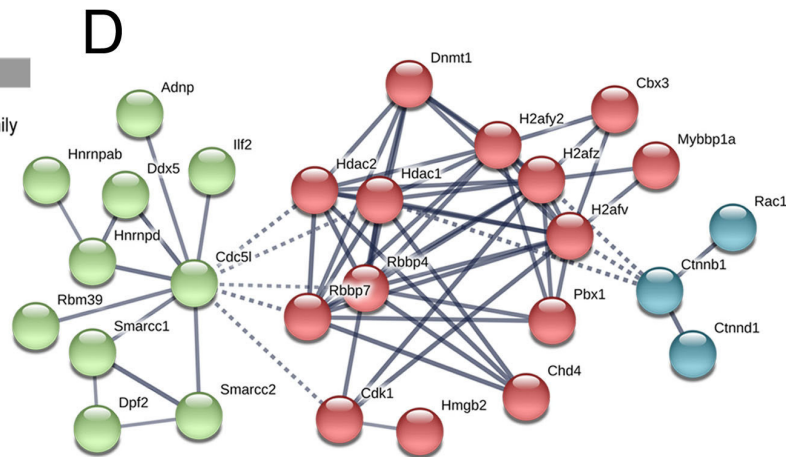


Figure 3. LC-MS/MS identifies TBX2 interaction partner in E14.5 lungs.

(A) Diagram depicting the strategy to identify TBX2 interacting proteins in embryonic lungs. Tissue of E14.5 wildtype formaldehyde fixed lungs was homogenized, cells were lysed, and nuclei extracted. Protein complexes containing TBX2 were purified with an α -TBX2 antibody. Subsequent LC-MS/MS analysis and statistical filtering (Student's t-test difference of ≥ 2) revealed an enrichment of 219 proteins within the α -TBX2 fraction compared to the control lacking the α -TBX2 antibody. Manual exclusion of mitochondrial, proteasomal, and ribosomal proteins as well as hemoglobins, immunoglobins and non-nuclear proteins lead to a list of 119 candidate proteins. Of these, 22 were associated with the GO term "transcriptional regulation", 7 with the terms "histone/histone modification". 7 proteins were in the intersection of both GO term lists. (B,C) List of enriched proteins associated with the GO term "transcription regulation" (B) and "histones" or "histone modification" (C) according to DAVID functional analysis. (D) STRING analysis of interactions of the candidate proteins shown in (B) and (C). Three clusters were identified using MCL clustering with an inflation parameter of 2, an interaction score of high confidence (0.700) and deactivating the interaction source "textmining".

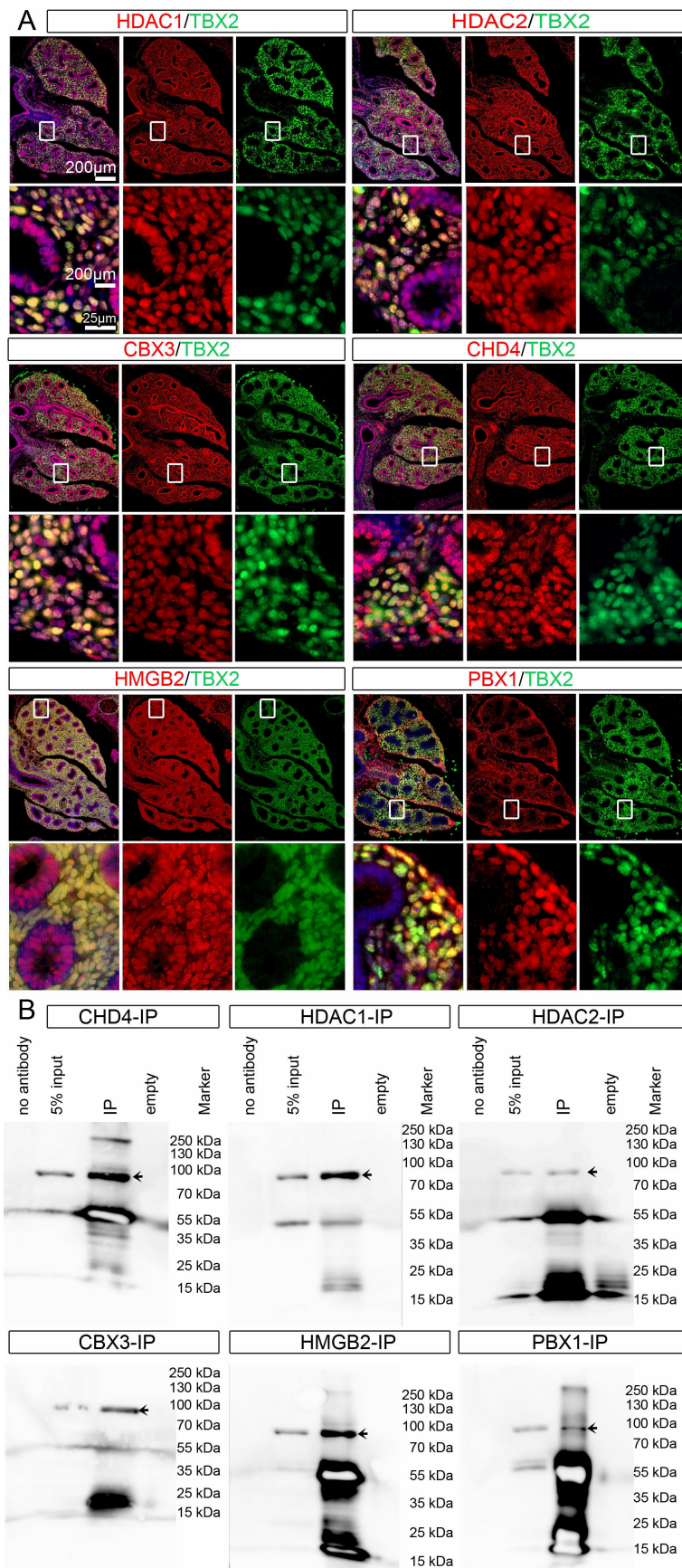


Figure 4. Interaction candidates are coexpressed with TBX2 in the pulmonary mesenchyme and interact in HEK293 cells.

(A) Co-immunofluorescence analysis of candidate interaction partners (red) and TBX2 (green) on frontal sections of the right lung of E14.5 *Tbx2^{cre/+}* embryos. Antigens are color-coded and nuclei were counterstained with DAPI (blue). Insets or selected regions in overview images are magnified in rows 2,4 and 6. (B) Western blot analysis of co-immunoprecipitation experiments for verification of TBX2 interaction of candidate proteins on 10% SDS polyacrylamide gels. Detection was performed with an anti-TBX2 primary antibody and developed with chemoluminescence-IHC. Arrows indicate TBX2 bands.

Lanes were loaded as follows: No antibody: IP without specific antibody resembling negative IP-control; 5% input: 5% of crude cell extract before precipitation; empty: no protein loaded; IP: co-immunoprecipitate with antibody for specific candidate. Expected molecular weight for TBX2.HA approx. 76.2 kDa.

Additional files

Additional file 1:

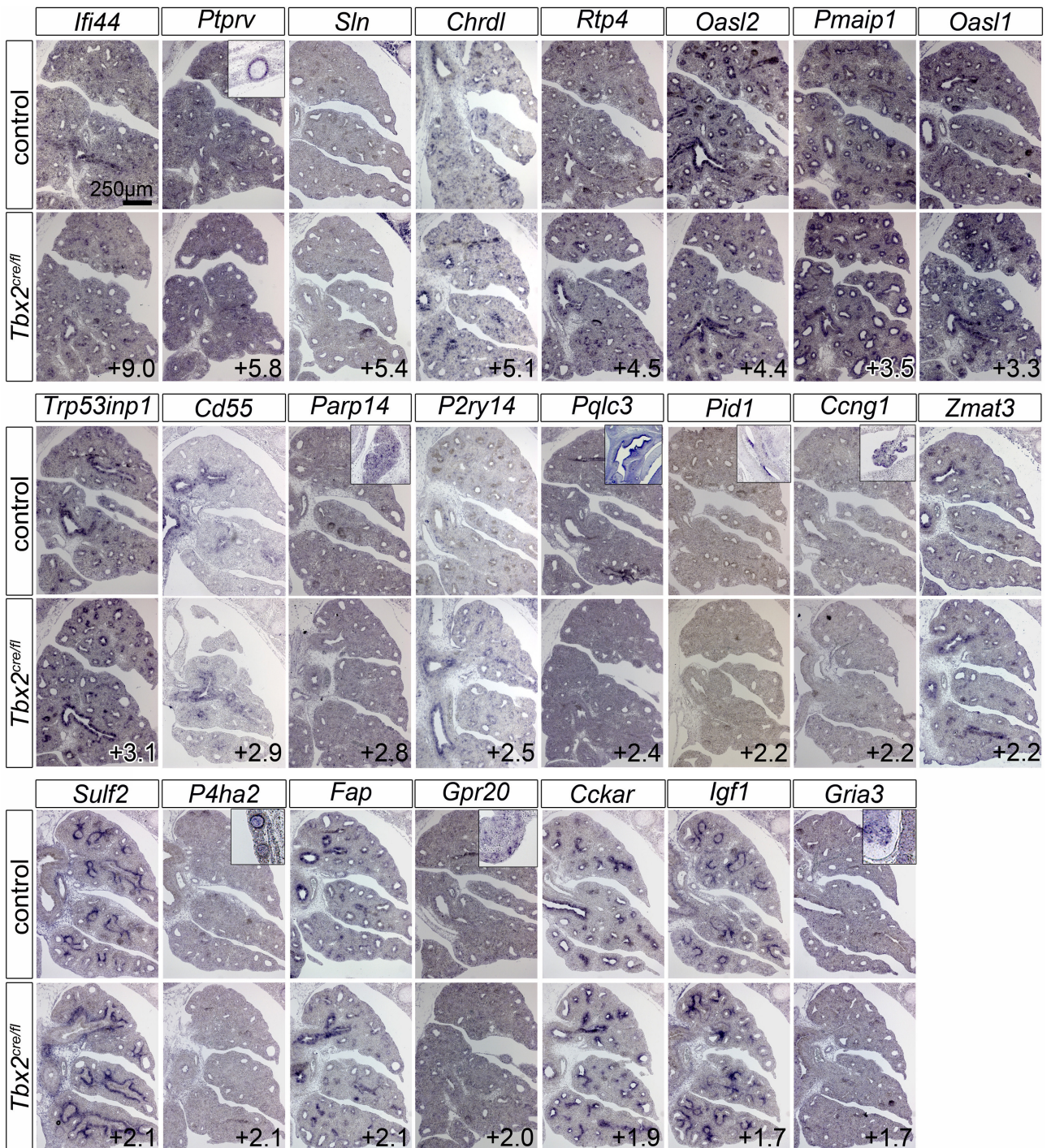


Figure S1. Expression analysis of candidate genes with increased expression in microarray analyses of TBX2-deficient lungs.

RNA *in situ* hybridizations were performed on frontal lung sections of E14.5 control (*Tbx2*^{+/fl}) and *Tbx2*-deficient (*Tbx2*^{cre/fl}) embryos. Insets show positive control regions. Numbers refer to fold change in the microarray analysis of *Tbx2*-deficient lungs. Probes and genotypes are as indicated.

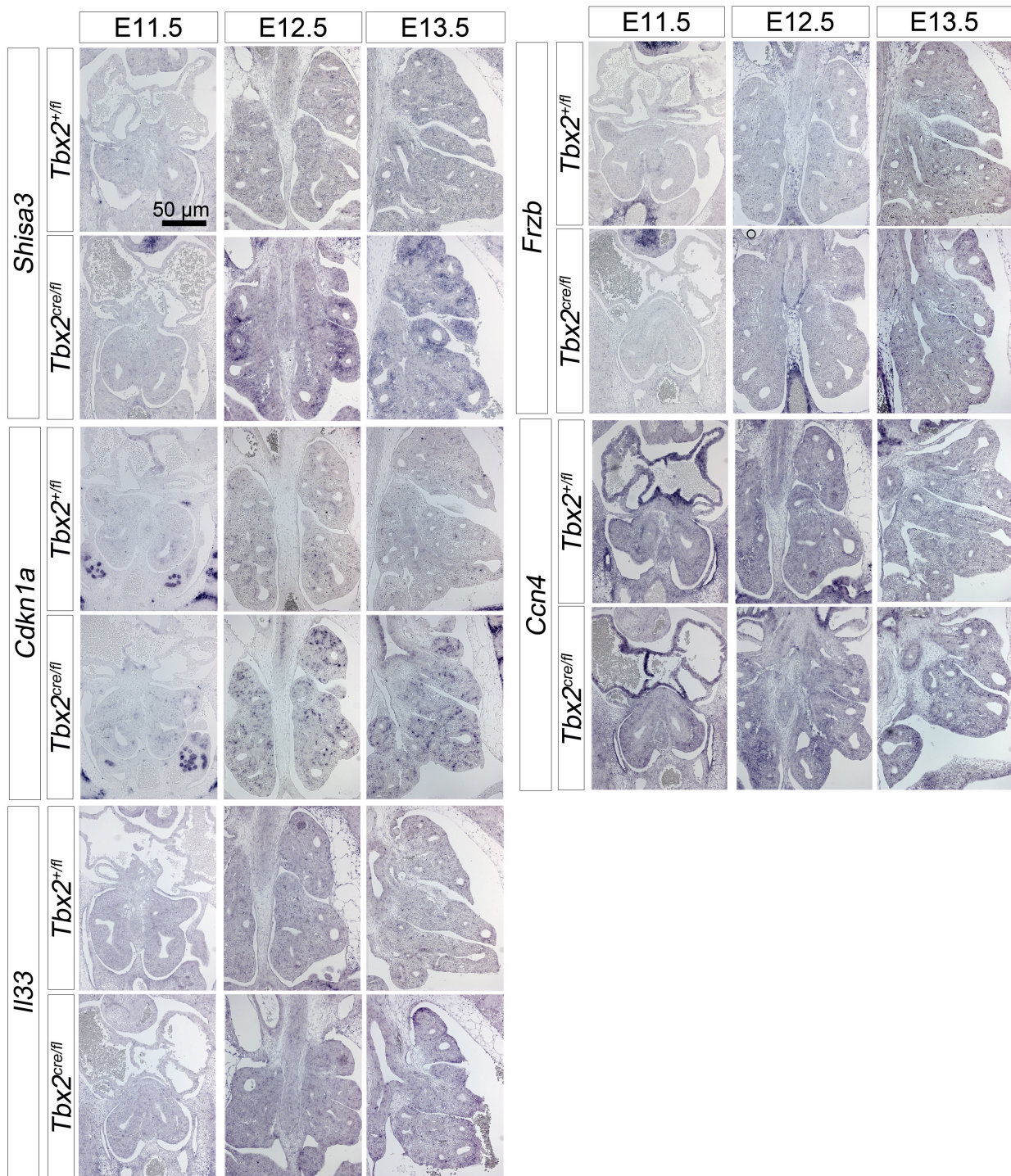


Figure S2. Derepression of TBX2 target genes occurs around E12.5 in TBX2-deficient pulmonary mesenchyme.

In situ hybridization on frontal lung sections of E11.5, E12.5 and E13.5 control (*Tbx2^{+/fl}*) and *Tbx2*-deficient (*Tbx2^{cre/fl}*) mice. Probes, genotypes and stages are as indicated.

Additional file 2:

Because of the extend of the tables, the complete data set of Additional file 2 is provided as electronic version on the attached compact disc. Table S1 and Table S10 are exclusively provided as electronic versions. Table S9 is partly provided in the printed version, while the complete list is provided as electronic version.

Table S1. TBX2 ChIP-seq peaks.

Shown are ChIP-seq peaks with a peak score threshold of 7 sorted by chromosomal position.

Because of the extend of the table, the complete data set is provided as electronic version on the attached compact disc.

Table S2. Functional annotation of enriched TBX2 ChIP-seq peaks.

Shown are gene enrichments determined by GREAT and associated with TBX2 ChIP peaks in clusters with annotated biological processes sorted by $-\log_{10}$ binomial p-value.

GO - Biological Processes

# Term Name	Binom Rank	Binom Raw P-Value	Binom FDR Q-Val	Binom Fold Enrichment	Binom Observed Region Hits	Binom Region Set Coverage	Hyper Rank	Hyper FDR Q-Val	Hyper Fold Enrichment	Hyper Observed Gene Hits	Hyper Total Genes	Hyper Gene Set Coverage
spleen development	60	7.39167e-6	1.61262e-3	2.1829	40	1.32%	401	1.55456e-3	2.6365	18	45	0.55%
positive regulation of Ras protein signal transduction	69	8.95426e-6	1.69871e-3	2.0973	43	1.42%	510	6.02107e-3	2.3728	18	50	0.55%
positive regulation of DNA replication	79	1.31358e-5	2.17655e-3	2.1762	38	1.26%	364	6.84036e-4	2.5632	21	54	0.65%
cellular response to vitamin D	95	2.44237e-5	3.36533e-3	2.6612	24	0.79%	619	1.51980e-2	3.8449	7	12	0.22%
cellular response to vitamin	97	2.81310e-5	3.79623e-3	2.4706	27	0.89%	647	1.84477e-2	3.1221	9	19	0.28%
negative regulation of stress fiber assembly	187	2.52657e-4	1.76860e-2	2.4957	20	0.66%	712	2.96011e-2	2.7463	10	24	0.31%
specification of animal organ identity	201	3.18392e-4	2.07351e-2	2.1570	26	0.86%	489	4.66036e-3	3.7075	9	16	0.28%
nephric duct morphogenesis	218	4.07560e-4	2.44723e-2	2.1980	24	0.79%	619	1.51980e-2	3.8449	7	12	0.22%
cardiac right ventricle morphogenesis	223	4.67781e-4	2.74586e-2	2.0676	27	0.89%	647	1.84477e-2	3.1221	9	19	0.28%
Roundabout signaling pathway	258	7.43845e-4	3.77400e-2	2.4092	18	0.60%	677	2.48674e-2	4.7080	5	7	0.15%
atrioventricular canal development	273	8.55612e-4	4.10255e-2	2.8657	13	0.43%	813	4.83056e-2	4.1195	5	8	0.15%
regulation of epithelial cell proliferation involved in lung morphogenesis	302	1.11352e-3	4.82647e-2	2.3227	18	0.60%	611	1.44242e-2	4.3941	6	9	0.18%

The test set of 3,025 genomic regions picked 3,246 genes (15%) of all 21,395 genes.

GO *Biological Process* has 13,090 terms covering 17,925 (84%) of all 21,395 genes.

13,090 ontology terms were tested (100%) using an annotation count range of [1, 1000].

GREAT version 4.0.4

Species assembly: mm10

Association rule: Basal+extension: 5000 bp upstream, 1000 bp downstream, 1000000 bp max extension, curated regulatory domains included

Table S2. Functional annotation of enriched TBX2 ChIP-seq peaks.

Shown are gene enrichments determined by GREAT and associated with TBX2 ChIP peaks in clusters with annotated biological processes sorted by $-\log_{10}$ binomial p-value.

Table S3. Functional annotation of enriched TBX2 ChIP-seq peaks.

Shown are gene enrichments determined by GREAT and associated with TBX2 ChIP peaks in clusters with annotated mouse phenotypes sorted by $-\log_{10}$ binomial p-value.

GO - Mouse Phenotype

# Term Name	Binom Rank	Binom Raw P-value	Binom FDR Q-Val	Binom Fold Enrichment	Binom Observed Region Hits	Binom Re-gion Set Coverage	Hyper Rank	Hyper FDR Q-Val	Hyper Fold Enrichment	Hyper Observed Gene Hits	Hyper Total Genes	Hyper Gene Set Coverage
abnormal pulmonary trunk morphology	18	3.67433e-7	1.95457e-4	2.9352	30	0.99%	334	3.11254e-4	4.0279	11	18	0.34%
dilated respiratory conducting tubes	20	5.35948e-7	2.56585e-4	2.4738	39	1.29%	264	5.22476e-5	3.8449	14	24	0.43%
abnormal primordial germ cell proliferation	23	7.19917e-7	2.99703e-4	4.1642	18	0.60%	668	1.03015e-2	3.8449	7	12	0.22%
interdigital webbing	25	1.14190e-6	4.37349e-4	2.4285	38	1.26%	249	2.73371e-5	3.6365	16	29	0.49%
abnormal digit development	33	3.08635e-6	8.95510e-4	2.1282	46	1.52%	195	4.04855e-6	3.4690	20	38	0.62%
abnormal epaxial muscle morphology	40	4.93022e-6	1.18017e-3	3.3376	20	0.66%	655	9.84215e-3	4.3941	6	9	0.18%
dilated esophagus	91	3.50163e-5	3.66441e-3	2.9019	20	0.66%	896	3.00625e-2	3.5952	6	11	0.18%
abnormal esophagus development	94	3.93148e-5	4.00468e-3	2.8773	20	0.66%	655	9.84215e-3	4.3941	6	9	0.18%
abnormal otic vesicle development	99	4.57307e-5	4.42295e-3	2.2772	30	0.99%	785	1.96389e-2	2.7463	10	24	0.31%
abnormal tympanic membrane morphology	111	8.06920e-5	6.95973e-3	2.6493	21	0.69%	772	1.81914e-2	3.9547	6	10	0.18%
decreased cochlear coiling	146	1.65556e-4	1.08575e-2	2.0556	32	1.06%	403	1.01289e-3	3.6252	11	20	0.34%
abnormal myometrium morphology	150	2.00807e-4	1.28178e-2	2.2248	26	0.86%	729	1.55424e-2	2.6853	11	27	0.34%
polycythemia	153	2.20664e-4	1.38095e-2	2.3981	22	0.73%	806	2.21641e-2	3.1017	8	17	0.25%
increased CD4-positive, alpha-beta memory T cell number	154	2.31732e-4	1.44080e-2	2.2442	25	0.83%	1019	4.22013e-2	2.4412	10	27	0.31%
failure of palatal shelf elevation	160	2.49749e-4	1.49459e-2	2.0069	32	1.06%	392	8.32411e-4	2.9960	15	33	0.46%
variable body spotting	171	3.22280e-4	1.80458e-2	2.3311	22	0.73%	649	9.68185e-3	3.5153	8	15	0.25%
abnormal citoris size	181	3.51310e-4	1.85845e-2	2.8707	15	0.50%	584	6.89131e-3	5.4927	5	6	0.15%
increased B-1 B cell number	185	3.74932e-4	1.94053e-2	2.0666	28	0.93%	821	2.37176e-2	2.2506	14	41	0.43%
abnormal diaphragm development	200	4.51463e-4	2.16138e-2	2.9266	14	0.46%	1038	4.52703e-2	3.2956	6	12	0.18%
abnormal germ cell physiology	246	7.24391e-4	2.81953e-2	2.1467	23	0.76%	476	2.68178e-3	3.2956	11	22	0.34%
prolonged diestrus	250	7.7264e-4	2.97692e-2	2.0961	24	0.79%	785	1.96389e-2	2.7463	10	24	0.31%
absent submandibular gland	256	8.07759e-4	3.02121e-2	2.7533	14	0.46%	742	1.65964e-2	4.7080	5	7	0.15%
absent ureteric bud	263	8.54282e-4	3.11017e-2	2.4513	17	0.56%	753	1.72098e-2	3.5491	7	13	0.22%
absent eyelids	264	8.78638e-4	3.18673e-2	2.1568	22	0.73%	452	1.82277e-3	3.6618	10	18	0.31%
absent alisphenoid bone	284	1.05736e-3	3.56486e-2	2.5706	15	0.50%	909	3.16026e-2	4.1195	5	8	0.15%
abnormal citoris morphology	287	1.07365e-3	3.58197e-2	2.3304	18	0.60%	339	3.60713e-4	5.7673	7	8	0.22%
abnormal spinal cord lateral column morphology	299	1.19261e-3	3.81916e-2	2.3751	17	0.56%	852	2.61216e-2	5.2730	4	5	0.12%
abnormal hindlimb bud morphology	305	1.25552e-3	3.94151e-2	2.1858	20	0.66%	649	9.68185e-3	3.5153	8	15	0.25%
increased macrophage nitric oxide production	328	1.49365e-3	4.36028e-2	6.1657	5	0.17%	949	3.52079e-2	6.5912	3	3	0.09%
abnormal auditory tube	340	1.66319e-3	4.68384e-2	2.9483	11	0.36%	742	1.65964e-2	4.7080	5	7	0.15%
abnormal olfactory tract morphology	341	1.67549e-3	4.70463e-2	2.0100	23	0.76%	753	1.72098e-2	3.5491	7	13	0.22%

The test set of 3,025 genomic regions picked 3,246 genes (15%) of all 21,395 genes.

Mouse Phenotype has 9,575 terms covering 9,654 (45%) of all 21,395 genes.

9,575 ontology terms were tested (100%) using an annotation count range of [1, 1000].

GREAT version 4.0.4

Species assembly: mm10

Association rule: Basal+extension: 5000 bp upstream, 1000 bp downstream, 1000000 bp max extension, curated regulatory domains included

Table S3. Functional annotation of enriched TBX2 ChIP-seq peaks.

Shown are gene enrichments determined by GREAT and associated with TBX2 ChIP peaks in clusters with annotated mouse phenotypes sorted by $-\log_{10}$ binomial p-value.

Table S4. Functional annotation of enriched TBX2 CHIP-seq peaks.

Shown are gene enrichments determined by GREAT and associated with TBX2 CHIP peaks in clusters with annotated human phenotypes sorted by $-\log_{10}$ binomial p-value.

GO - Human Phenotype

#_Term Name	Binom Rank	Binom P-Value	Binom Raw P-Value	Binom FDR Q-Val	Binom Fold Enrichment	Binom Observed Region Hits	Binom Region Coverage	Hyper Rank	Hyper FDR Q-Val	Hyper Enrichment	Hyper Observed Gene Hits	Hyper Total Genes	Hyper Gene Set Coverage
Myelomeningocele	10	3.54575e-4	2.33984e-1	3.3458	12	0.40%	166	5.83061e-2	3.9547	6	10	0.18%	
Meningocele	11	3.84161e-4	2.30462e-1	3.1297	13	0.43%	201	7.72708e-2	3.2956	7	14	0.22%	
Ulnar deviation of the hand or of fingers of the hand	12	4.56351e-4	2.50955e-1	2.1801	24	0.79%	178	6.24414e-2	2.5894	11	28	0.34%	
Short 2nd finger	34	2.03631e-3	3.95223e-1	2.3997	15	0.50%	155	5.47553e-2	4.7080	5	7	0.15%	
White forelock	49	2.99439e-3	4.03265e-1	2.4781	13	0.43%	223	8.87813e-2	4.1195	5	8	0.15%	
Oligodactyly	62	4.47491e-3	4.76289e-1	2.2741	14	0.46%	159	5.61705e-2	3.5491	7	13	0.22%	
Synostosis involving bones of the feet	67	4.99086e-3	4.91563e-1	2.0104	18	0.60%	120	3.60878e-2	3.5153	8	15	0.25%	
Partial albinism	80	5.60529e-3	4.62367e-1	2.5028	11	0.36%	195	7.86582e-2	5.2730	4	5	0.12%	
Lacrimal duct aplasia	125	9.61403e-3	5.07544e-1	2.5810	9	0.30%	195	7.86582e-2	5.2730	4	5	0.12%	

The test set of 3,025 genomic regions picked 3,246 genes (15%) of all 21,395 genes.
Human Phenotype has 6,599 terms covering 3,215 (15%) of all 21,395 genes.

GREAT version 4.0.4

Species assembly: mm10

Association rule: Basal+extension: 5000 bp upstream, 1000 bp downstream, 1000000 bp max extension, curated regulatory domains included

Table S4. Functional annotation of enriched TBX2 CHIP-seq peaks.

Shown are gene enrichments determined by GREAT and associated with TBX2 CHIP peaks in clusters with annotated human phenotypes sorted by $-\log_{10}$ binomial p-value.

Table S5. Genes with decreased expression in the microarrays of E14.5 control vs *Tbx2*-deficient lungs.

Shown are the individual intensities, the individual fold changes (FC) and the average FC over the four individual microarrays performed.

Gene Name	Intensities								Fold change (FC)				
	control 1	mutant 1	control 2	mutant 2	control 3	mutant 3	control 4	mutant 4	FC1	FC2	FC3	FC4	avgFC
<i>Ndp</i>	425	130	287	92	524	58	323	90	-3.3	-3.1	-9.1	-3.6	-4.8
<i>Asz1</i>	295	151	292	56	328	54	427	106	-1.9	-5.2	-6.1	-4.0	-4.3
<i>AW549542</i>	2284	646	1282	434	1728	466	1335	461	-3.5	-3.0	-3.7	-2.9	-3.3
<i>Dgkk</i>	127	79	234	66	177	39	162	59	-1.6	-3.5	-4.6	-2.8	-3.1
<i>Tmem27</i>	163	95	171	49	191	43	219	78	-1.7	-3.5	-4.5	-2.8	-3.1
<i>Dcx</i>	433	241	463	177	630	110	513	224	-1.8	-2.6	-5.7	-2.3	-3.1
<i>Tbx2</i>	9826	2499	5276	2059	8400	3200	5246	1758	-3.9	-2.6	-2.6	-3.0	-3.0
<i>Rspo2</i>	1459	948	1341	629	2245	354	1605	869	-1.5	-2.1	-6.3	-1.8	-3.0
<i>9230102K24Rik</i>	737	413	578	246	890	180	762	374	-1.8	-2.3	-4.9	-2.0	-2.8
<i>A_55_P2023176</i>	274	169	231	114	311	66	262	121	-1.6	-2.0	-4.7	-2.2	-2.6
<i>ENSMUST00000169692</i>	891	452	982	321	1491	604	952	402	-2.0	-3.1	-2.5	-2.4	-2.5
<i>Cpa3</i>	372	121	458	206	375	218	384	170	-3.1	-2.2	-1.7	-2.3	-2.3
<i>Dcpp1</i>	158	98	158	72	170	56	196	82	-1.6	-2.2	-3.0	-2.4	-2.3
<i>Rhox5</i>	2554	1365	1979	1071	2825	711	2540	1680	-1.9	-1.8	-4.0	-1.5	-2.3
<i>Asic4</i>	196	113	190	103	280	74	175	106	-1.7	-1.8	-3.8	-1.7	-2.3
<i>Plcb1</i>	232	140	316	91	255	168	216	96	-1.7	-3.5	-1.5	-2.2	-2.2
<i>Hist1h1b</i>	3500	2057	4094	1398	5939	2843	3890	1817	-1.7	-2.9	-2.1	-2.1	-2.2
<i>Colec10</i>	772	488	882	400	1127	477	1129	492	-1.6	-2.2	-2.4	-2.3	-2.1
<i>Adamdec1</i>	1551	870	984	609	1994	653	1428	734	-1.8	-1.6	-3.1	-1.9	-2.1
<i>Dcpp3</i>	190	122	222	106	221	91	260	117	-1.6	-2.1	-2.4	-2.2	-2.1
<i>Adh6a</i>	222	139	181	115	199	59	204	120	-1.6	-1.6	-3.4	-1.7	-2.1
<i>Lect1</i>	157	102	183	96	195	69	212	116	-1.5	-1.9	-2.8	-1.8	-2.0
<i>Arhgap20</i>	268	173	381	166	553	245	399	216	-1.6	-2.3	-2.3	-1.8	-2.0
<i>Meox1</i>	1819	792	1638	998	2041	835	1283	851	-2.3	-1.6	-2.4	-1.5	-2.0
<i>Snrpd3</i>	23872	15802	34613	14293	27304	14004	24132	12020	-1.5	-2.4	-1.9	-2.0	-2.0
<i>Fam162b</i>	5343	2850	5086	2347	4724	2854	5284	2760	-1.9	-2.2	-1.7	-1.9	-1.9
<i>Shisa9</i>	148	89	125	69	196	83	147	83	-1.7	-1.8	-2.4	-1.8	-1.9
<i>Sct</i>	609	387	492	283	706	281	605	377	-1.6	-1.7	-2.5	-1.6	-1.9
<i>Prpf38b</i>	476	314	669	253	661	389	513	334	-1.5	-2.6	-1.7	-1.5	-1.8
<i>Ptpn5</i>	1229	538	737	477	809	490	762	399	-2.3	-1.5	-1.7	-1.9	-1.8
<i>Fzd10</i>	607	328	565	324	592	320	466	294	-1.9	-1.7	-1.9	-1.6	-1.8
<i>Lhx6</i>	362	199	279	156	280	172	252	143	-1.8	-1.8	-1.6	-1.8	-1.8
<i>Nebi</i>	134	83	123	75	141	83	136	68	-1.6	-1.6	-1.7	-2.0	-1.7
<i>Parva</i>	149	95	186	106	210	115	132	85	-1.6	-1.7	-1.8	-1.5	-1.7
<i>Hpca</i>	753	382	439	289	639	391	447	289	-2.0	-1.5	-1.6	-1.5	-1.7
<i>Apln</i>	2389	1486	2231	1418	2320	1395	2134	1323	-1.6	-1.6	-1.7	-1.6	-1.6

Table S5. Genes with decreased expression in the microarrays of E14.5 control vs *Tbx2*-deficient lungs.

Shown are the individual intensities, the individual fold changes (FC) and the average FC over the four individual microarrays performed.

Table S6. Genes with increased expression in the microarrays of E14.5 control vs *Tbx2*-deficient lungs.

Shown are the individual intensities, the individual fold changes (FC) and the average FC over the four individual microarrays performed.

Gene Name	Intensities								Fold change (FC)				
	control 1	mutant 1	control 2	mutant 2	control 3	mutant 3	control 4	mutant 4	FC1	FC2	FC3	FC4	avgFC
<i>Iffi44</i>	24	143	43	359	16	264	43	213	6.0	8.3	16.8	5.0	9.0
<i>Ttn</i>	155	460	64	1168	101	300	49	199	3.0	18.2	3.0	4.0	7.0
<i>1700007K13Rik</i>	29	101	47	165	15	207	37	123	3.5	3.5	13.8	3.3	6.0
<i>Ptprv</i>	17	137	67	269	15	104	47	198	7.8	4.0	7.0	4.2	5.8
<i>Sln</i>	411	640	175	2523	481	1089	106	346	1.6	14.4	2.3	3.3	5.4
<i>Chrdl1</i>	23	121	47	117	16	155	37	100	5.3	2.5	9.9	2.7	5.1
<i>Cdkn1a</i>	156	736	423	1377	105	967	337	959	4.7	3.3	9.2	2.9	5.0
<i>Frzb</i>	44	279	64	242	34	241	81	227	6.3	3.8	7.0	2.8	5.0
<i>Iffi203</i>	70	147	80	406	73	682	102	230	2.1	5.1	9.3	2.3	4.7
<i>Rtp4</i>	478	2211	951	4290	529	2730	946	3537	4.6	4.5	5.2	3.7	4.5
<i>Oasl2</i>	114	382	201	849	115	669	144	583	3.3	4.2	5.8	4.1	4.4
<i>Asic2</i>	95	376	124	426	110	773	135	362	4.0	3.4	7.1	2.7	4.3
<i>Nell1</i>	303	479	235	554	201	1975	210	419	1.6	2.4	9.8	2.0	3.9
<i>Pmaip1</i>	210	941	402	1452	175	498	389	1139	4.5	3.6	2.8	2.9	3.5
<i>Usp18</i>	139	320	184	710	133	552	163	543	2.3	3.9	4.1	3.3	3.4
<i>Oasl1</i>	140	521	336	1164	123	452	307	730	3.7	3.5	3.7	2.4	3.3
<i>Gm9706</i>	134	398	351	1109	142	589	240	671	3.0	3.2	4.1	2.8	3.3
<i>Fabp4</i>	503	1038	512	1672	786	4383	490	923	2.1	3.3	5.6	1.9	3.2
<i>Isg15</i>	483	1484	1198	3467	498	1972	850	2249	3.1	2.9	4.0	2.6	3.1
<i>Trp53inp1</i>	2643	7008	5005	10575	2376	12179	4514	11530	2.7	2.1	5.1	2.6	3.1
<i>Mx2</i>	71	167	117	360	57	263	88	200	2.3	3.1	4.6	2.3	3.1
<i>Oas1a</i>	275	755	504	2037	383	1092	552	1458	2.7	4.0	2.9	2.6	3.1
<i>Ii33</i>	658	3130	1207	2178	627	2498	1530	2499	4.8	1.8	4.0	1.6	3.0
<i>Shisa3</i>	167	825	305	709	151	324	333	781	4.9	2.3	2.2	2.3	2.9
<i>Cd55</i>	950	2330	1012	2675	730	3010	1010	2280	2.5	2.6	4.1	2.3	2.9
<i>Parp14</i>	265	472	327	834	209	1082	332	588	1.8	2.5	5.2	1.8	2.8
<i>Ephx1</i>	456	845	554	1390	434	2159	557	1037	1.9	2.5	5.0	1.9	2.8
<i>Wispr1</i>	2542	6877	2826	8859	2163	6441	3072	6816	2.7	3.1	3.0	2.2	2.8
<i>Itga11</i>	227	848	344	1105	196	352	338	759	3.7	3.2	1.8	2.2	2.7
<i>Oas1f</i>	209	476	332	1161	281	685	364	905	2.3	3.5	2.4	2.5	2.7
<i>Iffih1</i>	222	358	243	706	156	635	221	407	1.6	2.9	4.1	1.8	2.6
<i>Mndal</i>	165	254	212	607	173	670	213	342	1.5	2.9	3.9	1.6	2.5
<i>P2ry14</i>	1196	1951	1200	2126	1001	4850	1251	2004	1.6	1.8	4.8	1.6	2.5
<i>Tgtp2</i>	134	262	202	555	145	462	171	336	2.0	2.7	3.2	2.0	2.5
<i>Xaf1</i>	72	143	119	263	59	226	122	204	2.0	2.2	3.8	1.7	2.4
<i>Gdnf</i>	76	188	69	192	51	129	76	132	2.5	2.8	2.5	1.7	2.4
<i>Pqlc3</i>	212	509	319	646	204	651	311	580	2.4	2.0	3.2	1.9	2.4
<i>Smoc2</i>	7026	14096	6969	20878	5702	9074	6322	17627	2.0	3.0	1.6	2.8	2.3
<i>Gpr17</i>	59	166	94	219	59	125	69	144	2.8	2.3	2.1	2.1	2.3
<i>Celf5</i>	283	536	338	848	224	620	268	547	1.9	2.5	2.8	2.0	2.3
<i>Pid1</i>	179	311	176	412	168	518	194	353	1.7	2.3	3.1	1.8	2.2
<i>Dner</i>	89	223	86	258	77	140	99	151	2.5	3.0	1.8	1.5	2.2
<i>Gdf15</i>	59	144	111	219	45	123	92	150	2.4	2.0	2.7	1.6	2.2
<i>Ccng1</i>	1628	4269	2666	5112	1583	3426	2358	4849	2.6	1.9	2.2	2.1	2.2
<i>Slc19a2</i>	1038	2448	1541	3053	876	2173	1357	2624	2.4	2.0	2.5	1.9	2.2
<i>Gbp3</i>	165	351	246	578	176	463	296	486	2.1	2.3	2.6	1.6	2.2
<i>Zmat3</i>	639	1316	944	2145	528	1415	715	1214	2.1	2.3	2.7	1.7	2.2
<i>Slc6a2</i>	106	239	87	205	136	347	110	165	2.2	2.4	2.5	1.5	2.2
<i>Sulf2</i>	1076	2778	1648	3437	976	2165	1326	2219	2.6	2.1	2.2	1.7	2.1
<i>P4ha2</i>	1750	4222	2114	3270	1530	4088	2003	3856	2.4	1.5	2.7	1.9	2.1
<i>2610507I01Rik</i>	443	1202	619	985	362	801	649	1295	2.7	1.6	2.2	2.0	2.1
<i>3110040M04Rik</i>	71	121	74	185	160	425	97	156	1.7	2.5	2.7	1.6	2.1
<i>Fap</i>	949	2558	1412	2669	1162	2508	1565	2616	2.7	1.9	2.2	1.7	2.1
<i>Ffar4</i>	82	157	117	230	72	169	93	189	1.9	2.0	2.3	2.0	2.1
<i>Lgals3bp</i>	148	302	258	485	201	508	227	398	2.0	1.9	2.5	1.8	2.0
<i>Edn1</i>	115	208	113	211	78	226	128	204	1.8	1.9	2.9	1.6	2.0
<i>Crispld2</i>	766	1244	677	1628	656	1242	652	1352	1.6	2.4	1.9	2.1	2.0
<i>Gpr20</i>	52	105	69	156	56	102	62	118	2.0	2.3	1.8	1.9	2.0
<i>Oas2</i>	109	177	148	387	115	233	140	243	1.6	2.6	2.0	1.7	2.0
<i>Cckar</i>	922	1543	1061	2106	767	1814	937	1559	1.7	2.0	2.4	1.7	1.9
<i>Eppk1</i>	583	885	677	1357	429	1052	464	719	1.5	2.0	2.5	1.5	1.9
<i>ENSMUST0000099050</i>	55653	141344	84314	133382	82215	124548	81061	152736	2.5	1.6	1.5	1.9	1.9
<i>Lmcd1</i>	1240	2094	1135	2154	760	1489	1084	2128	1.7	1.9	2.0	2.0	1.9
<i>Lgals9</i>	108	162	122	273	119	228	132	243	1.5	2.2	1.9	1.8	1.9
<i>Ms4a7</i>	653	1161	1023	2070	715	1227	992	1828	1.8	2.0	1.7	1.8	1.8
<i>Syn2</i>	80	139	111	222	147	297	83	130	1.7	2.0	2.0	1.6	1.8
<i>Sntg2</i>	552	847	444	675	381	799	465	795	1.5	1.5	2.1	1.7	1.7
<i>Rnf213</i>	3103	5389	3651	5878	2506	4870	3651	5609	1.7	1.6	1.9	1.5	1.7
<i>Igf1</i>	2904	4867	3373	5101	2830	5767	3319	5145	1.7	1.5	2.0	1.5	1.7
<i>Gria3</i>	445	737	520	835	454	843	547	832	1.7	1.6	1.9	1.5	1.7

Table S6. Genes with increased expression in the microarrays of E14.5 control vs Tbx2-deficient lungs.

Shown are the individual intensities, the individual fold changes (FC) and the average FC over the four individual microarrays performed.

Table S7. GO-Term analysis of upregulated genes in microarray analysis.

Shown are GO-terms of upregulated genes in the microarray determined by MouseMine sorted by raw p-value.

Category	Term	Count	%	PValue	Genes	List Total	Pop Hits	Pop Total	Fold Enrichment	Bonferroni	Benjamini	FDR
GOTERM_BP_DIRE CT	GO:0051607~defense response to virus	10	1.45E+16	3.89E+06	IFIH1, ISG15, OASL2, OASL1, PMAIP1, OAS1A, OAS2, IL33, OAS1F, MX2	61	167	18082	1.78E+15	2.36E+10	2.36E+10	5.75E+08
INTERPRO	IPR006117:2-5-oligoadenylate synthetase, conserved site	5	7.25E+15	5.51E+06	OASL2, OASL1, OAS1A, OAS2, OAS1F	64	8	20594	2.01E+10	1.00E+10	1.00E+10	6.80E+09
INTERPRO	IPR026774:2-5-oligoadenylate synthase	5	7.25E+15	3.86E+07	OASL2, OASL1, OAS1A, OAS2, OAS1F	64	12	20594	1.34E+16	7.03E+10	3.52E+09	4.77E+10
INTERPRO	IPR018952:2-5-oligoadenylate synthetase 1, domain 2/C-terminal	5	7.25E+15	3.86E+07	OASL2, OASL1, OAS1A, OAS2, OAS1F	64	12	20594	1.34E+16	7.03E+10	3.52E+09	4.77E+10
INTERPRO	IPR006116:2-5-oligoadenylate synthetase, N-terminal	5	7.25E+15	7.78E+06	OASL2, OASL1, OAS1A, OAS2, OAS1F	64	14	20594	1.15E+08	1.42E+11	4.72E+09	9.60E+10
GOTERM_BP_DIRE CT	GO:0009615~response to virus	7	1.01E+16	3.44E+09	IFIH1, OASL2, OASL1, TGTP2, OAS1A, OAS2, MX2	61	84	18082	2.47E+15	2.08E+12	1.04E+12	5.08E+11
UP_KEYWORDS	Antiviral defense	7	1.01E+16	4.23E+09	IFIH1, ISG15, OASL2, OASL1, OAS1A, OAS2, MX2	66	100	22680	2.41E+15	5.41E+10	5.41E+10	4.91E+11
GOTERM_MF_DIRE CT	GO:0003725~double-stranded RNA binding	6	8.70E+15	3.81E+10	IFIH1, OASL2, OASL1, OAS1A, OAS2, OAS1F	60	70	17446	2.49E+16	5.67E+11	5.67E+11	4.54E-03
UP_KEYWORDS	Innate immunity	8	1.16E+16	5.78E+10	IFIH1, CD55, OASL2, OASL1, TGTP2, OAS1A, OAS2, MX2	66	241	22680	1.14E+16	7.39E+11	3.70E+11	6.71E-03
GOTERM_MF_DIRE CT	GO:0001730~2-5-oligoadenylate synthetase activity	4	5.80E+15	5.95E+09	OASL2, OASL1, OAS1A, OAS2	60	11	17446	1.06E+16	8.86E+11	4.43E+11	7.09E-03

UP_KEYWORDS	Immunity	9	1.30E+16	1.86E+11	IFIH1, CD55, OASL2, OASL1, TGTP2, OAS1A, OAS2, MX2, LGALS9	66	401	22680	7.71E+15	2.38E-03	7.95E+11	2.16E-02
KEGG_PATHWAY	mmu04115:p53 signaling pathway	5	7.25E+15	4.11E+10	CDKN1A, ZMAT3, IGF1, PMAIP1, CCNG1	24	67	7691	2.39E+16	2.79E-03	2.79E-03	4.23E-02
UP_KEYWORDS	Glycoprotein	25	3.62E+16	7.91E+10	CCKAR, FFAR4, SLC6A2, NELL1, ITGA11, OAS2, GDNF, SMOG2, LGALS3BP, WISP1, P4HA2, CRISPLD2, DNER, FAP, GPR20, ASIC2, GRIA3, FRZB, CD55, CHRDL1, SULF2, PTPRV, P2RY14, GPR17, GD-F15	66	3815	22680	2.25E+16	1.01E-02	2.53E-03	9.18E-02
UP_KEYWORDS	Disulfide bond	22	3.19E+15	1.05E+12	CCKAR, SLC6A2, NELL1, EDN1, ASIC2, ITGA11, IGF1, GRIA3, FRZB, TTN, GDNF, SMOG2, CD55, LGALS3BP, WISP1, ISG15, CRISPLD2, DNER, FAP, P2RY14, GPR17, GDF15	66	3124	22680	2.42E+16	1.34E-02	2.69E-03	1.22E-01
UP_KEYWORDS	Secreted	15	2.17E+15	2.46E+12	NELL1, EDN1, IGF1, IL33, FRZB, GDNF, LGALS9, SMOG2, LGALS3BP, CHRDL1, WISP1, ISG15, CRISPLD2, FAP, GD-F15	66	1685	22680	3.06E+15	3.11E-02	5.25E-03	2.86E-01

UP_SEQ_FEATURE	glycosylation site: N-linked (GlcNAc...)	24	3.48E+15	2.84E+12	58	3563	18012	2.09E+16	1.81E-01	1.81E-01	4.28E-01
UP_SEQ_FEATURE	disulfide bond	19	2.75E+16	5.04E+10	58	2510	18012	2.35E+16	2.99E-01	1.63E-01	7.59E-01
	GO:0061051~positive regulation of cell growth involved in cardiac muscle cell development										
GOTERM_BP_DIRE	cardiac muscle cell development	3	4.35E+16	7.00E+11	61	12	18082	7.41E+15	3.46E-01	1.32E-01	1.03E+15
GOTERM_CC_DIRE	extracellular region	15	2.17E+15	7.80E+11	62	1753	19662	2.71E+15	7.51E-02	7.51E-02	8.62E-01
	IPR002934:Nucleotidyl transferase domain										
INTERPRO	GO:0045178~basal part of cell	3	4.35E+16	8.19E+11	64	14	20594	6.90E+07	1.38E-01	3.66E-02	1.01E+16
GOTERM_CC_DIRE	mmu05164:influenza A	3	4.35E+16	1.25E-03	62	17	19662	5.60E+16	1.18E-01	6.06E-02	1.38E+15
KEGG_PATHWAY	GO:0002376~immune system process	5	7.25E+15	1.50E-03	24	171	7691	9.37E+15	9.71E-02	4.98E-02	1.53E+16
GOTERM_BP_DIRE		7	1.01E+16	1.66E-03	61	383	18082	5.42E+15	6.34E-01	2.22E-01	2.42E+16

GOTERM_BP_DIRE CT	GO:0006164~purine nucleotide biosynthetic process	3	4.35E+16	1.98E-03	OASL2, OAS1A, OAS2	61	20	18082	4.45E+15	6.99E-01	2.14E-01	2.89E+16
GOTERM_BP_DIRE CT	GO:0045087~innate immune response	7	1.01E+16	2.06E-03	IFIH1, CD55, OASL2, OASL1, OAS1A, OAS2, MX2	61	400	18082	5.19E+15	7.14E-01	1.88E-01	3.01E+16
GOTERM_BP_DIRE CT	GO:0006955~immune response	6	8.70E+15	2.06E-03	P2RY14, OASL2, OASL1, TGTP2, OAS2, OAS1F	61	272	18082	6.54E+15	7.14E-01	1.64E-01	3.01E+16
UP_SEQ_FEATURE	signal peptide	20	2.90E+16	2.55E-03	NELL1, EDN1, ITGA11, IGF1, GRIA3, FRZB, GDNF, SMOC2, CD55, LGALS3BP, CHRDL1, WISP1, SULF2, P4HA2, SHISA3, PTPRV, CRISPLD2, DNER, GD-F15, PQLC3	58	3124	18012	1.99E+16	8.35E-01	4.51E-01	3.78E+15
GOTERM_BP_DIRE CT	GO:0072332~intrinsic apoptotic signaling pathway by p53 class mediator	3	4.35E+16	4.73E-03	PTPRV, ZMAT3, PMAIP1	61	31	18082	2.87E+16	9.44E-01	3.02E-01	6.78E+15
GOTERM_BP_DIRE CT	GO:0051482~positive regulation of cytosolic calcium ion concentration involved in phospholipase C-activating G-protein coupled signaling pathway	3	4.35E+16	4.73E-03	EDN1, GPR17, GPR20	61	31	18082	2.87E+16	9.44E-01	3.02E-01	6.78E+15
GOTERM_BP_DIRE CT	GO:0045071~negative regulation of viral genome replication	3	4.35E+16	5.04E-03	ISG15, OASL1, MX2	61	32	18082	2.78E+16	9.53E-01	2.88E-01	7.20E+15
UP_SEQ_FEATURE	domain:Ubiquitin-like 1	2	2.90E+15	6.32E-03	ISG15, GM9706	58	2	18012	3.11E+16	9.88E-01	6.72E-01	9.12E+15
UP_SEQ_FEATURE	domain:Ubiquitin-like 2	2	2.90E+15	6.32E-03	ISG15, GM9706	58	2	18012	3.11E+16	9.88E-01	6.72E-01	9.12E+15

UP_SEQ_FEATURE	2	2.90E+15	6.32E-03	ISG15, GM9706	58	2	18012	3.11E+16	9.88E-01	6.72E-01	9.12E+15
region of interest:Involved in the ligation of specific target proteins											
UP_SEQ_FEATURE	2	2.90E+15 <td>6.32E-03 <td>ISG15, GM9706 <td>58</td> <td>2</td> <td>18012</td> <td>3.11E+16 <td>9.88E-01 <td>6.72E-01 <td>9.12E+15</td> </td></td></td></td></td>	6.32E-03 <td>ISG15, GM9706 <td>58</td> <td>2</td> <td>18012</td> <td>3.11E+16 <td>9.88E-01 <td>6.72E-01 <td>9.12E+15</td> </td></td></td></td>	ISG15, GM9706 <td>58</td> <td>2</td> <td>18012</td> <td>3.11E+16 <td>9.88E-01 <td>6.72E-01 <td>9.12E+15</td> </td></td></td>	58	2	18012	3.11E+16 <td>9.88E-01 <td>6.72E-01 <td>9.12E+15</td> </td></td>	9.88E-01 <td>6.72E-01 <td>9.12E+15</td> </td>	6.72E-01 <td>9.12E+15</td>	9.12E+15
chain:Ubiquitin cross-reactive protein											
UP_SEQ_FEATURE	3	4.35E+16 <td>6.42E-03 <td>CHRD1, WISP1, NELL1</td> <td>37</td> <td>35</td> <td>10425</td> <td>2.42E+15 <td>2.94E-01 <td>2.94E-01 <td>6.12E+15</td> </td></td></td></td>	6.42E-03 <td>CHRD1, WISP1, NELL1</td> <td>37</td> <td>35</td> <td>10425</td> <td>2.42E+15 <td>2.94E-01 <td>2.94E-01 <td>6.12E+15</td> </td></td></td>	CHRD1, WISP1, NELL1	37	35	10425	2.42E+15 <td>2.94E-01 <td>2.94E-01 <td>6.12E+15</td> </td></td>	2.94E-01 <td>2.94E-01 <td>6.12E+15</td> </td>	2.94E-01 <td>6.12E+15</td>	6.12E+15
SMART											
GOTERM_BP_DIRE	3	4.35E+16 <td>6.69E-03 <td>CCKAR, SLN, IGF1</td> <td>61</td> <td>37</td> <td>18082</td> <td>2.40E+16 <td>9.83E-01 <td>3.34E-01 <td>9.45E+15</td> </td></td></td></td>	6.69E-03 <td>CCKAR, SLN, IGF1</td> <td>61</td> <td>37</td> <td>18082</td> <td>2.40E+16 <td>9.83E-01 <td>3.34E-01 <td>9.45E+15</td> </td></td></td>	CCKAR, SLN, IGF1	61	37	18082	2.40E+16 <td>9.83E-01 <td>3.34E-01 <td>9.45E+15</td> </td></td>	9.83E-01 <td>3.34E-01 <td>9.45E+15</td> </td>	3.34E-01 <td>9.45E+15</td>	9.45E+15
GO:0051924~regulation of calcium ion transport											
CT											
INTERPRO	3	4.35E+16 <td>6.99E-03 <td>CHRD1, WISP1, NELL1</td> <td>64</td> <td>41</td> <td>20594</td> <td>2.35E+15 <td>7.21E-01 <td>2.25E-01 <td>8.30E+15</td> </td></td></td></td>	6.99E-03 <td>CHRD1, WISP1, NELL1</td> <td>64</td> <td>41</td> <td>20594</td> <td>2.35E+15 <td>7.21E-01 <td>2.25E-01 <td>8.30E+15</td> </td></td></td>	CHRD1, WISP1, NELL1	64	41	20594	2.35E+15 <td>7.21E-01 <td>2.25E-01 <td>8.30E+15</td> </td></td>	7.21E-01 <td>2.25E-01 <td>8.30E+15</td> </td>	2.25E-01 <td>8.30E+15</td>	8.30E+15
IPR001007:~von Willebrand factor, type C											
KEGG_PATHWAY	4	5.80E+15 <td>7.39E-03 <td>IFIH1, OAS1A, OAS2, MX2</td> <td>24</td> <td>136</td> <td>7691</td> <td>9.43E+15 <td>3.96E-01 <td>1.55E-01 <td>7.35E+15</td> </td></td></td></td>	7.39E-03 <td>IFIH1, OAS1A, OAS2, MX2</td> <td>24</td> <td>136</td> <td>7691</td> <td>9.43E+15 <td>3.96E-01 <td>1.55E-01 <td>7.35E+15</td> </td></td></td>	IFIH1, OAS1A, OAS2, MX2	24	136	7691	9.43E+15 <td>3.96E-01 <td>1.55E-01 <td>7.35E+15</td> </td></td>	3.96E-01 <td>1.55E-01 <td>7.35E+15</td> </td>	1.55E-01 <td>7.35E+15</td>	7.35E+15
mmu05162:Measles											
GOTERM_BP_DIRE	3	4.35E+16 <td>8.17E-03 <td>TGTP2, IFI203, GBP3</td> <td>61</td> <td>41</td> <td>18082</td> <td>2.17E+16 <td>9.93E-01 <td>3.64E-01 <td>1.14E+16</td> </td></td></td></td>	8.17E-03 <td>TGTP2, IFI203, GBP3</td> <td>61</td> <td>41</td> <td>18082</td> <td>2.17E+16 <td>9.93E-01 <td>3.64E-01 <td>1.14E+16</td> </td></td></td>	TGTP2, IFI203, GBP3	61	41	18082	2.17E+16 <td>9.93E-01 <td>3.64E-01 <td>1.14E+16</td> </td></td>	9.93E-01 <td>3.64E-01 <td>1.14E+16</td> </td>	3.64E-01 <td>1.14E+16</td>	1.14E+16
GO:0035458~cellular response to interferon-beta											
CT											
GOTERM_BP_DIRE	4	5.80E+15 <td>8.29E-03 <td>CDKN1A, ZMAT3, MNDAL, FRZB</td> <td>61</td> <td>125</td> <td>18082</td> <td>9.49E+15 <td>9.94E-01 <td>3.43E-01 <td>1.16E+16</td> </td></td></td></td>	8.29E-03 <td>CDKN1A, ZMAT3, MNDAL, FRZB</td> <td>61</td> <td>125</td> <td>18082</td> <td>9.49E+15 <td>9.94E-01 <td>3.43E-01 <td>1.16E+16</td> </td></td></td>	CDKN1A, ZMAT3, MNDAL, FRZB	61	125	18082	9.49E+15 <td>9.94E-01 <td>3.43E-01 <td>1.16E+16</td> </td></td>	9.94E-01 <td>3.43E-01 <td>1.16E+16</td> </td>	3.43E-01 <td>1.16E+16</td>	1.16E+16
GO:0030308~negative regulation of cell growth											
CT											
UP_KEYWORDS	22	3.19E+15 <td>9.38E-03 <td>PID1, IFIH1, EPPK1, NELL1, LMCD1, IFI44, OAS2, TTN, RNF213, LGALS9, CDKN1A, ISG15, PARP14, OASL1, FABP4, TRP53INP1, TGTP2, XAF1, OAS1A, MX2, GBP3, SNTG2</td> <td>66</td> <td>4404</td> <td>22680</td> <td>1.72E+16 <td>7.01E-01 <td>1.58E-01 <td>1.04E+16</td> </td></td></td></td>	9.38E-03 <td>PID1, IFIH1, EPPK1, NELL1, LMCD1, IFI44, OAS2, TTN, RNF213, LGALS9, CDKN1A, ISG15, PARP14, OASL1, FABP4, TRP53INP1, TGTP2, XAF1, OAS1A, MX2, GBP3, SNTG2</td> <td>66</td> <td>4404</td> <td>22680</td> <td>1.72E+16 <td>7.01E-01 <td>1.58E-01 <td>1.04E+16</td> </td></td></td>	PID1, IFIH1, EPPK1, NELL1, LMCD1, IFI44, OAS2, TTN, RNF213, LGALS9, CDKN1A, ISG15, PARP14, OASL1, FABP4, TRP53INP1, TGTP2, XAF1, OAS1A, MX2, GBP3, SNTG2	66	4404	22680	1.72E+16 <td>7.01E-01 <td>1.58E-01 <td>1.04E+16</td> </td></td>	7.01E-01 <td>1.58E-01 <td>1.04E+16</td> </td>	1.58E-01 <td>1.04E+16</td>	1.04E+16
Cytoplasm											
SMART	3	4.35E+16 <td>1.38E-02 <td>ISG15, OASL2, OASL1</td> <td>37</td> <td>52</td> <td>10425</td> <td>1.63E+16 <td>5.28E-01 <td>3.13E-01 <td>1.27E+16</td> </td></td></td></td>	1.38E-02 <td>ISG15, OASL2, OASL1</td> <td>37</td> <td>52</td> <td>10425</td> <td>1.63E+16 <td>5.28E-01 <td>3.13E-01 <td>1.27E+16</td> </td></td></td>	ISG15, OASL2, OASL1	37	52	10425	1.63E+16 <td>5.28E-01 <td>3.13E-01 <td>1.27E+16</td> </td></td>	5.28E-01 <td>3.13E-01 <td>1.27E+16</td> </td>	3.13E-01 <td>1.27E+16</td>	1.27E+16
SM00213:UBQ											
GOTERM_MF_DIRE	4	5.80E+15 <td>1.45E-02 <td>SMOC2, WISP1, CRISPLD2, NELL1</td> <td>60</td> <td>151</td> <td>17446</td> <td>7.70E+14 <td>8.87E-01 <td>5.16E-01 <td>1.60E+16</td> </td></td></td></td>	1.45E-02 <td>SMOC2, WISP1, CRISPLD2, NELL1</td> <td>60</td> <td>151</td> <td>17446</td> <td>7.70E+14 <td>8.87E-01 <td>5.16E-01 <td>1.60E+16</td> </td></td></td>	SMOC2, WISP1, CRISPLD2, NELL1	60	151	17446	7.70E+14 <td>8.87E-01 <td>5.16E-01 <td>1.60E+16</td> </td></td>	8.87E-01 <td>5.16E-01 <td>1.60E+16</td> </td>	5.16E-01 <td>1.60E+16</td>	1.60E+16
GO:0008201~heparin binding											
CT											
GOTERM_BP_DIRE	3	4.35E+16 <td>1.54E-02 <td>CCKAR, TRP53INP1, IGF1</td> <td>61</td> <td>57</td> <td>18082</td> <td>1.56E+16 <td>1.00E+00 <td>5.14E-01 <td>2.05E+16</td> </td></td></td></td>	1.54E-02 <td>CCKAR, TRP53INP1, IGF1</td> <td>61</td> <td>57</td> <td>18082</td> <td>1.56E+16 <td>1.00E+00 <td>5.14E-01 <td>2.05E+16</td> </td></td></td>	CCKAR, TRP53INP1, IGF1	61	57	18082	1.56E+16 <td>1.00E+00 <td>5.14E-01 <td>2.05E+16</td> </td></td>	1.00E+00 <td>5.14E-01 <td>2.05E+16</td> </td>	5.14E-01 <td>2.05E+16</td>	2.05E+16
GO:0009408~response to heat											
CT											
GOTERM_BP_DIRE	2	2.90E+15 <td>1.65E-02 <td>ASIC2, IGF1</td> <td>61</td> <td>5</td> <td>18082</td> <td>1.19E+16 <td>1.00E+00 <td>5.13E-01 <td>2.18E+15</td> </td></td></td></td>	1.65E-02 <td>ASIC2, IGF1</td> <td>61</td> <td>5</td> <td>18082</td> <td>1.19E+16 <td>1.00E+00 <td>5.13E-01 <td>2.18E+15</td> </td></td></td>	ASIC2, IGF1	61	5	18082	1.19E+16 <td>1.00E+00 <td>5.13E-01 <td>2.18E+15</td> </td></td>	1.00E+00 <td>5.13E-01 <td>2.18E+15</td> </td>	5.13E-01 <td>2.18E+15</td>	2.18E+15
GO:0050974~detection of mechanical stimulus involved in sensory perception											
CT											

GOTERM_CC_DIRE CT	GO:0005615~extracellular space	11	1.59E+16	1.67E-02	LGALS3BP, SULF2, NELL1, FAP, EDN1, LMCD1, IGF1, IL33, FRZB, GDF15, GDNF	62	1504	19662	2.32E+15	8.14E-01	4.29E-01	1.70E+15
INTERPRO	IPR000626:Ubiquitin	3	4.35E+16	1.74E-02	ISG15, OASL2, OASL1	64	66	20594	1.46E+16	9.59E-01	4.13E-01	1.95E+15
UP_KEYWORDS	Nucleotidyltransferase	3	4.35E+16	2.01E-02	OASL2, OAS1A, OAS2	66	76	22680	1.36E+16	9.26E-01	2.78E-01	2.10E+16
KEGG_PATHWAY	mmu05410:Hypertrophic cardiomyopathy (HCM)	3	4.35E+16	2.29E-02	ITGA11, IGF1, TTN	24	79	7691	1.22E+16	7.93E-01	3.26E-01	2.12E+16
GOTERM_BP_DIRE CT	GO:0034340~response to type I interferon	2	2.90E+15	2.30E-02	ISG15, MX2	61	7	18082	8.47E+15	1.00E+00	6.09E-01	2.91E+15
UP_KEYWORDS	Endoplasmic reticulum	8	1.16E+16	2.36E-02	SLN, SULF2, P4HA2, SHISA3, EPHX1, TGT-P2, OAS1A, OAS2	66	997	22680	2.76E+15	9.53E-01	2.88E-01	2.43E+16
UP_SEQ_FEATURE	region of interest:A	2	2.90E+15	2.50E-02	SYN2, IGF1	58	8	18012	7.76E+15	1.00E+00	9.72E-01	3.18E+15
GOTERM_BP_DIRE CT	GO:0043065~positive regulation of apoptotic process	5	7.25E+15	2.51E-02	NELL1, ZMAT3, TRP53INP1, PMAIP1, FRZB	61	335	18082	4.42E+15	1.00E+00	6.17E-01	3.13E+16
KEGG_PATHWAY	mmu05414:Dilated cardiomyopathy	3	4.35E+16	2.51E-02	ITGA11, IGF1, TTN	24	83	7691	1.16E+16	8.23E-01	2.93E-01	2.30E+16
GOTERM_BP_DIRE CT	GO:0034392~negative regulation of smooth muscle cell apoptotic process	2	2.90E+15	2.62E-02	EDN1, IGF1	61	8	18082	7.41E+15	1.00E+00	6.12E-01	3.25E+15
UP_KEYWORDS	RNA-binding	6	8.70E+15	2.89E-02	IFIH1, OASL2, ZMAT3, OASL1, OAS1A, OAS2	66	601	22680	3.43E+16	9.76E-01	3.13E-01	2.88E+16
GOTERM_BP_DIRE CT	GO:0048661~positive regulation of smooth muscle cell proliferation	3	4.35E+16	2.90E-02	WISP1, EDN1, IGF1	61	80	18082	1.11E+16	1.00E+00	6.29E-01	3.53E+15
GOTERM_BP_DIRE CT	GO:0006977~DNA damage response, signal transduction by p53 class mediator resulting in cell cycle arrest	2	2.90E+15	2.95E-02	CDKN1A, PTPRV	61	9	18082	6.59E+15	1.00E+00	6.15E-01	3.58E+16

INTERPRO	IPR004021:HIN-200/IF120x	2	2.90E+15	3.02E-02	MNDAL, IFI203	64	10	20594	6.44E+06	9.96E-01	5.49E-01	3.15E+16
INTERPRO	IPR011029:Death-like domain	3	4.35E+16	3.04E-02	IFIH1, MNDAL, IFI203	64	89	20594	1.08E+16	9.96E-01	5.05E-01	3.17E+16
GOTERM_BP_DIRE	GO:0070886~positive regulation of calcineurin-NFAT signaling cascade	2	2.90E+15	3.27E-02	LMCD1, IGF1	61	10	18082	5.93E+15	1.00E+00	6.35E-01	3.88E+16
UP_SEQ_FEATURE	domain:Fibronectin type-III	2	2.90E+15	3.43E-02	PTPRV, TTN	58	11	18012	5.65E+15	1.00E+00	9.83E-01	4.09E+15
UP_KEYWORDS	Cleavage on pair of basic residues	4	5.80E+15	3.44E-02	FAP, EDN1, GDF15, GDNF	66	248	22680	5.54E+15	9.89E-01	3.34E-01	3.34E+15
KEGG_PATHWAY	mmu04066:HIF-1 signaling pathway	3	4.35E+16	3.68E-02	CDKN1A, EDN1, IGF1	24	102	7691	9.43E+15	9.22E-01	3.46E-01	3.20E+14
GOTERM_BP_DIRE	GO:0008285~negative regulation of cell proliferation	5	7.25E+15	3.85E-02	CDKN1A, PTPRV, TRP53INP1, IGF1, FRZB	61	384	18082	3.86E+16	1.00E+00	6.78E-01	4.41E+16
UP_SEQ_FEATURE	compositionally biased region:Poly-Ser	5	7.25E+15	3.97E-02	CCKAR, SHISA3, SYN2, IFI203, TTN	58	407	18012	3.82E+16	1.00E+00	9.83E-01	4.58E+15
UP_SEQ_FEATURE	domain:VWFC 3	2	2.90E+15	4.04E-02	CHRD1, NELL1	58	13	18012	4.78E+16	1.00E+00	9.73E-01	4.63E+15
GOTERM_MF_DIRE	GO:0005178~integrin binding	3	4.35E+16	4.51E-02	WISP1, FAP, IGF1	60	100	17446	8.72E+03	9.99E-01	8.20E-01	4.23E+16
GOTERM_BP_DIRE	GO:0071850~mitotic cell cycle arrest	2	2.90E+15	4.55E-02	CDKN1A, FAP	61	14	18082	4.23E+15	1.00E+00	7.23E-01	4.98E+15
GOTERM_CC_DIRE	GO:0005730~nucleolus	7	1.01E+16	4.58E-02	CDKN1A, ZMAT3, MNDAL, OASL1, TRP53INP1, IFI203, RN-F213	62	842	19662	2.64E+15	9.91E-01	6.90E-01	4.06E+15
UP_SEQ_FEATURE	topological domain:Extracellular	13	1.88E+15	4.73E-02	CCKAR, FFAR4, SLC6A2, ASIC2, ITGA11, GRIA3, SHISA3, PTPRV, P2RY14, FAP, DNER, GPR17, GPR20	58	2256	18012	1.79E+16	1.00E+00	9.77E-01	5.19E+16
GOTERM_CC_DIRE	GO:0043195~terminal bouton	3	4.35E+16	4.81E-02	CCKAR, SYN2, GRIA3	62	113	19662	8.42E+15	9.93E-01	6.27E-01	4.21E+15

UP_KEYWORDS	Signal	20	2.90E+16	4.91E-02	NELL1, EDN1, ITGA11, IGF1, GRIA3, FRZB, GDNF, SMOG2, CD55, LGALS3BP, CHRDL1, WISP1, SULF2, P4HA2, SHISA3, PTPRV, CRISPLD2, DNER, GD-F15, PQLC3	66	4543	22680	1.51E+16	9.98E-01	4.15E-01	4.42E+15
UP_SEQ_FEATURE	domain:Fibronectin type-III 9	2	2.90E+15	4.95E-02	PTPRV, TTN	58	16	18012	3.88E+15	1.00E+00	9.72E-01	5.35E+14
GOTERM_MF_DIRE	GO:0043539~protein serine/threonine kinase activator activity	2	2.90E+15	4.96E-02	IGF1, LGALS9	60	15	17446	3.88E+15	9.99E-01	7.80E-01	4.55E+15
GOTERM_CC_DIRE	GO:0005614~interstitial matrix	2	2.90E+15	5.15E-02	SMOG2, IGF1	62	17	19662	3.73E+16	9.95E-01	5.86E-01	4.44E+15
UP_KEYWORDS	Growth factor	3	4.35E+16	5.15E-02	IGF1, GDF15, GDNF	66	127	22680	8.12E+15	9.99E-01	4.06E-01	4.59E+15
UP_KEYWORDS	Apoptosis	5	7.25E+15	5.17E-02	FAP, ZMAT3, TRP53IN-P1, PMAIP1, XAF1	66	489	22680	3.51E+15	9.99E-01	3.84E-01	4.60E+15
GOTERM_BP_DIRE	GO:0071356~cellular response to tumor necrosis factor	3	4.35E+16	5.17E-02	PID1, EDN1, FABP4	61	110	18082	8.08E+14	1.00E+00	7.53E-01	5.44E+15
GOTERM_BP_DIRE	GO:2000679~positive regulation of transcription regulatory region DNA binding	2	2.90E+15	5.18E-02	IGF1, LGALS9	61	16	18082	3.71E+15	1.00E+00	7.39E-01	5.45E+15
UP_SEQ_FEATURE	domain:VWF C1	2	2.90E+15	5.25E-02	CHRDL1, NELL1	58	17	18012	3.65E+15	1.00E+00	9.68E-01	5.57E+15
UP_SEQ_FEATURE	domain:VWF C2	2	2.90E+15	5.25E-02	CHRDL1, NELL1	58	17	18012	3.65E+15	1.00E+00	9.68E-01	5.57E+15
UP_KEYWORDS	Microsome	3	4.35E+16	5.51E-02	EPHX1, OAS1A, OAS2	66	132	22680	7.81E+15	9.99E-01	3.84E-01	4.82E+16

GOTERM_CC_DIRE CT	GO:0005737~cytoplasm	28	4.06E+15	5.60E-02	62	6631	19662	1.34E+16	9.97E-01	5.61E-01	4.72E+16
GOTERM_BP_DIRE CT	GO:0010629~negative regulation of gene expression	4	5.80E+15	5.79E-02	61	265	18082	4.47E+15	1.00E+00	7.64E-01	5.86E+15
GOTERM_BP_DIRE CT	GO:0010613~positive regulation of cardiac muscle hypertrophy	2	2.90E+15	5.81E-02	61	18	18082	3.29E+15	1.00E+00	7.52E-01	5.87E+16
GOTERM_BP_DIRE CT	GO:0043032~positive regulation of macrophage activation	2	2.90E+15	5.81E-02	61	18	18082	3.29E+15	1.00E+00	7.52E-01	5.87E+16
INTERPRO	IPR009030:Insulin-like growth factor binding protein, N-terminal	3	4.35E+16	6.02E-02	64	130	20594	7.43E+15	1.00E+00	7.15E-01	5.35E+16
KEGG_PATHWAY	mmu05160:Hepatitis C	3	4.35E+16	6.17E-02	24	136	7691	7.07E+15	9.87E-01	4.61E-01	4.80E+15
UP_KEYWORDS	Magnesium	5	7.25E+15	6.23E-02	66	521	22680	3.30E+15	1.00E+00	4.02E-01	5.26E+16
GOTERM_BP_DIRE CT	GO:0019229~regulation of vasoconstriction	2	2.90E+15	6.43E-02	61	20	18082	2.96E+15	1.00E+00	7.75E-01	6.26E+14
GOTERM_BP_DIRE CT	GO:0010165~response to X-ray	2	2.90E+15	6.75E-02	61	21	18082	2.82E+15	1.00E+00	7.79E-01	6.44E+15
GOTERM_BP_DIRE CT	GO:0010001~glial cell differentiation	2	2.90E+15	6.75E-02	61	21	18082	2.82E+15	1.00E+00	7.79E-01	6.44E+15
GOTERM_BP_DIRE CT	GO:0071398~cellular response to fatty acid	2	2.90E+15	6.75E-02	61	21	18082	2.82E+15	1.00E+00	7.79E-01	6.44E+15
GOTERM_MF_DIRE CT	GO:0005539~glycosaminoglycan binding	2	2.90E+15	6.87E-02	60	21	17446	2.77E+16	1.00E+00	8.29E-01	5.72E+16

CCKAR, IFIH1, RTP4, NELL1, EDN1, OAS2, RNF213, WISP1, P4HA2, ISG15, OASL1, TRP53INP1, XAF1, MX2, PID1, EPPK1, MNDAL, LMCD1, IGF1, IFI44, LGALS9, CDKN1A, PARP14, FABP4, IFI203, GDF15, GBP3, SNTG2

CDKN1A, TRP53INP1, IGF1, LGALS9

EDN1, IGF1

IL33, LGALS9

WISP1, NELL1, DNER

CDKN1A, OAS1A, OAS2

OASL2, ITGA11, OAS1A, OAS2, TTN

EDN1, ASIC2

CDKN1A, PMAIP1

DNER, IGF1

PID1, EDN1

SMOC2, CRISPLD2

UP_SEQ_FEATURE domain:Fibronectin type-III 8	2	2.90E+15	7.33E-02	PTRPV, TTN	58	24	18012	2.59E+16	1.00E+00	9.89E-01	6.83E+15
GOTERM_CC_DIRE GO:0005578~proteinaceous extracellular matrix	4	5.80E+15	7.49E-02	SMOC2, LGALS3BP, WISP1, CRISPLD2	62	316	19662	4.01E+15	1.00E+00	6.22E-01	5.79E+14
UP_SEQ_FEATURE domain:Fibronectin type-III 7 binding site:Activating enzyme	2	2.90E+15	7.62E-02	PTRPV, TTN	58	25	18012	2.48E+16	1.00E+00	9.86E-01	6.98E+15
UP_SEQ_FEATURE me	2	2.90E+15	7.92E-02	ISG15, GM9706	58	26	18012	2.39E+16	1.00E+00	9.84E-01	7.12E+15
INTERPRO IPR004020:DAPIN domain	2	2.90E+15	7.94E-02	MNDAL, IFI203	64	27	20594	2.38E+15	1.00E+00	7.78E-01	6.40E+15
GOTERM_BP_DIRE GO:0014065~phosphatidylinositol 3-kinase signaling	2	2.90E+15	7.98E-02	EDN1, IGF1	61	25	18082	2.37E+15	1.00E+00	8.24E-01	7.08E+15
GOTERM_BP_DIRE GO:0010468~regulation of gene expression	4	5.80E+15	8.25E-02	NELL1, ASIC2, IGF1, GDNF	61	308	18082	3.85E+16	1.00E+00	8.24E-01	7.20E+15
GOTERM_CC_DIRE GO:0043025~neuronal cell body	5	7.25E+15	8.38E-02	DNER, ASIC2, IGF1, GRIA3, CCNG1	62	534	19662	2.97E+16	1.00E+00	6.22E-01	6.22E+15
GOTERM_MF_DIRE GO:0005504~fatty acid binding	2	2.90E+15	8.44E-02	FFAR4, FABP4	60	26	17446	2.24E+16	1.00E+00	8.47E-01	6.51E+14
UP_KEYWORDS Nucleus compositionally biased region:Ser/Thr-rich	19	2.75E+16	8.45E-02	IFIH1, ZMAT3, NELL1, MNDAL, LMCD1, IL33, OAS2, TTN, CCNG1, LGALS9, CDKN1A, PARP14, OASL1, FABP4, TRP53INP1, XAF1, OAS1A, IFI203, GBP3	66	4534	22680	1.44E+16	1.00E+00	4.85E-01	6.41E+15
UP_SEQ_FEATURE on:GO:0032689~negative regulation of interferon-gamma production	2	2.90E+15	8.50E-02	CD55, FRZB	58	28	18012	2.22E+16	1.00E+00	9.85E-01	7.38E+15
GOTERM_BP_DIRE GO:0035025~positive regulation of Rho protein signal transduction	2	2.90E+15	8.59E-02	IL33, LGALS9	61	27	18082	2.20E+16	1.00E+00	8.27E-01	7.35E+15
GOTERM_BP_DIRE mmu05202:Transcriptional misregulation in cancer	2	2.90E+15	8.59E-02	GPR17, GPR20	61	27	18082	2.20E+16	1.00E+00	8.27E-01	7.35E+15
KEGG_PATHWAY	3	4.35E+16	8.63E-02	CDKN1A, IGF1, GRIA3	24	165	7691	5.83E+15	9.98E-01	5.36E-01	6.05E+15

GOTERM_MF_DIRE GO:0008083~growth factor activity	3	4.35E+16	8.64E-02	IGF1, GDF15, GDNF	60	145	17446	6.02E+15	1.00E+00	8.14E-01	6.60E+15
UP_SEQ_FEATURE domain:Fibronectin type-III 6	2	2.90E+15	8.79E-02	PTPRV, TTN	58	29	18012	2.14E+16	1.00E+00	9.83E-01	7.51E+15
UP_KEYWORDS Calcium	6	8.70E+15	8.81E-02	SMOC2, SULF2, NELL1, DNER, ITGA11, TTN	66	827	22680	2.49E+16	1.00E+00	4.81E-01	6.57E+14
SMART SM01289:SM01289	2	2.90E+15	8.93E-02	MNDAL, IFI203	37	27	10425	2.09E+15	9.94E-01	8.14E-01	6.00E+15
GOTERM_BP_DIRE GO:0045840~positive regulation of mitotic nuclear division	2	2.90E+15	9.20E-02	EDN1, IGF1	61	29	18082	2.04E+16	1.00E+00	8.39E-01	7.60E+15
UP_KEYWORDS Hydrolase	9	1.30E+16	9.73E-02	IFIH1, USP18, SULF2, PTPRV, FAP, EPHX1, TGTP2, RNF213, GBP3	66	1646	22680	1.88E+16	1.00E+00	4.98E-01	6.95E+15
GOTERM_BP_DIRE GO:2000379~positive regulation of reactive oxygen species metabolic process	2	2.90E+15	9.80E-02	PID1, CDKN1A	61	31	18082	1.91E+16	1.00E+00	8.49E-01	7.82E+15
GOTERM_BP_DIRE GO:0042771~intrinsic apoptotic signaling pathway in response to DNA damage by p53 class mediator	2	2.90E+15	9.80E-02	CDKN1A, PMAIP1	61	31	18082	1.91E+16	1.00E+00	8.49E-01	7.82E+15
UP_KEYWORDS Metal-binding	15	2.17E+15	9.85E-02	IFIH1, SLC6A2, ZMAT3, LMCD1, ITGA11, OAS2, TTN, RNF213, SMOC2, CDKN1A, SULF2, P4HA2, OASL2, OAS1A, XAF1	66	3395	22680	1.52E+16	1.00E+00	4.85E-01	7.00E+15

Table S7. GO-Term analysis of upregulated genes in microarray analysis.

Shown are GO-terms of upregulated genes in the microarray determined by MouseMine sorted by raw p-value.

Table S8. Functional annotation analysis of upregulated genes in microarray analysis.

Shown are functional clusters of upregulated genes in the microarray determined by DAVID functional annotation tool sorted by enrichment score.

Annotation Cluster 1	Enrichment Score:	Term	Count	%	PValue	Genes	List Total	Pop Hits	Pop Total	Fold Enrichment	Bonferroni	Benjamini	FDR
	3.4238609883227045												
GOTERM_BP_DIRECT		GO:0051607~defense response to virus	10	1.45E+16	3.89E+06	IFIH1, ISG15, OASL2, OASL1, PMAIP1, OAS1A, OAS2, IL33, OAS1F, MX2	61	167	18082	1.78E+15	2.36E+10	2.36E+10	5.75E+08
INTERPRO		IPR006117~2-5-oligoadenylate synthetase, conserved site	5	7.25E+15	5.51E+06	OASL2, OASL1, OAS1A, OAS2, OAS1F	64	8	20594	2.01E+10	1.00E+10	1.00E+10	6.80E+09
INTERPRO		IPR026774~2'-5'-oligoadenylate synthase	5	7.25E+15	3.86E+07	OASL2, OASL1, OAS1A, OAS2, OAS1F	64	12	20594	1.34E+16	7.03E+10	3.52E+09	4.77E+10
INTERPRO		IPR018952~2'-5'-oligoadenylate synthetase 1, domain 2/C-terminal	5	7.25E+15	3.86E+07	OASL2, OASL1, OAS1A, OAS2, OAS1F	64	12	20594	1.34E+16	7.03E+10	3.52E+09	4.77E+10
INTERPRO		IPR006116~2-5-oligoadenylate synthetase, N-terminal	5	7.25E+15	7.78E+06	OASL2, OASL1, OAS1A, OAS2, OAS1F	64	14	20594	1.15E+08	1.42E+11	4.72E+09	9.60E+10
GOTERM_BP_DIRECT		GO:0009615~response to virus	7	1.01E+16	3.44E+09	IFIH1, OASL2, OASL1, TGTP2, OAS1A, OAS2, MX2	61	84	18082	2.47E+15	2.08E+12	1.04E+12	5.08E+11
UP_KEYWORDS		Antiviral defense	7	1.01E+16	4.23E+09	IFIH1, ISG15, OASL2, OASL1, OAS1A, OAS2, MX2	66	100	22680	2.41E+15	5.41E+10	5.41E+10	4.91E+11
GOTERM_MF_DIRECT		GO:0003725~double-stranded RNA binding	6	8.70E+15	3.81E+10	IFIH1, OASL2, OASL1, OAS1A, OAS2, OAS1F	60	70	17446	2.49E+16	5.67E+11	5.67E+11	4.54E+03
UP_KEYWORDS		Innate immunity	8	1.16E+16	5.78E+10	IFIH1, CD55, OASL2, OASL1, TGTP2, OAS1A, OAS2, MX2	66	241	22680	1.14E+16	7.39E+11	3.70E+11	6.71E+03
GOTERM_MF_DIRECT		GO:0001730~2'-5'-oligoadenylate synthetase activity	4	5.80E+15	5.95E+09	OASL2, OASL1, OAS1A, OAS2	60	11	17446	1.06E+16	8.86E+11	4.43E+11	7.09E+03
UP_KEYWORDS		Immunity	9	1.30E+16	1.86E+11	IFIH1, CD55, OASL2, OASL1, TGTP2, OAS1A, OAS2, MX2, LGALS9	66	401	22680	7.71E+15	2.38E+03	7.95E+11	2.16E+02
INTERPRO		IPR002934~Nucleotidyl transferase domain	3	4.35E+16	8.19E+11	OASL2, OAS1A, OAS2	64	14	20594	6.90E+07	1.38E+01	3.66E+02	1.01E+16
KEGG_PATHWAY		mmu05164:Influenza A	5	7.25E+15	1.50E+03	IFIH1, OAS1A, OAS2, IL33, MX2	24	171	7691	9.37E+15	9.71E+02	4.98E+02	1.53E+16

GOTERM_BP_DIRECT	GOTERM_BP_DIRECT	GO:0002376--immune system process	Count	%	PValue	Genes	List Total	Pop Hits	Fold Enrichment	Bonferroni	Benjamini	FDR	
GOTERM_BP_DIRECT	GO:0002376--immune system process	GO:0002376--immune system process	7	1.01E+16	1.66E-03	IFIH1, CD55, OASL2, OASL1, OAS2, MX2, LGALS9	61	383	18082	5.42E+15	6.34E-01	2.22E-01	2.42E+16
GOTERM_BP_DIRECT	GO:0006164--purine nucleotide biosynthetic process	GO:0006164--purine nucleotide biosynthetic process	3	4.35E+16	1.98E-03	OASL2, OAS1A, OAS2	61	20	18082	4.45E+15	6.99E-01	2.14E-01	2.89E+16
GOTERM_BP_DIRECT	GO:0045087--innate immune response	GO:0045087--innate immune response	7	1.01E+16	2.06E-03	IFIH1, CD55, OASL2, OASL1, OAS1A, OAS2, MX2	61	400	18082	5.19E+15	7.14E-01	1.88E-01	3.01E+16
GOTERM_BP_DIRECT	GO:0006955--immune response	GO:0006955--immune response	6	8.70E+15	2.06E-03	P2RY14, OASL2, OASL1, TGTP2, OAS2, OAS1F	61	272	18082	6.54E+15	7.14E-01	1.64E-01	3.01E+16
KEGG_PATHWAY	mmu05162:Measles Nucleotidyltransferase	mmu05162:Measles Nucleotidyltransferase	4	5.80E+15	7.39E-03	IFIH1, OAS1A, OAS2, MX2	24	136	7691	9.43E+15	3.96E-01	1.55E-01	7.35E+15
UP_KEYWORDS	RNA-binding	RNA-binding	6	8.70E+15	2.89E-02	IFIH1, OASL2, ZMAT3	66	76	22680	1.36E+16	9.26E-01	2.78E-01	2.10E+16
UP_KEYWORDS	Magnesium	Magnesium	5	7.25E+15	6.23E-02	OASL2, ITGA11, OAS1A, OAS2, TTN	66	521	22680	3.30E+15	1.00E+00	4.02E-01	5.26E+16
GOTERM_MF_DIRECT	GO:0003723--RNA binding	GO:0003723--RNA binding	6	8.70E+15	1.23E-01	IFIH1, OASL2, ZMAT3, OASL1, OAS2, OAS1F	60	780	17446	2.24E+15	1.00E+00	9.62E-01	7.91E+15
KEGG_PATHWAY	mmu05168:Herpes simplex infection	mmu05168:Herpes simplex infection	3	4.35E+16	1.27E-01	IFIH1, OAS1A, OAS2	24	208	7691	4.62E+16	1.00E+00	6.42E-01	7.53E+15
UP_KEYWORDS	Nucleotide-binding	Nucleotide-binding	8	1.16E+16	2.36E-01	IFIH1, OASL2, TGTP2, OAS1A, OAS2, TTN, GBP3, MX2	66	1754	22680	1.57E+16	1.00E+00	7.76E-01	9.56E+14
GOTERM_MF_DIRECT	GO:0005524--ATP binding	GO:0005524--ATP binding	8	1.16E+16	2.45E-01	IFIH1, OASL2, SYN2, OASL1, OAS1A, OAS2, OAS1F, TTN	60	1507	17446	1.54E+16	1.00E+00	9.70E-01	9.65E+15
UP_KEYWORDS	Transferase	Transferase	6	8.70E+15	5.18E-01	CDKN1A, OASL2, PARP14, OAS1A, OAS2, TTN	66	1654	22680	1.25E+16	1.00E+00	9.69E-01	1.00E+16
UP_KEYWORDS	ATP-binding	ATP-binding	5	7.25E+15	5.54E-01	IFIH1, OASL2, OAS1A, OAS2, TTN	66	1363	22680	1.26E+16	1.00E+00	9.64E-01	1.00E+16
GOTERM_MF_DIRECT	GO:0000166--nucleotide binding	GO:0000166--nucleotide binding	7	1.01E+16	6.51E-01	IFIH1, CELF5, OASL2, PARP14, OAS2, GBP3, MX2	60	1936	17446	1.05E+16	1.00E+00	1.00E+00	1.00E+16
GOTERM_MF_DIRECT	GO:0016740--transferase activity	GO:0016740--transferase activity	5	7.25E+15	7.45E-01	OASL2, PARP14, OASL1, OAS2, OAS1F	60	1472	17446	9.88E-01	1.00E+00	1.00E+00	1.00E+16
<p>Enrichment Score: Annotation Cluster 2 3.3310651707009664</p>													
Category	Term		Count	%	PValue	Genes	List Total	Pop Hits	Fold Enrichment	Bonferroni	Benjamini	FDR	

UP_KEYWORDS	Antiviral defense	Count	%	PValue	Genes	List Total	Pop Hits	Pop Total	Fold Enrichment	Bonferroni	Benjamini	FDR
SMART	SM00213:UBQ	7	1.01E+16	4.23E+09	IFIH1, ISG15, OASL2, OASL1, OAS1A, OAS2, MX2	66	100	22680	2.41E+15	5.41E+10	5.41E+10	4.91E+11
INTERPRO	IPR000626:Ubiquitin	3	4.35E+16	1.38E-02	ISG15, OASL2, OASL1	37	52	10425	1.63E+16	5.28E-01	3.13E-01	1.27E+16
		3	4.35E+16	1.74E-02	ISG15, OASL2, OASL1	64	66	20594	1.46E+16	9.59E-01	4.13E-01	1.95E+15
Enrichment Score: 3.035633030628498												
Annotation Cluster 3	Term	Count	%	PValue	Genes	List Total	Pop Hits	Pop Total	Fold Enrichment	Bonferroni	Benjamini	FDR
UP_KEYWORDS	Glycoprotein	25	3.62E+16	7.91E+10	CCKAR, FFAR4, SLC6A2, NELL1, ITGA11, OAS2, GDNF, SMOC2, LGALS3BP, WISPI, P4HA2, CRISPLD2, DNER, FAP, GPR20, ASIC2, GRIA3, FRZB, CD55, CHRDL1, SULF2, PTPRV, P2RY14, GPR17, GDF15	66	3815	22680	2.25E+16	1.01E-02	2.53E-03	9.18E-02
UP_KEYWORDS	Disulfide bond	22	3.19E+15	1.05E+12	CCKAR, SLC6A2, NELL1, EDN1, ASIC2, ITGA11, IGF1, GRIA3, FRZB, TTN, GDNF, SMOC2, CD55, LGALS3BP, WISPI, ISG15, CRISPLD2, DNER, FAP, P2RY14, GPR17, GDF15	66	3124	22680	2.42E+16	1.34E-02	2.69E-03	1.22E-01
UP_KEYWORDS	Secreted	15	2.17E+15	2.46E+12	NELL1, EDN1, IGF1, IL33, FRZB, GDNF, LGALS9, SMOC2, LGALS3BP, CHRDL1, WISPI, ISG15, CRISPLD2, FAP, GDF15	66	1685	22680	3.06E+15	3.11E-02	5.25E-03	2.86E-01

UP_SEQ_FEATURE	glycosylation site:N-linked (GlcNAc...)	24	3.48E+15	2.84E+12	58	3563	18012	2.09E+16	1.81E-01	1.81E-01	4.28E-01	
<p>CCKAR, FFAR4, SLC6A2, NELL1, ITGA11, ASIC2, GRIA3, FRZB, GDNF, SMOC2, CD55, LGALS3BP, CHRDL1, WISP1, SULF2, P4HA2, CRISPLD2, PTPRV, DNER, FAP, P2RY14, GPR17, GDF15, GPR20</p>												
UP_SEQ_FEATURE	disulfide bond	19	2.75E+16	5.04E+10	58	2510	18012	2.35E+16	2.99E-01	1.63E-01	7.59E-01	
<p>CCKAR, NELL1, EDN1, ASIC2, ITGA11, IGF1, FRZB, TTN, GDNF, SMOC2, CD55, LGALS3BP, WISP1, CRISPLD2, DNER, P2RY14, FAP, GPR17, GDF15</p>												
GOTERM_CC_DIRECT	GO:0005576~extracellular region	15	2.17E+15	7.80E+11	62	1753	19662	2.71E+15	7.51E-02	7.51E-02	8.62E-01	
<p>NELL1, EDN1, IGF1, IL33, FRZB, GDNF, LGALS9, SMOC2, LGALS3BP, CHRDL1, WISP1, IGF15, CRISPLD2, FAP, GDF15</p>												
UP_SEQ_FEATURE	signal peptide	20	2.90E+16	2.55E-03	58	3124	18012	1.99E+16	8.35E-01	4.51E-01	3.78E+15	
<p>NELL1, EDN1, ITGA11, IGF1, GRIA3, FRZB, GDNF, SMOC2, CD55, LGALS3BP, CHRDL1, WISP1, SULF2, P4HA2, SHISA3, PTPRV, CRISPLD2, DNER, GDF15, PQLC3</p>												
GOTERM_CC_DIRECT	GO:0005615~extracellular space	11	1.59E+16	1.67E-02	62	1504	19662	2.32E+15	8.14E-01	4.29E-01	1.70E+15	
<p>LGALS3BP, SULF2, NELL1, FAP, EDN1, LMCD1, IGF1, IL33, FRZB, GDF15, GDNF</p>												
UP_KEYWORDS	Signal	20	2.90E+16	4.91E-02	66	4543	22680	1.51E+16	9.98E-01	4.15E-01	4.42E+15	
<p>NELL1, EDN1, ITGA11, IGF1, GRIA3, FRZB, GDNF, SMOC2, CD55, LGALS3BP, CHRDL1, WISP1, SULF2, P4HA2, SHISA3, PTPRV, CRISPLD2, DNER, GDF15, PQLC3</p>												

Annotation Cluster 4		Enrichment Score: 1.269065734222906										
Category	Term	Count	%	PValue	Genes	List Total	Pop Hits	Pop Total	Fold Enrichment	Bonferroni	Benjamini	FDR
GOTERM_BP_DIRECT	GO:0043065~positive regulation of apoptotic process	5	7.25E+15	2.51E-02	NELL1, ZMAT3, TRP53INP1, PMAIP1, FRZB	61	335	18082	4.42E+15	1.00E+00	6.67E-01	3.13E+16
UP_KEYWORDS	Apoptosis	5	7.25E+15	5.17E-02	FAP, ZMAT3, TRP53INP1, PMAIP1, XAF1	66	489	22680	3.51E+15	9.99E-01	3.84E-01	4.60E+15
GOTERM_BP_DIRECT	GO:0006915~apoptotic process	5	7.25E+15	1.20E-01	FAP, ZMAT3, TRP53INP1, PMAIP1, XAF1	61	570	18082	2.60E+15	1.00E+00	9.75E-01	8.50E+15
Annotation Cluster 5		Enrichment Score: 0.9983796718279031										
Category	Term	Count	%	PValue	Genes	List Total	Pop Hits	Pop Total	Fold Enrichment	Bonferroni	Benjamini	FDR
UP_KEYWORDS	Endoplasmic reticulum	8	1.16E+16	2.36E-02	SLN, SULF2, P4HA2, SHISA3, EPHX1, TGTP2, OAS1A, OAS2	66	997	22680	2.76E+15	9.53E-01	2.88E-01	2.43E+16
UP_KEYWORDS	Microsome	3	4.35E+16	5.51E-02	EPHX1, OAS1A, OAS2	66	132	22680	7.81E+15	9.99E-01	3.84E-01	4.82E+16
GOTERM_CC_DIRECT	GO:0005783~endoplasmic reticulum	8	1.16E+16	1.14E-01	CCKAR, SLN, SULF2, P4HA2, SHISA3, EPHX1, OAS1A, OAS2	62	1323	19662	1.92E+15	1.00E+00	7.03E-01	7.40E+15
GOTERM_CC_DIRECT	GO:0043231~intracellular membrane-bounded organelle	3	4.35E+16	6.82E-01	P4HA2, EPHX1, OAS2	62	751	19662	1.27E+16	1.00E+00	9.95E-01	1.00E+16
Annotation Cluster 6		Enrichment Score: 0.6615117943565963										
Category	Term	Count	%	PValue	Genes	List Total	Pop Hits	Pop Total	Fold Enrichment	Bonferroni	Benjamini	FDR
INTERPRO	IPR027417~P-loop containing nucleoside triphosphate hydrolase	6	8.70E+15	1.45E-01	IFIH1, IFM44, TGTP2, RNF213, GBP3, MX2	64	909	20594	2.12E+15	1.00E+00	9.58E-01	8.55E+15
GOTERM_MF_DIRECT	GO:0003924~GTPase activity	3	4.35E+16	1.57E-01	TGTP2, GBP3, MX2	60	209	17446	4.17E+15	1.00E+00	9.74E-01	8.70E+15
UP_KEYWORDS	Nucleotide-binding	8	1.16E+16	2.36E-01	IFIH1, OASL2, TGTP2, OAS1A, OAS2, TTN, GBP3, MX2	66	1754	22680	1.57E+16	1.00E+00	7.76E-01	9.56E+14
UP_KEYWORDS	GTP-binding	3	4.35E+16	2.46E-01	TGTP2, GBP3, MX2	66	332	22680	3.11E+15	1.00E+00	7.79E-01	9.62E+15
GOTERM_MF_DIRECT	GO:0005525~GTP binding	3	4.35E+16	3.73E-01	TGTP2, GBP3, MX2	60	383	17446	2.28E+16	1.00E+00	9.90E-01	9.96E+15
Annotation Cluster 7		Enrichment Score: 0.5368923254839906										

Category	Term	Count	%	PValue	Genes	List Total	Pop Hits	Pop Total	Fold Enrichment	Bonferroni	Benjamini	FDR
UP_KEYWORDS	Metal-binding	15	2.17E+15	9.85E-02	IFIH1, SLC6A2, ZMAT3, LMCD1, ITGA11, OAS2, TTN, RNF213, SMOG2, CDKN1A, SULF2, P4HA2, OASL2, OAS1A, XAF1	66	3395	22680	1.52E+16	1.00E+00	4.85E-01	7.00E+15
GOTERM_MF_DIRECT	GO:0046872--metal ion binding	14	2.03E+15	3.41E-01	IFIH1, SLC6A2, ZMAT3, ITGA11, LMCD1, OAS2, RNF213, SMOG2, CDKN1A, SULF2, P4HA2, OASL2, XAF1, OAS1A	60	3355	17446	1.21E+16	1.00E+00	9.88E-01	9.93E+15
UP_KEYWORDS	Zinc	6	8.70E+15	7.30E-01	CDKN1A, IFIH1, ZMAT3, LMCD1, XAF1, RNF213	66	2099	22680	9.82E-01	1.00E+00	9.88E-01	1.00E+16
Enrichment Score: 0.5102827409297518												
Annotation Cluster 8												
Category	Term	Count	%	PValue	Genes	List Total	Pop Hits	Pop Total	Fold Enrichment	Bonferroni	Benjamini	FDR
UP_SEQ_FEATURE	topological domain:Extracellular	13	1.88E+15	4.73E-02	CCKAR, FFAR4, SLC6A2, ASIC2, ITGA11, GRIA3, SHISA3, PTPRV, P2RY14, FAP, DNER, GPR17, GPR20	58	2256	18012	1.79E+16	1.00E+00	9.99E-01	5.19E+16
GOTERM_CC_DIRECT	GO:0016020--membrane	28	4.06E+15	1.01E-01	CCKAR, RTP4, FFAR4, SLC6A2, ITGA11, OAS2, RNF213, LGALS3BP, SLN, SHISA3, FAP, DNER, OASL1, GPR20, PQLC3, MNDAL, ASIC2, EPHX1, GRIA3, CD55, PTPRV, PARP14, P2RY14, TGTP2, GPR17, IFI203, GBP3, SNTG2	62	6998	19662	1.27E+16	1.00E+00	6.94E-01	6.93E+15
UP_SEQ_FEATURE	topological domain:Cytoplasmic	14	2.03E+15	1.13E-01	CCKAR, RTP4, FFAR4, SLC6A2, ASIC2, ITGA11, GRIA3, SHISA3, PTPRV, P2RY14, FAP, DNER, GPR17, GPR20	58	2880	18012	1.51E+16	1.00E+00	1.00E+00	8.36E+15

UP_SEQ_FEATURE	transmembrane region	17	2.46E+16	2.76E-01	CCKAR, RTP4, FFAR4, SLC6A2, ASIC2, ITGA11, EPHX1, GRIA3, SLN, SHISA3, PTPRV, DNER, P2RY14, FAP, GPR17, GPR20, PQLC3	58	4312	18012	1.22E+16	1.00E+00	1.00E+00	9.92E+15
GOTERM_CC_DIRECT	GO:0005886~plasma membrane	17	2.46E+16	4.46E-01	CCKAR, FFAR4, SLC6A2, ASIC2, IGF1, EPHX1, GRIA3, SLC19A2, CD55, SULF2, DNER, P2RY14, FAP, SYN2, GPR17, GPR20, SNTG2	62	4874	19662	1.11E+15	1.00E+00	9.80E-01	9.99E+15
UP_KEYWORDS	Cell membrane	12	1.74E+16	5.21E-01	CCKAR, CD55, FFAR4, SLC6A2, P2RY14, DNER, FAP, ASIC2, GRIA3, GPR17, GPR20, SNTG2	66	3759	22680	1.10E+16	1.00E+00	9.66E-01	1.00E+16
UP_KEYWORDS	Transmembrane helix	20	2.90E+16	6.40E-01	CCKAR, MS4A7, RTP4, FFAR4, SLC6A2, ASIC2, ITGA11, EPHX1, GRIA3, SLC19A2, SLN, P4HA2, SHISA3, PTPRV, DNER, FAP, P2RY14, GPR17, GPR20, PQLC3	66	6938	22680	9.91E-01	1.00E+00	9.76E-01	1.00E+15
UP_KEYWORDS	Transmembrane	20	2.90E+16	6.45E-01	CCKAR, MS4A7, RTP4, FFAR4, SLC6A2, ASIC2, ITGA11, EPHX1, GRIA3, SLC19A2, SLN, P4HA2, SHISA3, PTPRV, DNER, FAP, P2RY14, GPR17, GPR20, PQLC3	66	6955	22680	9.88E-01	1.00E+00	9.72E-01	1.00E+16
GOTERM_CC_DIRECT	GO:0016021~integral component of membrane	21	3.04E+16	6.86E-01	CCKAR, MS4A7, RTP4, FFAR4, SLC6A2, ASIC2, ITGA11, EPHX1, GRIA3, FRZB, SLC19A2, SLN, P4HA2, SHISA3, PTPRV, DNER, FAP, P2RY14, GPR17, GPR20, PQLC3	62	6878	19662	9.68E-01	1.00E+00	9.93E-01	1.00E+16

INTERPRO	IPR000276:G-protein-coupled receptor, rhodopsin-like	5	7.25E+15	6.61E-01	CCKAR, FFAR4, P2RY14, GPR17, GPR20	64	1458	20594	1.10E+16	1.00E+00	1.00E+00	1.00E+16
GOTERM_BP_DIRECT	GO:0007186~G-protein coupled receptor for signaling pathway	6	8.70E+15	6.80E-01	CCKAR, FFAR4, P2RY14, EDN1, GPR17, GPR20	61	1706	18082	1.04E+15	1.00E+00	1.00E+00	1.00E+16
GOTERM_MF_DIRECT	GO:0004930~G-protein coupled receptor for activity	6	8.70E+15	7.18E-01	CCKAR, FFAR4, P2RY14, GPR17, FRZB, GPR20	60	1749	17446	9.97E-01	1.00E+00	1.00E+00	1.00E+15
UP_KEYWORDS	G-protein coupled receptor	5	7.25E+15	7.45E-01	CCKAR, FFAR4, P2RY14, GPR17, GPR20	66	1741	22680	9.87E-01	1.00E+00	9.89E-01	1.00E+16
UP_KEYWORDS	Transducer	5	7.25E+15	7.69E-01	CCKAR, FFAR4, P2RY14, GPR17, GPR20	66	1801	22680	9.54E-01	1.00E+00	9.90E-01	1.00E+16
INTERPRO	IPR017452:GPCR, rhodopsin-like, 7TM	5	7.25E+15	7.78E-01	CCKAR, FFAR4, P2RY14, GPR17, GPR20	64	1708	20594	9.42E-01	1.00E+00	1.00E+00	1.00E+16
Annotation Cluster 10												
Enrichment Score: 0.3277560757196918												
Category	Term	Count	%	PValue	Genes	List Total	Pop Hits	Pop Total	Fold Enrichment	Bonferroni	Benjamini	FDR
UP_KEYWORDS	Differentiation	4	5.80E+15	2.83E-01	CHRD1, NELL1, DNER, FRZB	66	646	22680	2.13E+16	1.00E+00	8.17E-01	9.79E+15
GOTERM_BP_DIRECT	GO:0030154~cell differentiation	4	5.80E+15	4.82E-01	CHRD1, NELL1, DNER, FRZB	61	780	18082	1.52E+15	1.00E+00	1.00E+00	1.00E+16
UP_KEYWORDS	Developmental protein	4	5.80E+15	5.34E-01	CHRD1, SHISA3, DNER, FRZB	66	976	22680	1.41E+16	1.00E+00	9.66E-01	1.00E+15
GOTERM_BP_DIRECT	GO:0007275~multicellular organism development	4	5.80E+15	6.71E-01	CHRD1, SHISA3, DNER, FRZB	61	1029	18082	1.15E+16	1.00E+00	1.00E+00	1.00E+15
Annotation Cluster 11												
Enrichment Score: 0.01866930672055855												
Category	Term	Count	%	PValue	Genes	List Total	Pop Hits	Pop Total	Fold Enrichment	Bonferroni	Benjamini	FDR
UP_KEYWORDS	Transcription	4	5.80E+15	9.10E-01	PARP14, LMCD1, TRP53INP1, IL33	66	1859	22680	7.39E-01	1.00E+00	9.99E-01	1.00E+16
GOTERM_BP_DIRECT	GO:0006351~transcription, DNA-templated	4	5.80E+15	9.57E-01	PARP14, LMCD1, TRP53INP1, IL33	61	1885	18082	6.29E-01	1.00E+00	1.00E+00	1.00E+02
UP_KEYWORDS	Transcription regulation	3	4.35E+16	9.70E-01	PARP14, LMCD1, TRP53INP1	66	1799	22680	5.73E-01	1.00E+00	1.00E+00	1.00E+02
GOTERM_BP_DIRECT	GO:0006355~regulation of transcription, DNA-templated	3	4.35E+16	9.97E-01	PARP14, LMCD1, TRP53INP1	61	2279	18082	3.90E-01	1.00E+00	1.00E+00	1.00E+02

Table S8. Functional annotation analysis of upregulated genes in microarray analysis.

Shown are functional clusters of upregulated genes in the microarray determined by DAVID functional annotation tool sorted by enrichment score.

Table S9. Mass Spectrometry.

Shown is the complete list of detected proteins in mass spectrometry analysis.

	A	B	C	D	E	F	G	H	I	J	K	L	M	N	O	P	Q	R	S	
1																				
2																				
3																				
4	700																			
5	35																			
6	42																			
7	119																			
8	919																			
9	Intensity 1- Tbx2_x- y_Mean	Intensity 2- Tbx2_x- y_Mean	Intensity 3- Tbx2_x- y_Mean	Intensity 1- IgG_x- y_Mean	Intensity 2- IgG_x- y_Mean	Intensity 3- IgG_x- y_Mean	Intensity 1- Tbx2	Intensity 2- Tbx2	Intensity 3- Tbx2	Intensity 1- IgG	Intensity 2- IgG	Intensity 3- IgG	Intensity 1- IgG-Input	Intensity 2- IgG-Input	Intensity 3- IgG-Input	Intensity 1- Tbx2-Input	Intensity 2- Tbx2-Input	Intensity 3- Tbx2-Input	Student's T-test Signifi- cant ERM- Tbx2_ERM- IgG	N: Razor + unique peptides
10	14.527	11.944	11.983	-0.133	0.558	-0.220	17.237	17.928	17.150	31.049	28.466	28.505	18.413	16.327	17.640	15.405	+	+	+	1
11	14.891	14.526	14.668	6.146	2.245	1.073	22.707	18.806	17.634	34.180	33.816	33.958	18.947	14.175	23.859	14.721	+	+	+	1
12	9.416	8.748	7.338	-2.110	-1.711	-0.390	17.286	17.685	19.006	25.170	24.502	23.032	20.011	18.779	18.866	14.642	+	+	+	11
13	14.100	14.393	14.676	6.040	1.470	-7.622	22.179	17.609	23.761	30.966	31.259	31.542	16.280	15.997	18.121	15.611	+	+	+	10
14	0.000	-1.776	3.912	-10.189	-8.166	-4.010	16.850	18.873	23.030	20.261	18.485	24.173	29.710	24.369	17.099	23.424	+	+	+	8
15	12.061	11.729	11.625	5.765	1.022	5.738	23.219	18.476	23.191	33.038	32.705	32.602	18.658	16.249	24.727	17.227	+	+	+	10
16	6.761	6.800	7.208	-0.194	0.412	-1.584	16.629	17.236	15.239	23.336	23.375	23.783	17.433	16.214	18.521	14.630	+	+	+	2
17	3.742	3.401	3.029	-1.007	-5.188	-5.362	21.366	17.185	17.011	22.508	22.167	21.795	24.558	20.188	21.317	16.214	+	+	+	4
18	-1.609	-0.964	2.728	-7.043	-6.998	-6.346	17.726	17.772	18.424	16.924	17.569	21.261	22.578	26.961	22.169	14.908	+	+	+	3
19	8.969	7.610	7.748	-0.162	4.135	0.147	16.543	20.841	16.852	25.733	24.373	24.512	17.432	15.978	17.732	15.795	+	+	+	8
20	-4.879	1.912	1.031	-7.588	-7.810	-6.736	16.355	16.133	17.207	17.041	23.833	22.952	26.126	21.761	24.265	19.576	+	+	+	6
21	3.615	3.796	1.986	-8.508	-0.950	-1.031	15.291	22.848	22.768	23.612	23.793	21.982	26.044	21.554	24.577	15.416	+	+	+	11
22	5.383	1.690	5.115	-3.304	-1.277	-2.932	16.630	18.657	17.002	21.406	17.713	21.138	22.370	17.497	16.609	15.437	+	+	+	4
23	-2.306	3.062	2.264	-5.541	-4.153	-6.955	17.460	18.848	16.046	17.041	22.409	21.611	26.102	19.899	23.513	15.192	+	+	+	3
24	-0.840	0.162	8.921	-3.407	-4.010	-3.497	17.433	16.830	17.343	16.696	17.697	26.457	24.030	17.650	20.774	14.297	+	+	+	6
25	6.942	8.347	8.093	-0.748	0.397	4.880	16.760	17.905	22.387	23.337	24.743	24.488	18.717	16.299	18.435	14.356	+	+	+	3
26	2.787	5.254	2.811	-1.419	-3.614	-2.967	18.804	16.609	17.256	21.759	24.226	21.783	18.481	21.965	23.037	14.907	+	+	+	8
27	5.193	4.916	6.071	-1.107	-1.256	0.041	16.961	16.812	18.108	20.421	20.143	21.299	21.045	15.090	15.727	14.728	+	+	+	4
28	4.891	6.813	4.026	-1.276	-0.465	-1.022	16.020	16.830	16.274	22.049	23.971	21.184	18.335	16.257	18.202	16.113	+	+	+	4
29	1.388	8.595	6.469	-1.050	-0.363	0.114	16.452	17.139	17.616	17.573	24.780	22.654	19.456	15.548	17.137	15.233	+	+	+	4
30	8.702	7.755	-0.003	-0.156	-0.595	-0.036	17.307	16.868	17.428	24.428	23.481	15.723	17.748	17.178	16.351	15.101	+	+	+	2
31	0.058	4.747	2.561	-3.246	-3.561	-2.792	17.153	16.838	17.607	16.257	20.946	18.760	23.263	17.534	17.458	14.940	+	+	+	1

Part 2 - TBX2 target genes and interaction partners

	A	B	C	D	E	F	G	H	I	J	K	L	M	N	O	P	Q	R	S
32	2.438	6.504	4.625	-2.211	1.758	-2.808	17.220	21.188	16.623	21.428	25.493	23.614	18.262	20.600	23.520	14.458	+	9	9
33	-0.648	6.104	1.879	-2.578	-3.905	-2.775	16.999	15.673	16.802	16.435	23.187	18.961	18.871	20.284	20.001	14.165		5	5
34																			
35	4.555	4.456	3.120	-3.827	0.646	-1.191	16.950	21.423	19.586	22.561	22.461	21.126	25.087	16.467	21.582	14.430	+	9	9
36	3.795	4.429	-0.711	-5.178	-3.420	-0.291	16.592	18.350	21.479	22.061	22.895	17.555	23.549	19.990	22.481	14.052		4	4
37	5.041	4.425	3.684	-0.346	-1.464	-1.428	17.999	16.880	16.916	21.358	20.742	20.000	19.250	17.439	17.366	15.266	+	1	1
38	-0.311	4.961	5.542	-3.265	1.522	-4.441	17.103	21.889	15.927	15.796	21.068	21.648	23.669	17.065	18.257	13.966		3	3
39	5.977	3.670	5.556	-0.978	0.210	-0.174	16.204	17.392	17.009	24.630	22.324	24.210	17.358	17.007	21.455	15.853	+	25	1
40	1.625	4.218	3.314	-2.732	-2.274	-1.926	16.764	17.222	17.570	20.087	22.860	21.775	19.103	19.889	22.853	14.071	+	3	3
41																			
42	-1.082	-3.448	-4.601	-10.222	-4.779	-10.181	15.500	20.943	15.541	20.834	18.478	17.324	27.685	23.759	25.410	18.440		12	12
43	0.537	9.235	6.444	-0.271	0.914	-0.467	16.199	17.384	16.003	16.145	24.843	22.052	18.398	14.541	15.724	15.462		5	5
44																			
45	7.460	5.900	5.991	-0.609	-1.023	4.967	16.859	16.445	22.434	23.739	22.179	22.269	19.326	15.610	17.684	14.873		1	1
46	0.136	10.943	7.324	0.153	1.048	1.331	17.448	18.343	18.627	16.273	27.080	23.461	17.986	16.605	17.363	14.911		15	15
47	3.683	5.397	2.376	-1.353	-1.174	-1.848	16.811	16.990	16.316	20.403	22.116	19.095	19.368	16.960	18.090	15.349	+	2	2
48	2.573	8.080	5.616	-0.027	-0.376	0.957	25.607	25.258	26.591	24.641	30.149	27.684	24.083	27.184	26.030	18.107	+	27	27
49	-2.321	5.513	3.363	-4.677	-0.193	-4.261	16.839	21.323	17.256	15.777	23.612	21.462	19.838	23.195	20.393	15.804		4	4
50	-0.488	3.179	0.615	-5.055	-4.408	-2.293	17.182	17.829	19.944	20.084	23.751	21.187	24.423	20.051	21.949	19.194	+	5	3
51	1.629	8.585	6.017	-0.107	-0.026	1.453	17.752	17.833	19.312	17.090	24.046	21.478	18.770	16.948	17.285	13.637		5	5
52	9.904	6.267	7.408	5.211	1.689	1.774	29.390	25.868	25.953	28.021	24.384	25.525	25.189	23.169	16.955	19.278	+	3	3
53	5.502	4.543	3.141	-0.114	-0.162	-1.239	22.564	22.515	21.439	27.715	26.755	25.354	24.387	20.968	22.438	21.988	+	38	38
54	-2.312	3.763	-2.901	-2.209	-5.677	-8.255	21.202	17.734	15.156	16.909	22.984	16.321	24.767	22.055	18.860	19.583		4	4
55	3.402	4.926	5.975	-2.249	1.028	0.933	22.009	25.287	25.192	22.483	24.007	25.055	25.322	23.194	24.518	13.643	+	5	5
56	2.606	-0.252	-0.788	-6.087	-6.357	-0.562	16.412	16.142	21.937	21.045	18.187	17.651	24.868	20.129	22.150	14.728		3	3
57	-0.661	5.866	3.999	-1.711	-0.938	-2.636	16.441	17.214	15.516	16.005	22.531	20.665	20.170	16.133	18.562	14.769		2	2
58	0.055	2.566	0.220	-3.983	-4.205	-3.320	17.496	17.273	18.159	20.426	22.937	20.590	23.645	19.313	22.223	18.518	+	3	3
59	1.143	-1.161	-0.500	-5.269	-4.977	-4.544	16.927	17.119	17.552	20.029	17.726	18.387	23.512	20.679	17.419	20.354	+	4	4
60	-3.796	2.376	1.580	-4.683	-3.551	-5.563	17.442	18.574	16.562	15.372	21.544	20.748	24.642	19.608	23.315	15.021		5	5
61	4.105	6.283	1.744	-0.908	-0.301	-0.506	16.221	16.827	16.623	20.072	22.250	17.712	18.973	15.284	17.081	14.854	+	2	2
62	-0.690	5.259	4.131	-1.828	-1.486	-1.578	16.657	16.998	16.907	16.495	22.444	21.316	21.820	15.149	20.376	13.994		2	2
63	0.880	-3.690	-0.439	-6.473	-2.782	-7.499	18.565	22.255	17.538	22.309	17.738	20.990	26.720	23.355	24.334	18.524		11	10

Part 2 - TBX2 target genes and interaction partners

	T	U	V	W	X	Y	Z	AA	AB	AC	AD	AE	AF
32	9	4.8	285.15	82.628	19.431	18.989	1.410	5.610	Q8BT18; Q8BT18; Q8BT18-2; Q8BT18 Z; Q8BT18; A0A087WFS9; A0A087W RX8	Q8BT18-3; Q8BT18-2; Q8BT18 F6ZDS4; Q7M739; F6RX08	Serine/arginine repetitive matrix protein 2 Nucleoprotein TPR	Srrm2 Tpr	1182 426
33	5	3	273.99	35.996	19.577	17.083	1.289	5.631	F6ZDS4; Q7M739; F6RX08	F6ZDS4; Q7M739; F6RX08			
34	9	11.4	104.92	56.13	20.777	18.006	1.789	5.501	P30999; E9Q084; E9Q8Z6; G3X9V2; E9 E9Q004; E9Q001; D3Z2H2; E9Q8Z9; E9Q E9Q8Z8; E9Q905; E9Q907; E9Q903; E9Q986; D3Z7H8; P30999- 2; E9Q8Z6; P30999- 3; E9Q906; D3Z2H7	P30999; E9Q084; E9Q8Z6; G3X9V2; E9 E9Q004; E9Q001; D3Z2H2; E9Q8Z9; E9Q E9Q8Z8; E9Q905; E9Q907; E9Q903; E9Q986; D3Z7H8; P30999- 2; E9Q8Z6; P30999- 3; E9Q906; D3Z2H7	Catenin delta-1	Ctndd1	301
35	4	8.4	51.373	24.412	21.770	18.266	1.190	5.467	O55222; D3YZA8; F6O5Z1	O55222	Integrin-linked protein kinase	Ilk	529
36	1	28.1	3.7112	6.5528	18.344	16.316	3.278	5.463	A0A0N4SVL7; A0A0N4SWF7; Q923 D5	A0A0N4SVL7; A0A0N4SWF7; Q923 D5	WW domain-binding protein 11	Wbp11	70
37	3	6.3	50.113	18.832	20.367	16.107	0.982	5.458	Q9Z219	Q9Z219	Succinyl-CoA ligase [ADP-forming] subunit beta, mitochondrial	Suclia2 Tuba1a; Tub a3a	1573 873
38	1	57.2	50.135	9.814	17.182	18.654	2.613	5.382	P68369; P05214	P68369; P05214	Tubulin alpha-1A chain; Tubulin alpha-3 chain		873
39	3	22.3	19.79	18.626	19.496	18.462	2.599	5.363	Q62376-2; Q62376	Q62376-2; Q62376	U1 small nuclear ribonucleoprotein 70 kDa	Snmp70	1069
40	12	21.5	82.669	119.23	25.722	21.925	1.207	5.347	Q8BMS1	Q8BMS1	Trifunctional enzyme subunit alpha, mit- ochondrial; Long-chain enoyl-CoA hydratase; Long chain 3-hydroxyacyl-CoA dehy- drogenase	Hadha	1176
41	5	14.6	50.063	33.381	16.470	15.608	0.963	5.346	A0A0M0M76; Q6DFV4; A0A087W Q46; A0A087WFP00; A0A087WSU5; A 0A0A087WV00	A0A0M0M76; Q6DFV4; Q6DFV4; A0A087WQ 46; A0A087WV00	Nucleolar protein 58	Nops58	25
42	1	10.8	13.214	15.077	17.468	16.279	1.265	5.339	A0A140T8M9; A0A140T8M0; A0A0B4 4; I10; A0A075BSN0; A0A075B5K8; F6X 6XWJ2; A0A140T8N1; A0A0G2JDE5; P0 ; P01631	A0A140T8M9; A0A140T8M0; A0A0B4 4; I10; A0A075BSN0; A0A075B5K8; F6X 6XWJ2; A0A140T8N1; A0A0G2JDE5; P0 ; P01631	Ig kappa chain V-J1 region 26-10	Igkv1- 110; Igvk1- 35; Igvk1- 99; Igvk1-115	2
43	15	22.8	93.55	116.5	17.295	16.137	0.761	5.290	Q9JJK5	Q9JJK5	Nucleolar RNA helicase 2	Ddx21	1494
44	2	4.9	52.572	12.607	18.164	16.719	2.378	5.277	Q9CTT0	Q9CTT0	Ran-binding protein 3	Ranbp3	1370
45	27	36.9	76.722	323.31	25.634	22.068	1.479	5.238	P09405	P09405	Nucleolin	Ncl	582
46	4	32.4	22.135	33.416	21.516	18.099	0.889	5.229	Q3TFP0; Q9R0U0-3; Q9R0U0- 2; Q9R0U0; A3K657	Q3TFP0; Q9R0U0-3; Q9R0U0- 2; Q9R0U0	Serine/arginine-rich splicing factor 10	Srsf10	949
47	3	17.3	37.54	19.66	22.237	20.572	1.669	5.021	P62137	P62137	Serine/threonine-protein phosphatase PP1- α - 1	Ppp1ca	808
48	5	14.6	50.421	53.118	17.859	15.461	1.117	4.871	Q8BVY0	Q8BVY0	Ribosomal L1 domain-containing protein 1	Rsl1d1	1186
49	3	34.8	10.275	119.42	24.179	18.117	1.469	4.969	P61514	P61514	60S ribosomal protein L37a	Rpl37a	798
50	38	28.8	188.85	317.06	22.677	22.213	2.489	4.900	B9EHJ3; P39447; A0A0U1RPW2; A0 A0U1RP52	B9EHJ3; P39447; A0A0U1RPW2	Tight junction protein ZO-1	Tjp1	220
51	4	17.1	36.511	30.901	23.411	19.222	0.823	4.897	P14152	P14152	Malate dehydrogenase, cytoplasmic	Mdh1	611
52	5	37.3	12.554	32.625	24.258	19.080	1.885	4.864	O55142	O55142	60S ribosomal protein L35a	Rpl35a	527
53	3	26	10.99	21.197	22.499	18.439	1.056	4.858	P62627; AZAVR9	P62627; AZAVR9	Dynein light chain roadblock-type 1	Dynlrb1	825
54	2	6.1	40.068	14.573	18.152	16.666	1.135	4.829	P54923	P54923	[Protein ADP-ribosylarginine] hydrolase	Adprh	761
55	3	34.7	11.225	18.513	21.479	20.371	2.303	4.783	Q8CFZ0; G5UYP0; P63280	Q8CFZ0; G5UYP0; P63280	SUMO-conjugating enzyme UBC9	Ube2i	460
56	4	9.3	73.417	25.416	22.096	18.887	2.573	4.757	A0A0R4J0G0; Q8BH04	A0A0R4J0G0; Q8BH04	Phosphoenolpyruvate carboxykinase [GTP], mitochondrial	Pck2	82
57	5	10.1	95.832	32.072	22.125	19.168	1.081	4.652	P56399; Q3U4W8; D3YYA5	P56399; Q3U4W8	Ubiquitin carboxyl-terminal hydrolase 5; Ubiquitin carboxyl-terminal hydrolase	Usp5	768
58	2	1.5	123.55	11.881	17.128	15.968	1.600	4.615	B7ZC27; Q99FV0	B7ZC27; Q99FV0	Pre-mRNA-processing-splicing factor 8	Prpf8	216
59	2	17.8	14.866	15.591	18.485	17.185	1.166	4.531	P16045	P16045	Galactin-1	Lgals1	619
60	9	31.1	50.648	70.48	25.037	21.429	1.072	4.502	E9Q1G8; E9Q9F5; O55131	E9Q1G8; E9Q9F5; O55131	Septin-7	Sept7	368

Part 2 - TBX2 target genes and interaction partners

	A	B	C	D	E	F	G	H	I	J	K	L	M	N	O	P	Q	R	S
61	-0.324	-0.525	-0.455	-6.179	-1.544	-7.067	17.023	21.659	16.136	17.708	17.507	17.577	24.251	22.155	21.811	14.253		3	3
62	0.845	5.395	5.406	-2.200	0.218	0.142	15.129	17.547	17.472	16.612	21.163	21.174	18.433	16.225	16.997	14.538		2	2
63	5.086	3.842	3.630	-0.990	-0.577	0.749	16.089	16.502	17.828	21.310	20.066	19.854	17.807	16.351	17.255	15.193	+	1	1
64	2.904	-2.194	-3.022	-1.918	-7.006	-6.754	23.027	17.939	18.190	22.842	17.743	16.916	27.214	22.675	24.428	15.447		5	5
65	-2.333	2.740	2.452	-3.607	-2.046	-4.806	17.938	19.499	16.739	16.526	21.598	21.311	22.822	20.268	22.229	15.488		1	1
66	-0.633	4.488	3.195	-1.601	-1.939	-2.666	17.641	17.303	16.576	19.417	24.539	23.246	18.796	19.687	24.964	15.137	+	11	11
67	5.335	11.185	8.667	2.847	3.953	5.142	20.188	21.295	22.483	20.951	26.800	24.282	18.818	15.864	16.507	14.723		18	18
68	-1.598	-1.573	-0.248	-6.819	-8.749	-1.084	18.131	16.200	23.865	22.277	22.302	23.627	29.373	20.526	23.597	24.153		10	10
69	1.862	-1.130	2.858	-6.917	-1.521	-1.187	15.687	21.083	21.417	20.463	17.471	21.459	23.912	21.296	22.761	14.441		5	5
70	-1.974	2.639	2.770	-3.995	-3.459	-2.001	15.503	16.039	17.497	16.979	21.792	21.723	19.034	19.962	23.390	14.516		4	4
71	-0.158	5.100	4.336	-1.882	-2.038	0.132	17.036	16.879	19.049	15.774	21.032	20.268	23.076	14.759	16.856	15.008		2	2
72	-4.048	2.002	-3.069	-6.203	-5.250	-6.700	17.471	18.424	16.974	16.205	22.255	17.184	23.113	24.235	24.514	15.992		8	7
73	0.088	4.931	5.361	-1.151	-0.795	-0.703	17.079	17.434	17.527	15.773	20.616	21.046	21.349	15.110	16.941	14.429		3	3
74	-0.541	1.255	0.531	-2.360	-3.998	-5.386	18.922	17.284	15.896	20.694	22.491	21.767	22.907	19.657	23.179	19.292	+	5	5
75	-3.526	-8.602	-3.341	-8.865	-9.321	-10.209	18.160	17.704	16.815	22.461	17.385	22.646	29.542	24.508	26.543	25.431		2	2
76	-2.389	5.418	2.925	-4.427	-4.164	1.730	16.791	17.063	22.947	16.687	24.494	22.000	18.740	23.695	24.729	13.422		8	8
77	4.044	4.474	2.503	-1.153	-1.018	0.434	16.543	16.678	18.130	22.437	22.866	20.896	19.439	15.953	18.261	18.525	+	3	3
78	3.253	6.421	4.710	-3.069	2.192	2.518	16.798	22.059	22.395	21.601	24.769	23.058	18.053	21.681	22.418	14.278		6	6
79	6.816	6.262	5.473	4.531	2.104	-0.711	28.142	25.715	22.900	27.258	26.704	25.916	21.902	25.320	24.623	16.262		7	5
80	-2.829	3.952	1.335	-2.134	-1.189	-6.761	21.003	21.949	16.376	17.590	24.371	21.755	24.730	21.545	25.176	15.663		6	6
81	-2.749	3.247	3.740	-5.090	-3.274	0.084	17.241	19.057	22.415	16.459	22.455	22.948	24.821	19.841	23.118	15.299		1	1
82	-4.936	1.262	1.751	-6.022	-3.453	-4.870	19.340	21.909	20.492	15.301	21.499	21.987	25.767	24.956	25.159	15.314		12	12
83	-2.269	2.513	1.749	-2.827	-3.478	-4.067	18.237	17.586	16.997	17.103	21.885	21.121	25.353	16.775	18.314	20.430		5	2
84	-2.755	5.320	2.020	-5.414	-1.396	-0.951	16.957	20.975	21.419	16.244	24.320	21.020	19.125	25.615	23.351	14.647		9	9
85	6.572	5.900	1.509	2.537	-0.925	0.144	19.206	15.744	16.813	22.967	22.295	17.904	17.752	15.587	17.733	15.057		2	2
86	13.176	11.360	10.139	10.040	9.647	2.785	29.665	29.272	22.410	29.353	27.537	26.316	19.812	19.439	18.807	13.546		5	5
87	1.109	6.756	7.886	0.391	-0.037	3.218	17.734	17.306	20.561	16.525	22.173	23.303	18.008	16.678	16.756	14.078		3	3
88	-0.103	8.432	5.296	0.479	0.971	0.035	17.311	17.802	16.867	15.762	24.297	21.161	18.356	15.308	17.574	14.155		3	3
89	-1.315	3.962	3.101	-3.307	-2.361	-0.649	16.152	17.088	18.810	17.973	23.250	22.389	18.343	20.575	23.457	15.119		11	2

Part 2 - TBX2 target genes and interaction partners

	T	U	V	W	X	Y	Z	AA	AB	AC	AD	AE	AF
61	3	22.3	17.263	17.354	23.203	18.032	1.232	4.495	G3UJ4:H3B:Q7,P99029-2,P99029	G3UJ4:H3B:Q7,P99029-2,P99029	Peroxisome assembly factor 3	Prdx5	462
62	2	5.8	58.841	12.432	17.329	15.768	1.232	4.495	Q9D554	Q9D554	Splicing factor 3A subunit 3	Sf3a3	1436
63	1	0.4	230.99	6.279	17.079	16.224	2.521	4.459	K3W4L0:B2RRE2;E9QAX2;Q9JMH9-9-4;Q9JMH9-1;Q9JMH9-1;Q9JMH9-6	K3W4L0:B2RRE2;E9QAX2;Q9JMH9-9-4;Q9JMH9-1;Q9JMH9-1;Q9JMH9-6	Unconventional myosin-XVIIia	Myo18a	208
64	5	10	67.277	34.547	24.944	19.938	0.831	4.465	P35564	P35564	Calnexin	Canx	684
65	1	12.8	10.102	6.3729	21.545	18.858	1.142	4.439	G6E919;F7CDT0;F6WMC0;P61082	G6E919;F7CDT0;F6WMC0;P61082	NEDD8-conjugating enzyme Ubc12	Ube2m	423
66	8	7.7	172.79	72.374	19.242	20.051	1.318	4.419	Q01320	Q01320	DNA topoisomerase 2-alpha	Top2a	920
67	18	15.1	152.04	214.91	17.341	15.615	1.141	4.415	Q7TPV4	Q7TPV4	Myb-binding protein 1A	Mybbp1a	1122
68	5	68.4	15.748	285.38	24.950	23.875	0.876	4.411	ABDUK4;EQ223;CON_P02070	ABDUK4;EQ223	Beta-globin	Hbbt1;Hbb-bs	190
69	5	10.9	67.314	31.284	22.604	18.601	0.932	4.405	P61222	P61222	ATP-binding cassette sub-family E member 1	Abce1	795
70	4	14.1	43.062	24.608	19.498	18.953	1.206	4.363	Q9CXV6	Q9CXV6	Interleukin enhancer-binding factor 2	Ilf2	1383
71	2	10	28.463	12.467	18.917	15.932	1.149	4.355	O88456;A0A0R4IZW8;A0A0R4J1C2	O88456;A0A0R4IZW8;A0A0R4J1C2	Calpain small subunit 1	Capns1	75
72	7	16	61.447	43.267	23.674	20.253	1.062	4.346	A2AJ72;Q3TX6;A0A0A6YV5;FTA	A2AJ72;Q3TX6;A0A0A6YV5	Far upstream element (FUSE)-binding protein 3	Fubp3	153
73	3	17	15.137	18.748	18.230	15.685	1.203	4.343	Q05816	Q05816	Fatty acid-binding protein, epidermal	Fabp5	934
74	3	16.5	37.186	38.734	21.282	21.235	1.881	4.330	P62141;A0A0J9YU8;A0A0J9YU8	P62141;A0A0J9YU8	Serine/threonine-protein phosphatase PP1-beta catalytic subunit	Ppp1cb	809
75	2	28.9	11.433	16.596	27.025	25.987	1.146	4.309	EQ3T0;P47955	EQ3T0;P47955	60S acidic ribosomal protein P1	Gm10073;Rplp1	377
76	8	9.9	122.78	58.529	21.217	19.076	0.629	4.271	Q3UNM4;P07496-2;P97466;Q3UID0;Q6PDG5-2;Q8PDG5;Q3UZD0	Q3UNM4;P07496-2;P97466;Q3UID0;Q6PDG5-2;Q8PDG5	SWI/SNF complex subunit SMARCC1;SWI/SNF complex subunit SMARCC2	Smarcc1;Smarrcc2	908
77	3	12.2	41.81	19.123	17.696	18.393	2.250	4.253	Q925F2;D3Z5Y0	Q925F2	Endothelial cell-selective adhesion molecule	Esam	1288
78	5	17.4	39.025	47.396	19.867	18.348	0.981	4.247	Q3TWW8;A0A0A6YXX6	Q3TWW8	Serine/arginine-rich splicing factor 6	Srsf6	958
79	5	56.2	13.509	72.166	23.611	20.443	1.263	4.209	Q3THW5;P0C0S6;Q8R029;Q3UA9	Q3THW5;P0C0S6;Q8R029;Q3UA9	Histone H2A.V;Histone H2A.Z;Histone H2A	H2afv;H2afz	584
80	6	5.7	136.33	71.316	23.138	20.419	0.731	4.181	Q6ZQ38;D3YWC5	Q6ZQ38	Cullin-associated NEDD8-dissociated protein 1	Cand1	1106
81	1	4.3	31.2	7.1701	22.331	19.208	0.743	4.172	D3Z0U5;D6RGM7;D3Z4J2;A0A0G2J	D3Z0U5;D6RGM7;D3Z4J2;A0A0G2J	Katanin p60 ATPase-containing subunit A-like 2;Spermatogenesis-associated protein 5	Katnal2;Spat	27
82	12	10.9	161.93	78.691	25.361	20.236	0.844	4.141	FY0;A0A0A0M0Q80;Q9D3R6-3;Q9D3R6;Q3UWC0	FY0;A0A0A0M0Q80;Q9D3R6-3;Q9D3R6;Q3UWC0	Eukaryotic translation initiation factor 3 subunit A	Eif3a	647
83	2	46.3	15.878	17.375	21.064	19.372	1.268	4.122	P02089	P02089	Hemoglobin subunit beta-2	Hbb-b2	555
84	6	14.9	70.887	117.32	22.370	18.999	0.683	4.115	Q8VHM5;F7B5B5;A2AW41	Q8VHM5;F7B5B5;A2AW41	Heterogeneous nuclear ribonucleoprotein R	HnmpR	429
85	2	2.5	84.185	12.638	16.669	16.395	1.012	4.075	Q8Z1P7;G3UXN4;Q6P8V1	Q8Z1P7;G3UXN4;Q6P8V1	KN motif and ankyrin repeat domain-containing protein 3	Kank3	456
86	5	24.6	13.916	42.384	19.625	16.177	0.742	4.068	P62320	P62320	Small nuclear ribonucleoprotein Sm D3	Smrpd3	823
87	2	27.6	12.678	30.082	17.343	15.417	0.805	4.060	A0A140T8Q1;P01635;A0A140T8P6	A0A140T8Q1;P01635	Ig kappa chain V-V region K2	Igkv12-41	117
88	3	12.2	33.828	24.254	16.832	15.865	0.740	4.047	F7AA45;E9Q8F0;Q8VH51-3;Q8VH51-2;Q8VH51;B7ZD63;B7ZD61	F7AA45;E9Q8F0;Q8VH51-3;Q8VH51-2;Q8VH51;B7ZD63;B7ZD61	RNA-binding protein 39	Rbm39	398
89	2	20.6	49.067	14.684	19.459	19.288	1.044	4.022	Q8VDW0;D6RHT5;G3UXI6;Q8VDW0-2	Q8VDW0	ATP-dependent RNA helicase DDX39A	Ddx39a	1255

Part 2 - TBX2 target genes and interaction partners

	A	B	C	D	E	F	G	H	I	J	K	L	M	N	O	P	Q	R	S
90	1.052	3.100	2.145	-2.380	-1.338	-2.028	17.036	18.078	17.388	19.581	21.629	20.673	18.500	20.332	21.401	15.666	+	2	2
91	-0.826	-4.244	-1.400	-6.517	-5.555	-6.163	17.004	17.966	17.358	20.952	17.535	20.378	25.360	21.681	23.823	19.735	+	9	9
92	-1.044	0.320	0.340	-3.436	-7.041	-1.433	20.041	18.435	22.044	21.471	22.835	22.854	25.054	21.899	23.456	21.574		9	7
93	3.583	2.917	-0.869	-1.171	-3.242	-1.430	16.242	14.171	15.983	20.351	19.685	15.899	17.956	16.870	17.524	16.013		2	2
94	-2.644	1.727	1.912	-4.389	-5.872	-0.192	18.425	16.943	22.623	16.962	21.334	21.519	25.801	19.828	22.780	16.433		5	5
95	-0.898	-0.631	-2.027	-8.868	-4.175	-1.947	17.058	21.751	23.979	23.213	23.480	22.084	28.202	23.651	26.397	21.825		9	9
96	0.794	5.349	2.666	-3.794	-0.424	1.697	17.576	20.947	23.067	21.563	26.118	23.435	18.190	24.551	25.527	16.011		7	7
97																			
98	2.168	6.354	5.025	0.702	0.334	1.240	23.916	23.548	24.454	22.203	26.389	25.060	20.469	25.958	25.673	14.396	+	17	17
99	4.175	4.491	3.443	0.959	0.651	-0.756	18.021	17.712	16.305	20.737	21.052	20.004	18.616	15.508	18.352	14.770	+	1	1
100	-2.587	2.650	2.371	-5.833	-4.405	1.458	15.104	16.532	22.395	16.807	22.044	21.766	23.356	18.517	20.437	18.352		3	1
101	-2.984	4.908	4.064	-3.356	-4.043	2.206	17.523	16.836	23.085	16.869	24.742	23.897	25.329	16.429	24.411	15.256		8	8
102	2.075	4.819	2.811	0.789	-3.663	1.384	22.122	17.671	22.718	21.616	24.360	22.352	18.864	23.803	23.096	15.986		12	12
103	1.462	5.184	3.722	-0.648	-0.583	0.447	16.662	16.728	17.757	17.994	21.716	20.254	17.929	16.692	17.181	15.883	+	1	1
104	-4.206	5.710	2.728	0.738	-3.353	-4.165	22.064	17.973	17.161	14.756	24.672	21.690	24.487	18.165	22.506	15.418		6	6
105	-7.743	-0.929	-1.280	-8.464	-5.173	-7.264	15.507	18.798	16.707	16.313	23.128	22.777	27.021	20.920	26.174	21.939		6	6
106	4.917	5.089	2.493	0.571	3.252	-2.238	18.872	21.563	16.063	24.237	24.409	21.814	21.207	15.395	19.164	19.478		11	11
107	4.038	7.760	6.305	2.534	2.300	2.392	24.323	24.089	24.181	22.950	26.672	25.217	22.234	21.344	23.905	13.919	+	9	9
108	-0.289	-0.397	-0.769	-3.761	-3.259	-5.306	16.928	17.429	15.383	20.771	20.663	20.291	21.346	20.030	21.234	20.888	+	3	3
109	1.531	2.031	1.972	0.373	-3.731	-1.952	22.218	18.114	19.893	22.038	22.538	22.479	24.169	19.521	22.578	18.437	+	5	5
110	-5.231	1.033	0.481	-5.935	-5.521	-3.102	17.774	18.188	20.608	16.696	22.961	22.409	26.715	20.703	25.135	18.720		11	11
111	-1.218	-0.315	0.460	-3.512	-4.378	-3.932	18.185	17.319	17.766	17.687	18.591	19.365	24.253	19.142	17.780	20.031	+	5	5
112	-2.359	0.233	-1.284	-5.918	-6.743	-1.452	17.271	16.446	21.738	20.144	22.735	21.219	24.591	21.788	23.980	21.025		4	4
113	3.501	2.879	2.870	0.377	-0.976	-0.841	17.507	16.154	16.288	20.377	19.754	19.745	18.048	16.211	18.752	15.000	+	1	1
114	-3.513	0.831	2.176	-6.149	-3.026	-1.901	16.941	20.064	21.189	15.776	20.220	21.465	23.452	22.729	24.783	13.784		6	6
115	-1.216	-5.822	-0.541	-3.232	-5.726	-9.274	23.551	21.058	17.510	22.604	17.998	23.278	26.437	27.130	26.255	21.384		5	5
115	6.342	8.637	6.627	5.426	4.776	0.677	22.205	21.555	17.456	22.208	24.403	22.493	17.319	16.238	17.154	14.578		2	2

Part 2 - TBX2 target genes and interaction partners

	T	U	V	W	X	Y	Z	AA	AB	AC	AD	AE	AF
90	2	11	32,646	14,824	19,416	18,528	2,418	4,014	E9Q715;Q05GXS;Q7TNC4-2;Q7TNC4-3;Q7TNC4-4;Q7TNC4-4;Q7TNC4-4;Q7TNC4-4	E9Q715;Q05GXS;Q7TNC4-2;Q7TNC4-3;Q7TNC4-4;Q7TNC4-4;Q7TNC4-4;Q7TNC4-4	Putative RNA-binding protein Luc7-like 2	Luc7I2	390
91	9	24	57,147	58,539	23,521	21,779	1,638	3,821	Q922B2;Q8BJY7	Q922B2	Aspartate--tRNA ligase, cytoplasmic	Dars	1282
92	5	40.7	28,086	75,46	23,476	22,515	1,060	3,842	Q9COV8;Q9COV8-2;A2A5N1;Q70456	Q9COV8;Q9COV8-2;A2A5N1	14-3-3 protein beta(alpha), 14-3-3 protein beta(alpha), N-terminally processed	Ywhab	1357
93	2	2.6	108,85	12,312	17,413	16,768	1,174	3,825	V9GWT6;V9GXH3;V9GXFO;V9GXFP;V9GXGXP;8;F8VPM7;Q99M11-4;Q99M11-2;Q99M11-2;Q99M11-2	V9GWT6;V9GXH3;V9GXFO;V9GXFP;V9GXGXP;8;F8VPM7;Q99M11-4;Q99M11-2;Q99M11-2;Q99M11-2	ELKS/Rab6-interacting/CAST family member 1	Erc1	433
94	5	28.9	16,924	30,636	22,815	19,607	0,778	3,816	Q3UY29;EQQ3P9;F8WGS1;P62492;P46638;G3UZD3;G3UZL4	Q3UY29;EQQ3P9;F8WGS1;P62492;P46638;G3UZD3;G3UZL4	Ras-related protein Rab-11A;Ras-related protein Rab-11B	Rab11b;Rab11a	376
95	3	23.8	32,931	65,133	25,926	24,111	0,850	3,811	P51881	P51881	ADP(ATP) translocase 2, ADP(ATP) translocase 2, N-terminally processed	Slc25a5	746
96	6	33.9	20,811	58,39	21,370	20,769	0,845	3,777	Q9DCC5;P23198;D3Z1;A9;D3Z313	Q9DCC5;P23198;D3Z1;A9;D3Z313	Chromobox protein homolog 3	Cbx3	648
97	14	29.9	67,443	125,55	23,214	20,035	1,388	3,757	Q3TUE1;A0A0G2JGWB;A0A0G2JFY5;Q3UUU2;Q91WJ8;Q91WJ8-2;A0A0G2JG00;A0A0G2JFK2;A0A0G2JGV9;A0A0G2JG96	Q3TUE1;A0A0G2JGWB;A0A0G2JFY5;Q3UUU2;Q91WJ8;Q91WJ8-2;A0A0G2JG00;A0A0G2JFK2;A0A0G2JGV9;A0A0G2JG96	Far upstream element-binding protein 1	Fubp1	50
98	1	8.1	14,098	6,703	17,062	16,561	2,444	3,752	Q9D937	Q9D937	Uncharacterized protein C11orf98 homolog	Fubp1	1454
99	1	22.8	20,396	9,0413	20,937	19,395	0,596	3,738	P61750;E9Q788;F6UFB9	P61750;E9Q788	ADP-ribosylation factor 4	Arf4	799
100	8	25.1	24,923	51,534	20,879	19,833	0,514	3,734	A2BE93;Q9EQU5-2;Q9EQU5;A2BE92;Q9EQU5-3	A2BE93;Q9EQU5-2;Q9EQU5;A2BE92	Protein SET	Set	180
101	12	12.3	135,55	80,654	21,334	19,541	0,976	3,732	Q921M3;Q921M3-2	Q921M3;Q921M3-2	Splicing factor 3B subunit 3	Sf3b3	1280
102	1	18.2	7,9577	6,3556	17,311	16,532	1,509	3,717	Q4FK66-2;Q4FK66	Q4FK66-2;Q4FK66	Pre-mRNA-splicing factor 38A	Ppfp38a	996
103	6	30.3	28,785	37,604	21,326	18,962	0,483	3,671	P17918;A0A140T8V5	P17918;A0A140T8V5	Proliferating cell nuclear antigen	Pcna	630
104	6	12.6	47,436	52,727	23,971	24,057	0,688	3,649	H2;G3UZ28;G3UY4;G3UZ33;G3UYL3	Q8BG32;G3UXL5;G3UWW7;G3UYH2;G3UZ28;G3UY4;G3UZ33;G3UYL3	26S proteasome non-ATPase regulatory subunit 11	Psmd11	1142
105	11	10.1	131,28	66,913	18,301	19,321	0,950	3,638	Q9Z0U1;Q921G9;Q9QXY1	Q9Z0U1	Tight junction protein ZO-2	Tjp2	1555
106	8	29.1	32,754	64,793	21,789	18,912	1,541	3,626	Q60668-3;Q60668;F6ZV59;G5E8G0;G3X9W0;Q60668-4;Q60668-2;E9Q5B6;Q60668-4;Q60668-2;E9Q5B6	Q60668-3;Q60668;F6ZV59;G5E8G0;G3X9W0;Q60668-4;Q60668-2;E9Q5B6;Q60668-4;Q60668-2;E9Q5B6	Heterogeneous nuclear ribonucleoprotein D0	Hnmpd	1020
107	3	16.4	39,834	18,854	20,688	21,061	2,337	3,623	Q8BFW7-5;Q8BFW7-4;Q8BFW7	Q8BFW7-5;Q8BFW7-4;Q8BFW7	Lipoma-preferred partner homolog	Lpp	1138
108	5	18	23,432	31,516	21,845	20,507	1,405	3,615	Q3TLP8;P63001;Q05144;A2AC13;P60764	Q3TLP8;P63001;Q05144;A2AC13;P60764	Ras-related C3 botulinum toxin substrate 1;Ras-related C3 botulinum toxin substrate 2	Rac1;Rac2	853
109	11	18.9	94,208	98,543	23,709	21,928	0,759	3,614	Q3UZG2;Q61316	Q3UZG2;Q61316	Heat shock 70 kDa protein 4	Hspa4	966
110	5	24.3	26,468	30,381	21,697	18,906	2,556	3,583	Q8WTP6;Q8WTP6-2;F7BP55	Q8WTP6;Q8WTP6-2	Adenylate kinase 2, mitochondrial, N-terminally processed	Ak2	1537
111	4	19.3	27,763	38,311	23,190	22,502	0,922	3,568	H3BK43;H3BLJ6;H3BLJ6;Q9ROP3;H3BJC6;H3BJP2;H3BK16;H3BL99;3BJC6;H3BJP2;H3BK46	H3BK43;H3BLJ6;H3BLJ6;Q9ROP3;H3BJC6;H3BJP2;H3BK16;H3BL99;3BJC6;H3BJP2;H3BK46	S-tryptophanase hydrolase	Esd	480
112	1	2.6	46,795	6,7267	17,130	16,876	2,760	3,563	Q5NDS2	Q5NDS2	rRNA methyltransferase 3, mitochondrial	Rnmtd1	1002
113	6	16.4	52,866	40,36	23,090	19,289	0,763	3,557	Q8BVQ9;P46471	Q8BVQ9;P46471	26S protease regulatory subunit 7	Psmc2	718
114	5	13.2	40,742	41,076	26,784	23,820	0,667	3,551	Q9CR16	Q9CR16	Peptidyl-prolyl cis-trans isomerase D	Ppid	1362
115	2	11.7	20,151	16,241	16,778	15,866	1,015	3,542	Q8OZM5	Q8OZM5	H1 histone family, member X (H1.10 linker histone)	H1fx	1136

Part 2 - TBX2 target genes and interaction partners

	A	B	C	D	E	F	G	H	I	J	K	L	M	N	O	P	Q	R	S
116	1.770	6.110	2.996	-0.982	2.061	-0.756	16.994	20.038	17.221	20.938	25.278	22.164	18.246	17.707	22.404	15.932		10	10
117	-7.020	-3.290	-1.619	-8.693	-5.050	-8.734	15.961	19.604	15.920	16.587	20.317	21.988	27.280	22.028	24.861	22.553		9	9
118	-1.744	3.592	3.010	-2.882	-3.922	1.165	17.128	16.088	21.175	16.245	21.581	20.999	25.343	14.677	18.314	17.665		4	4
119	-5.060	-0.560	-0.565	-7.185	-2.787	-6.702	17.089	21.487	17.571	17.297	21.797	21.792	25.353	23.195	23.853	21.061		6	6
120	2.027	4.568	4.203	1.607	3.469	-4.743	21.320	23.183	14.970	20.749	23.291	22.926	24.028	15.399	22.968	14.477		4	4
121	1.345	1.286	-3.633	-1.527	-2.251	-7.667	23.478	22.754	17.337	22.138	22.078	17.159	26.154	23.855	25.143	16.443		4	4
122	-4.632	-0.495	-2.359	-7.667	-8.469	-1.616	17.597	16.795	23.648	19.732	23.869	22.006	27.220	23.307	25.165	23.563		3	3
123	-0.213	7.769	4.223	0.572	0.313	0.685	16.968	16.710	17.082	15.925	23.907	20.361	17.129	15.664	17.007	15.268		4	4
124	-0.109	7.007	5.979	0.259	1.764	0.651	17.224	18.729	17.616	16.118	23.234	22.206	17.733	16.197	17.059	15.396		4	2
125	1.096	1.023	-3.391	-3.545	-3.186	-4.689	17.081	17.440	15.937	20.474	20.402	15.987	19.199	22.052	21.163	17.593		3	3
126	0.529	6.207	4.120	-0.597	2.903	-1.552	16.227	19.728	15.273	16.902	22.580	20.493	18.676	14.973	17.865	14.881		3	3
127	-2.519	2.789	-2.721	-3.194	-4.933	-4.408	18.366	16.627	17.152	15.845	21.153	15.643	23.307	19.813	22.489	14.239		2	2
128	0.953	11.255	9.212	4.743	0.740	5.884	21.400	17.397	22.541	15.516	25.818	23.776	19.089	14.226	16.737	12.390		10	10
129	6.036	7.233	6.240	4.236	1.795	3.453	21.561	19.119	20.777	23.830	25.027	24.034	19.371	15.278	20.604	14.983	+	9	9
130	3.791	6.003	4.801	1.998	1.121	1.500	23.802	22.925	23.304	23.096	25.308	24.106	24.266	19.342	24.619	13.991	+	13	13
131																			
132	3.017	4.902	2.969	-0.659	3.663	-1.988	18.012	22.334	16.683	22.216	24.101	22.167	22.181	15.161	23.519	14.878		9	9
133	14.147	13.302	12.958	9.852	10.753	9.944	33.962	34.864	34.055	33.984	33.139	32.794	24.988	23.234	18.277	21.397	+	1	1
134	4.356	3.588	3.341	-0.755	0.872	1.341	16.127	17.753	18.222	21.002	20.234	19.987	17.873	15.889	18.077	15.216	+	4	4
135	1.588	0.915	-0.249	-3.742	-1.803	-2.022	23.255	25.194	24.975	27.150	26.476	25.313	28.254	25.740	27.264	23.858	+	49	49
136	-4.857	0.757	-0.166	-2.336	-5.708	-6.041	20.659	17.287	16.954	17.027	22.640	21.717	24.768	21.231	23.530	20.236		5	5
137	2.227	6.053	4.256	-3.318	3.379	2.681	16.067	22.764	22.066	21.397	25.222	23.425	17.812	20.957	22.839	15.500		9	9
137	2.604	4.253	2.906	-0.634	0.003	0.618	17.091	17.728	18.343	20.025	21.675	20.328	19.397	16.052	20.759	14.084	+	1	1

	T	U	V	W	X	Y	Z	AA	AB	AC	AD	AE	AF
116	10	19.2	68.578	62.1	17.977	19.168	1.019	3.518	AOA0G2JG10;Q497W9;O35286;AOA0G2JG5;Q05BH3;G5X8X0;AZA4N9/AZA4FP	AOA0G2JG10;Q497W9;O35286	Pre-mRNA-splicing factor ATP-dependent RNA helicase DHX15	Dhx15	51
117	9	43.5	27.623	122.24	24.654	23.607	0.809	3.516	Q8DCV4;AOA0U1RQB4;AOA0U1RNG;AOA0N4SVE0;AOA0U1RNR3;AOA0U1RNP5;AOA0N4SWE9	Q8DCV4;AOA0U1RQB4;AOA0U1RNK3;AOA0N4SVE0;AOA0U1RNR3;AOA0U1RNP5;AOA0N4SWE9	Electron transfer flavoprotein subunit beta Retinol-binding protein 1	Etfb Rbp1	1479 918
118	4	34.1	15.846	27.629	20.010	17.989	0.695	3.499	Q00915	Q00915	Electron transfer flavoprotein subunit beta Retinol-binding protein 1	Rbp1	918
119	6	9.3	63.53	39.919	24.274	22.357	0.789	3.496	P46061	P46061	Ran GTPase-activating protein 1	Rangap1	716
120	4	3.4	182.29	31.073	19.714	18.723	0.598	3.488	EQQPX1;P39061-2;P39061-1;P39061-1;P39061-1	EQQPX1;P39061-2;P39061-1;P39061-1;P39061-1	Collagen alpha-1(XVII) chain;Endostatin Thioresoxin	Col18a1 Txn1	413 590
121	4	38.1	11.675	53.999	25.005	20.793	0.614	3.481	P10639	P10639	Thioresoxin	Txn1	590
122	3	68.2	5.0256	34.496	25.264	24.364	0.623	3.422	Q8ZVW8;AOA0N4SVF0	Q8ZVW8;AOA0N4SVF0	Thymosin beta-10	Tmsb10	1113
123	4	3.8	138.55	25.719	16.396	16.138	0.668	3.403	H3BL37;O08784;Q05CS0;H3BIX0	H3BL37;O08784;Q05CS0;H3BIX0	Treacle protein	Tcof1	484
124	2	12.1	36.983	15.72	16.965	16.227	0.682	3.401	P63087;P63087-2;AOA0G2JFF1;AOA0G2JGC1	P63087;P63087-2;AOA0G2JFF1;AOA0G2JGC1	Serine/threonine-protein phosphatase PPI-gamma catalytic subunit	Ppp1cc	860
125	3	15.8	25.352	17.467	20.626	19.378	1.024	3.382	Q8C266;P35278;A2A5F6;A2A5F5;Q8CQD1;P61021	Q8C266;P35278	Ras-related protein Rab-5C	Rab5c	689
126	3	11.2	37.048	20.103	16.825	16.373	0.719	3.367	D9JZV6;P41778-2;P41778;G3UXL9;Q3UR63;V9GXB8;O35317-2;O35984;O36317	D9JZV6;P41778-2;P41778	Pre-B-cell leukemia transcription factor 1	Pbx1	320
127	2	5.9	56.55	16.903	21.560	18.364	0.831	3.361	P62814	P62814	V-type proton ATPase subunit B, brain isoform	Atp6v1b2	831
128	10	13.4	112.72	60.847	16.657	14.563	0.404	3.351	Q921K2;P11103-2;P11103	Q921K2;P11103-2;P11103	Poly [ADP-ribose] polymerase 1	Parp1	1279
129	9	19.4	55.249	57.431	17.324	17.794	1.839	3.342	Q99LF4	Q99LF4	RNA-splicing ligase RtcB homolog	Rtcb	1309
130	13	26.9	47.688	85.957	21.804	19.305	2.073	3.325	P50247;AZALT5	P50247	Adenosylhomocysteinase	Ahey	738
131									P11440;D3Z2T9;P97377-2;Q80YP0;P97377;Q04735-2;E9PYC7;E3W997;Q3V3A1;Q14AX6;Q14AX6-3;Q69ZA1-2;Q14AX6-2;Q8K0D0;Q04735;O35495;Q3V3A1-3;Q04889;AOA0G2JDL3;Q99J95-3;Q8K0D0-2;O35495-2;Q99J95;O35495-3;Q64261;Q99J95-2;P49515;Q69ZA1	P11440;D3Z2T9	Cyclin-dependent kinase 1	Cdk1	597
132	1	0.6	135.87	7.9036	24.111	19.837	2.711	3.286	AOA087WS76;AOA140LHL6;EQQ3S4	AOA087WS76;AOA140LHL6;EQQ3S4	Mitogen-activated protein kinase kinase 19	Map3k19	24
133	2	27.1	20.697	27.438	16.881	16.646	2.015	3.276	P84078;P61205;Q8BSL7;P84084;3YU25;EQ02C2;A2A6T9	P84078;P61205;Q8BSL7;P84084	ADP-ribosylation factor 1;ADP-ribosylation factor 3;ADP-ribosylation factor 2;ADP-ribosylation factor 5	Arf1;Arf3;Arf2;Arf5	794
134	49	25.2	269.82	323.31	26.997	25.561	1.799	3.274	P26039;AZAIM2;E9PUM4;Q71LX4;F6S1V7;F6SX70	P26039	Talin-1	Tin1	657
135	5	20.4	33.081	35.76	22.995	21.883	0.711	3.273	D3YU12;Q8K2T1;G5E8S7;Q8K2T1-2;Q8K2T1-3	D3YU12;Q8K2T1;G5E8S7;Q8K2T1-2;Q8K2T1-3	NmIA-like family domain-containing protein 1	Nmral1	276
136	9	16.7	69.448	60.966	19.385	19.169	0.612	3.265	Q8C2Q3;EQ9L19;Q8C2Q3-2	Q8C2Q3;EQ9L19;Q8C2Q3-2	RNA-binding protein 14	Rbm14	1193
137	1	3.2	46.638	8.0052	17.725	17.421	2.196	3.259	O54941	O54941	SWI/SNF-related matrix-associated actin-dependent regulator of chromatin subfamily E member 1	Smarca1	524

Part 2 - TBX2 target genes and interaction partners

	A	B	C	D	E	F	G	H	I	J	K	L	M	N	O	P	Q	R	S
138	-1.607	1.341	0.044	-5.382	-3.726	-0.724	17.585	19.241	22.243	19.830	22.778	21.481	25.274	20.660	24.269	18.605		9	9
139	-4.135	-2.536	0.964	-6.392	-2.203	-6.890	16.952	21.140	16.654	16.402	18.000	21.501	24.324	22.363	25.328	15.745		6	6
140	5.762	5.105	5.542	1.817	3.349	1.774	26.147	27.680	26.105	25.668	25.011	25.448	25.508	23.154	25.454	14.357	+	7	7
141	-4.548	5.514	2.344	-3.538	-3.447	0.907	16.711	16.802	21.156	15.505	25.566	22.397	18.640	21.857	23.552	16.553		10	10
142	2.935	6.518	5.955	2.650	1.496	1.884	23.974	22.820	23.208	22.877	26.461	25.898	17.391	25.258	26.952	12.934		9	9
143	0.068	6.452	4.138	-3.109	2.477	1.969	17.188	22.775	22.287	19.410	25.794	23.480	18.643	21.952	24.466	14.218		12	12
144	-1.738	5.185	4.747	0.645	-0.538	-1.210	18.836	17.653	16.981	15.371	22.294	21.857	20.113	16.269	18.227	15.992		2	2
145	-0.559	4.400	3.525	-1.318	1.162	-1.745	17.049	19.529	16.623	15.676	20.635	19.760	22.349	14.387	17.833	14.637		3	3
146	1.758	4.886	3.318	-6.322	5.135	1.927	15.878	27.334	24.127	23.603	26.730	25.162	17.682	26.717	26.757	16.932		18	18
147	-1.522	5.324	4.050	-0.857	-0.265	-0.217	16.334	16.926	16.974	16.397	23.243	21.969	19.242	15.140	20.611	15.227		1	1
148	-1.452	-2.115	-1.768	-7.030	-2.544	-4.908	17.787	22.273	19.908	22.337	21.674	22.021	25.905	23.728	24.483	23.096		11	11
149	-0.917	-0.480	0.570	-3.923	-3.080	-2.824	24.294	25.137	25.393	23.879	24.316	25.365	29.149	27.286	27.972	21.619	+	21	21
150	0.387	-2.806	-3.869	-4.839	-5.327	-4.920	17.258	16.770	17.178	20.371	17.179	16.316	24.116	20.079	19.395	20.575		4	4
151	-1.347	1.109	2.305	-1.682	-1.300	-3.948	19.960	20.342	17.678	17.412	19.868	21.064	24.873	18.410	22.746	14.771		7	7
152	-0.697	0.942	0.656	-7.045	-0.494	-0.503	17.864	24.515	24.506	22.794	24.434	24.148	27.073	22.944	26.085	20.898		5	4
153	1.988	2.807	2.048	-1.026	-2.448	1.439	19.005	17.583	21.470	20.775	21.594	20.835	24.207	15.856	23.076	14.499		2	2
154	-2.348	-3.178	-3.551	-3.253	-7.109	-7.438	21.417	17.561	17.232	21.649	20.819	20.446	25.751	23.589	23.882	24.112		9	9
155	-2.841	2.335	1.374	0.529	-4.606	-3.723	21.623	16.488	17.370	17.194	22.370	21.409	21.181	21.006	22.365	17.705		2	2
156	-1.317	4.705	1.697	-4.492	-0.012	0.942	17.541	22.021	22.975	17.878	23.900	20.893	22.533	21.533	23.551	14.840		8	8
157	4.348	7.048	-0.492	4.058	-0.081	-1.674	21.421	17.282	15.689	21.346	24.046	16.507	18.589	16.137	16.792	17.205		2	2
158	6.002	4.198	0.319	0.425	1.472	0.027	16.732	17.780	16.334	22.463	20.659	16.780	16.827	15.788	18.130	14.792		1	1
159	8.402	5.603	5.444	3.903	3.307	3.721	24.089	23.494	23.907	24.644	21.845	21.686	22.482	17.881	16.715	15.769	+	5	5
160	0.325	8.951	4.235	-1.153	4.709	1.454	16.128	21.990	18.736	16.677	25.303	20.587	18.805	15.758	17.500	15.203		13	13
161	2.212	0.168	3.001	-1.532	-0.608	-0.885	23.785	24.709	24.432	25.458	23.414	26.247	27.676	22.958	27.161	19.331	+	5	5
162	8.535	5.888	7.080	5.606	4.509	3.016	29.778	28.681	27.188	29.678	27.031	28.223	26.998	21.347	26.125	16.162		12	12
163	-0.458	4.209	3.156	-0.971	-0.723	0.243	16.090	16.337	17.303	17.325	21.992	20.939	18.817	15.303	20.746	14.821		2	2
164	2.623	2.899	3.096	-1.770	1.572	0.519	19.893	23.235	22.182	23.321	23.597	23.794	18.005	25.321	27.392	14.003	+	8	8
165	-1.320	-2.726	-4.022	-4.129	-8.798	-3.434	21.862	17.183	22.556	23.587	22.181	20.885	27.480	24.501	24.995	24.820		12	12
166	-1.082	7.104	3.955	-0.032	-0.782	2.510	17.089	16.339	19.630	16.818	25.004	21.855	19.405	14.836	21.222	14.978		5	5
167	2.212	3.786	3.382	1.887	-2.176	1.446	21.779	17.717	21.339	21.316	22.890	22.485	24.356	15.429	22.620	15.588		3	3
168	-4.450	4.845	2.343	-4.049	-0.037	-1.389	18.180	22.192	20.840	16.717	26.013	23.511	20.746	23.712	23.722	18.614		10	10
169	-3.030	2.272	-1.710	-0.679	-4.975	-4.920	21.126	16.831	16.886	15.799	21.101	17.119	24.351	19.260	23.119	14.539		4	4
170	-7.308	-2.727	-5.584	-8.241	-7.375	-8.091	16.915	17.782	17.066	16.276	20.856	18.000	26.354	23.959	24.528	22.639		10	10

Part 2 - TBX2 target genes and interaction partners

	T	U	V	W	X	Y	Z	AA	AB	AC	AD	AE	AF
138	9	5	213.61	57.488	22.967	21.437	0.931	3.203	B1B1A8;Q6PDN3-3;Q6PDN3;Q6PDN3-2;Q6PDN3-4	B1B1A8;Q6PDN3-3;Q6PDN3;Q6PDN3-2	Myosin light chain kinase, smooth muscle; Myosin light chain kinase, smooth muscle, deglutamylated form		
139	6	12.7	47.408	36.245	23.343	20.537	0.696	3.193	P54775;A0A140LIZ5	P54775;A0A140LIZ5	26S protease regulatory subunit 6B	Myk	203
140	7	30.1	20.732	54.993	24.331	19.906	2.332	3.156	P62717;F6YIWA4	P62717	60S ribosomal protein L18a	Psmc4 Rpl18a	759 827
141	10	15.5	89.783	77.529	20.249	20.053	0.400	3.129	Q3JUG5;P97311	Q3JUG5;P97311	DNA helicase; DNA replication licensing factor MCM6	Mcm6	898
142	9	27.7	36.21	99.045	21.324	19.943	1.261	3.126	Q20BD0;Q80XR6;Q89020	Q20BD0;Q80XR6;Q89020	Heterogeneous nuclear ribonucleoprotein A/B	Hnrnpab	946
143	12	21	81.21	83.791	20.298	19.342	0.530	3.107	Q81881;D3Z6N3	Q81881	DNA replication licensing factor MCM7	Mcm7	1054
144	2	8	28.721	12.62	18.191	17.109	0.603	3.099	Q9DCC4	Q9DCC4	Pyruvate-5-carboxylate reductase 3	Pycrl	1471
145	3	1	333.73	18.456	18.368	16.235	0.804	3.089	EP9X70;Q60847-2;Q60847-5;Q60847;Q60847-4;Q60847-3	EP9X70;Q60847-2;Q60847-5;Q60847;Q60847-4;Q60847-3	Collagen alpha-1(XI) chain	Col12a1	348
146	14	25.7	69.265	178.59	22.200	21.944	0.364	3.074	Q8BTS0;Q61656;S4R116;B1ARCO;	Q8BTS0;Q61656;S4R116	Probable ATP-dependent RNA helicase DDX5	Ddx5	1045
147	1	2.2	45.854	7.3207	17.191	17.919	0.656	3.063	D3Z5N6;G61103	D3Z5N6;G61103	Zinc finger protein ubi-44	Dpif2	310
148	11	20.7	63.772	77.587	24.816	23.789	1.094	3.049	A2A6U3;Q80UG5-3;Q80UG5;Q80UG5-2;A2A6U5	A2A6U3;Q80UG5-3;Q80UG5;Q80UG5-2;A2A6U5	Septin-9	Sept9	128
149	21	45.4	58.004	240.8	28.217	24.795	2.255	3.000	P80317;Q61390;B1AT05	P80317	T-complex protein 1 subunit zeta	Cct6a	889
150	4	15.3	57.086	26.739	22.097	19.985	1.135	2.999	Q921L6;Q60598	Q921L6;Q60598	Src substrate cortactin	Ctn	1018
151	7	10.8	80.208	45.874	21.642	18.759	1.039	2.999	Q8CQK1	Q8CQK1	Heat shock protein 75 kDa, mitochondrial	Trap1	1347
152	4	17.9	31.052	29.597	25.009	23.492	0.595	2.981	O08807;B1AZS9	O08807;B1AZS9	Peroxisredoxin-4	Prdx4	504
153	2	5.7	49.03	13.825	20.031	18.787	1.193	2.959	Q8BWW3	Q8BWW3	Eukaryotic peptide chain release factor subunit 1	Etrf1	1188
154	9	20.3	72.544	71.86	24.670	23.997	0.981	2.908	AOA0R4JIE3;Q8QXS6-3;Q8QXS6;Q8QXS6-2;F7CPL2	AOA0R4JIE3;Q8QXS6-3;Q8QXS6;Q8QXS6-2	Drebrin	Dbn1	93
155	2	7.3	25.835	12.116	21.094	20.035	0.573	2.889	A2ALF0;A2ALF3;F6TQL3;Q6NZB0;F7CXJ2	A2ALF0;A2ALF3;F6TQL3;Q6NZB0;F7CXJ2	Dnaj homolog subfamily C member 8	Dnajc8	157
156	3	17.8	46.908	62.581	22.033	19.196	0.525	2.882	A2AFJ1;Q60973;A2AFI9;F6U539	A2AFJ1;Q60973;A2AFI9	Histone-binding protein RBBP7	Rbbp7	143
157	2	18.9	14.427	18.674	17.363	16.998	0.441	2.867	P11031	P11031	Activated RNA polymerase II transcriptional coactivator p15	Sub1	595
158	1	6.9	18.376	6.752	16.307	16.461	0.761	2.865	Q9D735	Q9D735	Uncharacterized protein C19orf43 homolog		1442
159	3	32.9	9.2327	41.243	20.186	16.242	1.358	2.839	AOA0G2JDW7;AOA0G2JG29;Q6ZWU9	AOA0G2JDW7;AOA0G2JG29;Q6ZWU9	40S ribosomal protein S27	Rps27	42
160	13	3.8	404.05	82.948	17.282	16.352	0.397	2.834	Q61001	Q61001	Laminin subunit alpha-5	Lama5	1029
161	5	36.2	15.069	33.561	25.317	23.246	1.465	2.801	P62849-2;P62849-3;P62849	P62849-2;P62849-3;P62849	40S ribosomal protein S24	Rps24	836
162	12	50.7	14.865	116.75	24.173	21.143	1.223	2.791	P62830;A2AF8	P62830	60S ribosomal protein L23	Rpl23	834
163	2	2.6	63.413	13.889	17.060	17.783	0.889	2.786	H8BJW3;H8BJU0;Q6NVF9	H8BJW3;H8BJU0;Q6NVF9	Cleavage and polyadenylation specificity factor subunit 6	Cpsf6	477
164	8	28.5	30.53	57.882	21.663	20.698	1.301	2.766	Q9CX86	Q9CX86	Heterogeneous nuclear ribonucleoprotein A0	Hnrnpa0	1380
165	12	35.4	38.676	102.14	25.991	24.907	0.676	2.764	P07356;B0V2N7;B0V2N8;B0V2N5	P07356;B0V2N7;B0V2N8;B0V2N5	Annexin A2; Annexin	Anxa2	569
166	4	21.2	40.092	35.297	17.121	17.900	0.461	2.760	Q8CCK0	Q8CCK0	Core histone macro-H2A.2	H2afy2	1198
167	3	19.6	19.667	19.442	19.893	19.104	0.935	2.741	P59899;Q3TX55;EPVMA7	P59899	Actin-related protein 2/3 complex subunit 4	Arc4	778
168	10	23.7	55.983	66.896	22.229	21.168	0.381	2.737	Q8BK67;A2AWQ2	Q8BK67	Protein RCC2	Rcc2	1168
169	4	16	38.442	25.155	21.805	18.829	0.561	2.702	Q8Z1Z2	Q8Z1Z2	Serine-threonine kinase receptor-associated protein	Strap	1568
170	10	29.4	43.688	66.95	25.157	23.584	0.925	2.696	Q3THS6;AOA0U1RNT6;AOA0U1RNK6;AOA0U1RQ95;Q91X83;AOA0U1RCB0;AOA0U1RPH4	Q3THS6;AOA0U1RNT6;AOA0U1RNK6;AOA0U1RQ95;Q91X83;AOA0U1RCB0;AOA0U1RPH4	S-adenosylmethionine synthase isoform type-2	Mat2a	952

	A	B	C	D	E	F	G	H	I	J	K	L	M	N	O	P	Q	R	S
171	2.932	-2.241	3.382	-0.468	-2.037	-1.418	17.754	16.175	16.794	21.608	16.435	22.058	20.428	15.996	21.983	15.368		2	2
172	-5.369	-3.068	-6.377	-8.062	-7.187	-7.498	17.165	18.040	17.729	17.978	20.278	16.969	27.024	23.430	24.302	22.391		5	5
173	0.828	5.156	4.138	0.777	1.285	0.169	16.741	17.250	16.134	16.648	20.976	19.958	17.434	14.496	17.832	13.807		1	1
174	-3.650	-1.388	-1.464	-5.604	-4.544	-4.237	21.158	22.218	22.525	21.092	23.353	23.277	27.292	26.232	26.910	22.573	+	27	27
175	-5.751	-1.991	0.413	-4.973	-4.941	-5.232	17.099	17.132	16.841	15.221	18.981	21.385	24.173	19.972	24.546	17.399		5	5
176	-0.084	5.276	4.717	-1.116	-0.281	3.496	17.077	17.912	21.688	17.652	23.013	22.454	20.235	16.150	21.134	14.339		1	1
177	-2.689	-3.339	-1.237	-9.591	-4.653	-0.787	18.350	23.288	27.154	24.143	23.493	25.596	31.689	24.193	26.787	26.878		10	10
178	-5.642	-2.016	-1.753	-5.766	-8.296	-3.081	17.830	15.300	20.515	16.838	20.465	20.727	26.482	20.710	24.472	20.488		13	13
179	0.349	4.708	3.084	0.503	-0.036	0.006	17.784	17.245	17.288	17.405	21.764	20.140	18.001	16.561	18.614	15.498		1	1
180	-5.171	0.247	0.061	-5.888	-0.486	-6.136	16.868	22.270	16.620	16.486	21.905	21.719	24.679	20.833	24.938	18.377		8	8
181	4.007	9.795	7.151	5.113	1.893	6.342	23.765	20.545	24.994	22.958	28.746	26.102	19.503	17.802	18.750	19.152		10	10
182	3.252	4.698	-2.014	-2.093	1.573	-1.085	16.825	20.491	17.834	20.913	22.360	15.648	21.444	16.393	20.681	14.642		6	6
183																			
184	-3.128	-1.444	1.257	-0.860	-5.623	-4.363	21.077	16.314	17.575	15.745	17.428	20.130	23.329	20.546	22.862	14.883		7	7
185	-1.336	0.660	-0.267	-6.647	-0.424	-1.370	16.970	23.193	22.247	21.607	23.603	22.676	28.018	19.215	25.743	20.142		12	12
186	-2.329	0.854	-0.546	0.405	-5.187	-4.669	22.003	16.410	16.929	15.685	18.867	17.468	23.140	20.055	20.864	15.163		2	2
187	7.276	9.480	7.865	4.831	6.681	5.689	24.675	26.525	25.533	24.254	26.459	24.844	19.945	19.743	17.567	16.390	+	1	1
188	1.048	1.132	1.462	0.566	-4.153	-0.126	21.577	16.857	20.885	20.516	20.600	20.930	26.262	15.759	24.502	14.434		13	13
189	2.987	7.555	5.810	1.986	2.453	4.584	22.221	22.688	24.820	21.586	26.154	24.409	18.095	22.375	23.424	13.772		8	6
190	-0.946	4.346	3.167	-0.888	-0.190	0.317	16.308	17.006	17.513	15.427	20.718	19.539	18.019	16.373	18.372	14.372		1	1
191	-2.336	3.558	1.898	1.225	-2.587	-2.832	20.786	16.974	16.729	16.193	22.087	20.427	17.333	21.790	21.659	15.398		5	5
192	9.469	9.089	9.106	6.138	7.890	6.383	23.707	25.459	23.952	24.938	24.557	24.575	19.615	15.524	16.403	14.534	+	2	1
193	-6.844	-2.751	-3.049	-5.862	-6.331	-7.689	18.647	18.178	16.810	16.659	20.753	20.455	25.543	23.475	25.169	21.839		3	3
194	0.861	0.416	1.547	-0.032	-2.526	-1.862	24.396	21.902	22.567	24.383	23.938	25.068	26.394	22.463	26.270	20.773	+	10	10
195	-4.931	-0.380	0.164	-6.006	-0.753	-5.624	16.504	21.757	16.885	17.329	21.881	22.425	25.121	19.889	24.478	20.044		13	6
196	-0.632	3.000	2.572	-1.285	-1.374	0.373	16.118	16.029	17.777	16.810	20.442	20.014	18.906	15.901	20.251	14.632		2	2

Part 2 - TBX2 target genes and interaction partners

	A	B	C	D	E	F	G	H	I	J	K	L	M	N	O	P	Q	R	S
196	-1.982	3.432	0.992	1.637	-3.072	-3.345	21.540	16.831	16.559	16.839	22.253	19.813	19.156	20.651	19.949	15.692		5	5
197	-2.222	1.627	2.527	-2.022	-1.943	-1.300	17.484	17.563	18.206	17.028	20.877	21.777	22.608	16.404	23.471	15.029		3	3
198	5.474	8.723	6.792	4.944	4.717	4.134	27.138	26.911	26.328	25.629	28.878	26.947	20.249	24.139	26.107	14.203		41	41
199	-2.484	-3.322	-4.453	-9.204	-3.570	-4.643	16.750	22.383	21.310	22.159	21.321	20.190	26.497	25.410	26.899	22.388		9	9
200	0.240	-2.286	-3.107	-3.879	-5.240	-3.089	17.247	15.886	18.037	20.025	17.500	16.678	23.617	18.634	22.566	16.984		3	3
201	-0.095	-2.924	-3.436	-3.026	-4.730	-5.735	19.327	17.622	16.617	21.109	18.280	17.768	25.667	19.037	23.653	18.755		5	5
202	2.052	4.889	3.811	0.432	1.682	1.641	21.984	23.234	23.193	21.561	24.398	23.320	22.660	20.444	23.985	15.033		7	2
203	11.028	9.139	8.870	8.209	8.288	5.611	27.829	27.909	25.232	29.071	27.182	26.913	24.295	14.946	22.422	13.664		9	9
204	-2.192	4.097	2.001	-2.024	-3.303	2.321	16.890	15.611	21.235	17.375	23.664	21.568	18.834	18.994	24.022	15.112		7	5
205	2.217	4.047	3.380	1.541	2.771	-1.567	20.969	22.199	17.861	20.405	22.235	21.568	23.244	15.612	21.256	15.120		3	3
206	-0.412	7.069	3.566	-0.757	0.376	3.739	16.742	17.875	21.238	17.701	25.183	21.680	18.692	16.306	21.813	14.414		8	8
207	-2.591	3.562	2.213	-3.404	1.688	-1.860	16.108	21.200	17.651	16.961	23.114	21.765	23.811	15.213	23.331	15.773		3	1
208	0.817	9.111	2.148	3.251	-0.202	2.397	20.775	17.321	19.920	16.982	25.275	19.312	17.690	17.357	16.915	15.414		14	14
209	-0.950	0.635	0.222	-0.024	-4.630	-2.066	21.767	17.162	19.726	20.030	21.515	21.202	24.686	18.897	23.618	18.341		5	5
210	7.625	2.819	2.829	6.526	0.001	0.032	23.899	17.374	17.405	22.753	17.948	17.757	18.746	16.000	16.835	13.422		3	3
211	-1.215	-0.012	-0.592	-2.813	-2.658	-2.846	26.077	26.232	26.044	25.877	27.080	26.500	30.610	27.170	28.650	25.534	+	10	10
212	3.106	3.134	2.288	0.133	1.662	0.238	23.688	25.217	23.793	26.232	26.260	25.414	24.864	22.246	25.096	21.156	+	21	21
213	-1.588	-5.078	-5.122	-1.590	-9.184	-7.501	26.152	18.558	20.241	24.433	20.943	20.899	29.386	26.098	26.534	25.508		7	7
214	-0.345	3.274	2.384	-0.774	0.612	-0.905	15.973	17.360	15.843	16.734	20.353	19.463	17.608	15.887	18.913	15.244		1	1
215	-1.340	5.414	5.242	-0.812	3.487	0.263	16.850	20.950	17.726	15.691	22.446	22.274	19.503	15.422	19.791	14.272		2	2
216	-1.647	-1.940	-2.577	-4.917	-4.537	-3.085	18.521	18.901	20.353	17.439	17.146	16.509	24.680	22.196	22.980	15.192	+	4	4
217	1.118	-0.589	-0.935	-1.948	0.749	-5.539	19.800	22.497	16.209	19.228	17.522	17.175	23.753	19.743	22.033	14.188		19	4
218	7.957	8.914	7.207	4.488	6.734	6.584	28.243	30.489	30.339	27.949	28.905	27.199	26.914	20.596	25.511	14.473		11	11
219	-0.880	6.310	4.348	1.895	0.144	1.478	18.385	16.635	17.969	15.894	23.084	21.123	17.409	15.573	17.183	16.365		2	2
220	-2.768	-0.778	-0.398	-3.013	-3.531	-3.572	24.398	23.880	23.840	22.438	24.418	24.799	28.740	26.082	27.172	23.221		18	18
221	-5.516	0.298	-0.321	-5.312	-2.179	-4.228	17.321	20.454	18.405	15.878	21.691	21.072	23.791	21.475	23.044	19.742		3	3
222	-1.116	7.530	5.345	0.647	1.586	3.360	17.542	18.481	20.255	14.320	22.966	20.781	16.943	16.847	15.934	14.938		2	2
223	0.906	2.266	2.649	0.533	-1.516	0.658	23.857	21.809	23.983	22.614	23.973	24.357	25.335	21.314	23.900	19.515		13	13
224	-1.882	-0.017	-1.138	-1.311	-6.847	-1.021	22.076	16.540	22.367	20.981	22.846	21.724	24.761	22.014	23.814	21.912		4	4
225	5.613	2.775	5.127	2.756	2.461	2.180	25.344	25.050	24.789	25.053	22.215	24.568	25.042	20.136	22.813	16.069		3	3
226	12.759	7.481	9.011	12.282	5.970	4.917	32.214	25.903	24.850	31.223	25.945	27.476	22.861	17.005	21.400	15.528		3	3
227	0.406	1.447	1.842	0.009	-0.160	-2.205	23.864	23.795	21.749	22.542	23.563	23.978	26.343	21.566	24.113	20.159		31	23
228	-7.527	-6.764	-2.981	-7.214	-7.124	-8.981	18.142	18.232	16.375	16.417	17.180	20.964	27.364	23.348	24.967	22.922		11	11
229	1.426	5.009	1.563	3.277	2.591	-3.862	22.786	22.100	15.647	21.371	24.954	21.508	17.843	21.176	24.692	15.198		7	7

Part 2 - TBX2 target genes and interaction partners

	T	U	V	W	X	Y	Z	AA	AB	AC	AD	AE	AF
196	5	5.4	145.81	31.481	19.903	18.821	0.462	2.408	Q99NB9;G5E866;A0A087WMS2	Q99NB9;G5E866	Splicing factor 3B subunit 1	Sf3b1	470
197	3	9.5	49.184	26.31	19.506	0.747	2.399	P62192	P62192	P62192	26S protease regulatory subunit 4	Psmc1	810
198	36	54.3	66.785	323.31	22.194	20.155	1.168	2.398	P14733	P14733	Lamin-B1	Lmnb1	614
199	9	27.4	36.46	62.98	25.953	24.643	0.585	2.386	Q9QZD9;A2AE03	Q9QZD9	Eukaryotic translation initiation factor 3 subunit 1	Eif3i	1522
200	3	22.7	16.534	19.09	21.125	19.785	0.926	2.352	O70591;F8WJ30	O70591;F8WJ30	Prefoldin subunit 2	Pfdn2	539
201	5	50.9	12.466	31.959	22.352	21.204	0.833	2.345	P97450;EQQAD6	P97450;EQQAD6	ATP synthase-coupling factor 6, mitochondrial	Atp5f1	906
202	2	17.6	47.655	23.213	21.552	19.509	1.188	2.332	Q60972;FBZLC6	Q60972	Histone-binding protein RBBP4	Rbbp4	1028
203	9	13.6	87.265	59.342	19.621	18.043	0.974	2.310	Q8Z110;Q9Z110-2;D3Z0B4	Q8Z110;Q9Z110-2	Delta-1-pyrroline-5-carboxylate synthetase;Glutamate 5-kinase;Gamma-glutamyl phosphate reductase	Aldh18a1	1557
204	5	8.3	108.34	32.245	18.914	19.567	0.386	2.304	G3UZ34;A2AH85;O08810	G3UZ34;A2AH85;O08810	116 kDa U5 small nuclear ribonucleoprotein component	Eftud2	150
205	3	13	25.378	19.485	19.428	18.188	0.757	2.300	Q60692	Q60692	Proteasome subunit beta type-6	Psmb6	1021
206	8	5.6	183.19	54.685	17.499	18.114	0.377	2.288	P13864;J3QNWD;P13864-2	P13864;J3QNWD;P13864-2	DNA (cytosine-5)-methyltransferase 1;DNA (cytosine-5)-methyltransferase	Dnmt1	606
207	1	18	19.854	7.337	19.512	19.552	0.397	2.253	Q8CQ19	Q8CQ19	Myosin regulatory light polypeptide 9	Myi9	1330
208	14	4.8	350.86	102.57	17.523	16.165	0.328	2.210	EP9YX6	EP9YX6	Proliferation marker protein Ki-67	Mki67	338
209	5	13.7	34.357	39.18	21.792	20.980	0.706	2.176	Q9CVB6;D3YXG6	Q9CVB6;D3YXG6	Actin-related protein 2/3 complex subunit 2	Arpc2	1372
210	3	29.9	11.163	17.743	17.373	15.128	0.329	2.171	G3UW56;Q0VGG2;A0A087WNR7;A0A087WNL9	G3UW56;Q0VGG2;A0A087WNR7;A0A087WNL9	Uncharacterized protein C8orf59 homolog	Rik	449
211	8	62.7	18.559	250.44	28.890	27.092	2.451	2.166	P18760;F8WGL3	P18760;F8WGL3	Cofilin-1	Cfl1	632
212	20	10.8	236.25	142.29	23.555	23.126	1.729	2.165	EQQA15;B2RQC6;G3UJWN2;B2RQC6-6-2;EQQAT6;F6S323	EQQA15;B2RQC6;G3UJWN2;B2RQC6-6-2;EQQAT6;F6S323	CAD protein;Glutamine-dependent carbamoyl-phosphate synthase;Aspartate carbamoyltransferase;Dihydroorotase	Cad	206
213	7	35.2	20.413	163.4	27.742	26.021	0.347	2.162	D3YYM6;Q91V55;P97461	D3YYM6;Q91V55;P97461	40S ribosomal protein S5;40S ribosomal protein S5, N-terminally processed	Rps5	288
214	1	1	141.55	6.3769	16.748	17.079	0.827	2.127	Q9CW03	Q9CW03	Structural maintenance of chromosomes protein 3	Smc3	1373
215									Q9QYS9-8;Q9QYS9-4;Q9QYS9-3;Q9QYS9-6;Q9QYS9-2;Q9QYS9-7;Q9QYS9-5	Q9QYS9-8;Q9QYS9-4;Q9QYS9-3;Q9QYS9-6;Q9QYS9-2;Q9QYS9-7;Q9QYS9-5	Protein quaking	Qk	1519
216	4	14.8	44.689	26.595	23.438	19.086	1.570	2.125	A2AGN7;O88865;B7ZCF1	A2AGN7;O88865;B7ZCF1	26S protease regulatory subunit 6A	Psmc3	148
217	4	70.2	28.696	25.419	21.748	18.110	0.475	2.110	G5E8R2;G5E8R1;G5E8R0;E9Q453;E9Q456;E9Q455;S4R261	G5E8R2;G5E8R1;G5E8R0;E9Q453;E9Q456;E9Q455;S4R261	Tropomyosin 1	Tpm1	472
218	11	71	7.8409	174.1	23.755	19.992	1.121	2.091	P62858;G3UY7;J3QNN8	P62858;G3UY7	40S ribosomal protein S28	Rps28	839
219	2	3.1	92.188	11.709	16.491	16.774	0.400	2.087	Q6A068	Q6A068	Cell division cycle 5-like protein	Cdc5l	1085
220	18	32.3	59.623	167.77	27.411	25.196	1.283	2.061	P80316;EOCZA1	P80316;EOCZA1	T-complex protein 1 subunit epsilon	Cct5	888
221	3	11.2	41.275	20.976	22.633	21.393	0.427	2.060	P63085	P63085	Mitogen-activated protein kinase 1	Mapk1	859
222	2	3.1	68.23	13.922	16.895	15.436	0.309	2.055	Q5SQ20;Q9EQD61	Q5SQ20;Q9EQD61	Pescadillo homolog	Pes1	1004
223	13	25.6	62.581	81.97	23.324	21.708	1.083	2.048	Q60864	Q60864	Stress-induced-phosphoprotein 1	Stip1	1024
224	4	15.9	32.237	27.995	23.388	22.863	0.446	2.047	Q8CDN6	Q8CDN6	Thioredoxin-like protein 1	Txn1f	1200
225	3	17.4	12.784	47.548	22.569	19.441	1.075	2.039	P62889	P62889	60S ribosomal protein L30	Rpl30	843
226	3	23.5	6.4066	34.892	19.933	18.464	0.295	2.028	P62892	P62892	60S ribosomal protein L39	Rpl39	844
227	21	15.7	233.45	158.75	23.954	22.136	1.142	2.017	Q3UH59;Q61879;Q5SV64;Q8BFX2	Q3UH59;Q61879;Q5SV64	Myosin-10	Myh10	977
228	11	33.9	48.354	106.39	25.356	23.945	0.588	2.016	P29758	P29758	Ornithine aminotransferase, mitochondrial	Oat	676
229	7	37	23.12	47.114	19.509	19.945	0.320	1.998	A2AU61;A2AU62;Q64012-2;Q64012;A2AU60	A2AU61;A2AU62;Q64012-2;Q64012;A2AU60	RNA-binding protein Raly	Raly	172

Table S9. Mass Spectrometry.

Complete list of detected proteins in mass spectrometry analysis.

Because of the extend of the table, Table S9 is only partly embedded in the printed version, while the complete data set is provided as electronic version on the attached compact disc.

Table S10. GO-Term analysis of interaction candidates.

Shown are GO-terms of candidate proteins for interaction with TBX2 determined by MouseMine sorted by Gene ID.

Because of the extend of the table, the complete data set is provided as electronic version on the attached compact disc.

Concluding remarks

The regulation of gene expression by TBX2 in the embryonic lung mesenchyme involves multiple molecular mechanisms.

To control gene transcription, regulatory proteins interfere either directly with the initiation of transcription by the RNA polymerase holoenzyme or modulate the accessibility of the DNA. Post-transcriptionally, gene expression is also regulated by RNA processing and protein modifications which influence the properties, the amount or the stability of a gene product. Utilizing microarray analysis, ChIP-seq data and an *in vivo* co-immunoprecipitation approach, the present study identified diverse mechanisms by which TBX2 regulates gene expression in the pulmonary mesenchyme.

The evaluation of the ChIP-seq data displayed several TBX2 peaks in promoter regions, but most frequently in regions between 50-500kbp away from the transcription start sites, demonstrating that TBX2 regulates target gene transcription via local (promoter), but more frequently via distal (enhancer/silencer) regulatory elements. In order to do so, TBX2 likely interacts with other transcription factors either antagonistically as described for the interaction with MSX1 [155] and EGR1 [156], cooperatively as shown for NKX2.5 [157] or synergistically as ascertained for RB1 [158]. Indeed, we were able to verify the interaction of TBX2 with the transcription factor PBX1 and the chromatin binding protein HMGB2 in the pulmonary mesenchyme. This indicates that DNA binding specificity and regulation of gene transcription in the pulmonary mesenchyme is realized by the coordinated interplay of TBX2 and additional proteins. However, the functional consequences of these interactions have not yet been addressed. Since mice deficient for *Hmgb2* do not exhibit any obvious lung defects [159], the interaction of TBX2 and HMGB2 might be irrelevant for general lung development. In contrast, the loss of PBX1 results in lung hypoplasia [160], but a regulation of proliferation by PBX1 has not yet been analyzed. However, closely related family members (*Hmgb1* and *Pbx2-4*) might act redundant, covering the functional requirement. TBX2 has been described to act as a transcriptional repressor [11, 12, 138] and the present as well as previous studies confirmed such a repressing function of TBX2 also in the developing lung mesenchyme.

In breast cancer cells, TBX2 has been shown to repress the tumor suppressor gene *NDRG1* by the recruitment of the DNA methyltransferase DNMT3B and histone methyl-

transferase complex components, which set a repressive mark (H3K9me₃) within the proximal promoter [126]. In other contexts the repression of target genes such as *Cdkn1a* and *Cdkn2a* depends on the deacetylation of lysine residues in N-terminal tails of histones by HDACs, which are recruited by TBX2 [161-163]. We verified the interaction of TBX2 with HDACs and observed a co-immunoprecipitation of the DNA methyltransferase DNMT1, suggesting that TBX2 is able to trigger DNA methylation and histone modifying enzymes associated with transcriptional repression in the embryonic lung. Although we were not able to identify a histone methyltransferase among the TBX2 interaction partner, we verified an interaction of TBX2 with CHD4 and CBX3, two proteins which recognize and bind methylated histone tails (H3K9me₃) [104, 107, 110, 164, 165], supporting the idea that TBX2 is also involved in histone modification. Furthermore, CHD4 is described as chromatin remodeling protein and as core protein of the NuRD complex, which also includes the verified TBX2 interaction partners HDAC1 and HDAC2 [166-170]. Interestingly, CHD4 contains an HMG-box-like domain in its N-terminal region [171], which possibly mediates a cooperative binding of TBX2 and the CHD4/NuRD complex to the DNA via the identified enrichment of HMG-box binding motifs close to TBX2 peak regions. Although no individual validation was performed, the MS analysis also identified the histone binding proteins RBBP4 and RBBP7, which are involved in the assembly of the NuRD complex [168, 172]. Together this strongly indicates the participation of TBX2 in the recruitment and/or function of the NuRD complex to regulate target gene repression. Moreover, TBX2 was suggested to recruit a novel repressing complex by the interaction with CBX3 and TRIM28 to co-repress EGR1-target genes in breast cancer cells. Our proteomics analysis co-immunoprecipitated both CBX3 and TRIM28, suggesting the possibility of a similar complex assembly in the pulmonary mesenchyme. Thus, TBX2 likely participates in different mechanisms of chromatin remodeling to (persistently) repress the transcription of its target genes in the pulmonary mesenchyme.

The identified protein interaction partners are able to act as transcriptional repressors in different contexts [168, 173-176], but PBX1 was described to have activating properties [177, 178] and moreover, was even shown to directly activate *Fgf10* expression in the lung mesenchyme [160]. Possibly the interaction of TBX2 with PBX1 is not cooperatively, but competitively as described for TBX2 and MSX1 during tooth development [155]. However, the repeatedly described synergistic interaction of T-box and homeobox proteins [132,

136, 157, 179] argues against such a competition for PBX1. It has been shown that a HOX-PBX protein complex turns from an activating into a repressing complex depending on the available co-factors [180]. The switch to a repressor depends on the interaction with HDAC1, suggesting that the activation of *Fgf10* by PBX1 in the pulmonary mesenchyme depends on other co-regulators than TBX2, while PBX1 has a repressive function in the lung upon the interaction with TBX2/HDACs. However, as described above, the functional requirement of such an interaction has to be analyzed in additional studies.

Although our analysis strongly supports the repressive function of TBX2 via DNA binding and recruitment of repressive histone and chromatin modifying proteins/complexes in the pulmonary mesenchyme, our analyses propose an additional possibility of transcription control by TBX2, which should be considered at least to some degree.

The MS analysis identified several proteins associated with the splicing machinery among the putative TBX2 interaction partners, suggesting that TBX2 may regulate gene expression also by RNA processing. Interestingly, TBX3 was shown to interact with multiple splicing factors and to directly bind to the RNA via a TBE to impinge on splicing [181]. The close structural and functional similarity of both TBX2 and TBX3, permits the assumption of similar abilities of TBX2. Moreover, the validated TBX2 interaction partner CBX3 facilitates the recruitment of the splicing machinery to its targets in human colorectal cancer cells [182], providing a second mechanism by which TBX2 might influence RNA splicing. However, additional analyses are needed to further investigate a possible function of TBX2 in RNA processing.

In summary, TBX2 controls transcription in the pulmonary mesenchyme via the binding of differentially localized regulatory elements of target genes and more globally by different mechanisms of chromatin remodeling and/or histone modification. For this, TBX2 interacts with different proteins as well as other TFs. Moreover TBX2 may even participate in RNA processing to regulate target gene expression. Together, this demonstrates the high potential and variability of TBX2 regarding the control of gene expression in the embryonic lung and stresses generally the complexity of TFs.

TBX2 regulates cell proliferation and lung growth rather than lineage commitment and cell differentiation in the lung.

It was shown that TBX2 supports proliferation in a multitude of cancer types by repressing

the cell cycle inhibitors *Cdkn1a*, *Cdkn1b* and *Cdkn2a* [156, 161, 183]. In the lung mesenchyme TBX2 controls proliferation by at least two independent mechanisms [7], one of which is the direct repression of *Cdkn1a* and *Cdkn1b*, emphasizing the importance of TBX2 function to precisely regulate proliferation and organ growth. Interestingly, Kumar *et al.* [51] demonstrated that single cells of the mesothelium stay rather coherent and locally proliferate to populate the organ surface. The TBX2 lineage positive mesothelial clusters observed upon TBX2 overexpression therefore most likely emerge from an increased proliferation of lineage positive descendants, suggesting conserved functions of TBX2 in the pulmonary mesenchyme and mesothelium.

Moreover, the study by Kumar *et al.* [51] showed that the proliferation rate of different mesenchymal cells originating from the same lineage vary substantially, indicating a local control of proliferation. Several of the interaction partners of TBX2 identified in the MS analysis are closely linked to the regulation of proliferation. PBX1 promotes proliferation during spleen development [177], while HMGB2 plays a role in neural stem cell proliferation [184] and represses *Cdkn1a* in cervical cancer [185]. The CHD4 containing version of the NuRD complex is associated with the proliferation of progenitor cells [186, 187] and the epigenetic repression of *Cdkn1a* in breast cancer cells [188]. CBX3 represses *Cdkn1a* in colon cancer [189] and was shown to interact with TBX2 and TRIM28 to repress EGR1 target genes and thereby strongly supports proliferation in breast cancer cells [126]. TRIM28 was identified in our MS analysis, although not strikingly enriched, suggesting the assembly of a similar complex during lung development. TBX2 and the verified interaction partners were co-expressed in the majority but not all mesenchymal cells. Possibly the combined expression of TBX2 and its interaction partners and the exact expression levels of each are responsible for the differential proliferation of mesenchymal cells. Together, these findings reinforce the importance of TBX2 in proliferation control.

To allow cell differentiation, the expression of cell type-specific genes needs to be coordinated with the cell cycle exit [190]. Particularly members of the CIP/KIP family of cyclin-dependent kinase (CDK) inhibitors reduce CDK-promoted proliferation and may overcome the CDK-mediated inhibition of transcription factors which are involved in the induction of differentiation. Furthermore, it has been proposed that expression of transcriptional repressors antagonize senescence and terminal differentiation of quiescent cells [190]. Lüdtke *et al.* [7, 8] hypothesized that TBX2 acts as such an TF, which prevents

the differentiation of the lung mesenchyme by repressing *Cdkn1a* and thereby preserving a proliferative state of mesenchymal cells. TBX2, and its closest relative TBX3, are involved in cell type specification and differentiation of organs such as the heart, the liver and the ureter [13, 14, 16, 144, 145, 191-193]. Furthermore, the TBX2 interaction partners validated in the present study (CBX3, CHD4, PBX1, HMGB2, HDAC1/2) are involved in the fate decisions of different cell types [28, 194-200], supporting a potential function of TBX2 in lineage commitment or differentiation of mesenchymal cells of the lung.

Lüdtke *et al.* [7] suggested that the observed reduction of interstitial fibroblasts in *Tbx2*-deficient mice is caused by a premature maturation of these cells. The reduction of S100A4⁺ interstitial fibroblasts at E14.5 was confirmed in the present study, but analysis of earlier embryonic stages showed no premature emergence of these cells upon *Tbx2* deletion. This argues for a general reduction of S100A4⁺ interstitial cells possibly due to a decreased proliferation rather than a premature differentiation. In wild type mice the entire endothelium derives from the TBX2⁺ cell lineage, while only a subset of endothelial cells expresses TBX2 at E14.5, indicating a specific downregulation of TBX2 possibly as prerequisite for differentiation. Although a hypervascularization was observed upon *Tbx2* overexpression, neither *Tbx2* deletion nor overexpression interfered with endothelial differentiation. Therefore, the TBX2⁺ endothelial cells might represent transit-amplifying cells of the endothelium [201], and therefore persistent TBX2 expression drastically increases endothelial proliferation leading to the observed hypervascularization. Thus, neither interstitial fibroblast nor endothelial cell differentiation depends on TBX2 function, but the proliferation of both cell types is impacted by TBX2.

The deletion of *Tbx2* mildly affects the temporal window of a subprogram of bSMC differentiation, molecularly characterized by the premature expression of S100A4. In rhabdomyosarcoma cells, TBX2 recruits HDAC1 to directly repress smooth muscle associated genes like *myogenic differentiation 1 (Myod1)* and prevents terminal differentiation of SMC by repressing *Cdkn1a* [162]. Although the confirmed interaction of TBX2 and HDAC1 as well as the validated repression of *Cdkn1a* by TBX2 permits the assumption of a similar regulatory network in bSMCs, the establishment and differentiation, examined by several SMC markers, was unaffected upon loss of *Tbx2*. Moreover, *Tbx2* deletion appears to have no effect on the proliferation of bSMCs at E12.5, the time point when premature S100A4 expression was observed. This supports the notion that lineage commitment, dif-

ferentiation and proliferation of SMCs in the lung are largely independent of TBX2.

We identified *I/33* and *Ccn4* as direct target genes of TBX2 in the pulmonary mesenchyme which were derepressed in the submesothelial- or subepithelial mesenchyme, respectively. *I/33* is a cytokine which acts via its receptors IL1RL1 and IL-1RAcP [202, 203] and mediates the immune responses as alarmin in several tissues including the lung [203]. *Ccn4*, a member of the WNT1 inducible signaling pathway protein (WISP) subfamily of the connective tissue growth factor/CCN family of matricellular proteins is implicated in development, tissue repair and disease, where it is involved in proliferation, cell survival, epithelial–mesenchymal transition (EMT) and differentiation [204–207]. Both, *I/33* and *Ccn4* are associated with the control of proliferation and the production of ECM [202, 204, 208], suggesting that derepression of both genes in the lung mesenchyme mediate these phenotypical aspects observed in *Tbx2*-deficient lungs. However, further analysis have to be performed to unveil the functions of *I/33* and *Ccn4* in this context.

Thus, the fate analysis of the pulmonary mesenchyme of *Tbx2*-deficient and constitutively overexpressing mutant mice showed that deregulation of TBX2 has only a marginal affect on the establishment of mesenchymal cell types. Detailed expression analyses of TBX2 during cell cycle revealed that TBX2 levels substantially varied between the different phases of the cell cycle [209]. TBX2 levels increased from mid to late S-phase and peaked in late S- and G2-phase, while TBX2 expression was very low in G1-phase. The G1-phase is proposed to be the phase in which cell fate decisions are manifested by the expression of differentiation-inducing TFs [190, 210]. The low levels of TBX2 during this phase might explain the minor affect of TBX2 on differentiation observed in our study, since the upregulation of any pro-differentiation factor might overcome the weak repressive effect of TBX2 during G1-phase.

All in all, the major function of TBX2 in the lung mesenchyme is the precise control of proliferation, but not of lineage commitment and differentiation. This indicates, that TBX2 is more important to assure lung growth rather than maintaining an undifferentiated state of the progenitor populations. Nonetheless, it is important to consider that TBX3 may partly take over TBX2 function, especially in the subepithelial mesenchyme where TBX3 is predominantly expressed.

TBX2 might be involved in the etiology and/or progression of chronic lung diseases

TBX2 is a well-described oncogene which is a key factor to bypass cellular senescence in many different cancer types, including lung cancer [11, 143, 183]. The present as well as previous studies [7, 8], suggest that TBX2 not only participates in lung cancer, but also in progressive, chronic pulmonary diseases. Chronic lung disease (CLD) is a collective term for a variety of pulmonary disorders, including asthma bronchiale, chronic obstructive pulmonary disease (COPD)/emphysema, pulmonary fibrosis (PF) and others. These diseases are not curable up to now and represent leading causes of death and disability worldwide [211], emphasizing the importance to unveil underlying cellular and molecular mechanisms.

PF is characterized by a decreased diffusion capacity due to reduced airspaces, while COPD causes a limited airflow and the disruption of alveoli structure, whereas asthma bronchiale is marked by airflow obstruction upon exaggerated airway constriction. CLDs, especially the ones of fibrotic character, but also COPD/emphysema and asthma are accompanied by massive mesenchymal remodeling such as disturbed deposition of ECM, increased proliferation of fibroblasts as well as alterations of SMC and myofibroblast differentiation [212-215].

Mesenchymal thickening, an increase of ECM [213] and a higher incidence of S100A4 positive fibroblast as well as an increase in S100A4 level were observed in lungs of PF patients and corresponding mouse models [216]. S100A4 has a crucial function in the proliferation of fibroblasts and the increase in nuclear S100A4 level is sufficient to induce fibrotic properties in fibroblasts [217, 218]. Constitutive expression of TBX2 into adulthood has been shown to increase mesenchymal proliferation, resulting in a mesenchymal thickening and reduced air spaces at P40, accompanied by an enhanced ECM deposition and an increase of S100A4 expressing fibroblasts in mice [7]. Moreover, a recent study identified a *Col13a1* expressing subpopulation of matrix producing fibroblasts, which is expanded in fibrotic lungs [49]. This subpopulation not only expressed TBX2 in normal lungs but upregulated TBX2 in fibrotic condition. Together, this supports a role of TBX2 in fibrotic remodeling of the mesenchyme, including proliferation and matrix deposition.

An increase in ECM deposition is not only a feature of the mesenchymal remodeling in pulmonary fibrosis but also in asthma bronchiale [208, 215, 219]. Since S100A4⁺ fibroblasts are reduced in *Tbx2*-deficient lungs, extensive ECM deposition has to be triggered by a

different process in the loss-of function mutant lungs. The TBX2 target gene *Il33* is derepressed in the mesothelium and the submesothelial mesenchyme of *Tbx2*-deficient lungs and has been repeatedly described to mediate inflammatory responses in several CLDs including COPD/emphysema and asthma bronchiale [220-222]. IL33 expression levels were significantly elevated in bronchial asthma patients [208, 223] and in a murine mouse model for asthma. There, IL33 was shown to significantly increase the proliferation of lung fibroblast and the deposition of several ECM components such as different collagens and FN1 [208]. Additionally, the TBX2 target gene *Ccn4* which was upregulated in the subepithelial layer of *Tbx2*-deficient lungs was shown to induce the expression of ECM components such as FN1 and collagens [224]. Moreover, *Ccn4* induces proliferation and hypertrophy of human bSMC and may therefore contribute to the pathogenic mesenchymal remodeling of asthma bronchiale [225]. Interestingly, we observed a functional anomaly of the bSMC, both in *Tbx2*-deficient and constitutively overexpressing mutant mice. Loss of *Tbx2* led to an increase in contraction strength and a decelerated muscle relaxation, while the constitutive TBX2 expression resulted in an opposite effect. Thus, physiologically the LOF mutant resembles the hypertension observed in asthma bronchiale.

Chronic inflammation, emphysematous lesions and arrested tissue repair due to premature senescence of mesenchymal stem cells are key processes which characterize COPD/emphysema lungs [226]. Previous studies showed that senescence markers such as CDKN2A and CDKN1A were elevated in lungs of COPD patients as result of the suppression of anti-senescence mediators including *Tbx2*, chromatin modifiers and histone deacetylases [227]. The development of an emphysema-like histological phenotype was not observed in *Tbx2*-deficient lungs yet, possibly due to the fact that these mutants die shortly after birth [16] and emphysema-like malformations become prominent after alveoli should have been formed. However, molecular alterations of *Tbx2*-deficient mice, such as reduced WNT-signaling upon derepression of its antagonists *Shisa3* and *Frzb* [7, 8], are similar to observations in COPD/emphysema lungs, where reduced WNT-signaling upon upregulation of its antagonists critically contributes to the initiation of mesenchymal remodeling [215, 228]. Thus, not only the reduction of *Tbx2* but also downstream pathways provide a link of *Tbx2*-deficient and COPD/emphysema lungs.

Together these findings suggest that *Tbx2* regulates different aspects of mesenchymal remodeling via a set of downstream target genes.

Interstitial lung diseases affect the pulmonary parenchyma, however the initial cause originates from epithelial irritations and chronic inflammation [213, 219]. Since TBX2 is exclusively expressed in non-epithelial cells of the lung, it might represent one of the links between an epithelial trigger and downstream mesenchymal remodeling. It has been shown, that TBX2 is specifically phosphorylated in response to an external stress-stimulus, leading to an increase in protein level and consequently to an enhanced repression of target genes including *Cdkn1a* [229]. This suggests, that stress-associated signals caused by an epithelial or mesothelial inflammation might be transmitted into the mesenchyme via the phosphorylation of TBX2. Moreover, Lüdtké *et al.* [8] showed that TBX2 is downstream of SHH-signaling in wild type lungs, indicating that altered epithelial SHH-signaling as in case of COPD/emphysema, PF and asthma [230-232], might serve as mediator from epithelial irritations into a modified mesenchymal TBX2 expression.

In summary, the *Tbx2* mutants analyzed in this and previous studies, reflect different mesenchymal phenotypes of chronic pulmonary diseases such as COPD/emphysema, PF and asthma, without an obvious external stimulus like airway inflammation. Since the deletion of TBX2 only mildly affects cellular composition and the functionality of the lung, TBX2 mutants might serve as a suitable model to study interstitial lung distortions separately from primary epithelial effects. Furthermore, TBX2 might be a suitable mesenchyme-specific therapeutic target to reduce severity or progression of chronic pulmonary diseases without critically interfering with other aspects of lung homeostasis. However, deeper analyses are needed to evaluate the possible therapeutic effects of TBX2 deregulation in mesenchymal remodeling of pulmonary diseases.

References

- [1] Gilmour, D., Rembold, M., and Leptin, M. (2017). From Morphogen to Morphogenesis and Back. *Nature*, 541(7637):311-320. doi: 10.1038/nature21348.
- [2] Etensohn, C.A. (2013). Encoding Anatomy: Developmental Gene Regulatory Networks and Morphogenesis. *Genesis*, 51(6):383-409. doi: 10.1002/dvg.22380.
- [3] Levine, M. and Tjian, R. (2003). Transcription Regulation and Animal Diversity. *Nature*, 424:147-51. doi: 10.1038/nature01763.
- [4] Rock, J.R. and Hogan, B.L.M. (2011). Epithelial Progenitor Cells in Lung Development, Maintenance, Repair, and Disease. *Annual Review of Cell and Developmental Biology*, 27(1):493-512. doi: 10.1146/annurev-cellbio-100109-104040.
- [5] Schilders, K.A.A., Eenjes, E., van Riet, S., Poot, A. A., Stamatialis, D., Truckenmüller, R., Hiemstra, P. S., and Rottier, R.J. (2016). Regeneration of the Lung: Lung Stem Cells and the Development of Lung Mimicking Devices. *Respiratory Research*, 17(1):44. doi: 10.1186/s12931-016-0358-z.
- [6] Chapman, D.L., Garvey, N., Hancock, S., Alexiou, M., Agulnik, S.I., Gibson-Brown, J.J., Cebra-Thomas, J., Bollag, R.J., Silver, L.M., and Papaioannou, V.E. (1996). Expression of the T-Box Family Genes, Tbx1-Tbx5, During Early Mouse Development. *Dev Dyn*, 206(4):379-90. doi: 10.1002/(sici)1097-0177(199608)206:4<379::aid-aja4>3.0.co;2-f.
- [7] Lüdtke, T.H.W., Farin, H.F., Rudat, C., Schuster-Gossler, K., Petry, M., Barnett, P., Christoffels, V.M., and Kispert, A. (2013). Tbx2 Controls Lung Growth by Direct Repression of the Cell Cycle Inhibitor Genes Cdkn1a and Cdkn1b. *PLOS Genetics*, 9(1). doi: 10.1371/journal.pgen.1003189.
- [8] Lüdtke, T.H.W., Rudat, C., Wojahn, I., Weiss, A-C., Kleppa, M-J., Kurz, J., Farin, H.F., Moon, A., Christoffels, V.M, and Kispert, A. (2016). Tbx2 and Tbx3 Act Downstream of Shh to Maintain Canonical Wnt Signaling During Branching Morphogenesis of the Murine Lung. *Developmental Cell*. doi: 10.1016/j.devcel.2016.08.007.
- [9] Arora, R., Metzger, R.J., and Papaioannou, V.E. (2012). Multiple Roles and Interactions of Tbx4 and Tbx5 in Development of the Respiratory System. *PLoS Genetics*, 8(8):e1002866. doi: 10.1371/journal.pgen.1002866.
- [10] Haarman, M.G., Kerstjens-Frederikse, W.S., and Berger, R.M.F. (2019). The Ever-Expanding Phenotypical Spectrum of Human Tbx4 Mutations: From Toe to Lung. *European Respiratory Journal*, 54(2):1901504. doi: 10.1183/13993003.01504-2019.
- [11] Abrahams, A., Parker, M. I., and Prince, S. (2010). The T-Box Transcription Factor Tbx2: Its Role in Development and Possible Implication in Cancer. *IUBMB Life*, 62(2):92-102. doi: 10.1002/iub.275.
- [12] Naiche, L.A., Harrelson, Z., Kelly, R.G., and Papaioannou, V.E. (2005). T-Box Genes in Vertebrate Development. *Annu Rev Genet*, 39:219-239. doi: 10.1146/annurev.genet.39.073003.105925.

-
- [13] Aydoğdu, N., Rudat, C., Trowe, M.-O., Kaiser, M., Lüdtke, T., Mark Taketo, Makoto, M., Christoffels, V., Moon, A., and Kispert, A. (2018). Tbx2 and Tbx3 Act Downstream of Canonical Wnt Signaling in Patterning and Differentiation of the Mouse Ureteric Mesenchyme. *Development*, 145(23):dev171827. doi: 10.1242/dev.171827.
- [14] Harrelson, Z., Kelly, R.G., Goldin, S.N., Gibson-Brown, J.J., Bollag, R.J., Silver, L.M., and Papaioannou, V.E. (2004). Tbx2 Is Essential for Patterning the Atrioventricular Canal and for Morphogenesis of the Outflow Tract During Heart Development. *Development*, 131(20):5041-52. doi: 10.1242/dev.01378.
- [15] Farin, H.F., Lüdtke, T. H. W., Schmidt, M. K., Placzko, S., Schuster-Gossler, K., Petry, M., Christoffels, V. M., and Kispert, A. (2013). Tbx2 Terminates Shh/Fgf Signaling in the Developing Mouse Limb Bud by Direct Repression of Gremlin1. *PLOS Genetics*, 9(4):e1003467. doi: 10.1371/journal.pgen.1003467.
- [16] Aanhaanen, W.T., Brons, J.F., Dominguez, J.N., Rana, M.S., Norden, J., Airik, R., Wakker, V., de Gier-de Vries, C., Brown, N.A., Kispert, A., Moorman, A.F., and Christoffels, V.M. (2009). The Tbx2+ Primary Myocardium of the Atrioventricular Canal Forms the Atrioventricular Node and the Base of the Left Ventricle. *Circ Res*, 104(11):1267-74. doi: 10.1161/circresaha.108.192450.
- [17] Gu, Q. and Lee, L.Y. (2006). Neurophysiology; Neural Control of Airway Smooth Muscle, In: *Encyclopedia of Respiratory Medicine*, Academic Press: Oxford. p.138-145. doi: 10.1016/B0-12-370879-6/00253-2.978-0-12-370879-3.
- [18] Batra, H. and Antony, V.B. (2014). The Pleural Mesothelium in Development and Disease. *Front Physiol*, 5:284. doi: 10.3389/fphys.2014.00284.
- [19] Navarro, M., Ruberte, J., and Carretero, A. (2017). Respiratory Apparatus, In: *Morphological Mouse Phenotyping*, Academic Press. p.147-178. doi: 10.1016/B978-0-12-812972-2.50006-4.978-0-12-812805-3.
- [20] McInnes, E. (2014). The Respiratory System, In: *A Practical Guide to the Histology of the Mouse*. p.179-194. doi: 10.1002/9781118789568.ch11.9781118789568.
- [21] Shannon, J.M., Nielsen, L.D., Gebb, S.A., and Randell, S.H. (1998). Mesenchyme Specifies Epithelial Differentiation in Reciprocal Recombinants of Embryonic Lung and Trachea. *Dev Dyn*, 212(4):482-94. doi: 10.1002/(sici)1097-0177(199808)212:4<482::aid-aja2>3.0.co;2-d.
- [22] Cardoso, W.V. and Lu, J. (2006). Regulation of Early Lung Morphogenesis: Questions, Facts and Controversies. *Development*, 133(9):1611-1624. doi: 10.1242/dev.02310.
- [23] Volckaert, T. and De Langhe, S.P. (2015). Wnt and Fgf Mediated Epithelial-Mesenchymal Crosstalk During Lung Development. *Dev Dyn*, 244(3):342-66. doi: 10.1002/dvdy.24234.
- [24] Kimura, S., Hara, Y., Pineau, T., Fernandez-Salguero, P., Fox, C.H., Ward, J.M., and Gonzalez, F.J. (1996). The T/Ebp Null Mouse: Thyroid-Specific Enhancer-Binding Protein Is Essential for the Organogenesis of the Thyroid, Lung, Ventral Forebrain, and Pituitary. *Genes Dev*, 10(1):60-9. doi: 10.1101/gad.10.1.60.
-

-
- [25] Goss, A.M., Tian, Y., Tsukiyama, T., Cohen, E.D., Zhou, D., Lu, M.M., Yamaguchi, T.P., and Morrisey, E.E. (2009). Wnt2/2b and Beta-Catenin Signaling Are Necessary and Sufficient to Specify Lung Progenitors in the Foregut. *Dev Cell*, 17(2):290-8. doi: 10.1016/j.devcel.2009.06.005.
- [26] Weaver, M., Yingling, J.M., Dunn, N.R., Bellusci, S., and Hogan, B.L. (1999). Bmp Signaling Regulates Proximal-Distal Differentiation of Endoderm in Mouse Lung Development. *Development*, 126(18):4005-4015.
- [27] Domyan, E.T., Ferretti, E., Throckmorton, K., Mishina, Y., Nicolis, S. K., and Sun, X. (2011). Signaling through Bmp Receptors Promotes Respiratory Identity in the Foregut Via Repression of Sox2. *Development*, 138(5):971-981. doi: 10.1242/dev.053694.
- [28] Wang, Y., Tian, Y., Morley, M.P., Lu, M.M., DeMayo, F.J., Olson, E.N., and Morrisey, E.E. (2013). Development and Regeneration of Sox2+ Endoderm Progenitors Is Regulated by a Hdac1/2-Bmp4/Rb1 Regulatory Pathway. *Developmental cell*, 24(4):345-358. doi: 10.1016/j.devcel.2013.01.012.
- [29] Bellusci, S., Grindley, J., Emoto, H., Itoh, N., and Hogan, B.L. (1997). Fibroblast Growth Factor 10 (Fgf10) and Branching Morphogenesis in the Embryonic Mouse Lung. *Development*, 124(23):4867-78.
- [30] Metzger, R., Wachowiak, R., and Kluth, D. (2011). Embryology of the Early Foregut. *Seminars in Pediatric Surgery*, 20(3):136-144. doi: 10.1053/j.sempedsurg.2011.03.004.
- [31] Spooner, B.S. and Wessells, N.K. (1970). Mammalian Lung Development: Interactions in Primordium Formation and Bronchial Morphogenesis. *Journal of Experimental Zoology*, 175(4):445-454. doi: 10.1002/jez.1401750404.
- [32] Williams, A., Quan, Q., and Beasley, S. (2003). Three-Dimensional Imaging Clarifies the Process of Tracheoesophageal Separation in the Rat. *Journal of pediatric surgery*, 38:173-7. doi: 10.1053/jpsu.2003.50037.
- [33] deMello, D.E., Sawyer, D., Galvin, N., and Reid, L.M. (1997). Early Fetal Development of Lung Vasculature. *Am J Respir Cell Mol Biol*, 16(5):568-81. doi: 10.1165/ajrcmb.16.5.9160839.
- [34] Gebb, S.A. and Shannon, J.M. (2000). Tissue Interactions Mediate Early Events in Pulmonary Vasculogenesis. *Developmental Dynamics*, 217(2):159-169. doi: 10.1002/(SICI)1097-0177(200002)217:2<159::AID-DVDY3>3.0.CO;2-9.
- [35] Beck Jr, L. and D'Amore, P.A. (1997). Vascular Development: Cellular and Molecular Regulation. *The FASEB Journal*, 11(5):365-373. doi: 10.1096/fasebj.11.5.9141503.
- [36] Chao, C.-M., El Agha, E., Tiozzo, C., Minoo, P., and Bellusci, S. (2015). A Breath of Fresh Air on the Mesenchyme: Impact of Impaired Mesenchymal Development on the Pathogenesis of Bronchopulmonary Dysplasia. *Frontiers in Medicine*, 2(27). doi: 10.3389/fmed.2015.00027.
- [37] Herriges, M. and Morrisey, E.E. (2014). Lung Development: Orchestrating the Generation and Regeneration of a Complex Organ. *Development*, 141(3):502-13. doi: 10.1242/dev.098186.
-

-
- [38] Warburton, D., El-Hashash, A., Carraro, G., Tiozzo, C., Sala, F., Rogers, O., De Langhe, S., Kemp, P.J., Riccardi, D., Torday, J., Bellusci, S., Shi, W., Lubkin, S.R., and Jesudason, E. (2010). Lung Organogenesis. *Curr Top Dev Biol*, 90:73–158. doi: 10.1016/S0070-2153(10)90003-3.
- [39] Liu, Y. and Hogan, B.L.M. (2002). Differential Gene Expression in the Distal Tip Endoderm of the Embryonic Mouse Lung. *Gene Expression Patterns*, 2(3):229-233. doi: 10.1016/S1567-133X(02)00057-1.
- [40] Herriges, J.C., Yi, L., Hines, E. A., Harvey, J. F., Xu, G., Gray, P. A., Ma, Q., and Sun, X. (2012). Genome-Scale Study of Transcription Factor Expression in the Branching Mouse Lung. *Developmental dynamics*, 241(9):1432-1453. doi: 10.1002/dvdy.23823.
- [41] Que, J., Okubo, Tadashi, Goldenring, J. R., Nam, K.-T., Kurotani, R., Morrissey, E. E., Taranova, O., Pevny, L. H. and Hogan, B.L.M. (2007). Multiple Dose-Dependent Roles for Sox2 in the Patterning and Differentiation of Anterior Foregut Endoderm. *Development*, 134(13):2521. doi: 10.1242/dev.003855.
- [42] Ishii, Y., Rex, M., Scotting, P. J., and Yasugi, S. (1998). Region-Specific Expression of Chicken Sox2 in the Developing Gut and Lung Epithelium: Regulation by Epithelial-Mesenchymal Interactions. *Developmental Dynamics*, 213(4):464-475. doi: 10.1002/(SICI)1097-0177(199812)213:4<464::AID-AJA11>3.0.CO;2-Z.
- [43] Metzger, R.J., Klein, O.D., Martin, G.R., and Krasnow, M.A. (2008). The Branching Programme of Mouse Lung Development. *Nature*, 453:745-751. doi: 10.1038/nature07005.
- [44] Pepicelli, C.V., Lewis, P.M., and McMahon, A.P. (1998). Sonic Hedgehog Regulates Branching Morphogenesis in the Mammalian Lung. *Current Biology*, 8:1083-1086.
- [45] Warburton, D., Bellusci, S., De Langhe, S., Del Moral, P.M., Fleury, V., Mailleux, A., Tefft, D., Unbekandt, M., Wang, K., and Shi, W. (2005). Molecular Mechanisms of Early Lung Specification and Branching Morphogenesis. *Pediatr Res*, 57(5 Pt 2):26r-37r. doi: 10.1203/01.pdr.0000159570.01327.ed.
- [46] Weaver, M., Dunn, N.R., and Hogan, B.L. (2000). Bmp4 and Fgf10 Play Opposing Roles During Lung Bud Morphogenesis. *Development*, 127(12):2695-704.
- [47] Volckaert, T. and De Langhe, S.P. (2014). Lung Epithelial Stem Cells and Their Niches: Fgf10 Takes Center Stage. *Fibrogenesis Tissue Repair*, 7:8. doi: 10.1186/1755-1536-7-8.
- [48] Hogan, B.L.M., Barkauskas, C. E., Chapman, H. A., Epstein, J. A., Jain, R., Hsia, C. C. W., Niklason, L., Calle, E., Le, A., Randell, S. H., Rock, J., Snitow, M., Krummel, M., Stripp, B. R., Vu, T., White, E. S., Whitsett, J. A., and Morrissey, E.E. (2014). Repair and Regeneration of the Respiratory System: Complexity, Plasticity, and Mechanisms of Lung Stem Cell Function. *Cell Stem Cell*, 15(2):123-138. doi: 10.1016/j.stem.2014.07.012.
- [49] Xie, T., Wang, Y., Deng, N., Huang, G., Taghavifar, F., Geng, Y., Liu, N., Kulur, V., Yao, C., Chen, P., Liu, Z., Stripp, B., Tang, J., Liang, C. J., Noble, P., and Jiang, D. (2018). Single-Cell Deconvolution of Fibroblast Heterogeneity in Mouse Pulmonary Fibrosis. *Cell Reports*, 22:3625-3640. doi: 10.1016/j.celrep.2018.03.010.
-

-
- [50] Peng, T., Tian, Y., Boogerd, C. J., Lu, M. M., Kadzik, R. S., Stewart, K. M., Evans, S.M., and Morrissey, E.E. (2013). Coordination of Heart and Lung Co-Development by a Multipotent Cardiopulmonary Progenitor. *Nature*, 500(7464):589-592. doi: 10.1038/nature12358.
- [51] Kumar, M.E., Bogard, P. E., Espinoza, F. H., Menke, D. B., Kingsley, D. M., and Krasnow, M.A. (2014). Defining a Mesenchymal Progenitor Niche at Single Cell Resolution. *Science*, 346(6211):1258810-1258810. doi: 10.1126/science.1258810.
- [52] Li, C., Li, M., Li, S., Xing, Y., Yang, C-Y., Li, A., Borok, Z., De Langhe, S., and Minoo, P. (2015). Progenitors of Secondary Crest Myofibroblasts Are Developmentally Committed in Early Lung Mesoderm. *Stem Cells*, 33:999-1012. doi: 10.1002/stem.1911.
- [53] Zhang, W., Menke, D. B., Jiang, M., Chen, H., Warburton, D., Turcatel, G., Lu, C. H., Xu, W., Luo, Y., and Shi, W. (2013). Spatial-Temporal Targeting of Lung-Specific Mesenchyme by a Tbx4 Enhancer. *BMC Biol*, 11:111. doi: 10.1186/1741-7007-11-111.
- [54] Xie, T., Liang, J., Liu, N., Huan, C., Zhang, Y., Liu, W., Kumar, M., Xiao, R., D'Armiento, J., Metzger, D., Chambon, P., Papaioannou, V. E., Stripp, B. R., Jiang, D., and Noble, P.W. (2016). Transcription Factor Tbx4 Regulates Myofibroblast Accumulation and Lung Fibrosis. *The Journal of Clinical Investigation*, 126(8):3063-3079. doi: 10.1172/JCI85328.
- [55] El Agha, E., Herold, S., Alam, D. A., Quantius, J., MacKenzie, B. A., Carraro, G., Moiseenko, A., Chao, C.-M., Minoo, P., Seeger, W., and Bellusci, S. (2014). Fgf10-Positive Cells Represent a Progenitor Cell Population During Lung Development and Postnatally. *Development*, 141(2):296-306. doi: 10.1242/dev.099747.
- [56] Lütke, T.H., Rudat, C., Kurz, J., Häfner, R., Greulich, F., Wojahn, I., Aydoğdu, N., Mamo, T.M., Kleppa, M.-J., Trowe, M. O., Bohnenpoll, T., Taketo, M.M., and Kispert, A. (2019). Mesothelial Mobilization in the Developing Lung and Heart Differs in Timing, Quantity, and Pathway Dependency. *American Journal of Physiology-Lung Cellular and Molecular Physiology*, 316(5):L767-L783. doi: 10.1152/ajplung.00212.2018.
- [57] von Gise, A., Stevens, S. M., Honor, L. B., Oh, J. H., Gao, C., Zhou, B., and Pu, W.T. (2016). Contribution of Fetal, but Not Adult, Pulmonary Mesothelium to Mesenchymal Lineages in Lung Homeostasis and Fibrosis. *American Journal of Respiratory Cell and Molecular Biology*, 54(2):222-230. doi: 10.1165/rcmb.2014-0461OC.
- [58] Que, J., Wilm, B., Hasegawa, H., Wang, F., Bader, D., and Hogan, B.L.M. (2008). Mesothelium Contributes to Vascular Smooth Muscle and Mesenchyme During Lung Development. *Proceedings of the National Academy of Sciences*, 105(43):16626-16630. doi: 10.1073/pnas.0808649105.
- [59] Cano, E., Carmona, R., and Muñoz-Chápuli, R. (2013). Wt1-Expressing Progenitors Contribute to Multiple Tissues in the Developing Lung. *Am J Physiol Lung Cell Mol Physiol*, 305:322-332. doi: 10.1152/ajplung.00424.2012.
- [60] Snitow, M., Lu, M.M., Cheng, L., Zhou, S., and Morrissey, E.E. (2016). Ezh2 Restricts the Smooth Muscle Lineage During Mouse Lung Mesothelial Development. *Development*, 143(20):3733-3741. doi: 10.1242/dev.134932.
-

-
- [61] Yin, Y., Wang, F., and Ornitz, D.M. (2011). Mesothelial- and Epithelial-Derived Fgf9 Have Distinct Functions in the Regulation of Lung Development. *Development*, 138(15):3169-77. doi: 10.1242/dev.065110.
- [62] Weaver, M., Batts, L., and Hogan, B.L. (2003). Tissue Interactions Pattern the Mesenchyme of the Embryonic Mouse Lung. *Dev Biol*, 258(1):169-84. doi: 10.1016/S0012-1606(03)00117-9.
- [63] White, A.C., Xu, J., Yin, Y., Smith, C., Schmid, G., and Ornitz, D.M. (2006). Fgf9 and Shh Signaling Coordinate Lung Growth and Development through Regulation of Distinct Mesenchymal Domains. *Development*, 133(8):1507-17. doi: 10.1242/dev.02313.
- [64] Ornitz, D.M. and Yin, Y. (2012). Signaling Networks Regulating Development of the Lower Respiratory Tract. *Cold Spring Harb Perspect Biol*, 4(5). doi: 10.1101/cshperspect.a008318.
- [65] Maillieux, A.A., Kelly, R.G., Veltmaat, J.M., De Langhe, S.P., Zaffran, S., Thiery, J.P., and Bellusci, S. (2005). Fgf10 Expression Identifies Parabronchial Smooth Muscle Cell Progenitors and Is Required for Their Entry into the Smooth Muscle Cell Lineage. *Development*, 132(9):2157-2166. doi: 10.1242/dev.01795.
- [66] Ustiyani, V., Bolte, C., Zhang, Y., Han, L. Xu, Y., Yutzey, K. E., Zorn, A. M., Kalin, T. V., Shannon, J. M., and Kalinichenko, V.V. (2018). Foxf1 Transcription Factor Promotes Lung Morphogenesis by Inducing Cellular Proliferation in Fetal Lung Mesenchyme. *Developmental biology*, 443(1):50-63. doi: 10.1016/j.ydbio.2018.08.011.
- [67] Morrisey, E.E. and Hogan, B.L. (2010). Preparing for the First Breath: Genetic and Cellular Mechanisms in Lung Development. *Dev Cell*, 18(1):8-23. doi: 10.1016/j.devcel.2009.12.010.
- [68] Goss, A.M., Tian, Y., Cheng, L., Yang, J., Zhou, D., Cohen, E.D., and Morrisey, E.E. (2011). Wnt2 Signaling Is Necessary and Sufficient to Activate the Airway Smooth Muscle Program in the Lung by Regulating Myocardin/Mrtf-B and Fgf10 Expression. *Dev Biol*, 356(2):541-52. doi: 10.1016/j.ydbio.2011.06.011.
- [69] De Langhe, S.P., Carraro, G., Tefft, D., Li, C., Xu, X., Chai, Y., Minoo, P., Hajihosseini, M. K., Drouin, J., Kaartinen, V., and Bellusci, S. (2008). Formation and Differentiation of Multiple Mesenchymal Lineages During Lung Development Is Regulated by Beta-Catenin Signaling. *PLoS One*, 3(1):e1516. doi: 10.1371/journal.pone.0001516.
- [70] Cohen, E.D., Ihida-Stansbury, K., Lu, M.M., Panettieri, R.A., Jones, P.L. and Morrisey, E.E. (2009). Wnt Signaling Regulates Smooth Muscle Precursor Development in the Mouse Lung Via a Tenascin C/Pdgfr Pathway. *The Journal of Clinical Investigation*, 119(9):2535-2549. doi: 10.1172/JCI38079.
- [71] Mahlapuu, M., Enerbäck, S., and Carlsson, P. (2001). Haploinsufficiency of the Forkhead Gene Foxf1, a Target for Sonic Hedgehog Signaling, Causes Lung and Foregut Malformations. *Development*, 128(12):2397.
- [72] Hines, E.A., Jones, M.-K. N., Verheyden, J. M., Harvey, J. F., and Sun, X. (2013). Establishment of Smooth Muscle and Cartilage Juxtaposition in the Developing Mouse Upper Airways. *Proceedings of the National Academy of Sciences*, 110(48):19444-19449. doi: 10.1073/pnas.1313223110.
-

-
- [73] Young, R.E., Jones, M.-K., Hines, E. A., Li, R., Luo, Y., Shi, W., Verheyden, J. M., and Sun, X. (2020). Smooth Muscle Differentiation Is Essential for Airway Size, Tracheal Cartilage Segmentation, but Dispensable for Epithelial Branching. *Developmental Cell*, 53(1):73-85.e5. doi: 10.1016/j.devcel.2020.02.001.
- [74] Tacchetti, C., Tavella, S., Dozin, B., Quarto, R., Robino, G. and Cancedda, R. (1992). Cell Condensation in Chondrogenic Differentiation. *Experimental Cell Research*, 200(1):26-33. doi: 10.1016/S0014-4827(05)80067-9.
- [75] de Crombrugge, B., Lefebvre, V., and Nakashima, K. (2001). Regulatory Mechanisms in the Pathways of Cartilage and Bone Formation. *Current Opinion in Cell Biology*, 13(6):721-728. doi: 10.1016/S0955-0674(00)00276-3.
- [76] Snowball, J., Ambalavanan, M., Whitsett, J., and Sinner, D. (2015). Endodermal Wnt Signaling Is Required for Tracheal Cartilage Formation. *Developmental Biology*, 405(1):56-70. doi: 10.1016/j.ydbio.2015.06.009.
- [77] Geng, Y., Dong, Y., Yu, M., Zhang, L., Yan, X., Sun, J., Qiao, L., Geng, H., Nakajima, M., Furuichi, T., Ikegawa, S., Gao, X., Chen, Y.-G., Jiang, D., and Ning, W. (2011). Follistatin-Like 1 (Fstl1) Is a Bone Morphogenetic Protein (Bmp) 4 Signaling Antagonist in Controlling Mouse Lung Development. *Proceedings of the National Academy of Sciences*, 108(17):7058-7063. doi: 10.1073/pnas.1007293108.
- [78] Park, J., Zhang, J.J., Moro, A., Kushida, M., Wegner, M., and Kim, P.C. (2010). Regulation of Sox9 by Sonic Hedgehog (Shh) Is Essential for Patterning and Formation of Tracheal Cartilage. *Dev Dyn*, 239(2):514-26. doi: 10.1002/dvdy.22192.
- [79] Bell, S.M., Schreiner, C. M., Wert, S. E., Mucenski, M.L., Scott, W. J., and Whitsett, J.A. (2008). R-Spondin 2 Is Required for Normal Laryngeal-Tracheal, Lung and Limb Morphogenesis. *Development*, 135(6):1049-1058. doi: 10.1242/dev.013359.
- [80] Hatakeyama, Y., Tuan, R.S., and Shum, L. (2004). Distinct Functions of Bmp4 and Gdf5 in the Regulation of Chondrogenesis. *J Cell Biochem*, 91(6):1204-17. doi: 10.1002/jcb.20019.
- [81] Sein, K., Wells, T. R., Landing, B. H., and Chow, C.R. (1985). Short Trachea, with Reduced Number of Cartilage Rings—a Hitherto Unrecognized Feature of Digeorge Syndrome. *Pediatric Pathology*, 4(1-2):81-88. doi: 10.3109/15513818509025905.
- [82] Vermot, J., Niederreither, K., Garnier, J.-M., Chambon, P., and Dollé, P. (2003). Decreased Embryonic Retinoic Acid Synthesis Results in a Digeorge Syndrome Phenotype in Newborn Mice. *Proceedings of the National Academy of Sciences of the United States of America*, 100(4):1763-1768. doi: 10.1073/pnas.0437920100.
- [83] Drake, C.J., Hungerford, J.E., and Little, C.D. (1998). Morphogenesis of the First Blood Vessels. *Annals of the New York Academy of Sciences*, 857(1):155-179. doi: 10.1111/j.1749-6632.1998.tb10115.x.
- [84] Risau, W. (1997). Mechanisms of Angiogenesis. *Nature*, 386(6626):671-674. doi: 10.1038/386671a0.
-

-
- [85] White, A.C., Lavine, K.J., and Ornitz, D.M. (2007). Fgf9 and Shh Regulate Mesenchymal Vegfa Expression and Development of the Pulmonary Capillary Network. *Development*, 134(20):3743-52. doi: 10.1242/dev.004879.
- [86] Healy, A.M., Morgenthau, L., Zhu, X., Farber, H. W., and Cardoso, W.V. (2000). Vegf Is Deposited in the Subepithelial Matrix at the Leading Edge of Branching Airways and Stimulates Neovascularization in the Murine Embryonic Lung. *Developmental Dynamics*, 219(3):341-352. doi: 10.1002/1097-0177(2000)9999:9999<::AID-DVDY1061>3.0.CO;2-M.
- [87] Ramasamy, S.K., Mailleux, A. A., Gupte, V. V., Mata, F., Sala, F. G., Veltmaat, J. M., Del Moral, P. M., De Langhe, S., Parsa, S., Kelly, L. K., Kelly, R., Shia, W., Keshet, E., Minoo, P., Warburton, D., and Bellusci, S. (2007). Fgf10 Dosage Is Critical for the Amplification of Epithelial Cell Progenitors and for the Formation of Multiple Mesenchymal Lineages During Lung Development. *Developmental biology*, 307(2):237-247. doi: 10.1016/j.ydbio.2007.04.033.
- [88] Ren, X., Ustiyanyan, V., Pradhan, A., Cai, Y., Havrilak, J. A., Bolte, C. S., Shannon, J. M., Kalin, T. V., and Kalinichenko, V.V. (2014). Foxf1 Transcription Factor Is Required for Formation of Embryonic Vasculature by Regulating Vegf Signaling in Endothelial Cells. *Circulation Research*, 115(8):709-720. doi: 10.1161/CIRCRESAHA.115.304382.
- [89] Shalaby, F., Rossant, J., Yamaguchi, T. P., Gertsenstein, M., Wu, X.-F., Breitman, M. L., and Schuh, A.C. (1995). Failure of Blood-Island Formation and Vasculogenesis in Flk-1-Deficient Mice. *Nature*, 376(6535):62-66. doi: 10.1038/376062a0.
- [90] Yamaguchi, T.P., Dumont, D.J., Conlon, R.A., Breitman, M.L., and Rossant, J. (1993). Flk-1, an Flt-Related Receptor Tyrosine Kinase Is an Early Marker for Endothelial Cell Precursors. *Development*, 118(2):489-498.
- [91] Greif, D.M., Kumar, M., Lighthouse, J. K., Hum, J., An, A., Ding, L., Red-Horse, K., Espinoza, F. H., Olson, L., Offermanns, S., and Krasnow, M.A. (2012). Radial Construction of an Arterial Wall. *Developmental Cell*, 23(3):482-493. doi: 10.1016/j.devcel.2012.07.009.
- [92] Hirschi, K.K., Rohovsky, S.A., and D'Amore, P.A. (1998). Pdgf, Tgf-Beta, and Heterotypic Cell-Cell Interactions Mediate Endothelial Cell-Induced Recruitment of 10t1/2 Cells and Their Differentiation to a Smooth Muscle Fate. *The Journal of cell biology*, 141(3):805-814. doi: 10.1083/jcb.141.3.805.
- [93] Nicosia, R.F. and Villaschi, S. (1995). Rat Aortic Smooth Muscle Cells Become Pericytes During Angiogenesis in Vitro. *Laboratory investigation*, 73(5):658-666.
- [94] Benjamin, L.E., Hemo, I., and Keshet, E. (1998). A Plasticity Window for Blood Vessel Remodelling Is Defined by Pericyte Coverage of the Preformed Endothelial Network and Is Regulated by Pdgf-B and Vegf. *Development*, 125(9):1591.
- [95] Rajagopal, J., Carroll, T.J., Guseh, J.S., Bores, S.A., Blank, L.J., Anderson, W. J., Yu, J., Zhou, Q., McMahon, A.P., and Melton, D.A. (2008). Wnt7b Stimulates Embryonic Lung Growth by Coordinately Increasing the Replication of Epithelium and Mesenchyme. *Development*, 135(9):1625-1634. doi: 10.1242/dev.015495.
-

-
- [96] Hellstrom, M., Kalen, M., Lindahl, P., Abramsson, A., and Betsholtz, C. (1999). Role of Pdgf-B and Pdgfr-Beta in Recruitment of Vascular Smooth Muscle Cells and Pericytes During Embryonic Blood Vessel Formation in the Mouse. *Development*, 126(14):3047-3055.
- [97] De Langhe, S.P., Sala, F.G., Del Moral, P-M., Fairbanks, T.J., Yamada, K.M., Warburton, D., Burns, R.C., and Bellusci, S. (2005). Dickkopf-1 (Dkk1) Reveals That Fibronectin Is a Major Target of Wnt Signaling in Branching Morphogenesis of the Mouse Embryonic Lung. *Developmental Biology*, 277:316–331. doi: 10.1016/j.ydbio.2004.09.023.
- [98] Bostrom, H., Willetts, K., Pekny, M., Leveen, P., Lindahl, P., Hedstrand, H., Pekna, M., Hellstrom, M., Gebre-Medhin, S., Schalling, M., Nilsson, M., Kurland, S., Tornell, J., Heath, J.K., and Betsholtz, C. (1996). Pdgf-a Signaling Is a Critical Event in Lung Alveolar Myofibroblast Development and Alveogenesis. *Cell*, 85(6):863-73.
- [99] Li, B., Carey, M., and Workman, J.L. (2007). The Role of Chromatin During Transcription. *Cell*, 128(4):707-719. doi: 10.1016/j.cell.2007.01.015.
- [100] Längst, G. and Manelyte, L. (2015). Chromatin Remodelers: From Function to Dysfunction. *Genes*, 6(2):299-324. doi: 10.3390/genes6020299.
- [101] Clapier, C.R. and Cairns, B.R. (2009). The Biology of Chromatin Remodeling Complexes. *Annu Rev Biochem*, 78:273-304. doi: 10.1146/annurev.biochem.77.062706.153223.
- [102] Varga-Weisz, P. (2001). Atp-Dependent Chromatin Remodeling Factors: Nucleosome Shufflers with Many Missions. *Oncogene*, 20(24):3076-3085. doi: 10.1038/sj.onc.1204332.
- [103] Zhang, Y. (2006). It Takes a Phd to Interpret Histone Methylation. *Nat Struct Mol Biol*, 13(7):572-4. doi: 10.1038/nsmb0706-572.
- [104] Musselman, C.A., Mansfield, R. E., Garske, A. L., Davrazou, F., Kwan, A. H., Oliver, S. S., O'Leary, H., Denu, J. M., Mackay, J. P., and Kutateladze, T.G. (2009). Binding of the Chd4 Phd2 Finger to Histone H3 Is Modulated by Covalent Modifications. *The Biochemical journal*, 423(2):179-187. doi: 10.1042/BJ20090870.
- [105] Bannister, A.J. and Kouzarides, T. (2011). Regulation of Chromatin by Histone Modifications. *Cell research*, 21(3):381-395. doi: 10.1038/cr.2011.22.
- [106] Li, X.-Y., Thomas, S., Sabo, P. J., Eisen, M. B., Stamatoyannopoulos, J. A., and Biggin, M.D. (2011). The Role of Chromatin Accessibility in Directing the Widespread, Overlapping Patterns of Drosophila Transcription Factor Binding. *Genome Biology*, 12(4):R34. doi: 10.1186/gb-2011-12-4-r34.
- [107] Dong, X. and Weng, Z. (2013). The Correlation between Histone Modifications and Gene Expression. *Epigenomics*, 5(2):113-116. doi: 10.2217/epi.13.13.
- [108] Martin, C. and Zhang, Y. (2005). The Diverse Functions of Histone Lysine Methylation. *Nature Reviews Molecular Cell Biology*, 6(11):838-849. doi: 10.1038/nrm1761.
- [109] Sims, R.J., III, Nishioka, K., and Reinberg, D. (2003). Histone Lysine Methylation: A Signature for Chromatin Function. *Trends in Genetics*, 19(11):629-639. doi: 10.1016/j.tig.2003.09.007.
-

-
- [110] Bannister, A.J., Zegerman, P., Partridge, J. F., Miska, E. A., Thomas, J. O., Allshire, R. C. and Kouzarides, T. (2001). Selective Recognition of Methylated Lysine 9 on Histone H3 by the Hp1 Chromo Domain. *Nature*, 410(6824):120-124. doi: 10.1038/35065138.
- [111] Eissenberg, J.C. and Elgin, S.C.R. (2000). The Hp1 Protein Family: Getting a Grip on Chromatin. *Current Opinion in Genetics & Development*, 10(2):204-210. doi: 10.1016/S0959-437X(00)00058-7.
- [112] Maison, C. and Almouzni, G. (2004). Hp1 and the Dynamics of Heterochromatin Maintenance. *Nature Reviews Molecular Cell Biology*, 5(4):296-305. doi: 10.1038/nrm1355.
- [113] Fujita, N., Watanabe, S., Ichimura, T., Tsuruzoe, S., Shinkai, Y., Tachibana, M., Chiba, T., and Nakao, M. (2003). Methyl-Cpg Binding Domain 1 (Mbd1) Interacts with the Suv39h1-Hp1 Heterochromatic Complex for DNA Methylation-Based Transcriptional Repression. *Journal of Biological Chemistry*, 278(26):24132-24138. doi: 10.1074/jbc.M302283200.
- [114] Honda, S. and Selker, E.U. (2008). Direct Interaction between DNA Methyltransferase Dim-2 and Hp1 Is Required for DNA Methylation in *Neurospora Crassa*. *Molecular and cellular biology*, 28(19):6044-6055. doi: 10.1128/MCB.00823-08.
- [115] Miranda, T.B. and Jones, P.A. (2007). DNA Methylation: The Nuts and Bolts of Repression. *J Cell Physiol*, 213(2):384-90. doi: 10.1002/jcp.21224.
- [116] Ludwig, C.H. and Bintu, L. (2019). Mapping Chromatin Modifications at the Single Cell Level. *Development*, 146(12):dev170217. doi: 10.1242/dev.170217.
- [117] Wu, C. (1997). Chromatin Remodeling and the Control of Gene Expression. *J Biol Chem*, 272(45):28171-4. doi: 10.1074/jbc.272.45.28171.
- [118] Campbell, N.A. and Reece, J.B. (2006). *Biologie*. 6. ed, München [u.a.]: Pearson Studium.
- [119] Alberts, B., Johnson, A., Lewis, J., Raff, M., Roberts, K., and Walter, P. (2008). *Molecular Biology of the Cell*. 5. ed: Garland Science, Taylor & Francis Group.
- [120] Weaver, R.F. (2011). *Molecular Biology*. 5. ed: McGraw-Hill Companies.
- [121] Waldron, L., Steimle, J. D., Greco, T. M., Gomez, N. C., Dorr, K. M., Kweon, J., Temple, B., Yang, X. H., Wilczewski, C. M., Davis, I. J., Cristea, I. M., Moskowitz, I. P., and Conlon, F.L. (2016). The Cardiac Tbx5 Interactome Reveals a Chromatin Remodeling Network Essential for Cardiac Septation. *Developmental cell*, 36(3):262-275. doi: 10.1016/j.devcel.2016.01.009.
- [122] Hota, S.K., Johnson, J. R., Verschueren, E., Thomas, R., Blotnick, A. M., Zhu, Y., Sun, X., Pennacchio, L. A., Krogan, N. J., and Bruneau, B.G. (2019). Dynamic Baf Chromatin Remodeling Complex Subunit Inclusion Promotes Temporally Distinct Gene Expression Programs in Cardiogenesis. *Development*, 146(19):dev174086. doi: 10.1242/dev.174086.
- [123] Hosokawa, H., Tanaka, T., Suzuki, Y., Iwamura, C., Ohkubo, S., Endoh, K., Kato, M., Endo, Y., Onodera, A., Tumes, D. J., Kanai, A., Sugano, S., and Nakayama, T. (2013). Functionally Distinct Gata3/Chd4 Complexes Coordinately Establish T Helper 2 (Th2) Cell Identity. *Proceedings of the National Academy of Sciences of the United States of America*, 110(12):4691-4696. doi: 10.1073/pnas.1220865110.
-

-
- [124] Kaltenbrun, E., Greco, T. M., Slagle, C. E., Kennedy, L. M., Li, T., Cristea, I. M., and Conlon, F.L. (2013). A Gro/Tle-Nurd Corepressor Complex Facilitates Tbx20-Dependent Transcriptional Repression. *Journal of proteome research*, 12(12):5395-5409. doi: 10.1021/pr400818c.
- [125] Rivera-Reyes, R., Kleppa, M.-J., and Kispert, A. (2018). Proteomic Analysis Identifies Transcriptional Cofactors and Homeobox Transcription Factors as Tbx18 Binding Proteins. *PLOS ONE*, 13(8):e0200964. doi: 10.1371/journal.pone.0200964.
- [126] Crawford, N.T., McIntyre, A. J., McCormick, A., D'Costa, Z. C., Buckley, N. E., and Mullan, P.B. (2019). Tbx2 Interacts with Heterochromatin Protein 1 to Recruit a Novel Repression Complex to Egr1-Targeted Promoters to Drive the Proliferation of Breast Cancer Cells. *Oncogene*, 38(31):5971-5986. doi: 10.1038/s41388-019-0853-z.
- [127] Agulnik, S.I., Bollag, R.J., and Silver, L.M. (1995). Conservation of the T-Box Gene Family from *Mus Musculus* to *Caenorhabditis Elegans*. *Genomics*, 25(1):214-219. doi: 10.1016/0888-7543(95)80128-9.
- [128] Bollag, R.J., Siegfried, Z., Cebra-Thomas, J. A., Garvey, N., Davison, E. M., and Silver, L.M. (1994). An Ancient Family of Embryonically Expressed Mouse Genes Sharing a Conserved Protein Motif with the T Locus. *Nature Genetics*, 7(3):383-389. doi: 10.1038/ng0794-383.
- [129] Kispert, A. and Herrmann, B.G. (1993). The Brachyury Gene Encodes a Novel DNA Binding Protein. *The EMBO journal*, 12(8):3211-3220.
- [130] Müller, C.W. and Herrmann, B.G. (1997). Crystallographic Structure of the T Domain–DNA Complex of the Brachyury Transcription Factor. *Nature*, 389(6653):884-888. doi: 10.1038/39929.
- [131] Papapetrou, C., Edwards, Y.H., and Sowden, J.C. (1997). The T Transcription Factor Functions as a Dimer and Exhibits a Common Human Polymorphism Gly-177-Asp in the Conserved DNA-Binding Domain. *FEBS Letters*, 409(2):201-206. doi: 10.1016/S0014-5793(97)00506-1.
- [132] Stennard, F.A., Costa, M.W., Elliott, D.A., Rankin, S., Haast, S.J., Lai, D., McDonald, L.P., Niederreither, K., Dolle, P., Bruneau, B.G., Zorn, A.M., and Harvey, R.P. (2003). Cardiac T-Box Factor Tbx20 Directly Interacts with Nkx2-5, Gata4, and Gata5 in Regulation of Gene Expression in the Developing Heart. *Dev Biol*, 262(2):206-24. doi: 10.1016/S0012-1606(03)00385-3.
- [133] Fan, C., Liu, M., and Wang, Q. (2003). Functional Analysis of Tbx5 Missense Mutations Associated with Holt-Oram Syndrome. *The Journal of biological chemistry*, 278(10):8780-8785. doi: 10.1074/jbc.M208120200.
- [134] Garg, V., Kathiriya, I. S., Barnes, R., Schluterman, M. K., King, I. N., Butler, C. A., Rothrock, C. R., Eapen, R. S., Hirayama-Yamada, K., Joo, K., Matsuoka, R., Cohen, J. C., and Srivastava, D. (2003). Gata4 Mutations Cause Human Congenital Heart Defects and Reveal an Interaction with Tbx5. *Nature*, 424(6947):443-447. doi: 10.1038/nature01827.
-

-
- [135] Lamolet, B., Pulichino, A.-M., Lamonerie, T., Gauthier, Y., Brue, T., Enjalbert, A., and Drouin, J. (2001). A Pituitary Cell-Restricted T Box Factor, Tpit, Activates Pomc Transcription in Cooperation with Pitx Homeoproteins. *Cell*, 104(6):849-859. doi: 10.1016/S0092-8674(01)00282-3.
- [136] Hiroi, Y., Kudoh, S., Monzen, K., Ikeda, Y., Yazaki, Y., Nagai, R., and Komuro, I. (2001). Tbx5 Associates with Nkx2-5 and Synergistically Promotes Cardiomyocyte Differentiation. *Nat Genet*, 28(3):276-80. doi: 10.1038/90123.
- [137] Takeuchi, J.K., Lou, X., Alexander, J. M., Sugizaki, H., Delgado-Olguín, P., Holloway, A.K., Mori, A.D., Wylie, J.N., Munson, C., Zhu, Y., Zhou, Y.-Q., Yeh, R.-F., Henkelman, R.M., Harvey, R.P., Metzger, D., Chambon, P., Stainier, D.Y.R., Pollard, K.S., Scott, I.C., and Bruneau, B.G. (2011). Chromatin Remodelling Complex Dosage Modulates Transcription Factor Function in Heart Development. *Nature Communications*, 2(1):187. doi: 10.1038/ncomms1187.
- [138] Papaioannou, V.E. (2014). The T-Box Gene Family: Emerging Roles in Development, Stem Cells and Cancer. *Development*, 141(20):3819-3833. doi: 10.1242/dev.104471.
- [139] Kispert, A. (1995). The Brachyury Protein: A T-Domain Transcription Factor. *Seminars in Developmental Biology*, 6(6):395-403. doi: 10.1016/S1044-5781(06)80003-4.
- [140] Ouimette, J.-F., Jolin, M. L., L'Honoré, A., Gifuni, A., and Drouin, J. (2010). Divergent Transcriptional Activities Determine Limb Identity. *Nature Communications*, 1(1):35. doi: 10.1038/ncomms1036.
- [141] Paxton, C., Zhao, H., Chin, Y., Langner, K., and Reecy, J. (2002). Murine Tbx2 Contains Domains That Activate and Repress Gene Transcription. *Gene*, 283(1-2):117-24. doi: 10.1016/s0378-1119(01)00878-2.
- [142] Agulnik, S.I., Garvey, N., Hancock, S., Ruvinsky, I., Chapman, D. L., Agulnik, I., Bollag, R., Papaioannou, V., and Silver, L.M. (1996). Evolution of Mouse T-Box Genes by Tandem Duplication and Cluster Dispersion. *Genetics*, 144(1):249-54.
- [143] Peres, J., Davis, E., Mowla, S., Bennett, D. C., Li, J. A., Wansleben, S., and Prince, S. (2010). The Highly Homologous T-Box Transcription Factors, Tbx2 and Tbx3, Have Distinct Roles in the Oncogenic Process. *Genes & Cancer*, 1(3):272-282. doi: 10.1177/1947601910365160.
- [144] Singh, R., Hoogaars, W.M., Barnett, P., Grieskamp, T., Rana, M. S., Buermans, H., Farin, H.F., Petry, M., Heallen, T., Martin, J.F., Moorman, A.F., Hoen, P A., Kispert, A., and Christoffels, V.M. (2012). Tbx2 and Tbx3 Induce Atrioventricular Myocardial Development and Endocardial Cushion Formation. *Cell Mol Life Sci*, 69(8):1377-89. doi: 10.1007/s00018-011-0884-2.
- [145] Lüdtke, T.H.-W., Christoffels, V. M., Petry, M., and Kispert, A. (2009). Tbx3 Promotes Liver Bud Expansion During Mouse Development by Suppression of Cholangiocyte Differentiation. *Hepatology*, 49(3):969-978. doi: 10.1002/hep.22700.
-

-
- [146] Zirzow, S., Lüdtke, T.H.W., Brons, J.F., Petry, M., Christoffels, V.M., and Kispert, A. (2009). Expression and Requirement of T-Box Transcription Factors Tbx2 and Tbx3 During Secondary Palate Development in the Mouse. *Developmental Biology*, 336(2):145-155. doi: 10.1016/j.ydbio.2009.09.020.
- [147] Ghosh, T.K., Brook, J.D., and Wilsdon, A. (2017). T-Box Genes in Human Development and Disease, In: Current Topics in Developmental Biology, Academic Press. p.383-415. doi: 10.1016/bs.ctdb.2016.08.006.0070-2153.
- [148] Jerome, L.A. and Papaioannou, V.E. (2001). Digeorge Syndrome Phenotype in Mice Mutant for the T-Box Gene, Tbx1. *Nature Genetics*, 27(3):286-291. doi: 10.1038/85845.
- [149] Davenport, T.G., Jerome, Majewska, L.A., and Papaioannou, V.E. (2003). Mammary Gland, Limb and Yolk Sac Defects in Mice Lacking Tbx3, the Gene Mutated in Human Ulnar Mammary Syndrome. *Development*, 130(10):2263-73. doi: 10.1242/dev.00431.
- [150] Basson, C.T., Bachinsky, D. R., Lin, R. C., Levi, T., Elkins, J. A., Soultz, J., Grayzel, D., Kroumpouzou, E., Traill, T. A., Leblanc-Straceski, J., Renault, B., Kucherlapati, R., Seidman, J. G., and Seidman, C.E. (1997). Mutations in Human Tbx5 Cause Limb and Cardiac Malformation in Holt-Oram Syndrome. *Nature genetics*, 15(1):30-35. doi: 10.1038/ng0197-30.
- [151] Takahashi, T., Friedmacher, F., Zimmer, J., and Puri, P. (2017). Expression of T-Box Transcription Factors 2, 4 and 5 Is Decreased in the Branching Airway Mesenchyme of Nitrofen-Induced Hypoplastic Lungs. *Pediatr Surg Int*, 33(2):139-143. doi: 10.1007/s00383-016-4005-z.
- [152] Holder, A.M., Klaassens, M., Tibboel, D., de Klein, A., Lee, B., and Scott, D.A. (2007). Genetic Factors in Congenital Diaphragmatic Hernia. *American journal of human genetics*, 80(5):825-845. doi: 10.1086/513442.
- [153] Du, W.-L., Fang, Q., Chen, Y., Teng, J.-W., Xiao, Y.-S., Xie, P., Jin, B., and Wang, J.-Q. (2017). Effect of Silencing the T-Box Transcription Factor Tbx2 in Prostate Cancer Pc3 and Lncap Cells. *Molecular Medicine Reports*, 16(5):6050-6058. doi: 10.3892/mmr.2017.7361.
- [154] Cebra-Thomas, J.A., Bromer, J., Gardner, R., Lam, G.K., Sheipe, H., and Gilbert, S.F. (2003). T-Box Gene Products Are Required for Mesenchymal Induction of Epithelial Branching in the Embryonic Mouse Lung. *Developmental Dynamics*, 226:82-90. doi: 10.1002/dvdy.10208.
- [155] Saadi, I., Das, P., Zhao, M., Raj, L., Ruspita, I., Xia, Y., Papaioannou, V. E., and Bei, M. (2013). Msx1 and Tbx2 Antagonistically Regulate Bmp4 Expression During the Bud-to-Cap Stage Transition in Tooth Development. *Development*, 140(13):2697-2702. doi: 10.1242/dev.088393.
- [156] Mohamad, T., Kazim, N., Adhikari, A., and Davie, J.K. (2018). Egr1 Interacts with Tbx2 and Functions as a Tumor Suppressor in Rhabdomyosarcoma. *Oncotarget*, 9(26):18084-18098. doi: 10.18632/oncotarget.24726.
-

-
- [157] Habets, P.E., Moorman, A.F., Clout, D.E., van Roon, M.A., Lingbeek, M., van Lohuizen, M., Campione, M., and Christoffels, V.M. (2002). Cooperative Action of Tbx2 and Nkx2.5 Inhibits Anf Expression in the Atrioventricular Canal: Implications for Cardiac Chamber Formation. *Genes Dev*, 16(10):1234-46. doi: 10.1101/gad.222902.
- [158] Vance, K.W., Shaw, H. M., Rodriguez, M., Ott, S., and Goding, C.R. (2010). The Retinoblastoma Protein Modulates Tbx2 Functional Specificity. *Mol Biol Cell*, 21(15):2770-9. doi: 10.1091/mbc.E09-12-1029.
- [159] Ronfani, L., Ferraguti, M., Croci, L., Ovitt, C. E., Scholer, H. R., Consalez, G. G., and Bianchi, M.E. (2001). Reduced Fertility and Spermatogenesis Defects in Mice Lacking Chromosomal Protein Hmgb2. *Development*, 128(8):1265.
- [160] Li, W., Lin, C. Y., Shang, C., Han, P, Xiong, Y., Lin, C. J., Yang, J., Selleri, L., and Chang, C.P. (2014). Pbx1 Activates Fgf10 in the Mesenchyme of Developing Lungs. *Genesis*, 52(5):399-407. doi: 10.1002/dvg.22764.
- [161] Vance, K.W., Carreira, S., Brosch, G., and Goding, C.R. (2005). Tbx2 Is Overexpressed and Plays an Important Role in Maintaining Proliferation and Suppression of Senescence in Melanomas. *Cancer Research*, 65(6):2260. doi: 10.1158/0008-5472.CAN-04-3045.
- [162] Zhu, B., Zhang, M., Byrum, S. D., Tackett, A. J., and Davie, J.K. (2014). Tbx2 Blocks Myogenesis and Promotes Proliferation in Rhabdomyosarcoma Cells. *Int J Cancer*, 135(4):785-797. doi: 10.1002/ijc.28721.
- [163] Zhu, B., Zhang, M., Williams, E. M., Keller, C., Mansoor, A., and Davie, J.K. (2016). Tbx2 Represses Pten in Rhabdomyosarcoma and Skeletal Muscle. *Oncogene*, 35(32):4212-4224. doi: 10.1038/onc.2015.486.
- [164] Ruan, J., Ouyang, H., Amaya, M. F., Ravichandran, M., Loppnau, P., Min, J., and Zang, J. (2012). Structural Basis of the Chromodomain of Cbx3 Bound to Methylated Peptides from Histone H1 and G9a. *PLOS ONE*, 7(4):e35376. doi: 10.1371/journal.pone.0035376.
- [165] Zocco, M., Marasovic, M., Pisacane, P., Bilokapic, S., and Halic, M. (2016). The Chp1 Chromodomain Binds the H3k9me Tail and the Nucleosome Core to Assemble Heterochromatin. *Cell Discovery*, 2(1):16004. doi: 10.1038/celldisc.2016.4.
- [166] Basta, J. and Rauchman, M. (2015). The Nucleosome Remodeling and Deacetylase Complex in Development and Disease. *Translational research : the journal of laboratory and clinical medicine*, 165(1):36-47. doi: 10.1016/j.trsl.2014.05.003.
- [167] Denslow, S.A. and Wade, P.A. (2007). The Human Mi-2/Nurd Complex and Gene Regulation. *Oncogene*, 26(37):5433-5438. doi: 10.1038/sj.onc.1210611.
- [168] Lai, A.Y. and Wade, P.A. (2011). Nurd: A Multi-Faceted Chromatin Remodelling Complex in Regulating Cancer Biology. *Nature reviews. Cancer*, 11(8):588-596. doi: 10.1038/nrc3091.
- [169] Smith, R., Sellou, H., Chapuis, C., Huet, S., and Timinszky, G. (2018). Chd3 and Chd4 Recruitment and Chromatin Remodeling Activity at DNA Breaks Is Promoted by Early Poly(Adp-Ribose)-Dependent Chromatin Relaxation. *Nucleic acids research*, 46(12):6087-6098. doi: 10.1093/nar/gky334.
-

-
- [170] Xue, Y., Wong, J., Moreno, G. T., Young, M. K., Côté, J., and Wang, W. (1998). Nurd, a Novel Complex with Both Atp-Dependent Chromatin-Remodeling and Histone Deacetylase Activities. *Mol Cell*, 2(6):851-61. doi: 10.1016/s1097-2765(00)80299-3.
- [171] Silva, A.P.G., Ryan, D. P., Galanty, Y., Low, J. K. K., Vandevenne, M., Jackson, S. P., and Mackay, J.P. (2016). The N-Terminal Region of Chromodomain Helicase DNA-Binding Protein 4 (Chd4) Is Essential for Activity and Contains a High Mobility Group (Hmg) Box-Like-Domain That Can Bind Poly(Adp-Ribose). *The Journal of biological chemistry*, 291(2):924-938. doi: 10.1074/jbc.M115.683227.
- [172] Murzina, N.V., Pei, X.-Y., Zhang, W., Sparkes, M., Vicente-Garcia, J., Pratap, J. V., McLaughlin, S. H., Ben-Shahar, T. R., Verreault, A., Luisi, B. F., and Laue, E.D. (2008). Structural Basis for the Recognition of Histone H4 by the Histone-Chaperone Rbap46. *Structure*, 16(7):1077-1085. doi: 10.1016/j.str.2008.05.006.
- [173] Lu, Q. and Kamps, M.P. (1996). Selective Repression of Transcriptional Activators by Pbx1 Does Not Require the Homeodomain. *Proceedings of the National Academy of Sciences*, 93(1):470. doi: 10.1073/pnas.93.1.470.
- [174] Nielsen, A.L., Ortiz, J. A., You, J., Oulad-Abdelghani, M., Khechumian, R. Gansmuller, A., Chambon, P., and Losson, R. (1999). Interaction with Members of the Heterochromatin Protein 1 (Hp1) Family and Histone Deacetylation Are Differentially Involved in Transcriptional Silencing by Members of the Tif1 Family. *The EMBO journal*, 18(22):6385-6395. doi: 10.1093/emboj/18.22.6385.
- [175] Stelzer, G., Goppelt, A., Lottspeich, F., and Meisterernst, M. (1994). Repression of Basal Transcription by Hmg2 Is Counteracted by TfiIh-Associated Factors in an Atp-Dependent Process. *Molecular and Cellular Biology*, 14(7):4712. doi: 10.1128/MCB.14.7.4712.
- [176] Kwon, S.H. and Workman, J. (2011). The Changing Faces of Hp1: From Heterochromatin Formation and Gene Silencing to Euchromatic Gene Expression: Hp1 Acts as a Positive Regulator of Transcription. *BioEssays : news and reviews in molecular, cellular and developmental biology*, 33:280-9. doi: 10.1002/bies.201000138.
- [177] Brendolan, A., Ferretti, E., Salsi, V., Moses, K., Quaggin, S., Blasi, F., Cleary, M. L., and Selleri, L. (2005). A Pbx1-Dependent Genetic and Transcriptional Network Regulates Spleen Ontogeny. *Development*, 132(13):3113-26. doi: 10.1242/dev.01884.
- [178] Chung, E.Y., Liu, J., Homma, Y., Zhang, Y., Brendolan, A., Saggese, M., Han, J., Silverstein, R., Selleri, L., and Ma, X. (2007). Interleukin-10 Expression in Macrophages During Phagocytosis of Apoptotic Cells Is Mediated by Homeodomain Proteins Pbx1 and Prep-1. *Immunity*, 27(6):952-64. doi: 10.1016/j.immuni.2007.11.014.
- [179] Jain, D., Nemec, S., Luxey, M., Gauthier, Y., Bemmo, A., Balsalobre, A., and Drouin, J. (2018). Regulatory Integration of Hox Factor Activity with T-Box Factors in Limb Development. *Development*, 145(6):dev159830. doi: 10.1242/dev.159830.
- [180] Saleh, M., Rambaldi, I., Yang, X. J., and Featherstone, M.S. (2000). Cell Signaling Switches Hox-Pbx Complexes from Repressors to Activators of Transcription Mediated by Histone Deacetylases and Histone Acetyltransferases. *Molecular and cellular biology*, 20(22):8623-8633. doi: 10.1128/mcb.20.22.8623-8633.2000.
-

-
- [181] Kumar P, P., Franklin, S., Emechebe, U., Hu, H., Moore, B., Lehman, C., Yandell, M., and Moon, A.M. (2014). Tbx3 Regulates Splicing in Vivo: A Novel Molecular Mechanism for Ulnar-Mammary Syndrome. *PLOS Genetics*, 10(3):e1004247. doi: 10.1371/journal.pgen.1004247.
- [182] Smallwood, A., Hon, G. C., Jin, F., Henry, R. E., Espinosa, J. M., and Ren, B. (2012). Cbx3 Regulates Efficient Rna Processing Genome-Wide. *Genome research*, 22(8):1426-1436. doi: 10.1101/gr.124818.111.
- [183] Jacobs, J.J., Keblusek, P., Robanus-Maandag, E., Kristel, P., Lingbeek, M., Nederlof, P.M., van Welsem, T., van de Vijver, M.J., Koh, E.Y., Daley, G.Q., and van Lohuizen, M. (2000). Senescence Bypass Screen Identifies Tbx2, Which Represses Cdkn2a (P19(Arf)) and Is Amplified in a Subset of Human Breast Cancers. *Nat Genet*, 26(3):291-9. doi: 10.1038/81583.
- [184] Abraham, A.B., Bronstein, R., Chen, E. I., Koller, A., Ronfani, L., Maletic-Savatic, M., and Tsirka, S.E. (2013). Members of the High Mobility Group B Protein Family Are Dynamically Expressed in Embryonic Neural Stem Cells. *Proteome Science*, 11(1):18. doi: 10.1186/1477-5956-11-18.
- [185] Zhang, P., Lu, Y., and Gao, S. (2019). High-Mobility Group Box 2 Promoted Proliferation of Cervical Cancer Cells by Activating Akt Signaling Pathway. *Journal of Cellular Biochemistry*, 120. doi: 10.1002/jcb.28998.
- [186] Nitarska, J., Smith, J. G., Sherlock, W. T., Hillege, M. M. G., Nott, A., Barshop, W. D., Vashisht, A. A., Wohlschlegel, J. A., Mitter, R. and Riccio, A. (2016). A Functional Switch of Nurd Chromatin Remodeling Complex Subunits Regulates Mouse Cortical Development. *Cell Reports*, 17(6):1683-1698. doi: 10.1016/j.celrep.2016.10.022.
- [187] Yoshida, T., Hu, Y., Zhang, Z., Emmanuel, A. O., Galani, K., Muhire, B., Snippert, H. J., Williams, C. J., Tolstorukov, M. Y., Gounari, F., and Georgopoulos, K. (2019). Chromatin Restriction by the Nucleosome Remodeler Mi-2beta and Functional Interplay with Lineage-Specific Transcription Regulators Control B-Cell Differentiation. *Genes Dev*, 33(13-14):763-781. doi: 10.1101/gad.321901.118.
- [188] Hou, M.-F., Luo, C.-W., Chang, T.-M., Hung, W.-C., Chen, T.-Y., Tsai, Y.-L., Chai, C.-Y., and Pan, M.-R. (2017). The Nurd Complex-Mediated P21 Suppression Facilitates Chemoresistance in Brca-Proficient Breast Cancer. *Experimental Cell Research*, 359(2):458-465. doi: 10.1016/j.yexcr.2017.08.029.
- [189] Fan, Y., Li, H., Liang, X., and Xiang, Z. (2017). Cbx3 Promotes Colon Cancer Cell Proliferation by Cdk6 Kinase-Independent Function During Cell Cycle. *Oncotarget*, 8(12):19934-19946. doi: 10.18632/oncotarget.15253.
- [190] Ruijtenberg, S. and van den Heuvel, S. (2016). Coordinating Cell Proliferation and Differentiation: Antagonism between Cell Cycle Regulators and Cell Type-Specific Gene Expression. *Cell cycle (Georgetown, Tex.)*, 15(2):196-212. doi: 10.1080/15384101.2015.1120925.
- [191] Christoffels, V.M., Hoogaars, W. M., Tessari, A., Clout, D. E., Moorman, A. F., and Campione, M. (2004). T-Box Transcription Factor Tbx2 Represses Differentiation and Formation of the Cardiac Chambers. *Dev Dyn*, 229(4):763-70. doi: 10.1002/dvdy.10487.
-

-
- [192] Ribeiro, I., Kawakami, Y., Büscher, D., Raya, Á., Rodríguez-León, J., Morita, M., Rodríguez Esteban, C., and Izpisua Belmonte, J.C. (2007). Tbx2 and Tbx3 Regulate the Dynamics of Cell Proliferation During Heart Remodeling. *PLOS ONE*, 2(4):e398. doi: 10.1371/journal.pone.0000398.
- [193] Singh, M.K., Christoffels, V. M., Dias, J. M., Trowe, M.-O., Petry, M., Schuster-Gossler, K., Bürger, A., Ericson, J., and Kispert, A. (2005). Tbx20 Is Essential for Cardiac Chamber Differentiation and Repression of Tbx2. *Development*, 132(12):2697-2707. doi: 10.1242/dev.01854.
- [194] Selleri, L., Depew, M. J., Jacobs, Y., Chanda, S. K., Tsang, K. Y., Cheah, K. S. E., Rubenstein, J. L. R., O’Gorman, S., and Cleary, M.L. (2001). Requirement for Pbx1 in Skeletal Patterning and Programming Chondrocyte Proliferation and Differentiation. *Development*, 128(18):3543.
- [195] Huang, C., Su, T., Xue, Y., Cheng, C., Lay, F. D., McKee, R. A., Li, M., Vashisht, A., Wohlschlegel, J., Novitch, B. G., Plath, K., Kurdistani, S. K., and Carey, M. (2017). Cbx3 Maintains Lineage Specificity During Neural Differentiation. *Genes & Development*, 31(3):241-246. doi: 10.1101/gad.292169.116.
- [196] Kimura, A., Matsuda, T., Sakai, A., Murao, N., and Nakashima, K. (2018). Hmgb2 Expression Is Associated with Transition from a Quiescent to an Activated State of Adult Neural Stem Cells. *Developmental Dynamics*, 247(1):229-238. doi: 10.1002/dvdy.24559.
- [197] Morikawa, K., Ikeda, N., Hisatome, I., and Shirayoshi, Y. (2013). Heterochromatin Protein 1 γ Overexpression in P19 Embryonal Carcinoma Cells Elicits Spontaneous Differentiation into the Three Germ Layers. *Biochemical and Biophysical Research Communications*, 431(2):225-231. doi: 10.1016/j.bbrc.2012.12.128.
- [198] Villaescusa, J.C., Li, B., Toledo, E. M., Rivetti di Val Cervo, P., Yang, S., Stott, S.R.W., Kaiser, K., Islam, S., Gyllborg, D., Laguna-Goya, R., Landreh, M., Lönnerberg, P., Falk, A., Bergman, T., Barker, R.A., Linnarsson, S., Selleri, L., and Arenas, E. (2016). A Pbx1 Transcriptional Network Controls Dopaminergic Neuron Development and Is Impaired in Parkinson's Disease. *The EMBO Journal*, 35(18):1963-1978. doi: 10.15252/embj.201593725.
- [199] Zhang, C.L., McKinsey, T.A., and Olson, E.N. (2002). Association of Class II Histone Deacetylases with Heterochromatin Protein 1: Potential Role for Histone Methylation in Control of Muscle Differentiation. *Molecular and cellular biology*, 22(20):7302-7312. doi: 10.1128/mcb.22.20.7302-7312.2002.
- [200] Micucci, J.A., Sperry, E.D., and Martin, D.M. (2015). Chromodomain Helicase DNA-Binding Proteins in Stem Cells and Human Developmental Diseases. *Stem cells and development*, 24(8):917-926. doi: 10.1089/scd.2014.0544.
- [201] Yoder, M.C. (2018). Endothelial Stem and Progenitor Cells (Stem Cells): (2017 Grover Conference Series). *Pulmonary circulation*, 8(1):1-9. doi: 10.1177/2045893217743950.
- [202] Chen, X., Lu, K., Timko, N. J., Weir, D. M., Zhu, Z., Qin, C., Mann, J. D., Bai, Q., Xiao, H., Nicholl, M. B., Wakefield, M. R., and Fang, Y. (2018). IL-33 Notably Inhibits the Growth of Colon Cancer Cells. *Oncol Lett*, 16(1):769-774. doi: 10.3892/ol.2018.8728.
-

-
- [203] Cayrol, C. and Girard, J.-P. (2018). Interleukin-33 (Il-33): A Nuclear Cytokine from the Il-1 Family. *Immunological Reviews*, 281(1):154-168. doi: 10.1111/imr.12619.
- [204] Berschneider, B. and Königshoff, M. (2011). Wnt1 Inducible Signaling Pathway Protein 1 (Wisp1): A Novel Mediator Linking Development and Disease. *The International Journal of Biochemistry & Cell Biology*, 43(3):306-309. doi: 10.1016/j.biocel.2010.11.013.
- [205] Deng, W., Fernandez, A., McLaughlin, S. L., and Klinke, D.J. (2019). Wnt1-Inducible Signaling Pathway Protein 1 (Wisp1/Ccn4) Stimulates Melanoma Invasion and Metastasis by Promoting the Epithelial–Mesenchymal Transition. *Journal of Biological Chemistry*, 294(14):5261-5280. doi: 10.1074/jbc.RA118.006122.
- [206] Schlegelmilch, K., Keller, A., Zehe, V., Hondke, S., Schilling, T., Jakob, F., Klein-Hitpass, L., and Schütze, N. (2014). Wisp 1 Is an Important Survival Factor in Human Mesenchymal Stromal Cells. *Gene*, 551(2):243-254. doi: 10.1016/j.gene.2014.09.002.
- [207] Zemans, R.L., McClendon, J., Aschner, Y., Briones, N. Young, S. K., Lau, L.F., Kahn, M., and Downey, G.P. (2013). Role of B-Catenin-Regulated Ccn Matricellular Proteins in Epithelial Repair after Inflammatory Lung Injury. *American Journal of Physiology - Lung Cellular and Molecular Physiology*, 304(6):415-427. doi: 10.1152/ajplung.00180.2012.
- [208] An, G., Zhang, X., Wang, W., Huang, Q., Li, Y., Shan, S., Corrigan, C., Wang, W., and Ying, S. (2018). The Effects of Il-33 on Airways Collagen Deposition and Matrix Metalloproteinase Expression in a Murine Surrogate of Asthma. *Immunology*. doi: 10.1111/imm.12911.
- [209] Bilican, B. and Goding, C.R. (2006). Cell Cycle Regulation of the T-Box Transcription Factor Tbx2. *Experimental Cell Research*, 312(12):2358-2366. doi: 10.1016/j.yexcr.2006.03.033.
- [210] Boward, B., Wu, T., and Dalton, S. (2016). Control of Cell Fate through Cell Cycle and Pluripotency Networks. *Stem cells*, 34(6):1427-1436. doi: 10.1002/stem.2345.
- [211] Soriano, J.B., Kendrick, P. J., Paulson, K R., *et al.* (2020). Prevalence and Attributable Health Burden of Chronic Respiratory Diseases, 1990-2017: A Systematic Analysis for the Global Burden of Disease Study 2017. *The Lancet Respiratory Medicine*, 8(6):585-596. doi: 10.1016/S2213-2600(20)30105-3.
- [212] Bara, I., Ozier, A., Tunon de Lara, J. M., Marthan, R., and Berger, P. (2010). Pathophysiology of Bronchial Smooth Muscle Remodelling in Asthma. *European Respiratory Journal*, 36(5):1174. doi: 10.1183/09031936.00019810.
- [213] Barratt, S.L., Creamer, A., Hayton, C., and Chaudhuri, N. (2018). Idiopathic Pulmonary Fibrosis (Ipf): An Overview. *Journal of clinical medicine*, 7(8):201. doi: 10.3390/jcm7080201.
- [214] Karakioulaki, M., Papakonstantinou, E., and Stolz, D. (2020). Extracellular Matrix Remodelling in Copd. *European Respiratory Review*, 29(158):190124. doi: 10.1183/16000617.0124-2019.
- [215] Shi, J., Li, F., Luo, M., Wei, J., and Liu, X. (2017). Distinct Roles of Wnt/B-Catenin Signaling in the Pathogenesis of Chronic Obstructive Pulmonary Disease and Idiopathic Pulmonary Fibrosis. *Mediators of Inflammation*, 2017:3520581. doi: 10.1155/2017/3520581.
-

-
- [216] Lawson, W.E., Polosukhin, V.V., Zoia, O., Stathopoulos, G.T., Han, W., Plieth, D., Loyd, J.E., Neilson, E.G., and Blackwell, T.S. (2005). Characterization of Fibroblast-Specific Protein 1 in Pulmonary Fibrosis. *Am J Respir Crit Care Med*, 171(8):899-907. doi: 10.1164/rccm.200311-1535OC.
- [217] Lee, J.-U., Chang, H. S., Shim, E.-Y., Park, J.-S., Koh, E.-S., Shin, H.-K., Park, J.-S., and Park, C.-S. (2020). The S100 Calcium-Binding Protein A4 Level Is Elevated in the Lungs of Patients with Idiopathic Pulmonary Fibrosis. *Respiratory Medicine*, 171:105945. doi: 10.1016/j.rmed.2020.105945.
- [218] Xia, H., Gilbertsen, A., Herrera, J., Racila, E. Smith, K., Peterson, M., Griffin, T., Benyumov, A., Yang, L., Bitterman, P. B., and Henke, C.A. (2017). Calcium-Binding Protein S100a4 Confers Mesenchymal Progenitor Cell Fibrogenicity in Idiopathic Pulmonary Fibrosis. *The Journal of Clinical Investigation*, 127(7):2586-2597. doi: 10.1172/JCI90832.
- [219] Ito, J.T., Lourenço, J. D., Righetti, R. F., Tibério, I. F. L. C., Prado, C. M., and Lopes, F.D.T.Q.S. (2019). Extracellular Matrix Component Remodeling in Respiratory Diseases: What Has Been Found in Clinical and Experimental Studies? *Cells*, 8(4):342. doi: 10.3390/cells8040342.
- [220] Xia, J., Zhao, J., Shang, J., Li, M., Zeng, Z., Zhao, J., Wang, J., Xu, Y., and Xie, J. (2015). Increased Il-33 Expression in Chronic Obstructive Pulmonary Disease. *American Journal of Physiology - Lung Cellular and Molecular Physiology*, 308(7):L619-L627. doi: 10.1152/ajplung.00305.2014.
- [221] Yagami, A., Orihara, K., Morita, H., Futamura, K., Hashimoto, N., Matsumoto, K., Saito, H., and Matsuda, A. (2010). Il-33 Mediates Inflammatory Responses in Human Lung Tissue Cells. *The Journal of Immunology*, 185(10):5743-5750. doi: 10.4049/jimmunol.0903818.
- [222] Liew, F.Y., Pitman, N.I., and McInnes, I.B. (2010). Disease-Associated Functions of Il-33: The New Kid in the Il-1 Family. *Nat Rev Immunol*, 10(2):103-110. doi: 10.1038/nri2692.
- [223] Préfontaine, D., Lajoie-Kadoch, S., Foley, S., Audusseau, S., Olivenstein, R., Halayko, A. J., Lemièrre, C., Martin, J. G., and Hamid, Q. (2009). Increased Expression of Il-33 in Severe Asthma: Evidence of Expression by Airway Smooth Muscle Cells. *J Immunol*, 183(8):5094-103. doi: 10.4049/jimmunol.0802387.
- [224] Königshoff, M., Kramer, M., Balsara, N., Wilhelm, J., Amarie, O.V., Jahn, A., Rose, F., Fink, L., Seeger, W., Schaefer, L., Günther, A., and Eickelberg, O. (2009). Wnt1-Inducible Signaling Protein-1 Mediates Pulmonary Fibrosis in Mice and Is Upregulated in Humans with Idiopathic Pulmonary Fibrosis. *The Journal of Clinical Investigation*, 119(4):772-787. doi: 10.1172/JCI33950.
- [225] Yang, M., Du, Y., Xu, Z., and Jiang, Y. (2016). Functional Effects of Wnt1-Inducible Signaling Pathway Protein-1 on Bronchial Smooth Muscle Cell Migration and Proliferation in Ova-Induced Airway Remodeling. *Inflammation*, 39(1):16-29. doi: 10.1007/s10753-015-0218-x.
- [226] Chilosi, M., Carloni, A., Rossi, A., and Poletti, V. (2013). Premature Lung Aging and Cellular Senescence in the Pathogenesis of Idiopathic Pulmonary Fibrosis and Copd/Emphysema. *Translational Research*, 162(3):156-173. doi: 10.1016/j.trsl.2013.06.004.
-

-
- [227] Acquaaah-Mensah, G.K., Malhotra, D., Vulimiri, M., McDermott, Jason. E., and Biswal, S. (2012). Suppressed Expression of T-Box Transcription Factors Is Involved in Senescence in Chronic Obstructive Pulmonary Disease. *PLoS Computational Biology*, 8(7):e1002597. doi: 10.1371/journal.pcbi.1002597.
- [228] Kneidinger, N., Yildirim, A. O., Callegari, J., Takenaka, S., Stein, M. M., Dumitrascu, R., Bohla, A., Bracke, K. R., Morty, R. E., Brusselle, G. G., Schermuly, R. T., Eickelberg, O., and Konigshoff, M. (2011). Activation of the Wnt/Beta-Catenin Pathway Attenuates Experimental Emphysema. *Am J Respir Crit Care Med*, 183(6):723-33. doi: 10.1164/rccm.200910-1560OC.
- [229] Abrahams, A., Mowla, S., Parker, M. I., Goding, C. R., and Prince, S. (2008). Uv-Mediated Regulation of the Anti-Senescence Factor Tbx2. *J Biol Chem*, 283(4):2223-30. doi: 10.1074/jbc.M705651200.
- [230] Belgacemi, R., Luczka, E., Ancel, J., Diabasana, Z., Perotin, J.-M., Germain, A., Lalun, N., Birembaut, P., Dubernard, X., Mérol, J.-C., Delepine, G., Polette, M., Deslée, G., and Dormoy, V. (2020). Airway Epithelial Cell Differentiation Relies on Deficient Hedgehog Signalling in Copd. *EBioMedicine*, 51:102572-102572. doi: 10.1016/j.ebiom.2019.11.033.
- [231] Hu, B., Liu, J., Wu, Z., Liu, T., Ullenbruch, M.R., Ding, L., Henke, C.A., Bitterman, P.B., and Phan, S.H. (2014). Reemergence of Hedgehog Mediates Epithelial-Mesenchymal Crosstalk in Pulmonary Fibrosis. *AJRCMB Articles in Press*. doi: 10.1165/rcmb.2014-0108OC.
- [232] Kugler, M.C., Joyner, A.L., Loomis, C.A., and Munger, J.S. (2015). Sonic Hedgehog Signaling in the Lung. From Development to Disease. *Am J Respir Cell Mol Biol*, 52(1):1-13. doi: 10.1165/rcmb.2014-0132TR.

Acknowledgment

I would like to thank Prof. Dr. Andreas Kispert for the fascinating and challenging project and the opportunity to participate in his research group. I appreciated the constructive discussions and continuous support over the last years, which promoted my personal development not only as a researcher.

I would like to thank Prof. Dr. Hansjörg Küster for his kind acceptance to be in chair of the examiners and Prof. Dr. Nico Lachmann for his kind acceptance to be referee of my dissertation.

I would like to thank Prof. Dr. Achim Gossler for the fantastic working environment within the institute, which was maintained despite all catastrophes.

Further, I would like to thank Prof. Dr. Andreas Pich and the complete team of the Research Core Unit Proteomics of the MHH, who very quickly performed the initial MS analysis and further sample preparations. A huge thank you also to Dr. Holger Eubel and Patrick Künzel from the Department of Plant Proteomics from the Leibniz University Hannover, who spontaneously provided their help and took over the MS measurements after the water damage in the I6.

Particularly I would like to thank Dr. Timo Lüdtko for constantly supporting me, for many helpful discussions and great ideas which advanced the project.

A special thanks also to Dr. Mark-Oliver Trowe who introduced me during my undergraduate studies to all basic lab work and thereby laid the foundation for this thesis.

A huge thank you to all the past and present lab members for helpful discussions, support, fantastic team-work, funny situations, cheering up, constant supply of cookies and chocolate and all the nice evenings in and outside the lab.

And a special thanks to Marina Kaiser, for so many years of working, laughing, supporting and simply spending together. The end of an era!

Finally, I want to thank my entire family who facilitated not only my university studies, but also supported me in each period of life and backed and cheered me up during all this time.

THANK YOU!

Curriculum Vitae

Personal information:

Name: Irina Wojahn
Date of birth: 20.02.1990
Place of birth: Cuxhaven
Citizenship: German

School education:

1996 - 2000 Amandus Abendroth Grundschule, Cuxhaven
2000 - 2002 Bleickenschule (Orientierungsstufe), Cuxhaven
2002 - 2009 Amandus Abendroth Gymnasium, Cuxhaven
Graduation grade: European baccalaureate

University studies:

2009 - 2013 Gottfried Wilhelm Leibniz Universität, Hannover
Graduation grade: B. Sc. Biology
Thesis title: "Phänotypische Charakterisierung der Innenohrentwicklung in *Tbx2*- und *Tbx3*- mutanten Mäusen" ("Phenotypical characterization of inner ear development in *Tbx2*- and *Tbx3*- mutant mice")

2014 - 2016 Carl-von-Ossietzky University, Oldenburg
Graduation grade: M. Sc.
Thesis title: "Molekulare Analyse von *Tbx2* in der murinen Lungenentwicklung" ("Molecular analysis of *Tbx2* in murine lung development")

2016 - expected 2021 Gottfried Wilhelm Leibniz Universität, Hannover
PhD student
Thesis title: "Analysis of the expression, the cellular and the molecular functions of TBX2 in murine lung development"

Working experience:

1.10.2013 - Research Assistant; Institute for Molecular Biology, Hannover

31.07.2014 and Medical School

1.09.2014 - Research project: "Initial analysis of the function of TBX2 and

30.09.2014 TBX3 in the development of the mouse inner ear"

16.09.2015 - Research Assistant; Institut of Biology and Enviromental

31.10.2015 Science, AG Neurosensorik/Animal Navigation, Carl-von-

Ossietzky Universität, Oldenburg

Research project: "Migratory behavior of migratory songbirds in consideration of anthropogenic and endogenous magnetic fields"

15.12.2016 - Research Assistant; Institute for Molecular Biology, Hannover

30.04.2020 Medical School

Research project: "Analysis of the molecular function of *Tbx2* in murine lung development"

Publications

Irina Wojahn, Timo H. Lüdtkke, Vincent M. Christoffels, Mark-Oliver Trowe and Andreas Kispert. TBX2-positive cells represent a multi-potent mesenchymal progenitor pool in the developing lung. *Respiratory Research*, 2019, 20:292; DOI:10.1186/s12931-019-1264-y.

Timo H. Lüdtkke*, **Irina Wojahn***, Marc-Jens Kleppa, Jasper Schierstaedt, Vincent M. Christoffels, Patrick Künzler and Andreas Kispert. Combined genomic and proteomic approaches reveal DNA binding sites and interaction partners of TBX2 in the developing lung. *Respiratory Research*, 2021, 22:85; DOI:10.1186/s12931-021-01679-y.

*Gleichwertiger Beitrag (geteilte Erstautorenschaft).

Timo Lüdtkke, Carsten Rudat, **Irina Wojahn**, Anna-Carina Weiss, Marc-Jens Kleppa, Jennifer Kurz, Henner F. Farin, Anne Moon, Vincent M. Christoffels, Andreas Kispert. *Tbx2* and *Tbx3* act downstream of Shh to maintain canonical Wnt-signaling during branching morphogenesis of the murine lung. *Developmental Cell*, 2016, 39:1-15; DOI:10.1016/j.devcel.2016.08.007.

Lüdtkke TH., Rudat C., Kurz J., Häfner R., Greulich F., **Wojahn I.**, Aydoğdu N., Mamo TM., Kleppa MJ., Trowe MO., Bohnenpoll T., Taketo MM., Kispert A. Mesothelial mobilization in the developing lung and heart differs in timing, quantity, and pathway dependency. *Am J Physiol Lung Cell Mol Physiol.*, 2019, May 1;316(5):L767-L783. DOI:10.1152/ajplung.00212.201.

Marina Kaiser, **Irina Wojahn**, Carsten Rudat, Timo H. Lüdtkke, Robert Kelly, Vincent M. Christoffels, Anne Moon, Andreas Kispert and Mark-Oliver Trowe. Regulation of otocyst patterning by *Tbx2* and *Tbx3* is required for inner ear morphogenesis in the mouse. *Development*, 2021, DOI:10.1242/dev.195651.

Bohnenpoll, T., Wittern, AB., Mamo TM., Weiss AC., Rudat C., Kleppa MJ., Schuster-Gossler K., **Wojahn I.**, Lüdtké TH., Trowe MO., Kispert A. A SHH-FOXF1-BMP4 signaling axis regulating growth and differentiation of epithelial and mesenchymal tissues in ureter development. *PLoS Genet.*, 2017, Aug 10;13(8):e1006951. DOI:10.1371/journal.pgen.1006951.

Tobias Bohnenpoll, Mark-Oliver Trowe, **Irina Wojahn**, Makoto Mark Taketo, Marianne Petry, Andreas Kispert. Canonical Wnt signaling regulates the proliferative expansion and differentiation of fibrocytes in the murine inner ear. *Developmental Biology*, 2014, 391(1):54-65; DOI:10.1016/j.ydbio.2014.03.023.

Petra Bolte, Angelika Einwich, Pranav K. Seth, Raisa Chetverikova, Dominik Heyers, **Irina Wojahn**, Ulrike Janssen-Bienhold, Regina Feederle, P. J. Hore, Karin Dedek, Henrik Mouritsen. Cryptochrome 1a Localisation in Light- and Dark-Adapted Retinae of Several Migratory and Non-Migratory Bird Species: No Signs of Light-Dependent Activation. *Ethology Ecology & Evolution*, 2021, DOI: 10.1080/03949370.2020.1870571.

Declaration

I hereby declare and confirm that this dissertation is entirely the result of my own work except otherwise indicated. As indicated (see "Erklärung zur kumulativen Dissertation") some data were already part of my master thesis. Apart from that, this thesis has not been part of any other examination.

Erklärung zur Dissertation

Gemäß §6(1) der Promotionsordnung der Naturwissenschaftlichen Fakultät der Gottfried Wilhelm Leibniz Universität Hannover für die Promotion zum Dr. rer. nat.

Hiermit erkläre ich, dass ich meine Dissertation mit dem Titel

“Analysis of the expression, the cellular and the molecular functions of TBX2 in murine lung development”

selbstständig verfasst sowie die Hilfsmittel und Quellen und gegebenenfalls die zu Hilfeleistungen herangezogenen Institutionen vollständig angegeben habe. Wie Angegeben wurden wenige Daten dieser Dissertation bereits während meiner Masterarbeit generiert (siehe "Erklärung zur kumulativen Dissertation"). Abgesehen davon wurden die Inhalte dieser Disseration nicht zuvor als Bachelorarbeit, Masterarbeit, oder andere Prüfungsarbeit verwendet.

Hannover, _____

Irina Wojahn